PROTEOMICS FOR STUDYING FOODBORNE MICROORGANISMS AND THEIR IMPACT ON FOOD QUALITY AND HUMAN HEALTH

EDITED BY: Rosa Anna Siciliano, Sergio Uzzau and Maria Fiorella Mazzeo
PUBLISHED IN: Frontiers in Microbiology

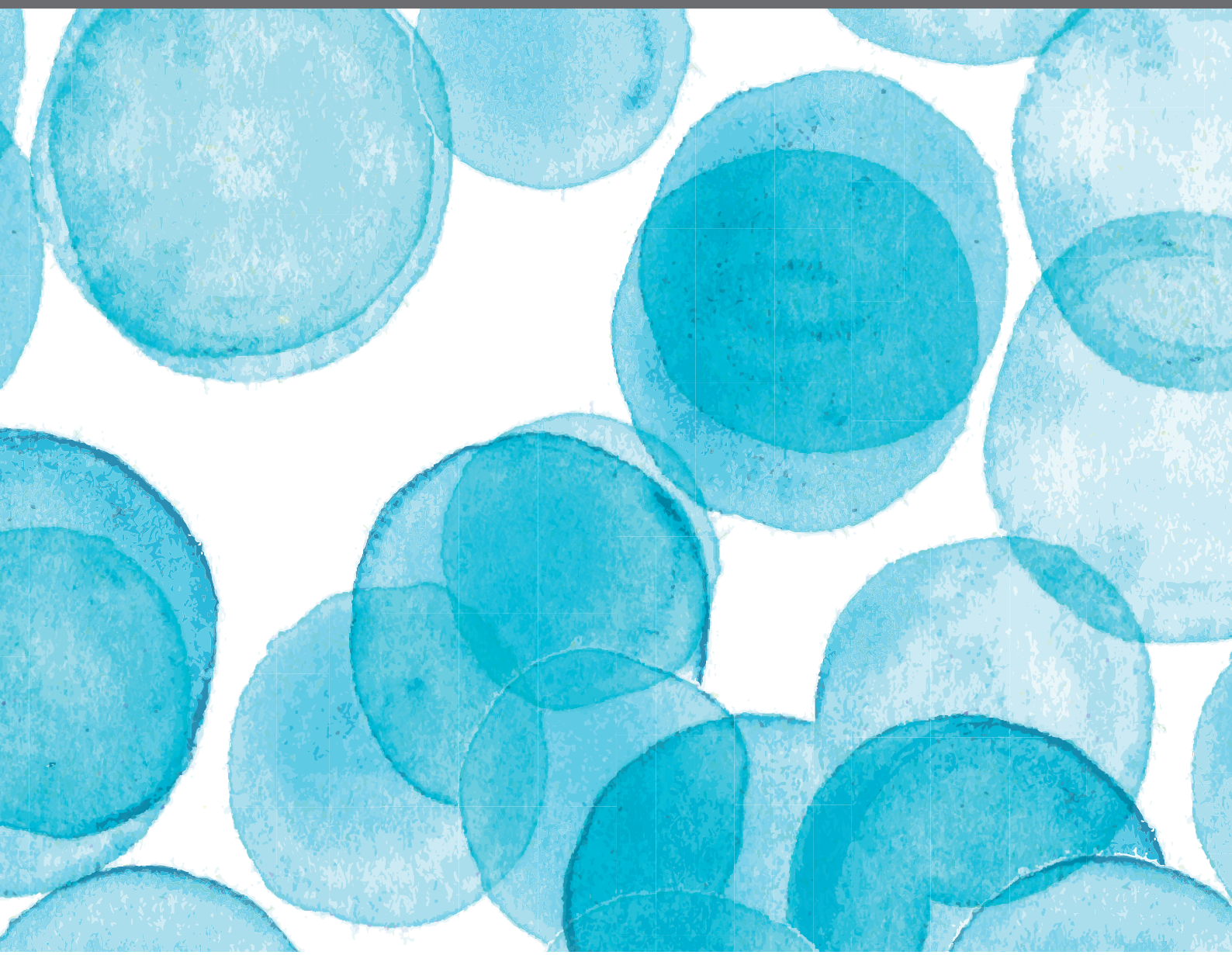

frontiers Research Topics

ISSN 1664-8714
ISBN 978-2-88963-076-9
DOI 10.3389/978-2-88963-076-9

About Frontiers

Frontiers is more than just an open-access publisher of scholarly articles: it is a pioneering approach to the world of academia, radically improving the way scholarly research is managed. The grand vision of Frontiers is a world where all people have an equal opportunity to seek, share and generate knowledge. Frontiers provides immediate and permanent online open access to all its publications, but this alone is not enough to realize our grand goals.

Frontiers Journal Series

The Frontiers Journal Series is a multi-tier and interdisciplinary set of open-access, online journals, promising a paradigm shift from the current review, selection and dissemination processes in academic publishing. All Frontiers journals are driven by researchers for researchers; therefore, they constitute a service to the scholarly community. At the same time, the Frontiers Journal Series operates on a revolutionary invention, the tiered publishing system, initially addressing specific communities of scholars, and gradually climbing up to broader public understanding, thus serving the interests of the lay society, too.

Dedication to Quality

Each Frontiers article is a landmark of the highest quality, thanks to genuinely collaborative interactions between authors and review editors, who include some of the world's best academicians. Research must be certified by peers before entering a stream of knowledge that may eventually reach the public - and shape society; therefore, Frontiers only applies the most rigorous and unbiased reviews.
Frontiers revolutionizes research publishing by freely delivering the most outstanding research, evaluated with no bias from both the academic and social point of view. By applying the most advanced information technologies, Frontiers is catapulting scholarly publishing into a new generation.

What are Frontiers Research Topics?

Frontiers Research Topics are very popular trademarks of the Frontiers Journals Series: they are collections of at least ten articles, all centered on a particular subject. With their unique mix of varied contributions from Original Research to Review Articles, Frontiers Research Topics unify the most influential researchers, the latest key findings and historical advances in a hot research area! Find out more on how to host your own Frontiers Research Topic or contribute to one as an author by contacting the Frontiers Editorial Office: researchtopics@frontiersin.org

PROTEOMICS FOR STUDYING FOODBORNE MICROORGANISMS AND THEIR IMPACT ON FOOD QUALITY AND HUMAN HEALTH

Topic Editors:
Rosa Anna Siciliano, Institute of Food Sciences, National Research Council, Italy
Sergio Uzzau, University of Sassari, Italy
Maria Fiorella Mazzeo, Institute of Food Sciences, National Research Council, Italy

Foodborne microorganisms play a pivotal role in mediating the tight relation between food and human health from a dual perspective. In fact, notwithstanding the introduction of strict regulations and new technologies to ensure food quality and safety, foodborne pathogens continue to cause infections and diseases and represent a serious public health concern, while spoilage bacteria can severely affect food quality thus leading to major industry and commercial losses. On the other hand, probiotics positively affect human health, promoting digestion and uptake of dietary nutrients, strengthening intestinal barrier function, modulating immune response and enhancing antagonism towards pathogens. Nowadays, proteomics represents a key discipline to perform high-throughput studies in the field of food microbiology and enables the most accurate identification of complex networks of proteins involved in the cell adaptation to different growth conditions as well as in beneficial or harmful effects on human health. The present eBook offers an overview of the most up to date proteomic methodologies and further assesses the strength of proteomics in exploring different aspects of the foodborne microorganism life-style and defining biomarkers of food quality and safety.

Citation: Siciliano, R. A., Uzzau, S., Mazzeo, M. F., eds. (2019). Proteomics for Studying Foodborne Microorganisms and Their Impact on Food Quality and Human Health. Lausanne: Frontiers Media. doi: 10.3389/978-2-88963-076-9

Table of Contents

frontiers in Nutrition

EDITORIAL
published: 10 July 2019
doi: 10.3389/fnut.2019.00104

Editorial: Proteomics for Studying Foodborne Microorganisms and Their Impact on Food Quality and Human Health

Rosa Anna Siciliano[1]*, *Sergio Uzzau*[2] *and Maria Fiorella Mazzeo*[1]

[1] *Institute of Food Sciences, National Research Council (CNR-ISA), Avellino, Italy,* [2] *Department of Biomedical Sciences, University of Sassari, Sassari, Italy*

Keywords: proteomics, microorganisms, food quality, food, human health

Editorial on the Research Topic

Proteomics for Studying Foodborne Microorganisms and Their Impact on Food Quality and Human Health

Foodborne microorganisms may play a pivotal role in mediating the tight relation between food and human health from a dual perspective. In fact, notwithstanding the introduction of strict regulations and new technologies to ensure food quality and safety, foodborne pathogens continue to cause infections and diseases, representing a serious public health concern, while spoilage bacteria can severely affect food quality thus leading to major industry and commercial losses.

On the other hand, probiotics positively affect human health, promoting digestion and uptake of dietary nutrients, strengthening intestinal barrier function, modulating immune response, and enhancing antagonism toward pathogens.

The present Research Topic of Frontiers in Nutrition was aimed to bring together research findings that further assess the strength of proteomics in exploring different aspects of the foodborne microorganisms' world.

Proteomics represents a key discipline to investigate physiology of foodborne bacteria since it enables the most accurate identification of complex networks of proteins underlying beneficial or harmful effects and cellular adaptation to different growth conditions, such as low temperatures. In this regard, refrigeration is still a widely used method for food storage and bacterial acclimation can favor food contamination and spoilage.

In their exemplary study, Santos et al. characterized the surface proteins of *Listeria monocytogenes,* grown in biofilm, to explore cold stress adaptation mechanisms boosted by this microorganism. In fact, capability to survive and proliferate at low temperature represents an essential feature of this foodborne pathogen enabling contamination of refrigerated and ready-to-eat foods.

Similarly, the cold tolerance features of *Vibrio parahaemolyticus*, a foodborne pathogen commonly isolated in seafood, have been elucidated. The integration of transcriptomic and proteomic data, collected from frozen squid and clinical isolates revealed the role of pyruvate metabolism in the processes of cold adaptation (Xie et al.).

This interesting microorganism is also able to survive in a viable but not culturable (VBNC) state when exposed to adverse conditions, such as refrigeration, and it can regain culturability (resuscitation state) under appropriate conditions. The molecular processes involved in this resuscitation process have been investigated by Zhong et al.

OPEN ACCESS

Edited and reviewed by:
Giovanna Suzzi,
University of Teramo, Italy

***Correspondence:**
Rosa Anna Siciliano
rsiciliano@isa.cnr.it

Specialty section:
This article was submitted to Food Microbiology, a section of the journal Frontiers in Nutrition

Received: *18 June 2019*
Accepted: *27 June 2019*
Published: *10 July 2019*

Citation:
Siciliano RA, Uzzau S and Mazzeo MF (2019) Editorial: Proteomics for Studying Foodborne Microorganisms and Their Impact on Food Quality and Human Health. Front. Nutr. 6:104. doi: 10.3389/fnut.2019.00104

The stress response mechanisms of bacteria are tightly regulated at transcriptional level and RpoS is known as an alternative sigma factor controlling stress resistance and virulence in many pathogens. Liu et al. defined the regulatory network of RpoS and assessed its role in biofilm formation and spoilage potential of *Pseudomonas fluorescens*, a bacterium often responsible for the deterioration of proteinaceous foods.

The development of innovative methods for the detection of pathogens and spoilage bacteria is still an indispensable research issue that can successfully take advantage of proteomic methodologies. As reported in this Research Topic, immune-proteomics was applied by Shi et al. to identify cell surface associated proteins in *Alicyclobacillus acidoterrestris*, a major putrefying bacterium mainly contaminating juice, and to select antigens potentially useful for the development of an immunological method for the detection of this contaminant.

Interestingly, different strains of the same bacterial species can exhibit either probiotic or pathogenic features. As matter of fact, *Enterococcus faecalis* is a controversial microorganism since, on one side, different strains can be used as food starters and probiotics, while, on the other, *E. faecalis* clinical isolates are now considered emergent nosocomial pathogens, exhibiting resistance to antibiotics and putative virulence factors. The high-throughput proteomic study performed on three different strains of this microorganism by Cirrincione et al. provided additional evidence to assess their food safety and highlight potential probiotic or pathogenic traits.

To gain a thorough view of the molecular mechanisms associated to probiotic or pathogenic features of bacteria, it is of the outmost importance the analysis of the surface exposed proteins that represent the front-line of interaction of the bacterial cells with their environmental niches. In the last decade, *ad hoc* designed proteomic strategies have been developed to analyze this complex class of molecules, taking advantages of the recent technological improvements in mass spectrometry and bioinformatics and thus providing direct evidence of protein cell localization and cell wall topology. These methods and the most updated and relevant results in the probiotics field have been reviewed by Siciliano et al.

In this frame, the analysis of the surfaceome of the well-known probiotic strain *Lactobacillus rhamnosus* GG highlighted that different growth conditions (glucose or fructose as carbon source of cells grown in planktonic or biofilm state) qualitatively and quantitatively modified the pattern of surface exposed proteins thus affecting probiotic (adherence and immunomodulatory) and industrially relevant (proteolytic activity) features (Savijoki et al.).

On the other hand, surface proteins are directly involved in bacteria pathogenicity and virulence and, for instance, in *Salmonella enterica* subspecies *enterica* (SEE), these features can vary considerably across serovars (and even strains). In this context, Fagerquist and Zaragoza confirmed the presence of flagella proteins in the surfaceome of three different SEE serovars and that of secreted invasion/effector proteins (Sip) in the Newport and Thompson strains.

In conclusion, the articles gathered in this Research Topic offer an overview of the most up to date proteomic methodologies and further highlight the relevance of this discipline in exploring different aspects of the foodborne microbial lifestyle, enabling the definition of microbial biomarkers of food quality and safety and, in turn, the design of new food preservative strategies.

We hope that this Research Topic will be interesting for the readers of the journal and we are grateful to all authors, reviewers and editorial staff who contributed to the realization of this initiative.

AUTHOR CONTRIBUTIONS

All authors listed have made a substantial, direct and intellectual contribution to the work, and approved it for publication.

Conflict of Interest Statement: The authors declare that the research was conducted in the absence of any commercial or financial relationships that could be construed as a potential conflict of interest.

frontiers in Nutrition

ORIGINAL RESEARCH
published: 14 June 2019
doi: 10.3389/fnut.2019.00089

Listeria monocytogenes Biofilm Adaptation to Different Temperatures Seen Through Shotgun Proteomics

Tiago Santos[1], *Didier Viala*[2], *Christophe Chambon*[2], *Julia Esbelin*[1] *and Michel Hébraud*[1,2]*

[1] *Université Clermont Auvergne, INRA, UMR Microbiologie Environnement Digestif Santé (MEDiS), Saint-Genès-Champanelle, France,* [2] *INRA, Plateforme d'Exploration du Métabolisme, Composante Protéomique (PFEMcp), Saint-Genès-Champanelle, France*

Listeria monocytogenes is a foodborne pathogen that can cause invasive severe human illness (listeriosis) in susceptible patients. Most human listeriosis cases appear to be caused by consumption of refrigerated ready-to-eat foods. Although initial contamination levels in foods are usually low, the ability of these bacteria to survive and multiply at low temperatures allows it to reach levels high enough to cause disease. This study explores the set of proteins that might have an association with *L. monocytogenes* adaptation to different temperatures. Cultures were grown in biofilm, the most widespread mode of growth in natural and industrial realms. Protein extractions were performed from three different growth temperatures (10, 25, and 37°C) and two growth phases (early stage and mature biofilm). *L. monocytogenes* subproteomes were targeted using three extraction methods: trypsin-enzymatic shaving, biotin-labeling and cell fractionation. The different subproteomes obtained were separated and analyzed by shotgun proteomics using high-performance liquid chromatography combined with tandem mass spectrometry (LC-OrbiTrap LTQVelos, ThermoFisher Scientific). A total of 141 (biotinylation), 98 (shaving) and 910 (fractionation) proteins were identified. Throughout the 920 unique proteins identified, many are connected to basic cell functions, but some are linked with thermoregulation. We observed some noteworthy protein abundance shifts associated with the major adaptation to cold mechanisms present in *L. monocytogenes*, namely: the role of ribosomes and the stressosome with a higher abundance of the general stress protein Ctc (Rl25) and the general stress transcription factor sigma B (σ^B), changes in cell fluidity and motility seen by higher levels of foldase protein PrsA2 and flagellin (FlaA), the uptake of osmolytes with a higher abundance of glycine betaine (GbuB) and carnitine transporters (OpucA), and the relevance of the overexpression of chaperone proteins such as cold shock proteins (CspLA and Dps). As for 37°C, we observed a significantly higher percentage of proteins associated with transcriptional or translational activity present in higher abundance upon comparison with the colder settings. These contrasts of protein expression throughout several conditions will enrich databases and help to model the regulatory circuitry that drives adaptation of *L. monocytogenes* to environments.

Keywords: *Listeria monocytogenes*, temperature adaptation, biofilm, subproteomes, shotgun proteomics

OPEN ACCESS

Edited by:
Maria Fiorella Mazzeo, Institute of Food Sciences, National Research Council (CNR-ISA), Italy

Reviewed by:
Bin Zhu, Virginia Commonwealth University, United States
Janet R. Donaldson, University of Southern Mississippi, United States

***Correspondence:**
Michel Hébraud
michel.hebraud@inra.fr

Specialty section:
This article was submitted to Food Microbiology, a section of the journal Frontiers in Nutrition

Received: *26 November 2018*
Accepted: *24 May 2019*
Published: *14 June 2019*

Citation:
Santos T, Viala D, Chambon C, Esbelin J and Hébraud M (2019) Listeria monocytogenes Biofilm Adaptation to Different Temperatures Seen Through Shotgun Proteomics. Front. Nutr. 6:89. doi: 10.3389/fnut.2019.00089

INTRODUCTION

The ready-to-eat (RTE) food sector is in constant expansion, offering a wide variety and number of products to consumers. Unfortunately, with that comes an increased chance of microbial contamination, as is the case of *Listeria monocytogenes* (1), a Gram-positive foodborne pathogen bacterium and the causative agent of the illness listeriosis (2). The European Food Safety Authority (EFSA) reported, in Europe, from 2008 to 2015, 37 food-borne outbreaks caused by *L. monocytogenes* that lead to 37 deaths (3). Just from June of 2018, 47 cases have been reported, and nine patients have died due to or with the infection (4). Even if the annual number of listeriosis cases comes behind other major foodborne pathogens (∼23,150 listeriosis cases were estimated worldwide in 2010), the mortality among infected individuals is very high, reaching levels up to 30% (5). This ubiquitous biofilm-forming bacterium is found throughout the environment, including soil, vegetation, and animals (6). The agroecosystems play a major role in the spread of such pathogens in the food chain through the production of contaminated raw products (7).

Bacterial cells are often found in complex communities, termed biofilms, that provide resources and protection to harsh environments (8). The trifactor, that includes pathogenic power, ability to form biofilm and ubiquity qualify *L. monocytogenes* as huge risk for human health. Remarkably, most stress-related reports were performed in planktonic cultures (9), even if there is a clear need to study the bacterial responses associated with stress tolerance and the features and benefits conferred by the sessile mode of growth to bacterial cells. One other *L. monocytogenes* attribute is its proteosurfaceome. Surface proteins are the link between bacteria and its environment, playing a significant role in communication, chemical sensing, stress resistance and balance of nutrients and toxins in the cell (10). *L. monocytogenes* genome sequence revealed 133 genes coding for surface proteins. Notably, the phylogenetically close but non-pathogenic *L. innocua* genome presented despair results regarding this protein family, unveiling for the first time its potential role in virulence (11). Even with the clear importance of proteomes and proteosurfaceome, protein studies have a higher level of complexity in comparison to DNA or RNA, mainly due to its variations in abundance, physicochemical features and subcellular localization (10). As for surface proteins, these are especially hard to work, since they require a carefully balanced hydrophilic and lipophilic environment (12). In regards to the role of surface proteins in virulence, the *L. monocytogenes* proteosurfaceome has been well explored (13), but the same cannot be said for its part in the adaptation and resistance to different environmental settings. Even scarcer are the studies in the sessile mode of growth, the predominant growth state in food workshops (14). To overcome the challenges associated with properly identifying surface-associated proteins, three different but complementary extraction methods were used in this study. First, the biotinylation method which is based on the treatment of intact cells with sulfo-NHS-SS-Biotin, to which the cell membrane is impermeable. This marker molecule reacts specifically with the ε-amino-group of lysine residues of surface-exposed proteins. Subsequently, labeled proteins can be separated from non-labeled proteins by affinity chromatography with neutravidin and then analyzed by liquid chromatography-tandem mass spectrometry (LC-MS/MS) (15). Secondly, the shaving method which consists on treating intact bacterial cells with proteases in an isotonic solution to promote the release exposed peptides (16). The third and final extraction method, the fractionation which allows to explore the proteome in separated subcellular fractions.

L. monocytogenes is an opportunistic bacterial pathogen that has the capacity to survive under extreme environmental conditions encountered in nature and in the food chain, such as high salt concentrations (17), large range of pH (18), desiccation (19, 20), and low temperatures (21). Maintaining the cold chain is an essential parameter throughout the processing and distribution of food, protecting it from the growth of mesophilic microorganisms and thus extending its shelflife. However, the temperatures used for refrigerated storage do not prevent the growth of psychrotrophic germs such as *L. monocytogenes* (22). Even if cold environments lead to a decrease in the rate of bacterial growth, they do not inhibit it completely (21). Temperature variation also has its role in virulence. As for many other bacterial pathogens, *L. monocytogenes* activates the expression of virulence genes at host body temperature (23). Throughout the years, multiple studies have been published exploring *Listeria*'s temperature adaptation, either through physicochemical tests (21, 24–29), genomic and transcriptomic methods (30–38), and also through metabolic and proteomic approaches (39–44). However, there is still a knowledge gap in the comparison of subproteomic changes to different temperatures, particularly in the biofilm mode of growth.

L. monocytogenes adaptation to low temperatures is one of its crucial attributes that supports *Listeria* persistence and dissemination in refrigerated products. This adaptation to cold temperatures renders the use of such physical setting insufficient for the control of *L. monocytogenes* presence in long-term storage under refrigeration products (45). *L. monocytogenes* is able to growth at temperatures as low as −0.4°C but also survive in freezing temperature such as −18°C (21, 46). In short, upon exposure to low temperatures, bacterial membranes become more rigid and the metabolic rate decreases. To overcome the hurdles imposed by a cold stress, bacteria have to increase the expression of genes involved in cell membrane function, production of cold shock proteins and multiple other molecular strategies to maintain homeostasis (47).

One of the major adaptative strategies is the induction of osmolyte and peptide transporters which will increase the amount of this molecules in the cytosol and maintain turgor pressure (48). The critical uptake of osmoprotectant molecules for *Listeria*'s adaptation to low temperature is made through auto transporters for compatible osmolytes and short oligopeptides (49). The main carnitine transporter, OpuC, encoded by the opuCABCD operon, was observed in high abundance in *Listeria* cells exposed to low temperatures (48, 50).

In cold environments, bacteria also duel with protein damage, particularly protein misfolding and aggregation. To counteract this damage, cells have at their disposal a network of molecular

chaperones that assist in maintaining proteins in their native states. A key role of chaperones is preventing protein aggregation (51). *L. monocytogenes* harbors three proteins from the CspA family (CspLA, CspLB, and CspD) and genome-wide expression studies showed a significant increase in expression of CspL at low temperatures (52).

L. monocytogenes response to the ever-changing environmental factors and stress conditions is linked to the activation of the alternative sigma factor sigma B (σ^B) that controls the general stress response (GSR). Functions of genes regulated by this transcriptional factor include a diversity of metabolic pathways, transport associated proteins, stress proteins, and other transcriptional factors (53). Particularly the osmolyte carnitine, which as mentioned before is transported via OpuC. The expression of this autotransporter is also regulated by σ^B. Other genes associated with cold stress resistance, *ltrC* (54) and *fri* (55), are also controlled by σ^B regulon. In short, even if a direct link between cryotolerance and σ^B has not yet been obtained, there are clear signs that this transcriptional factor has a role in *Listeria*'s adaptation to low temperature (47).

A combination with other mechanisms of cellular homeostasis maintenance, such as: control of membrane fluidity, gene expression events, protein folding and degradation, assimilation of carbon sources, oxidative stress response, and production of specific amino acids and lipids culminate in *Listeria*'s successful persistence in the cold temperatures of the food processing environment (56).

An understanding of how *L. monocytogenes* proteome changes in the biofilm mode of growth at different temperatures can help to unveil how it establishes and survives in the processing environment. To this point, this study aimed to explore the *Listeria monocytogenes* biofilm subproteomes and surface proteins under the influence of three temperatures: 10°C mimicking a common setting found in the food industry environment, 25°C as a baseline temperature, and 37°C as the human host setting.

MATERIALS AND METHODS

Strain and Biofilm Settings for Protein Extraction

The sequenced *L. monocytogenes* EGD-e strain, serogroup 1/2a, was used throughout this study (57). Routine pre-culturing and culturing were carried out in Tryptic Soy Broth (TSB, Difco, Fisher Scientific) at 25°C and 150 rpm. Bacterial growth was monitored by measuring the absorbance at 600 nm (OD_{600}). Precultured cells in stationary phase were used to inoculate cultures to obtain a final OD_{600} of 0.005. After 6 h of growth, cells were harvested by centrifugation (7,500 × g, 15 min) and resuspended in TSB diluted by 1:5 with sterile water in a volume equal to that of the supernatant collected, reaching an OD_{600} between 0.6 and 0.7. Seven milliliters of the bacterial suspension was poured on each stainless steel (SS) disk (38.5 cm^2), corresponding to an inoculation of 10^8 to 10^9 CFU/cm^2 (colony-forming unit/ square centimeter). The SS disks were then placed in a sterile Petri dish (55-mm diameter) and incubated at 25°C. Bacterial cells were allowed to adhere onto the disk for 3 h in static mode, before removing the medium to eliminate planktonic cells and add fresh medium. The disks incubation settings were dependent on the desired temperature (10, 25, or 37°C) and growth stage (early stage or mature biofilm) (**Supplementary Table 1**). To harvest the biofilm, the medium was removed and adherent cells were detached in 10 ml of Tryptone-salt (tryptone 0.1%, NaCl 0.85%, pH 7.0) by scraping the SS disk with a sterile spatula. Three biological replicates with 10 disks per each were used for every analyzed setting. Cell adhesion and population in biofilm were evaluated by cell enumeration. Serial dilutions were plated on Tryptic Soy Agar (TSA, Difco, Fisher Scientific) and incubated for 24 h at 37°C.

Protein Extraction Methods

The three extraction methods used in this study were biotin labeling, trypsin-enzymatic shaving and cell fractionation. All methods used were based on the protocol optimized for the extraction of surface exposed proteins developed by (58). In the biotinylation method, bacterial cells are treated with Sulfo-NHS-SS-Biotin, a marker molecule that is supposed to be membrane impermeable and interacts with surface exposed proteins. The shaving method consists of treating intact cells with proteases in an isotonic solution to release exposed peptides. The third method is the fairly well-established separation of membrane and cell wall components by cell fractionation. The technical details and result output of these extraction methods can be found in the Supporting information document and **Supplementary Figures 1, 2**.

Nano-LC-MS/MS and Bioinformatic Analysis

In order to obtain triplicate protein extracts, three independent biofilm cultures were used for each of the three methods described above. All samples, except those from the shaving method, were loaded onto SDS-PAGE gels to concentrate in one single band in the first few millimeters of the resolution gel. Excised bands were washed in 25 mM ammonium bicarbonate with 5% acetonitrile (ACN) for 30 min and twice in 25 mM ammonium bicarbonate with 50% ACN for 30 min. Reduction and alkylation reactions were performed with 10 mM DTT and 55 mM iodoacetamide solutions, respectively, and all bands were finally dehydrated with 100% ACN. The samples were hydrolyzed overnight at 37°C using 48 µl of a 25 mM NH_4HCO_3/12.5 ng.μl^{-1} trypsin solution (Promega) per band. Peptides were extracted from the gel bands in an ultrasonic field during 10 min with 38.4 µl of 100% acetonitrile representing 80% of digestion volume. Supernatants were transferred in eppendorf vials and dried using Speed Vac for 45 min and 40 µl of equilibration solution (H_2O/Trifluoroacetic Acid −99.95/0.05) was added.

All peptide mixtures were analyzed by nano-LC-MS/MS (Thermo Fisher Scientific) using an Ultimate 3000 system coupled to a LTQ Orbitrap Velos mass spectrometer (MS) with a nanoelectrospray ion source. For each sample, one microliter of peptide mixture was first preconcentrated on a C18 pre-column 5 cm length X 100 µm I.D. (Acclaim PepMap 100 C18, 5 µm, 100 A nanoViper), equilibrated with Trifluoroacetic Acid

0.05% in water at 30 μL/min. After 6 min of desalting and preconcentration, the pre-column was switched online with the analytical C18 column (75 μm inner diameter × 15 cm length; 2 μm, Acclaim PepMap 100 C18 Pepmap RSLC) equilibrated with 96 % solvent A (99.5 % H_2O, 0.5 % formic acid) and 4 % solvent B (80%ACN, 19.5% H_2O, 0.5% formic acid). Peptides were eluted according to their hydrophobicity at 300 nL/min flow rate using, respectively, a 4 to 52% gradient of solvent B for 31 min for biotin labeled and trypsin-enzymatic shaved fractions and a 4 to 40% gradient of solvent B for 56 min for cell fractions. Eluates were electrosprayed in positive-ion mode at 1.6 kV through a nanoelectrospray ion source heated to 250°C. The LTQ Orbitrap Velos MS was used in CID top 15 mode (i.e., 1 full scan MS and the 15 major peaks in the full scan were selected for MS/MS). The full scan MS was realized in the FTMS ion trap at a resolution of 60,000 (tolerance 10 ppm) and spectra were acquired with 1 microscan (m/z 400–1,400). For MS/MS, the following parameters were used: dynamic exclusion with 1 repeat counts, 20 s repeat duration and 80 s exclusion duration, isolation width for ion precursor was fixed at 1 m/z, single charged species were rejected, fragmentation used 37% normalized collision energy as the default activation of 0.25 and 10 ms activation time. For raw data processing, MS/MS ion search was performed with Mascot v2.5 for database search (http://www.matrixscience.com). The following parameters were considered for the searches: precursor mass tolerance of 10 ppm and fragment mass tolerance of 0.5 Da, a maximum of two missed cleavage sites of trypsin, carbamidomethylation (C) and oxidation (M) set as variable modifications. Protein identification was validated when at least two peptides originating from one protein showed statistically significant identity above Mascot scores 13 with a False Dicovery Rate of 1% (adjusted significance threshold $p < 0.05$). Ions score is $-10\log(P)$, where P is the probability that the observed match is a random event. Individual ions score >13 indicate identity or extensive homology. Interrogations were performed against a custom database containing distinct entries corresponding to raw protein sequences and the different predicted mature proteins of *L. monocytogenes* EGD-e (i.e., DB-Mature-LmoEGDe v2.0, 5838 sequences) based on putative cleavage sites of the SP (59). The subcellular location of identified proteins was determined with the rational secretomics based strategy for genomic and proteomic analyses developed by Renier et al. (60). For protein quantitation analysis, LC-Progenesis was used with Mascot v2.3 and the same identification parameters described above. Normalization was based on the LC-Progenesis process with Log10 ratio calculation and scalar estimation in log space. The statistical method used was the comparison in groups of two temperature settings in a "Between-subject design." For each temperature setting three biological replicas with three technical replicas were used. Venn diagrams were performed by the jvenn online tool (61). Functional category of proteins was based on the clusters of orthologous groups (COGs) via the eggNOG online framework (62). For proteins of interest, the average abundance from the 3 biological replicates in each condition was represented in a bar chart with standard deviation and statistical significance was tested by one-way ANOVA. Protein-protein association networks were made by the String database (63). Heat map displaying the normalized protein abundances were obtained via Xlstat (2018.5). Volcano plots were performed by the R software with the integration of the ggplot2 and ggrepel graphical packages for data analysis (64).

RESULTS

Overall Protein Identification Results

From all extraction methods and temperature settings, 920 unique proteins were identified (**Figure 1A**), representing a significant proportion of the *Listeria monocytogenes* proteome (32.2%) (57). The vast majority, 79% of the identified proteins, were characterized as cytoproteins, followed by membrane-associated proteins, extracellular and cell wall-associated proteins represent 17, 3, and 1%, respectively. Functional category of this set of proteins was based on the clusters of orthologous groups (COGs) (**Figure 1B**). Taking into consideration that the majority of identified proteins are from the cytoplasmic subcellular localization, it is not surprising that the functional category with the highest percentage of identified proteins is "Translation, ribosomal structure, and biogenesis" (13%), followed by "Transcription" and 'Cell wall/membrane/envelope biogenesis," 6% each. In addition, there are a multitude of normal molecular functions with a similar number of identified proteins. Although the genome sequence of *L. monocytogenes* was performed 18 years ago, a significant part of its proteome is still unannotated and lacks relevant information. This is reinforced by the large number of proteins whose function is not known here (192, 21%). In regards to the subproteomic extraction approach here implemented, we identified a high percentage of the *L. monocytogenes* intracellular proteome and also a significant amount of its surfaceome. In order to look for potential protein biomarkers of temperature adaptation, the protein identification data was structured by temperature and growth condition. The column chart in **Figure 4A** illustrates the stable and steady amount of identified proteins that were found in the different settings. The six branched Venn diagram shows that the vast majority of proteins were shared between all settings (531 proteins). Nevertheless, 122 proteins were identified only in one of the six settings in the study. Some of them with potential interest with temperature adaptation. In the case of early stage biofilm (Biof Es) grown at 10°C (**Figure 2A**), 40 uniquely identified proteins were registered, including the RNA polymerase sigma factor SigB, documented as regulating the expression of genes necessary for survival under environmental stress conditions (65). We have also identified three proteins of the flagellar motility system (Lmo0713, Lmo0714, and Lmo0697) and a DNA replication, recombination and repair associated protein (ssb2). Interestingly, OpuCA which is part of a documented carnitine solute auto transporter was identified only at the 10°C settings. Likewise, a unique heat shock protein involved in cell division and virulence (clpE) was identified in the 37°C condition at mature biofilm growth (66). The distribution of molecular functions in each setting follows the same trend as in the analysis of the whole protein identification data set seen previously (**Figure 2B**). A higher amount of proteins related to translational machinery was present and a similar amount of

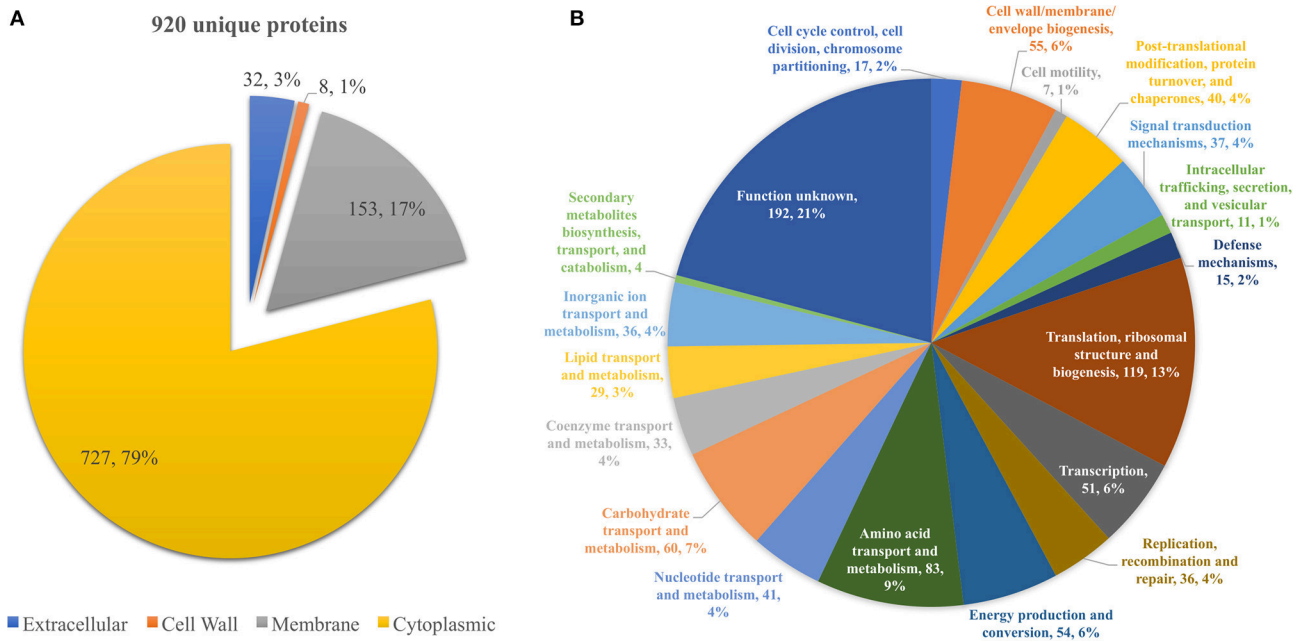

FIGURE 1 | (A) Pie chart showing the distribution of the 920 unique proteins identified by their predicted subcellular localization. **(B)** Pie chart illustrating the distribution of the 920 unique proteins identified by their predicted COG molecular function.

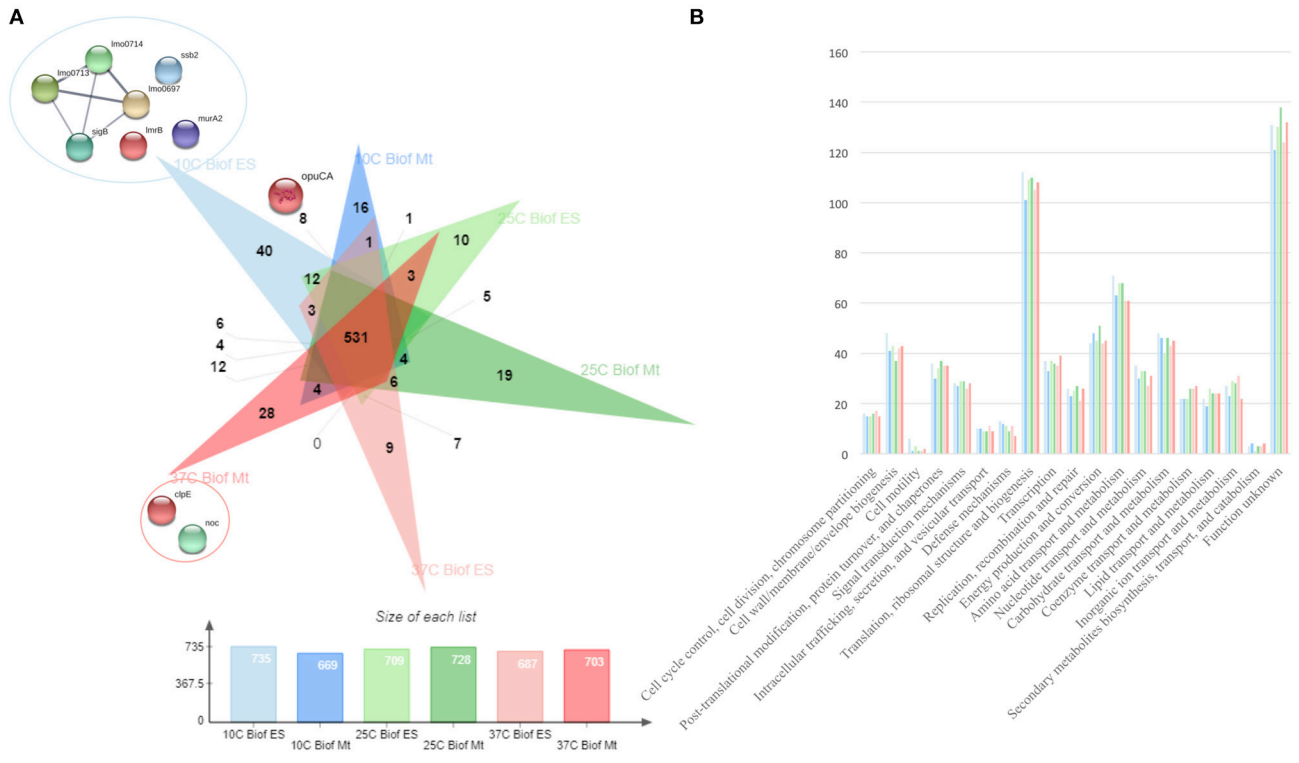

FIGURE 2 | (A) Venn diagram exposing the distribution of the 920 unique proteins identified by the three sets of temperature (10, 25, and 37°C) and two growth stages (ES—Early Stage biofilm and Mt—Mature biofilm) here analyzed. **(B)** Vertical bar chart showing the distribution of the 920 unique proteins identified by their predicted COG molecular function and separated by the conditions in study.

proteins identified for each molecular function across the six different settings. Though, a comparison of protein flows and changes that might have a relation to temperature adaptation can only be achieved by quantitation analysis.

Cross-Comparison of Temperature Adaptation Through Protein Quantitation

The quantitative analysis of protein abundance made by LC-Progenesis enabled the comparison of protein abundance through pairs of temperature settings, 10 vs. 37°C (**Figure 3**; **Supplementary Figure 4** and **Supplementary Table 2**), 10 vs. 25°C (**Figure 4**; **Supplementary Figure 5** and **Supplementary Table 3**), and 25 vs. 37°C (**Figure 5**; **Supplementary Figure 6** and **Supplementary Table 4**). In all cases, LC-Progenesis normalized abundances of the statistically significant identified proteins ($p < 0.05$) were used in order to compare the flows of proteins in each setting.

The Xlstat heat map in **Figure 3A** shows the relative abundance of each of the 380 statistically significant proteins retrieved when comparing the two growth phases at 10 and 37°C. This was the most contrasting comparison of growth temperatures, between a temperature mimicking the settings found in the food industry (10°C) and the temperature of the human host (37°C) to which *L. monocytogenes* expresses a higher level of virulence. A similar sum of proteins with higher abundance was detected in both temperatures, i.e., 196 at 10°C and 184 at 37°C. In some instances, there is a variance in one or more biological replicates regarding its abundance. The comparison of proteome changes can also be viewed by the shifts of protein abundance in regards to molecular function (**Figure 3B**). Regarding to transcriptional or translational activity, at 37°C, there are more proteins with higher abundance annotated with this molecular function. On the other hand, a higher percentage of proteins associated with a repair system mechanism were more abundant in the cold condition than at 37°C. The repair system molecular function is one of the categories COG (EggNOG orthologs). A temperature stress as 10°C induces DNA, RNA and protein damage in the cell (45). Some of the proteins that were more abundant at 10°C in this category have annotated involvement in solving protein aggregation and DNA damage (as for example DNAA chaperone protein, **Supplementary Table 2**). Similar result was seen for inorganic ion and amino acid transport associated proteins. A String map of protein interaction (**Supplementary Figure 4**) provides a graphical representation of the statistically significant proteins from this quantitation. Highlighted in blue are some of the proteins associated with the adaptation to harsh environmental conditions that were more abundant in the 10°C condition (**Supplementary Figure 4A**), as is the case of: the GTP-sensing transcriptional pleiotropic repressor CodY; the carnitine transporter OpuCA; the redox regulated molecular chaperone HslO, that protects both thermally unfolding and oxidatively damaged proteins from irreversible aggregation (67); the foldase protein PrsA2, which protects the cell by controlling the folding and stability of secreted proteins in stress conditions (68); the DNA protection during starvation Dps, that protects DNA from oxidative damage by sequestering intracellular Fe^{2+} ion and storing it in the form of Fe^{3+} oxyhydroxide mineral (56); the ATP-dependent zinc metalloprotease FtsH, which plays a role in the quality control of integral membrane proteins (69); the DNA ligase LigA, essential for DNA replication and repair of damaged DNA under stress conditions (70); the superoxide dismutase SodA, responsible for destroying superoxide anion radicals which are produced within the cells (71); and the ATP-dependent RNA helicases CshA and CshB, which are involved in RNA degradation during cold tolerance, motility and alcohol tolerance (72).

The large sum of ribosomal proteins at 37°C validates the higher percentage of proteins previously associated with translational function (**Supplementary Figure 4B**). Likewise, highlighted in red are some of the chaperone proteins associated with heat adaptation and the general stress response system, that were more abundant at 37°C. They participate actively in the response to hyperosmotic and heat shock by the recognition and processing of DNA lesions, and preventing the aggregation of stress-denatured proteins and by disaggregating proteins (73), such proteins as: DnaK, DnaJ, GroES, GroEL, GrpE, UvrA, and ClpB. The virulence capacity of *L. monocytogenes* is also here underlined by the higher abundance of the endopeptidase p60 (Iap) which is a major extracellular protein involved in the invasion of phagocytic cells (11).

The quantitation appraisal of the cold condition to the control temperature setting in this study (25°C) resulted in 336 statistically significant proteins (**Figure 4A**). We observed 26% more proteins with a higher abundance at 10°C than at 25°C. In agreement with the previous comparison, sessile cells at 10°C showed a lower percentage of abundance of proteins associated with translational machinery and, once again, a higher percentage of proteins with higher abundance involved in amino acid transport. The mapping of this set of proteins reveals the same trend as previous results with stress response associated proteins being more abundant in the cold condition (e.g., ClspL and SigB) (**Supplementary Figure 5**). The higher number of ribosomal proteins at 25°C confirms the tendency toward fewer translation mechanisms at the cold condition. Furthermore, chaperone proteins (DnaK, GroEL) and some virulence associated proteins, like the internalin A (InlA) which mediates the entry of *L. monocytogenes* into host intestinal epithelial cells (74) and chemotaxis CheA involved in the transmission of sensory signals from the chemoreceptors to the flagellar motors in intracellular movement (75), were also present in lower levels at the colder setting.

The last quantitative comparison of protein abundance was between 25 and 37°C, which gave the lowest amount of statistically significant proteins among the three comparisons (233 proteins, **Figure 5A**). A similar number of proteins with higher abundance was found under both conditions, probably related to the proximity of this two temperature settings. However, changes in proteome abundance can be retrieved upon analysis of molecular functional categories (**Figure 5B**). As in the previous two analyses, the highest temperature showed a greater number of proteins associated with translation. At 37°C, there is a higher amount of proteins

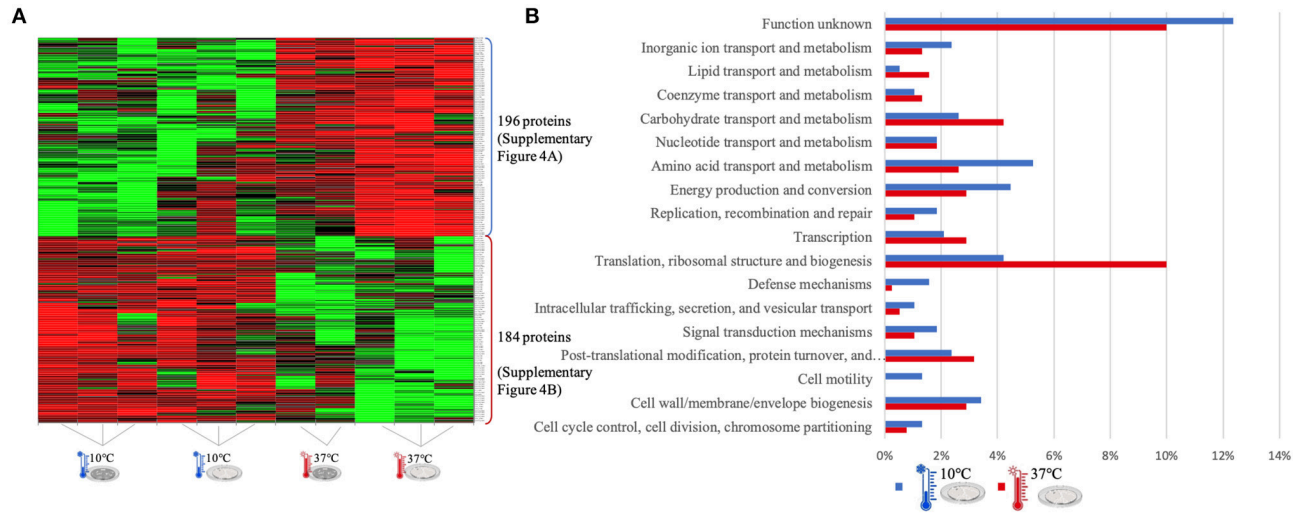

FIGURE 3 | LC-Progenesis ANOVA comparing the biofilm at 10 and at 37°C (**Supplementary Table 2**) The two biofilm stages are represented either by dark SS (stainless still) disks for early stage or cell filled gray SS disks for mature biofilm. **(A)** Heat map illustrating the abundance of each of the 380 statistical significantly different proteins obtained in this comparison. **(B)** Horizontal bar chart showing the percentage of proteins with higher abundance in each temperature setting by their predicted COG molecular function.

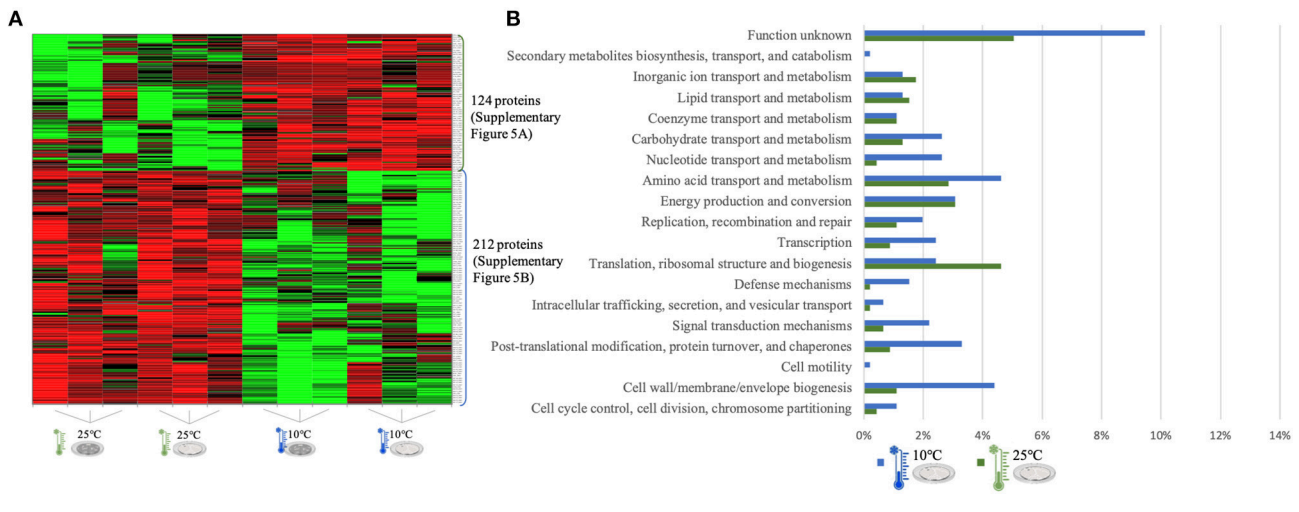

FIGURE 4 | LC-Progenesis ANOVA comparing the biofilm at 10 and at 25°C (**Supplementary Table 3**). The two biofilm stages are represented either by dark SS (stainless still) disks for early stage or cell filled gray SS disks for mature biofilm. **(A)** Heat map illustrating the abundance of each of the 336 statistical significantly different proteins obtained in this comparison. **(B)** Horizontal bar chart showing the percentage of proteins with higher abundance in each temperature setting by their predicted COG molecular function.

with higher abundance related to carbohydrate metabolism and also coenzyme transport. The flagella motor system was more abundant at 25°C (**Supplementary Figure 6A**). As in the first quantitative appraisal (10 vs. 37°C), the ribosomal, chaperone and virulence associated proteins were more abundant at 37°C (**Supplementary Figure 4B**).

Proteins of Interest for Temperature Adaptation

For an additional understanding of the *L. monocytogenes* proteome changes under different conditions, it was important to have a look at sets of proteins of interest and also outliers that could be potential biomarkers for the adaptation to this environmental and food industry setting. **Figures 6**, **7** represent the average abundances of some of these proteins of interest between the two extreme poles of temperatures and across the two stages of biofilm growth (early stage, represented by dark SS disks, and mature biofilm, represented by cell filled SS disks). For each protein, average abundances were obtained from the three biological replicates in each condition. In the case of the DNA protection to starvation protein (Dps), a higher abundance was obtained at 10°C, particularly in the mature biofilm stage.

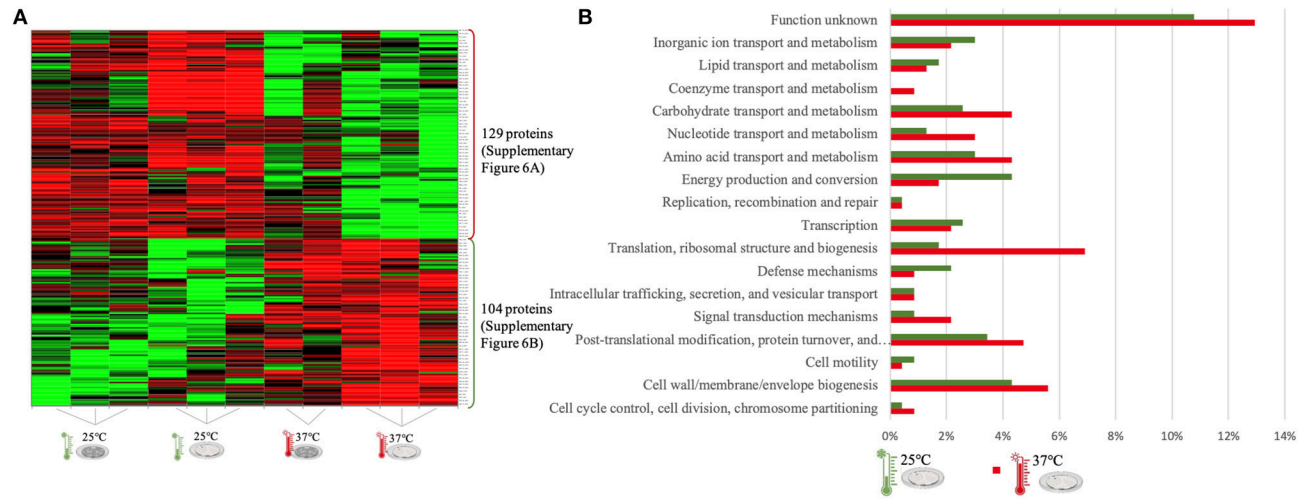

FIGURE 5 | LC-Progenesis ANOVA comparing the biofilm at 25 and at 37°C (**Supplementary Table 4**). The two biofilm stages are represented either by dark SS (stainless still) disks for early stage or cell filled gray SS disks for mature biofilm. **(A)** Heat map illustrating the abundance of each of the 233 statistical significantly different proteins obtained in this comparison. **(B)** Horizontal bar chart showing the percentage of proteins with higher abundance in each temperature setting by their predicted COG molecular function.

Dps is important for full resistance to heat and cold shocks and is essential for full virulence of this bacterium (56). The abundance of other three cold adaptation associated proteins was also greater at 10°C than at 37°C (**Figure 6**), namely: the cold shock protein (CspLA); ABC transporter OpuCA; and Kat, a catalase suggested to be one of the contributors to the ability of *L. monocytogenes* to grow at low temperatures (76). The cell motility associated proteins were more abundant at temperatures under 37°C, as it is the case of flagellin (FlaA) and flagellar hook (FlgE) with a higher abundance at 10°C, particularly in the early stage biofilm (**Figure 7**). A different tendency was seen for the cellular trafficking proteins, the abundance of these proteins were registered with higher levels at 37°C. Heat adaptation associated protein chaperones were detected, in most instances, with higher abundance at 37°C, particularly in the mature biofilm. To further retrieve protein drifts and outliers, volcano plots were generated from the three groups of temperature comparison, with cut-offs at p-value = 0.05 (log10(p-value) = 1.30103) and fold change (FC) = 2 (log2(fold change) = 1). Each of the quantitative comparisons was represented in a different volcano plot, 10 vs. 37°C (**Figure 8A**), 10 vs. 25°C (**Figure 8B**), and 25 vs. 37°C (**Figure 8C**). A total of 139, 68, and 58 proteins respected these cut-offs criteria, respectively. In all three plots, the top 50 proteins with higher fold change were marked with the color to which they presented higher mean condition (blue for 10°C, green for 25°C, and red for 37°C). In the 10 vs. 37°C plot, the proteins with the highest fold change at 10°C are associated with metabolism and amino acid transport. In the 10°C highlighted set of proteins are also included stress adaptation proteins, such as OpuCA (Q7AP65_LISMO) and CspLA (CSPA_LISMO), and cell motility associated proteins (Q8Y954_LISMO, Lmo0680). In the pool of proteins with high fold change at 37°C, there are proteins associated with virulence as LmaA (Q7AP93_LISMO), LmaB (Q7AP94_LISMO), CspLB (CSPB_LISMO) and proteins involved in heat adaptation (Lmo1580, Q8Y6V1_LISMO, and CcpA, Q8Y6T3_LISMO). In regards to the evaluation between 10 and 25°C, transport associated proteins were observed with the highest fold change in the cold condition. This was particularly the case for amino acid transporter such as multiple ATP-binding cassette transporter (ABC) OpuCA, (Q7AP65_LISMO), Lmo0538 (Q8Y9J0_LISMO), and SerC (SERC_LISMO). At 25°C, most of proteins had a connection with energy production and translation machinery. At the level of the 25 vs. 37°C comparison, the majority of proteins were associated with translation or carbohydrate functions. To note the presence of two virulence associated proteins with FC>2 at 37°C, Iap (P60_LISMO) and UvrC (UVRC_LISMO).

DISCUSSION

Listeria monocytogenes is the causative agent of listeriosis, a highly fatal disease to fetuses, newborns, infants, pregnant women, elderly and immunocompromised individuals (77). Invasive listeriosis is considered the leading cause of death from foodborne infections in industrialized countries. Despite the application of the food safety criteria (FSC) for *L. monocytogenes* in RTE foods from 2006 onwards, a statistically significant increase in listeriosis cases has been reported in the European Union between 2009 and 2013 (3, 78).

The cleaning and disinfection of surfaces and materials in food industries is difficult to achieve due to *L. monocytogenes* capacity to survive under harsh condition, such as a wide pH range (79), desiccated environments (9, 20), and low temperatures (80). Since *L. monocytogenes* is a psychrotrophic microorganism able to multiply in food stored under refrigerated temperatures, a low contamination number present in RTE products can grow to a level which threatens consumer health (81). At low temperatures, *Listeria* faces multiple molecular constraints such as increased

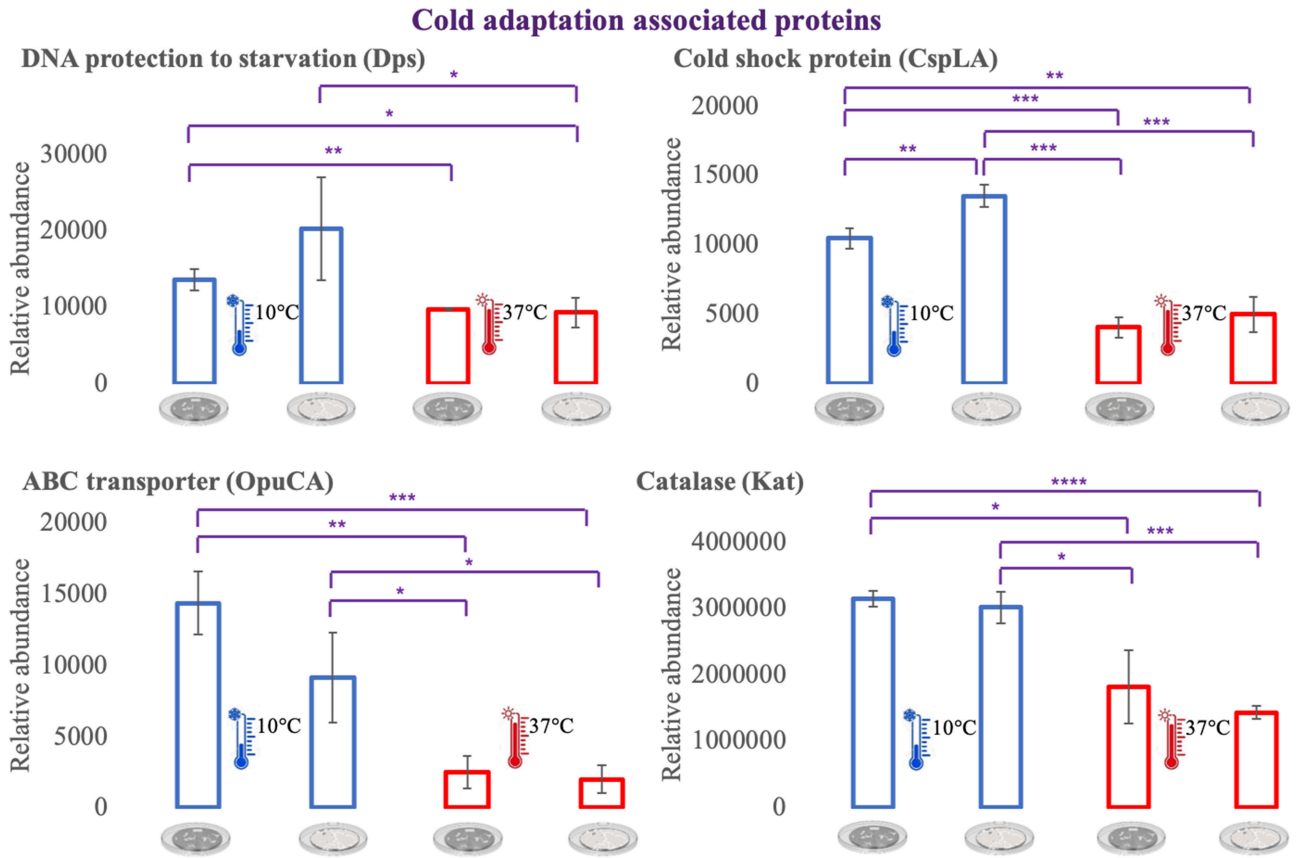

FIGURE 6 | Vertical bar charts showing the average abundance of some cold adaptation associated proteins by the different condition in analysis. Statistical significance was tested by one-way ANOVA (*$P \leq 0.05$; **$P \leq 0.01$; ***$P \leq 0.00$; ****$P \leq 0.0001$). The two biofilm stages are represented either by dark SS (stainless still) disks for early stage or cell filled gray SS disks for mature biofilm.

membrane rigidity, amino acid starvation, oxidative stress, aberrant protein synthesis, cell surface remodeling, reduced protein and enzyme activity, slow transport, and nutrient uptake processes (56, 82). *L. monocytogenes* response mechanisms to these hurdles has been extensively studied by transcriptomic approaches. Contrasting are the few studies to the changes at the proteome level that allow *Listeria* to survive at refrigeration temperatures (41, 43, 83), and none performed in a biofilm mode of growth. The present study sought to investigate the influence of three temperatures in the proteome changes of *L. monocytogenes* grown in the biofilm mode of growth. In the next subsections, we overview some noteworthy protein abundance shifts associated with the major adaptation to cold mechanisms present in *L. monocytogenes*, namely: the role of ribosomes and the stressosome, changes in cell fluidity and motility, the uptake of osmolytes, and the relevance of the overexpression of chaperone proteins such as cold shock proteins. Based on the proteomic data obtained in this study it is highly unlikely that a set of surface proteins play a unique role in the adaptation to the different temperatures. Hence, adaptation to low temperature growth is a complex response involving many aspects of the cell molecular biology and biochemistry (45). The typical molecular mechanisms of cold stress adaptation referenced in bacteria include: overexpression of stability mechanisms by the modulation of nucleic acid structures, maintenance of structural integrity in cell membranes, uptake of compatible solutes, production of various cold stress proteins, including cold shock proteins (Csps), and nonspecific stress response mechanisms.

Cold Stress Adaptation and the Role of Ribosomes

One of the first side effects of exposure to low temperatures is the compromise of ribosomal structural stability and this deterioration causes a general reduction in the bacteria's protein synthesis capacity (45). In this study, the majority of ribosomal proteins were less abundant in the cold condition, and in some instances, ribosomal proteins had a high fold change in the warmer setting (**Figure 8**). The 50S ribosomal proteins (Rl) are referenced as the first cold stress sensors in microbes, as is the case of Rl11. The former is essential for the activation of sigma B (σ^B) transcription factor in *Bacillus subitilis* (84), the general stress response transcriptional factor that controls the expression of dozens of stress adaptation related genes. We observed an increased level of Rl11 protein at 10°C, as well as the initiation factor IF2 which is implicated in the formation of 30S preinitiation complex, suggesting a role in ribosome assembling

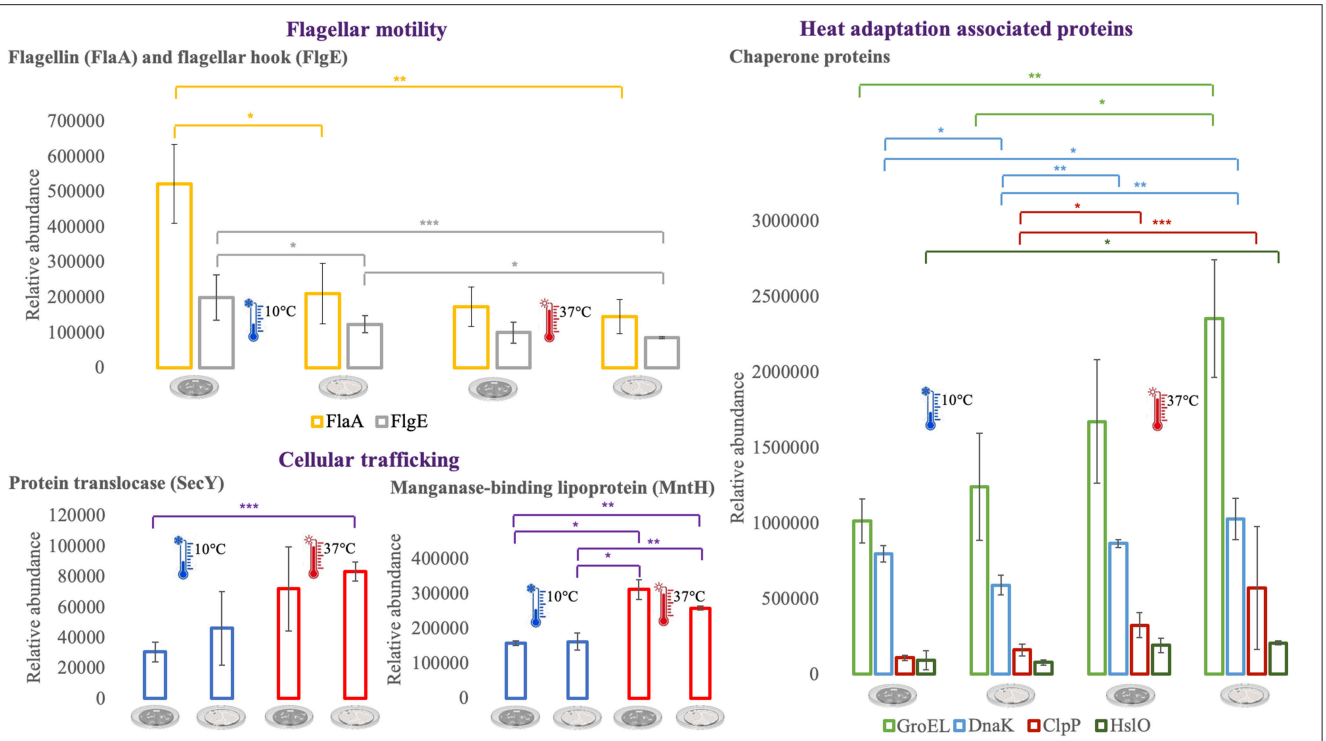

FIGURE 7 | Vertical bar charts showing the average abundance of flagellar, cellular trafficking and heat adaptation associated proteins by the different condition in analysis. Statistical significance was tested by one-way ANOVA (*$P \leq 0.05$; **$P \leq 0.01$; ***$P \leq 0.00$). The two biofilm stages are represented either by dark SS (stainless still) disks for early stage or cell filled gray SS disks for mature biofilm.

(41). The general stress protein Ctc (Rl25), was here more abundant at 10°C and the same was seen in *L. monocytogenes* upon exposure to a salt condition (85). Concerning σ^B, this general stress transcription factor was more abundant at 10°C than at the room temperature (**Supplementary Table 3**). The σ^B enables *Listeria* pathogenicity in two different ways. First, by controlling the expression of genes that enhance the survival during food industry pipeline settings. Second, σ^B plays a role upon infection by indirectly regulating PrfA, the main virulence regulator (86, 87). This transcriptional factor has also been associated with the efficient accumulation of betaine and carnitine as cryoprotectants (88), which will be further discussed in the next sections. On the contrary, it has been suggested that σ^B does not, in fact, play a pivotal role during cold adaptation in *L. monocytogenes*. So, it seems to contribute to the adaptation in a growth phase-dependent manner, particularly in the early stages of growth (89). This result was not seen here, since σ^B was more abundant in the mature biofilm than in the early stage one. The reasoning behind this can be linked with the different modes of growth applied in the two studies and the fact that σ^B also has a determinant role in biofilm formation (90).

Cell Membrane Fluidity, Chemotaxis, and Their Involvement in Cold Adaptation

Changes in the cell membrane fluidity and surface proteins are part of the bacterial adaptation to cold stress (30). For example, Lmo0624 has a role in lipid metabolism and higher transcripts of this gene were reported at 4°C (91). In agreement with this result we also observed Lmo0624 (Q8Y9A8) more abundant in the cold condition with one of the highest fold changes (FC = 9.27) (**Figure 8A**). The foldase protein PrsA2, here found more abundant in the colder setting (FC = 2.41, **Supplementary Table 2**) is a member of a family of membrane-associated lipoproteins that play a role in the folding and stability of secreted proteins as they pass the bacterial membrane. PrsA2 contributes to the integrity of the *L. monocytogenes* cell wall as well as swimming motility and bacterial resistance to different stresses (92). Cell stability and bacterial attachment to surfaces are influenced not only by cell surface properties but also by the presence of surface appendages, such as flagella (93). All the cell motility associated proteins identified in this study, namely flagellin (FlaA), flagellar hooks FlgK and FlgE, Lmo0689 (Q8Y948), Flha (Lmo0680, Q8Y954), MotA (Lmo0685, Q7AP82) were more abundant at 10 and 25°C when compared with the *in vivo* setting (37°C). FlaA is the bacterial flagella main protein (94) and *L. monocytogenes* strains are motile and flagellated below 30°C (95), and typically not motile at 37°C (96). However, the role of the flagellum in biofilm formation is controversial. There are observations that give it an important role in biofilm formation (97), and in other reports strains with this gene deleted had improved sessile development (98). In regards to the putative role of the flagella, it was described to be required for the initial cell attachment phase by overcoming the van der Waals forces (93). We have observed several motility associated proteins with

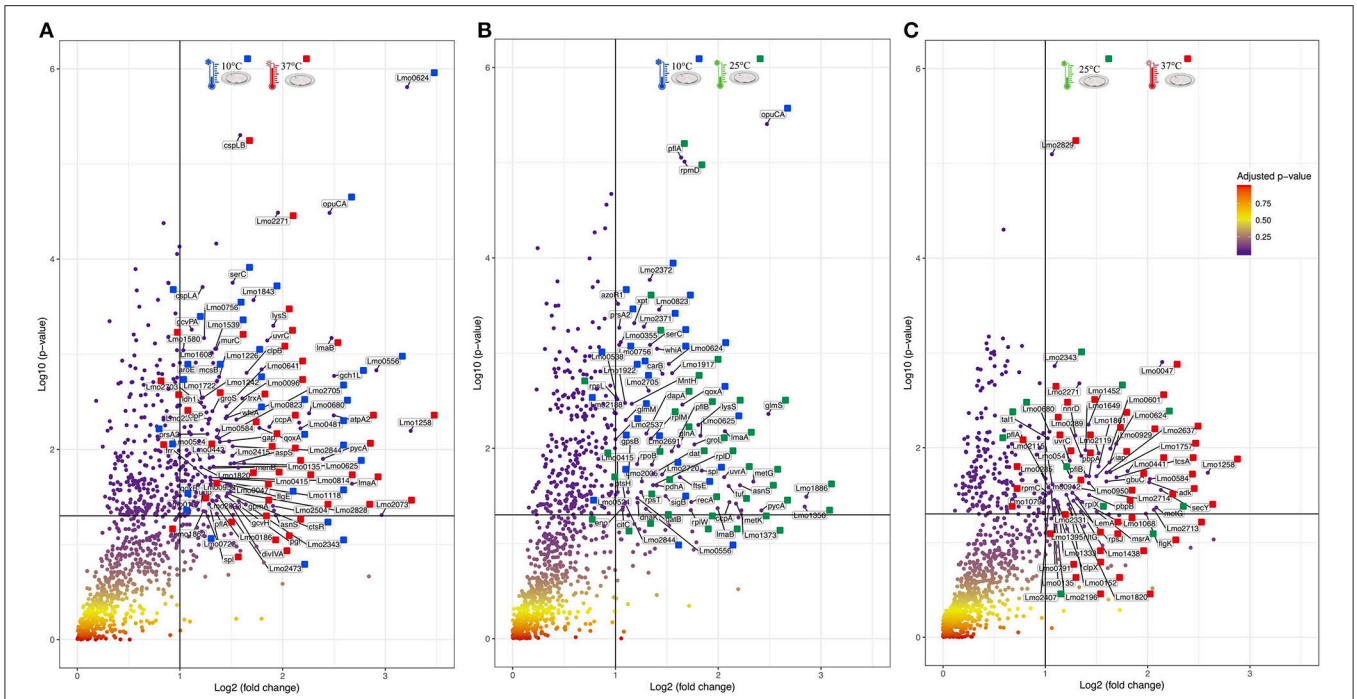

FIGURE 8 | Volcano plots representing the distribution of the identified proteins taking into account their fold change and *p*-value, Cut-off are represented by black lines at fold change two [Log_2(fold change) = 1] and *p*-value 0,05 [Log_{10}(*p*-value) = 1.30103]. The top 50 proteins with highest fold change are marked with their respective color that represent in which setting they were more abundant (blue for 10°C, green for 25°C, and red for 37°C). **(A)** Volcano plot for the comparison between 10 and 37°C. **(B)** Volcano plot for the comparison between 10 and 25°C. **(C)** Volcano plot for the comparison between 25 and 37°C.

significant abundance shifts that support the hypothesis that motile flagellum is needed for an optimal cold stress response in *L. monocytogenes*. Moreover, we have detected that all these cell motility proteins were more abundant in the early stage of biofilm. A flagellum-associated operon (consisting of Lmo0675 to Lmo0689) has been previously retrieved in high transcript levels from *L. monocytogenes* exposed to 4°C in log phase (91). Lmo0689 was also observed in this study to be more abundant at 10°C and in the early stage biofilm. Similarly, FlhA and MotA play a role in the cold tolerance of *L. monocytogenes* (99). This is consistent with our observation that MotA was one of the proteins with the highest fold change (FC = 4.78) in the 10 vs. 37°C comparison. Likewise, the ability to modulate membrane fatty acid composition and improve membrane fluidity is a crucial step for temperature adaptation (100). FabH, which was here more abundant at 10°C, is connected with the increased formation of anteiso branched-chain fatty acids during cold temperature adaptation, which ultimately is responsible for the increase in membrane fluidity (101).

The Crucial Role of Cryoprotective Solutes

The uptake of compatible solutes/osmolytes is one of the key steps for the survival of bacteria in stress conditions. Osmolytes are low-molecular weight organic compounds that are stored in high intracellular concentrations with minimal effects on the normal functioning of the cell. At low temperatures, cryoprotective solutes act through stabilization of enzymatic functions and the cell membrane lipid bilayer (102). Organic compounds such as glycine betaine and carnitine help to relieve turgor pressure, in this manner they have an essential role in the survival of *Listeria* under elevated osmolarity and cold settings (25, 50). In the food industry, *L. monocytogenes* has access to these solutes from carnitine rich meat and dairy products, and glycine betaine from plants and shellfish (54). There are three solute import systems known to operate in *L. monocytogenes*: glycine betaine porter I (BetL), glycine betaine porter II (Gbu), and the carnitine transporter OpuC (25). Here, we have identified GbuB (Q7AP75) and OpuCA (Q7AP65). The non-identification of a BetL can be reasoned with the described more pronounced role of Gbu and OpuC as preferential cryoprotection systems in *L. monocytogenes* (49). Regarding the cryoprotective impact between Gbu and OpuC, a report comparing their role concluded that carnitine uptake at low temperatures is higher than betaine after cold temperature (48). Supporting this result, GbuB (Q7AP75) and OpuCA (Q7AP65) were in this study more abundant at 10°C. Interestingly, OpuCA had one of the highest fold changes (FC = 4.91, **Figure 8A**; FC = 5.56, **Figure 8B**), one more hint that cryoprotectants are essential for *Listeria* rapid response to the conditions typically found in food preservation.

Cold Shock Proteins and Other Proteins Potential Involved in Temperature Adaptation

A second key point into the adaptation of a microbe to a cold stress is the production of various stress-related proteins,

including cold shock proteins (Csps) (31). Our results showed a higher abundance of the cold shock protein CspLA (CSPA) at 10°C and with high fold change (FC = 2.33, **Figure 8A**). CspA deletion mutants have showed to abolish *L. monocytogenes* growth at refrigeration temperatures (31). However, there are also Csps downregulated at low temperature, pointing to their potential role under conditions other than cold growth (91). Similar result was here obtained with the cold shock protein CspLB (CSPB) more abundant in the warmer condition (FC = 3, **Figure 8A**). This infers that CspLB also have a function during normal growth (40).

Various other cold response associated proteins were identified in this study. The GTP-sensing transcriptional pleiotropic repressor CodY was more abundant at 10°C. CodY has a role in the regulation of relevant genes implicated in *Listeria* growth at low temperature (91). *L. monocytogenes* CodY also has a recognized role in virulence (65), in this matter, from the 16 proteins identified here encoded by CodY regulated genes there are cases of stress adaptation associated proteins (Dps and SerC—more abundant at 10°C) and virulence-associated proteins (LmaA, LmaB, GroES, GroEL, and ClpB—more abundant at 37°C) (**Supplementary Table 2**). DNA protection during starvation protein (Dps or Fri) is a 18 kDa *L. monocytogenes* major cold shock protein that is required for iron storage and protection against reactive oxygen species (55, 103). This major protein for low-temperature adaptation was here detected in high levels at 10°C. Similar result was obtained for enolase (Eno) (**Supplementary Table 2**), which has been found to be upregulated at low temperatures by others (43). Eno does not possess an N-terminal signal peptide, but it was found before to be exposed on the bacterial cell surface or extracellularly, thus meaning there should be an uncharacterized secretion pathway (94). Further proteins connected to cold adaptation mechanisms in *L. monocytogenes* were more abundant at 10°C, such as folding catalysts Lmo1583 and Lmo2376, that have been detected before in increased levels at 4°C (41). Proteins with a role in protection from reactive oxygen species (superoxide dismutase-Sod, catalase-Cat, Lmo0640, and Lmo1967) and in iron metabolism (Lmo2415-SufD and Lmo2411-SufB) were also more abundant in the cold condition. SufD and SufB are part of the Suf system, which in *Escherichia coli* is activated to enable the increase of *de novo* Fe–S assembly, maintaining Fe–S cluster biosynthesis under oxidative stress conditions (104). Two-component-system histidine kinases (TCSs) are among the major systems that aid bacteria in overcoming many of arduous stress factors encountered in nature and during food processing environment (28). LisK which is part of the TCSs was here more abundant at 10°C. As for RNA chaperones, like DEAD-box RNA helicases, they act by resolving secondary structures in mRNA that can be developed in a cell subjected to cold (105). The three putative DEAD-box RNA helicase genes (Lmo0866, Lmo1450, and Lmo1722) are required for cold tolerance and motility in *L. monocytogenes* (37, 106). We have observed the three helicases with higher abundances at 10°C. The overall protein abundance data obtained also showed some nonspecific stress response mechanisms or shared responses to other stress conditions. Such a case is the amino acid, lipid and carbohydrate transport which have at least a double role in the protection against cold temperatures and salt exposure (83). In respect to the proteins associated with the amino acid transport and metabolism, the majority of them was more abundant in the cold condition (66.7% in 10 vs. 37°C, **Figure 3B**; 61.8% 10 vs. 25°C, **Figure 4B**). This suggests that the cells endure starvation in certain amino acids during a cold condition, counterbalancing this lack with the increase expression of such transportation systems. Moreover, some amino acid biosynthetic enzymes were also more abundant at 10°C, for example Cysteine tRNA ligase (CysS) and Shikimate dehydrogenase (AroE, Q8Y733), indicating that the stressed cell responds by increasing the production of enzymes needed to upturn the production of scarce amino acids (45, 82). Additionally, six proteins with amino acid transport presented a high fold change, including AroE with FC = 2.23.

Abundance Flows of Virulence-Associated Proteins

The comparison made between a food processing low temperature setting and the *in vivo* temperature enabled an outlook over the changes in heat shock proteins (HSP) and proteins typically associated with virulence. HSPs main function is to repair damage to proteins via chaperone activity, for example DnaK, GroEL, GroES, GrpE, ClpB, and HtpG (27). One might assume their importance in resolving protein damage from cold stress, however this class of stress response genes are usually less transcribed at lower temperatures (91). In this study, the majority of these chaperone proteins were more abundant in the warmer condition, particularly at 37°C. This is also connected to the fact that *L. monocytogenes* is a psychrotroph microorganism and growth in temperatures above 35°C may result in the induction of a stress response (107). Moreover, chaperone proteins are also required for *L. monocytogenes* maximum virulence potential (82). To approach the topic of virulence-associated proteins, it is pertinent to look into Lmo0443, a potential factor for low virulence. Lmo0443 is overexpressed in less virulent *L. monocytogenes* strains and underexpressed in more virulent ones (108). In this *L. monocytogenes* EGD-e strain, Lmo0443 had higher abundance at 37°C, consistent with its lower pathogenicity when compared with EGD or 10403S *Listeria* strains (109). In the same trend of results, internalins are essential for *Listeria* pathogenicity (110). Only one internalin was detected in this study. InlA which was observed with higher abundance at 25°C (10 vs. 25°C comparison, **Supplementary Table 3**). Internalins have a diversity of functions amongst the Listeriae, InlA in particular is documented as being crucial for *Listeria* capacity to invade human epithelial cell lines (111). The crucial topological factor (DivIVA) required for completion of cell division in *L. monocytogenes* and associated with host cell invasion was more abundant in the 37°C condition with high fold change (FC = 2.84) (13). Lastly, the *agr* locus of *L. monocytogenes* is recognized to be important in bacterial virulence. The open reading frame *lmo0047* that proceeds the *agrB* encodes a protein of unknown function (112), that was here more abundant at 37°C and with

high fold change (FC = 4.41), suggesting a potential role in a virulence mechanism.

Consistent with previous studies (30, 32, 35, 37, 38, 41, 43, 44, 56, 82, 83, 85, 91), we have observed a significant remodeling of protein abundance as a function of temperature, highlighting once again the predominant influence of this environmental parameter on protein expression and the need for the bacteria to adapt to it and maintain its homeostasis.

CONCLUSION

Listeria monocytogenes overcomes various kinds of stress, including the low temperatures present in food processing and storage. Cold stress adaptation mechanisms are therefore an essential skill of *Listeria*, enabling it to survive and proliferate to reach minimal infectious levels on refrigerated foods. In this aspect, the cold conditions in food plants may, in fact, be selecting for *L. monocytogenes* subtypes with the appropriate adaptive physiological attributes that lead to efficient survival and spread during food handling (45). Analogous approaches in the future will aid in highlighting additional potential target genes of cold stress resistance in *Listeria monocytogenes*. It will be of particular interest to make a direct comparison between this biofilm proteomic data and similar planktonic approaches. Thus, enabling the study of possible molecular cold response and biofilm targets that currently await additional assessment.

AUTHOR CONTRIBUTIONS

TS and MH designed the study. TS wrote the manuscript. TS, CC, DV, and JE performed the experiments. TS, DV, and MH analyzed the data. All authors reviewed the manuscript.

FUNDING

TS was seconded by List_MAPS project, which received funding from the European Union's Horizon 2020 research and Innovation programme under the Marie-Slodowska Curie grant agreement n°641984. JE was seconded from the Agence Nationale de la Recherche (ANR) (France) as part of an EcoSec contract.

SUPPLEMENTARY MATERIAL

The Supplementary Material for this article can be found online at: https://www.frontiersin.org/articles/10.3389/fnut.2019.00089/full#supplementary-material

REFERENCES

1. Malley TJ, Butts J, Wiedmann M. Seek and destroy process: *Listeria monocytogenes* process controls in the ready-to-eat meat and poultry industry. *J Food Prot.* (2015) 78:436–45. doi: 10.4315/0362-028X.JFP-13-507
2. Renier S, Hebraud M, Desvaux M. Molecular biology of surface colonization by *Listeria monocytogenes*: an additional facet of an opportunistic Gram-positive foodborne pathogen. *Environ Microbiol.* (2011) 13:835–50. doi: 10.1111/j.1462-2920.2010.02378.x
3. Ricci A, Allende A, Bolton D, Chemaly M, Davies R, Fernandez PS, et al. *Listeria Monocytogenes Contamination of Ready-to-Eat Foods and the Risk for Human Health in the EU*. Parma: European Food Safety Authority (2018).
4. EFSA. *Multi-Country Outbreak of Listeria monocytogenes Serogroup IVb, Multi-Locus Sequence Type 6, Infections Linked to Frozen Corn and Possibly to Other Frozen Vegetables – First Update*. Parma: European Food Safety Authority (2018).
5. De Noordhout CM, Devleesschauwer B, Angulo FJ, Verbeke G, Haagsma J, Kirk M, et al. The global burden of listeriosis: a systematic review and meta-analysis. *Lancet Infect Dis.* (2014) 14:1073–82. doi: 10.1016/S1473-3099(14)70870-9
6. Allerberger F, Wagner M. Listeriosis: a resurgent foodborne infection. *Clin Microbiol Infect.* (2010) 16:16–23. doi: 10.1111/j.1469-0691.2009.03109.x
7. Vivant AL, Garmyn D, Piveteau P. *Listeria monocytogenes*, a down-to-earth pathogen. *Front Cell Infect Microbiol.* (2013) 3:87. doi: 10.3389/fcimb.2013.00087
8. Vogeleer P, Tremblay YD, Mafu AA, Jacques M, Harel J. Life on the outside: role of biofilms in environmental persistence of Shiga-toxin producing *Escherichia coli*. *Front Microbiol.* (2014) 5:317. doi: 10.3389/fmicb.2014.00317
9. Esbelin J, Santos T, Hebraud M. Desiccation: an environmental and food industry stress that bacteria commonly face. *Food Microbiol.* (2018) 69:82–8. doi: 10.1016/j.fm.2017.07.017
10. Cordwell SJ. Technologies for bacterial surface proteomics. *Curr Opin Microbiol.* (2006) 9:320–9. doi: 10.1016/j.mib.2006.04.008
11. Cabanes D, Dehoux P, Dussurget O, Frangeul L, Cossart P. Surface proteins and the pathogenic potential of *Listeria monocytogenes*. *Trends Microbiol.* (2002) 10:238–45. doi: 10.1016/S0966-842X(02)02342-9
12. Rabilloud T. Membrane proteins and proteomics: love is possible, but so difficult. *Electrophoresis.* (2009) 30(Suppl. 1):S174–80. doi: 10.1002/elps.200900050
13. Carvalho F, Sousa S, Cabanes D. How *Listeria monocytogenes* organizes its surface for virulence. *Front Cell Infect Microbiol.* (2014) 4:48. doi: 10.3389/fcimb.2014.00048
14. Giaouris E, Heir E, Hebraud M, Chorianopoulos N, Langsrud S, Moretro T, et al. Attachment and biofilm formation by foodborne bacteria in meat processing environments: causes, implications, role of bacterial interactions and control by alternative novel methods. *Meat Sci.* (2014) 97:298–309. doi: 10.1016/j.meatsci.2013.05.023
15. Hempel K, Pane-Farre J, Otto A, Sievers S, Hecker M, Becher D. Quantitative cell surface proteome profiling for SigB-dependent protein expression in the human pathogen *Staphylococcus aureus* via biotinylation approach. *J Proteome Res.* (2010) 9:1579–90. doi: 10.1021/pr901143a
16. Tiong HK, Hartson S, Muriana PM. Comparison of five methods for direct extraction of surface proteins from *Listeria monocytogenes* for proteomic analysis by orbitrap mass spectrometry. *J Microbiol Methods.* (2015) 110:54–60. doi: 10.1016/j.mimet.2015.01.004
17. Cole MB, Jones MV, Holyoak C. The effect of pH, salt concentration and temperature on the survival and growth of *Listeria monocytogenes*. *J Appl Bacteriol.* (1990) 69:63–72. doi: 10.1111/j.1365-2672.1990.tb02912.x
18. Davis MJ, Coote PJ, O'byrne CP. Acid tolerance in *Listeria monocytogenes*: the adaptive acid tolerance response (ATR) and growth-phase-dependent acid resistance. *Microbiology.* (1996) 142(Pt 10):2975–82. doi: 10.1099/13500872-142-10-2975
19. Vogel BF, Hansen LT, Mordhorst H, Gram L. The survival of *Listeria monocytogenes* during long term desiccation is facilitated by sodium chloride and organic material. *Int J Food Microbiol.* (2010) 140:192–200. doi: 10.1016/j.ijfoodmicro.2010.03.035
20. Santos T, Theron L, Chambon C, Viala D, Centeno D, Esbelin J, et al. MALDI mass spectrometry imaging and in situ microproteomics

of *Listeria monocytogenes* biofilms. *J Proteomics*. (2018) 187:152–60. doi: 10.1016/j.jprot.2018.07.012
21. Walker SJ, Archer P, Banks JG. Growth of *Listeria monocytogenes* at refrigeration temperatures. *J Appl Bacteriol.* (1990) 68:157–62. doi: 10.1111/j.1365-2672.1990.tb02561.x
22. Junttila JR, Niemela SI, Hirn J. Minimum growth temperatures of *Listeria monocytogenes* and non-haemolytic *Listeria*. *J Appl Bacteriol.* (1988) 65:321–7. doi: 10.1111/j.1365-2672.1988.tb01898.x
23. Johansson J, Mandin P, Renzoni A, Chiaruttini C, Springer M, Cossart P. An RNA thermosensor controls expression of virulence genes in *Listeria monocytogenes*. *Cell.* (2002) 110:551–61. doi: 10.1016/S0092-8674(02)00905-4
24. Giovannacci I, Ermel G, Salvat G, Vendeuvre JL, Bellon-Fontaine MN. Physicochemical surface properties of five *Listeria monocytogenes* strains from a pork-processing environment in relation to serotypes, genotypes and growth temperature. *J Appl Microbiol.* (2000) 88:992–1000. doi: 10.1046/j.1365-2672.2000.01057.x
25. Angelidis AS, Smith GM. Role of the glycine betaine and carnitine transporters in adaptation of *Listeria monocytogenes* to chill stress in defined medium. *Appl Environ Microbiol.* (2003) 69:7492–8. doi: 10.1128/AEM.69.12.7492-7498.2003
26. Chan YC, Hu Y, Chaturongakul S, Files KD, Bowen BM, Boor KJ, et al. Contributions of two-component regulatory systems, alternative sigma factors, and negative regulators to *Listeria monocytogenes* cold adaptation and cold growth. *J Food Prot.* (2008) 71:420–5. doi: 10.4315/0362-028X-71.2.420
27. Hayman MM, Anantheswaran RC, Knabel SJ. Heat shock induces barotolerance in *Listeria monocytogenes*. *J Food Prot.* (2008) 71:426–30. doi: 10.4315/0362-028X-71.2.426
28. Pontinen A, Markkula A, Lindstrom M, Korkeala H. Two-component-system histidine kinases involved in growth of *Listeria monocytogenes* EGD-e at low temperatures. *Appl Environ Microbiol.* (2015) 81:3994–4004. doi: 10.1128/AEM.00626-15
29. Lee B-H, Hébraud M, Bernardi T. Increased adhesion of *Listeria monocytogenes* strains to abiotic surfaces under cold stress. *Front Microbiol.* (2017) 8:2221. doi: 10.3389/fmicb.2017.02221
30. Tasara T, Stephan R. Evaluation of housekeeping genes in *Listeria monocytogenes* as potential internal control references for normalizing mRNA expression levels in stress adaptation models using real-time PCR. *FEMS Microbiol Lett.* (2007) 269:265–72. doi: 10.1111/j.1574-6968.2007.00633.x
31. Schmid B, Klumpp J, Raimann E, Loessner MJ, Stephan R, Tasara T. Role of cold shock proteins in growth of *Listeria monocytogenes* under cold and osmotic stress conditions. *Appl Environ Microbiol.* (2009) 75:1621–7. doi: 10.1128/AEM.02154-08
32. Arguedas-Villa C, Stephan R, Tasara T. Evaluation of cold growth and related gene transcription responses associated with *Listeria monocytogenes* strains of different origins. *Food Microbiol.* (2010) 27:653–60. doi: 10.1016/j.fm.2010.02.009
33. Ivy RA, Wiedmann M, Boor KJ. Grown at 7°C shows reduced acid survival and an altered transcriptional response to acid shock compared to *L. monocytogenes* grown at 37°C. *Appl Environ Microbiol.* (2012) 78:3824–36. doi: 10.1128/AEM.00051-12
34. Mattila M, Somervuo P, Rattei T, Korkeala H, Stephan R, Tasara T. Phenotypic and transcriptomic analyses of Sigma L-dependent characteristics in *Listeria monocytogenes* EGD-e. *Food Microbiol.* (2012) 32:152–64. doi: 10.1016/j.fm.2012.05.005
35. Durack J, Ross T, Bowman JP. Characterisation of the transcriptomes of genetically diverse *Listeria monocytogenes* exposed to hyperosmotic and low temperature conditions reveal global stress-adaptation mechanisms. *PLoS ONE.* (2013) 8:e73603. doi: 10.1371/journal.pone.0073603
36. Kaspar D, Auer F, Schardt J, Schindele F, Ospina A, Held C, et al. Temperature- and nitrogen source-dependent regulation of GlnR target genes in *Listeria monocytogenes*. *FEMS Microbiol Lett.* (2014) 355:131–41. doi: 10.1111/1574-6968.12458
37. Cabrita P, Trigo MJ, Ferreira RB, Brito L. Differences in the expression of cold stress-related genes and in the swarming motility among persistent and sporadic strains of *Listeria monocytogenes*. *Foodborne Pathog Dis.* (2015) 12:576–84. doi: 10.1089/fpd.2014.1918
38. Cordero N, Maza F, Navea-Perez H, Aravena A, Marquez-Fontt B, Navarrete P, et al. Different transcriptional responses from slow and fast growth rate strains of *Listeria monocytogenes* adapted to low temperature. *Front Microbiol.* (2016) 7:229. doi: 10.3389/fmicb.2016.00229
39. Bayles DO, Annous BA, Wilkinson BJ. Cold stress proteins induced in *Listeria monocytogenes* in response to temperature downshock and growth at low temperatures. *Appl Environ Microbiol.* (1996) 62:1116–9.
40. Wemekamp-Kamphuis HH, Karatzas AK, Wouters JA, Abee T. Enhanced levels of cold shock proteins in *Listeria monocytogenes* LO28 upon exposure to low temperature and high hydrostatic pressure. *Appl Environ Microbiol.* (2002) 68:456–63. doi: 10.1128/AEM.68.2.456-463.2002
41. Cacace G, Mazzeo MF, Sorrentino A, Spada V, Malorni A, Siciliano RA. Proteomics for the elucidation of cold adaptation mechanisms in *Listeria monocytogenes*. *J Proteomics.* (2010) 73:2021–30. doi: 10.1016/j.jprot.2010.06.011
42. Singh AK, Ulanov AV, Li Z, Jayaswal RK, Wilkinson BJ. Metabolomes of the psychrotolerant bacterium *Listeria monocytogenes* 10403S grown at 37 degrees C and 8 degrees C. *Int J Food Microbiol.* (2011) 148:107–14. doi: 10.1016/j.ijfoodmicro.2011.05.008
43. Cabrita P, Batista S, Machado H, Moes S, Jeno P, Manadas B, et al. Comparative analysis of the exoproteomes of *Listeria monocytogenes* strains grown at low temperatures. *Foodborne Pathog Dis.* (2013) 10:428–34. doi: 10.1089/fpd.2012.1385
44. He L, Deng QL, Chen MT, Wu QP, Lu YJ. Proteomics analysis of *Listeria monocytogenes* ATCC 19115 in response to simultaneous triple stresses. *Arch Microbiol.* (2015) 197:833–41. doi: 10.1007/s00203-015-1116-1
45. Tasara T, Stephan R. Cold stress tolerance of *Listeria monocytogenes*: a review of molecular adaptive mechanisms and food safety implications. *J Food Prot.* (2006) 69:1473–84. doi: 10.4315/0362-028X-69.6.1473
46. Nowak J, Cruz CD, Palmer J, Fletcher GC, Flint S. Biofilm formation of the *L. monocytogenes* strain 15G01 is influenced by changes in environmental conditions. *J Microbiol Methods.* (2015) 119:189–95. doi: 10.1016/j.mimet.2015.10.022
47. Nicaogain K, O'byrne CP. The role of stress and stress adaptations in determining the fate of the bacterial pathogen *Listeria monocytogenes* in the food chain. *Front Microbiol.* (2016) 7:1865. doi: 10.3389/fmicb.2016.01865
48. Miladi H, Elabed H, Ben Slama R, Rhim A, Bakhrouf A. Molecular analysis of the role of osmolyte transporters opuCA and betL in *Listeria monocytogenes* after cold and freezing stress. *Arch Microbiol.* (2017) 199:259–65. doi: 10.1007/s00203-016-1300-y
49. Wemekamp-Kamphuis HH, Sleator RD, Wouters JA, Hill C, Abee T. Molecular and physiological analysis of the role of osmolyte transporters BetL, Gbu, and OpuC in growth of *Listeria monocytogenes* at low temperatures. *Appl Environ Microbiol.* (2004) 70:2912–8. doi: 10.1128/AEM.70.5.2912-2918.2004
50. Cetin MS, Zhang C, Hutkins RW, Benson AK. Regulation of transcription of compatible solute transporters by the general stress sigma factor, sigmaB, in *Listeria monocytogenes*. *J Bacteriol.* (2004) 186:794–802. doi: 10.1128/JB.186.3.794-802.2004
51. Kim YE, Hipp MS, Bracher A, Hayer-Hartl M, Hartl FU. Molecular chaperone functions in protein folding and proteostasis. *Annu Rev Biochem.* (2013) 82:323–55. doi: 10.1146/annurev-biochem-060208-092442
52. Chan YC, Wiedmann M. Physiology and genetics of *Listeria monocytogenes* survival and growth at cold temperatures. *Crit Rev Food Sci Nutr.* (2009) 49:237–53. doi: 10.1080/10408390701856272
53. Cossart P. Molecular and cellular basis of the infection by *Listeria monocytogenes*: an overview. *Int J Med Microbiol.* (2002) 291:401–9. doi: 10.1078/1438-4221-00146
54. Chan YC, Boor KJ, Wiedmann M. SigmaB-dependent and sigmaB-independent mechanisms contribute to transcription of *Listeria monocytogenes* cold stress genes during cold shock and cold growth. *Appl Environ Microbiol.* (2007) 73:6019–29. doi: 10.1128/AEM.00714-07
55. Hebraud M, Guzzo J. The main cold shock protein of *Listeria monocytogenes* belongs to the family of ferritin-like proteins. *FEMS Microbiol Lett.* (2000) 190:29–34. doi: 10.1016/S0378-1097(00)00310-4

56. Soni KA, Nannapaneni R, Tasara T. The contribution of transcriptomic and proteomic analysis in elucidating stress adaptation responses of *Listeria monocytogenes*. *Foodborne Pathog Dis.* (2011) 8:843–52. doi: 10.1089/fpd.2010.0746
57. Glaser P, Frangeul L, Buchrieser C, Rusniok C, Amend A, Baquero F, et al. Comparative genomics of *Listeria* species. *Science.* (2001) 294:849–52. doi: 10.1126/science.1063447
58. Esbelin J, Santos T, Ribiére C, Desvaux M, Viala D, Chambon C, Hébraud M. Comparison of three methods for cell surface proteome extraction of Listeria monocytogenes biofilms. *OMICS J Integr Biol.* (2018) 22:779–87. doi: 10.1089/omi.2018.0144
59. Renier S, Chafsey I, Chambon C, Caccia N, Charbit A, Hebraud M, et al. Contribution of the multiple Type I signal peptidases to the secretome of *Listeria monocytogenes*: deciphering their specificity for secreted exoproteins by exoproteomic analysis. *J Proteomics.* (2015) 117:95–105. doi: 10.1016/j.jprot.2015.01.007
60. Renier S, Micheau P, Talon R, Hebraud M, Desvaux M. Subcellular localization of extracytoplasmic proteins in monoderm bacteria: rational secretomics-based strategy for genomic and proteomic analyses. *PLoS ONE.* (2012) 7:e42982. doi: 10.1371/journal.pone.0042982
61. Bardou P, Mariette J, Escudie F, Djemiel C, Klopp C. jvenn: an interactive Venn diagram viewer. *BMC Bioinformatics.* (2014) 15:293. doi: 10.1186/1471-2105-15-293
62. Huerta-Cepas J, Szklarczyk D, Forslund K, Cook H, Heller D, Walter MC, et al. eggNOG 4.5: a hierarchical orthology framework with improved functional annotations for eukaryotic, prokaryotic and viral sequences. *Nucleic Acids Res.* (2016) 44:D286–93. doi: 10.1093/nar/gkv1248
63. Szklarczyk D, Morris JH, Cook H, Kuhn M, Wyder S, Simonovic M, et al. The STRING database in 2017: quality-controlled protein-protein association networks, made broadly accessible. *Nucleic Acids Res.* (2017) 45:D362–8. doi: 10.1093/nar/gkw937
64. Wickham H. *ggplot2: Elegant Graphics for Data Analysis*. New York, NY: Springer-Verlag (2009).
65. Kazmierczak MJ, Mithoe SC, Boor KJ, Wiedmann M. *Listeria monocytogenes* sigma B regulates stress response and virulence functions. *J Bacteriol.* (2003) 185:5722–34. doi: 10.1128/JB.185.19.5722-5734.2003
66. Nair S, Frehel C, Nguyen L, Escuyer V, Berche P. ClpE, a novel member of the HSP100 family, is involved in cell division and virulence of *Listeria monocytogenes*. *Mol Microbiol.* (1999) 31:185–96. doi: 10.1046/j.1365-2958.1999.01159.x
67. Hain T, Ghai R, Billion A, Kuenne CT, Steinweg C, Izar B, et al. Comparative genomics and transcriptomics of lineages I, II, and III strains of *Listeria monocytogenes*. *BMC Genomics.* (2012) 13:144. doi: 10.1186/1471-2164-13-144
68. Forster BM, Zemansky J, Portnoy DA, Marquis H. Posttranslocation chaperone PrsA2 regulates the maturation and secretion of *Listeria monocytogenes* protein virulence factors. *J Bacteriol.* (2011) 193:5961–70. doi: 10.1128/JB.05307-11
69. Ito K, Akiyama Y. Cellular functions, mechanisms of action, and regulation of FtsH protease. *Annu Rev Microbiol.* (2005) 59:211–31. doi: 10.1146/annurev.micro.59.030804.121316
70. Matsunaga J, Sanchez Y, Xu X, Haake DA. Osmolarity, a key environmental signal controlling expression of leptospiral proteins LigA and LigB and the extracellular release of LigA. *Infect Immun.* (2005) 73:70–8. doi: 10.1128/IAI.73.1.70-78.2005
71. Brehm K, Haas A, Goebel W, Kreft J. A gene encoding a Superoxide dismutase of the facultative intracellular bacterium *Listeria monocytogenes*. *Gene.* (1992) 118:121–5. doi: 10.1016/0378-1119(92)90258-Q
72. Hunger K, Beckering CL, Wiegeshoff F, Graumann PL, Marahiel MA. Cold-induced putative DEAD box RNA helicases CshA and CshB are essential for cold adaptation and interact with cold shock protein B in *Bacillus subtilis*. *J Bacteriol.* (2006) 188:240–8. doi: 10.1128/JB.188.1.240-248.2006
73. Feder ME, Hofmann GE. Heat-shock proteins, molecular chaperones, and the stress response: evolutionary and ecological physiology. *Annu Rev Physiol.* (1999) 61:243–82. doi: 10.1146/annurev.physiol.61.1.243
74. Bierne H, Sabet C, Personnic N, Cossart P. Internalins: a complex family of leucine-rich repeat-containing proteins in *Listeria monocytogenes*. *Microb Infect.* (2007) 9:1156–66. doi: 10.1016/j.micinf.2007.05.003
75. Dons L, Eriksson E, Jin Y, Rottenberg ME, Kristensson K, Larsen CN, et al. Role of flagellin and the two-component CheA/CheY system of *Listeria monocytogenes* in host cell invasion and virulence. *Infect Immun.* (2004) 72:3237–44. doi: 10.1128/IAI.72.6.3237-3244.2004
76. Azizoglu RO, Kathariou S. Temperature-dependent requirement for catalase in aerobic growth of *Listeria monocytogenes* F2365. *Appl Environ Microbiol.* (2010) 76:6998–7003. doi: 10.1128/AEM.01223-10
77. Hernandez-Milian A, Payeras-Cifre A. What is new in listeriosis? *Biomed Res Int.* (2014) 2014:358051. doi: 10.1155/2014/358051
78. ECDC (2015). *The European Union Summary Report on Trends and Sources of Zoonoses, Zoonotic Agents and Foodborne Outbreaks in 2013*.
79. Mcclure PJ, Kelly TM, Roberts TA. The effects of temperature, pH, sodium chloride and sodium nitrite on the growth of *Listeria monocytogenes*. *Int J Food Microbiol.* (1991) 14:77–91. doi: 10.1016/0168-1605(91)90039-R
80. Gandhi M, Chikindas ML. *Listeria*: a foodborne pathogen that knows how to survive. *Int J Food Microbiol.* (2007) 113:1–15. doi: 10.1016/j.ijfoodmicro.2006.07.008
81. Szczawinski J, Ewa Szczawinska M, Lobacz A, Tracz M, Jackowska-Tracz A. Modelling the growth rate of *Listeria monocytogenes* in cooked ham stored at different temperatures. *J Vet Res.* (2017) 61:45–51. doi: 10.1515/jvetres-2017-0006
82. Liu S, Graham JE, Bigelow L, Morse PD II, Wilkinson BJ. Identification of *Listeria monocytogenes* genes expressed in response to growth at low temperature. *Appl Environ Microbiol.* (2002) 68:1697–705. doi: 10.1128/AEM.68.4.1697-1705.2002
83. Pittman JR, Buntyn JO, Posadas G, Nanduri B, Pendarvis K, Donaldson JR. Proteomic analysis of cross protection provided between cold and osmotic stress in *Listeria monocytogenes*. *J Proteome Res.* (2014) 13:1896–904. doi: 10.1021/pr401004a
84. Zhang S, Scott JM, Haldenwang WG. Loss of ribosomal protein L11 blocks stress activation of the *Bacillus subtilis* transcription factor sigma(B). *J Bacteriol.* (2001) 183:2316–21. doi: 10.1128/JB.183.7.2316-2321.2001
85. Duche O, Tremoulet F, Namane A, Labadie J, European Listeria Genome C. A proteomic analysis of the salt stress response of *Listeria monocytogenes*. *FEMS Microbiol Lett.* (2002) 215:183–8. doi: 10.1111/j.1574-6968.2002.tb11389.x
86. Sleator RD, Watson D, Hill C, Gahan CGM. The interaction between *Listeria monocytogenes* and the host gastrointestinal tract. *Microbiology.* (2009) 155:2463–75. doi: 10.1099/mic.0.030205-0
87. Shin JH, Brody MS, Price CW. Physical and antibiotic stresses require activation of the RsbU phosphatase to induce the general stress response in *Listeria monocytogenes*. *Microbiology.* (2010) 156:2660–9. doi: 10.1099/mic.0.041202-0
88. Becker LA, Evans SN, Hutkins RW, Benson AK. Role of ζB in adaptation of *Listeria monocytogenes* to growth at low temperature. *J Bacteriol.* (2000) 182:7083–7. doi: 10.1128/JB.182.24.7083-7087.2000
89. Utratna M, Cosgrave E, Baustian C, Ceredig RH, Byrne CP. Effects of growth phase and temperature on activity within a *Listeria monocytogenes* population: evidence for RsbV-independent activation of at refrigeration temperatures. *Biomed Res Int.* (2014) 2014:641647. doi: 10.1155/2014/641647
90. Lee JJ, Lee G, Shin JH. sigma(B) affects biofilm formation under the dual stress conditions imposed by adding salt and low temperature in *Listeria monocytogenes*. *J Microbiol.* (2014) 52:849–55. doi: 10.1007/s12275-014-4369-5
91. Chan YC, Raengpradub S, Boor KJ, Wiedmann M. Microarray-based characterization of the *Listeria monocytogenes* cold regulon in log- and stationary-phase cells. *Appl Environ Microbiol.* (2007) 73:6484–98. doi: 10.1128/AEM.00897-07
92. Cahoon LA, Freitag NE. *Listeria monocytogenes* virulence factor secretion: don't leave the cell without a chaperone. *Front Cell Infect Microbiol.* (2014) 4:13. doi: 10.3389/fcimb.2014.00013
93. Di Bonaventura G, Piccolomini R, Paludi D, D'orio V, Vergara A, Conter M, et al. Influence of temperature on biofilm formation by *Listeria monocytogenes* on various food-contact surfaces: relationship with motility and cell surface hydrophobicity. *J Appl Microbiol.* (2008) 104:1552–61. doi: 10.1111/j.1365-2672.2007.03688.x

94. Desvaux M, Hébraud M. The protein secretion systems in *Listeria*: inside out bacterial virulence. *FEMS Microbiol Rev.* (2006) 30:774–805. doi: 10.1111/j.1574-6976.2006.00035.x
95. Griffin AM, Robbins ML. The flagellation of *Listeria monocytogenes*. *J Bacteriol.* (1944) 48:114–5.
96. Way SS, Thompson LJ, Lopes JE, Hajjar AM, Kollmann TR, Freitag NE, et al. Characterization of flagellin expression and its role in *Listeria monocytogenes* infection and immunity. *Cell Microbiol.* (2004) 6:235–42. doi: 10.1046/j.1462-5822.2004.00360.x
97. Chang Y, Gu W, Fischer N, Mclandsborough L. Identification of genes involved in *Listeria monocytogenes* biofilm formation by mariner-based transposon mutagenesis. *Appl Microbiol Biotechnol.* (2012) 93:2051–62. doi: 10.1007/s00253-011-3719-z
98. Todhanakasem T, Young GM. Loss of flagellum-based motility by *Listeria monocytogenes* results in formation of hyperbiofilms. *J Bacteriol.* (2008) 190:6030–4. doi: 10.1128/JB.00155-08
99. Mattila M, Lindstrom M, Somervuo P, Markkula A, Korkeala H. Role of flhA and motA in growth of *Listeria monocytogenes* at low temperatures. *Int J Food Microbiol.* (2011) 148:177–83. doi: 10.1016/j.ijfoodmicro.2011.05.022
100. Zhang YM, Rock CO. Membrane lipid homeostasis in bacteria. *Nat Rev Microbiol.* (2008) 6:222–33. doi: 10.1038/nrmicro1839
101. Singh AK, Zhang Y-M, Zhu K, Subramanian C, Li Z, Jayaswal RK, et al. FabH selectivity for anteiso branched-chain fatty acid precursors in low-temperature adaptation in *Listeria monocytogenes*. *FEMS Microbiol Lett.* (2009) 301:188–92. doi: 10.1111/j.1574-6968.2009.01814.x
102. Lippert K, Galinski EA. Enzyme stabilization be ectoine-type compatible solutes: protection against heating, freezing and drying. *Appl Microbiol Biotechnol.* (1992) 37. doi: 10.1007/BF00174204
103. Dussurget O, Dumas E, Archambaud C, Chafsey I, Chambon C, Hebraud M, et al. *Listeria monocytogenes* ferritin protects against multiple stresses and is required for virulence. *FEMS Microbiol Lett.* (2005) 250:253–61. doi: 10.1016/j.femsle.2005.07.015
104. Ayala-Castro C, Saini A, Outten FW. Fe-S cluster assembly pathways in bacteria. *Microbiol Mol Biol Rev.* (2008) 72:110–25. doi: 10.1128/MMBR.00034-07
105. Markkula A, Mattila M, Lindstrom M, Korkeala H. Genes encoding putative DEAD-box RNA helicases in *Listeria monocytogenes* EGD-e are needed for growth and motility at 3 degrees C. *Environ Microbiol.* (2012) 14:2223–32. doi: 10.1111/j.1462-2920.2012.02761.x
106. Bareclev C, Vaitkevicius K, Netterling S, Johansson J. DExD-box RNA-helicases in *Listeria monocytogenes* are important for growth, ribosomal maturation, rRNA processing and virulence factor expression. *RNA Biol.* (2014) 11:1457–66. doi: 10.1080/15476286.2014.996099
107. Folio P, Chavant P, Chafsey I, Belkorchia A, Chambon C, Hebraud M. Two-dimensional electrophoresis database of *Listeria monocytogenes* EGDe proteome and proteomic analysis of mid-log and stationary growth phase cells. *Proteomics.* (2004) 4:3187–201. doi: 10.1002/pmic.200300841
108. Dumas E, Meunier B, Berdague JL, Chambon C, Desvaux M, Hebraud M. The origin of *Listeria monocytogenes* 4b isolates is signified by subproteomic profiling. *Biochim Biophys Acta.* (2009) 1794:1530–6. doi: 10.1016/j.bbapap.2009.06.029
109. Bécavin C, Bouchier C, Lechat P, Archambaud C, Creno S, Gouin E, et al. Comparison of widely used *Listeria monocytogenes* strains EGD, 10403S, and EGD-e highlights genomic variations underlying differences in pathogenicity. *MBio.* (2014) 5:e00969–14. doi: 10.1128/mBio.00969-14
110. Mcgann P, Ivanek R, Wiedmann M, Boor KJ. Temperature-dependent expression of *Listeria monocytogenes* internalin and internalin-like genes suggests functional diversity of these proteins among the listeriae. *Appl Environ Microbiol.* (2007) 73:2806–14. doi: 10.1128/AEM.02923-06
111. Dramsi S, Kocks C, Forestier C, Cossart P. Internalin-mediated invasion of epithelial cells by *Listeria monocytogenes* is regulated by the bacterial growth state, temperature and the pleiotropic activator prfA. *Mol Microbiol.* (1993) 9:931–41. doi: 10.1111/j.1365-2958.1993.tb01223.x
112. Autret N, Raynaud C, Dubail I, Berche P, Charbit A. Identification of the agr locus of *Listeria monocytogenes*: role in bacterial virulence. *Infect Immun.* (2003) 71:4463–71. doi: 10.1128/IAI.71.8.4463-4471.2003

Conflict of Interest Statement: The authors declare that the research was conducted in the absence of any commercial or financial relationships that could be construed as a potential conflict of interest.

frontiers in Microbiology

ORIGINAL RESEARCH
published: 06 February 2019
doi: 10.3389/fmicb.2019.00178

Cold Tolerance Regulated by the Pyruvate Metabolism in *Vibrio parahaemolyticus*

Tengfei Xie[1†], Rui Pang[1†], Qingping Wu[1], Juemei Zhang[1], Tao Lei[1], Yanping Li[1], Juan Wang[2], Yu Ding[3], Moutong Chen[1] and Jianlin Bai[1]*

[1] Guangdong Institute of Microbiology, State Key Laboratory of Applied Microbiology Southern China, Guangdong Provincial Key Laboratory of Microbial Culture Collection and Application, Guangdong Open Laboratory of Applied Microbiology, Guangzhou, China, [2] College of Food Science, South China Agricultural University, Guangzhou, China, [3] Department of Food Science & Technology, Jinan University, Guangzhou, China

OPEN ACCESS

Edited by:
Maria Fiorella Mazzeo, Istituto di Scienza dell'Alimentazione (ISA), Italy

Reviewed by:
José Ángel Huerta Ocampo, Centro de Investigación en Alimentación y Desarrollo (CIAD), Mexico
Inés Arana, University of the Basque Country, Spain

***Correspondence:**
Qingping Wu
wuqp203@163.com

[†] These authors have contributed equally to this work

Specialty section:
This article was submitted to Food Microbiology, a section of the journal Frontiers in Microbiology

Received: *19 August 2018*
Accepted: *22 January 2019*
Published: *06 February 2019*

Citation:
Xie T, Pang R, Wu Q, Zhang J, Lei T, Li Y, Wang J, Ding Y, Chen M and Bai J (2019) Cold Tolerance Regulated by the Pyruvate Metabolism in Vibrio parahaemolyticus. Front. Microbiol. 10:178. doi: 10.3389/fmicb.2019.00178

Vibrio parahaemolyticus is a common foodborne pathogen found in seafood, and represents a major threat to human health worldwide. Low-temperature storage is an important seafood processing method, but is not sufficient to completely eliminate the bacteria and avoid foodborne illness. To determine the mechanisms behind such cold tolerance, RNA-seq and iTRAQ analyses were first performed to obtain the global transcriptomic and proteomic patterns of frozen squid and clinical *V. parahaemolyticus* isolates under cold conditions. The integrated analysis revealed the modulation of multiple pathways such as the co-occurrence of down-regulated pyruvate metabolism and up-regulated fatty acid biosynthesis, which likely contribute to *V. parahaemolyticus* cold tolerance. Furthermore, we found that increasing concentrations of pyruvate can reduce the fatty acid content to influence *V. parahaemolyticus* growth in cold conditions. Thus, regulation of pyruvate concentration may be an effective method to control this seafood-borne pathogen.

Keywords: *Vibrio parahaemolyticus*, cold, pyruvate, transcriptome, proteome

INTRODUCTION

The causative agent of diarrheal disease, *Vibrio parahaemolyticus*, is the major pathogen responsible for seafood associated gastroenteritis in humans worldwide (Samoĭlenko et al., 2003). Seafood is very popular in China, and its higher consumption is correlated with an increase in the overall living standard of the population. However, this high rate of seafood consumption is also accompanied by high rates of foodborne illness. In the city of Sanya, China alone, there were 29 outbreaks caused by *V. parahaemolyticus* resulting in 499 illnesses from 2010 to 2016, accounting for about half of all cases of microbiological food poisoning (Deng et al., 2017). Raw seafood is generally subject to low-temperature storage as an important food preservation method, which can effectively limit bacterial growth and metabolism (Graumann and Marahiel, 1996). However, *V. parahaemolyticus* has still been isolated from seafood that has gone through the low-temperature treatment to ultimately cause foodborne illness (Wang et al., 2016) suggesting a specific mechanism of cold tolerance that has yet to be elucidated.

Previous studies have indicated various adaptations of microorganisms to low temperature, including reduced affinity of enzymes for their substrates, decreased thermal energy and reaction rates, and increased aqueous viscosity (D'Amico et al., 2006). Complex cold shock responses, including cold shock protein (CSP) production, DNA supercoiling modifications, and membrane fluidity maintenance, can help a bacterium survive under detrimental cold conditions (Horn et al., 2007). Nevertheless, different microorganisms have evolved unique strategies in response to low temperatures. For example, unsaturated fatty acids were shown to be effective cold-tolerant factors in *Pseudomonas* sp. (Garba et al., 2016). Another four proteins (ATP-dependent, ClpP, pyruvate kinase and a putative glycoprotein endopeptidase) appear to play important roles in cold adaptation for *Lactobacillus acidophilus*. Despite this basic information on bacterial cold adaptation, the complete strategies, pathways, and signals that compensate for low-temperature metabolism in *V. parahaemolyticus* remain poorly understood (Amato and Christner, 2009).

High-throughput sequencing technology has now made it possible to obtain detailed transcriptomic profiles and improve our understanding of the genetic variation involved in pathogen infection and virulence (Jiang et al., 2016; Sun et al., 2016). The proteome, a term coined by Wilkins in 1992, refers to all of the proteins expressed by the genome, which includes those assessed at the cellular or organismal level (Wasinger et al., 1995). Isobaric tags for relative and absolute quantitation (iTRAQ) is a relatively advanced quantitative proteomic technique that enables relative protein measurements simultaneously with determination of the absolute levels of a target protein using synthetic isobaric peptide standards (Ross et al., 2004), To date, analysis of the *V. parahaemolyticus* proteome has mostly been based on the results of sodium dodecyl sulfate (SDS)-polyacrylamide gel electrophoresis and two-dimensional electrophoresis methods (Chen et al., 2016), but a comprehensive understanding of the components involved in the activation, regulation, and tolerance of low-temperature remains incomplete. The recent advent of sequencing technologies has now made it possible to obtain detailed transcriptomic and proteome profiles of this pathogen in different environments. Indeed, microarray analysis helped to elucidate the effects of salt and acid stress on the *V. parahaemolyticus* transcriptome (Yang et al., 2010; Sun et al., 2014).

To further illustrate the molecular mechanisms driving the low-temperature adaptation of *V. parahaemolyticus,* we employed RNA-sequencing (RNA-seq) and iTRAQ methods to obtain the global transcriptome and proteome patterns of *V. parahaemolyticus* under low-temperature, respectively. Analysis of these transcriptional and proteome profiles is expected to broaden our understanding of the pathways induced in *V. parahaemolyticus* to facilitate survival under low-temperature, which can help to identify potential targets for developing food processing strategies to achieve more effective control of this pathogen and prevent widespread outbreaks of foodborne illness.

MATERIALS AND METHODS

Culture and Incubation Conditions

Vibrio parahaemolyticus strains V82 (isolated from frozen squid) and VL8 (clinical isolate, Xie et al., 2017) were grown overnight at 37°C in tryptic soytone broth (TSB) medium (HuanKai Microbial, Guangzhou, China). Dilutions of each culture were prepared up to $1{:}10^3$ dilution (TSB medium), further incubated at 37°C for 12 h, and then transferred to 4°C for 12 h. The control group was cultured at 37°C for 24 h continuously. Growth status was measured spectrophotometrically based on the optical density at 600 nm. According to the growth curve, stable phase strains were selected for RNA-seq and iTRAQ analysis (**Supplementary Figure S1**).

RNA-Seq Analysis

The total RNA was extracted using Bacterial RNA Kit (Omega Bio-Tek, Salt Lake City, UT, United States) according to the manufacturer's instructions. The complementary DNA (cDNA) libraries from two replicates of all samples were constructed and sequenced by GENE DENOVO, Ltd. (Guangzhou, China) on the Illumina sequencing platform (HiSeq^{TM} 2500), producing 150-bp single-end reads. All clean reads were aligned to the reference genome (GCF_001558495.1) of *V. parahaemolyticus* using Tophat2, and the fragments per kilobases per million values for the genes were estimated by Cufflinks software (Trapnell et al., 2012). Based on the threshold of $\log_2$ fold change ≥ 1 and false discovery rate (FDR) ≤ 0.05, the differentially expressed genes (DEGs) in each comparison were determined by the Cuffdiff module. All DEGs were annotated to the Gene Ontology database[1] and the Kyoto Encyclopedia of Genes and Genomes (KEGG) pathway database (Kanehisa et al., 2008). The functional enrichment was determined by comparison to the annotation of reference transcripts (FDR ≤ 0.05). To support this analysis, 20 DEGs were randomly selected for measurement of expression levels in each sample by quantitative reverse transcription-polymerase chain reaction (qRT-PCR).

iTRAQ Analysis

To enrich the total proteins, three biological replicates of all samples were separately ground into powder in liquid nitrogen, homogenized in 1 mL lysis buffer (10% w/v SDS, 0.1 M dithiothreitol in 0.1 M Tris-HCl, pH 7.6). Then sonication was in an ice bath for 15 cycles (work 5 s, stop 2 s) at 35 kHz. After super-centrifugation (30000 *g,* 4°C for 15 min), the supernatant was precipitated in 10% trichloroacetic acid /acetone, centrifuged at 30,000 *g*, 15 min at 4°C. Three acetone washes were performed on the protein precipitate. Protein precipitates were dissolved in the lysis buffer, protein concentration was measured by Bradford assay protein assay kit (Bio-Rad, United States) and 100 μg aliquots of each sample were used for proteomic experiments. The Filter-aided sample preparation-method (FASP) by Wiśniewski et al. (2009) that, employing ultrafiltration devices, allows to perform SDS removal, buffer exchange, chemical modification, and protein digestion to

[1] http://www.geneontology.org/

obtain peptides mixtures suitable for mass-spectrometric analysis was used to prepare peptide samples for iTRAQ experiments. Trypsin digestion (enzyme to protein ratio 1:50) was carried out at 37°C for 4 h. 4-plex iTRAQ labeling experiments were performed according to the manual provided by AB SCIEX, Pte. Ltd. (Redwood City, CA, United States) (Ross et al., 2004). Strong cation exchange were conducted in a Gemini-NX 5u C18 110A 150 mm × 4.6 mm column (Phenomenex, Guangzhou, China) by using a LC-20AB HPLC Pump system (Shimadzu, Japan). The process is as follows: uv wavelength: 214 nm; flow rate, 1000 μL/min; washing-gradient of liquid chromatography: Time(min), B%: 1, 5%; 18, 30%; 20, 80%; 24, 80%; 24.1, 5%; 30, stop. Reversed-phase liquid chromatography-tandem mass spectrometry were performed by SAGENE, Co., Ltd. (Guangzhou, China) in C18 enriching column (3 μm, ID 100 μm, 20 mm length) and separation column (1.9 μm, ID75 μm, 100 mm length) by using a Triple TOF 6600 (Applied Biosystems, United States). The process is as follows: flow rate, 300 nL/min; washing-gradient of liquid chromatography: Time(min), B%: 0.1, 8%; 55, 25%; 65, 80%; 70, 80%; 70.1, 2%; 75, 2%; stop. The peptides were identified by ProteinPilot 5.0 (AB Sciex) and matched to the reference transcripts of protein sequences of *V. parahaemolyticus* in SwissProt/UniProt database (identification parameters are shown in the **Supplementary Table S1**). The statistically significant differentially-accumulated proteins between treatment groups were determined based on the threshold of protein abundance ratio ≥ 1.5 (up-accumulation) or ≤ 0.667 (down-accumulation) (p-value ≤ 0.05, t-test). The protein–protein interaction network of differentially-accumulated proteins was analyzed using STRING (Szklarczyk et al., 2017). KEGG pathway annotation was performed as above description, and pathway overlaps with DEGs were identified with a custom Perl script.

Quantitative Real-Time PCR (qRT-PCR) Analysis

The total RNA was extracted using Bacterial RNA Kit (Omega Bio-Tek) according to the manufacturer's instructions. RNA degradation and contamination were monitored on 1% agarose

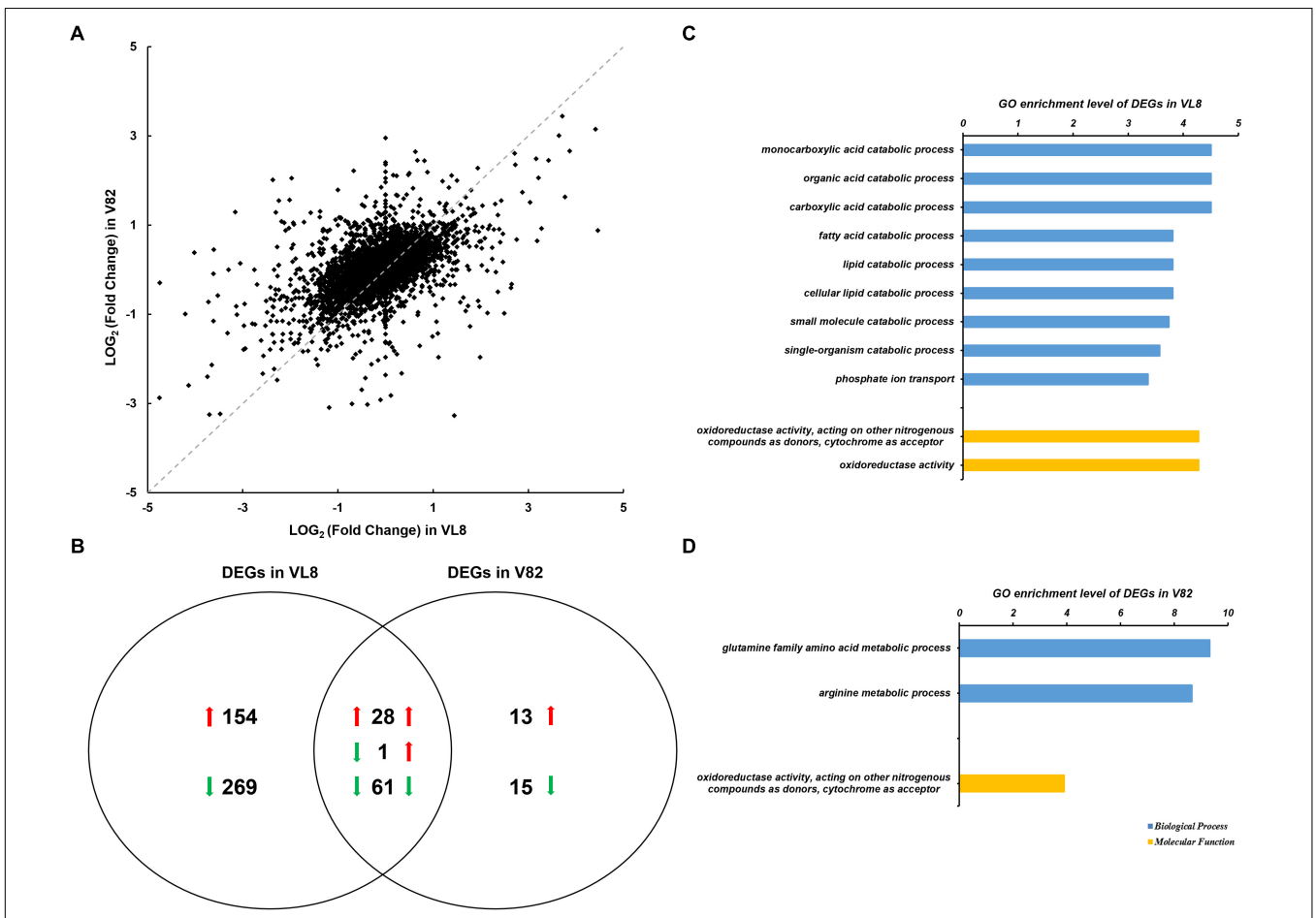

FIGURE 1 | Analyses of the RNA-seq data of two *Vibrio parahaemolyticus* strains under cold stress. The comparison was performed on the 4°C (supplemented) to 37°C (control) in each strain. **(A)** Scatter plots of log2 (Fold Change) per gene from the comparisons of two strains. **(B)** Venn diagrams of differentially expressed genes (DEGs) from the comparisons of two strains. GO enrichment analysis of DEGs from the comparison of VL8 **(C)** and V82 **(D)**, the GO annotation of whole transcripts of *V. parahaemolyticus* was used as background.

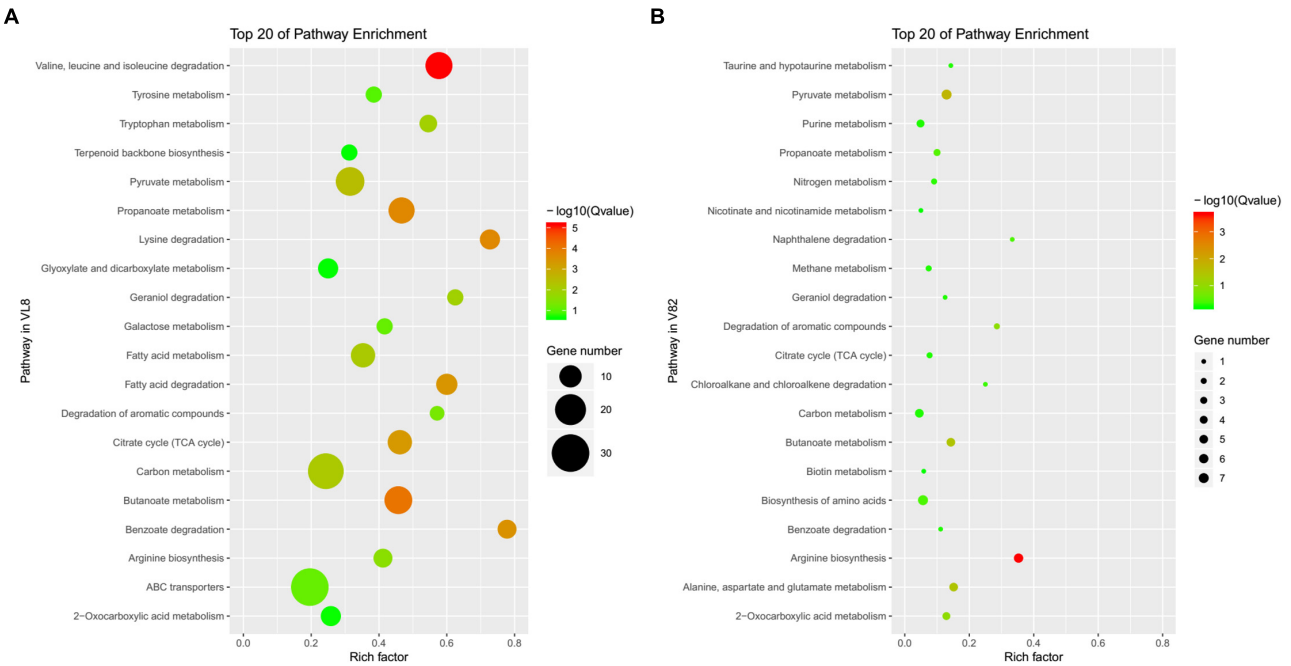

FIGURE 2 | The top 20 of enriched pathways annotated in the KEGG data library of DEGs from the comparisons of strains VL8 **(A)** and V82 **(B)**.

gels and the RNA concentration was quantified cDNA was synthesized using M-MLV First Strand cDNA Synthesis Kit (Omega Bio-Tek) and was quantified using Perfectstart SYBR Green qPCR master mix (Omega Bio-Tek). qRT-PCR was performed on the QuanStudio™ Real-Time PCR system (Applied Biosystems, Foster City, CA, United States). The mRNA level of each gene was normalized to that of 16S rRNA. A list of all primers used in this study is provided in **Supplementary Table S2**.

Fatty Acids Detection

Vibrio parahaemolyticus strain V82 was grown in TSB at 37°C, and then transferred to 4°C for the low-temperature treatment. The cultures were harvested by centrifugation (5000 × *g*, 4°C) and the fatty acid compositions were determined as described by Zhu et al. (2005) and the National Food Safety Standards of China guideline GB5009.168-2016 for examination of fatty acids.

Detection of *V. parahaemolyticus* by Confocal Laser Scanning Microscopy

Confocal laser scanning microscopy (CLSM) (Zeiss, Berlin, Germany) analysis was performed using a LIVE/DEAD® BacLight™ Bacterial Viability and Counting Kit (Invitrogen, Carlsbad, CA, United States) with an appropriate mixture of the SYTO 9 and propidium iodide (PI).

Statistical Analysis

Integrated analysis of the transcriptome and proteome data was conducted using locally designed Perl scripts. For the statistical analysis of qRT-PCR, the relative mRNA levels and $-\Delta\Delta CT$ values were calculated from the obtained cycle threshold values of three biological replicates (Livak and Schmittgen, 2012). The results of fatty acids detection are indicated as mean standard error of the mean ($n = 3$), and analyzed using significant range tests. Differences between groups were considered significant at $P < 0.05$.

RESULTS

Transcriptome Profiles for Strains VL8 and V82 Under Cold Stress

RNA-seq analysis was conducted to determine global changes at the transcript level for *V. parahaemolyticus* strains VL8 and V82 under cold stress, which revealed numerous DEGs for both strains cultured at 4 and 37°C. There was also obvious variation in *V. parahaemolyticus* gene expression profiles between the pathogenic strain VL8 and environmental strain V82 (**Figure 1A**, $R^2 = 0.2498$). The cold stress elicited 513 DEGs in VL8, representing approximately 11.01% of all genes in *V. parahaemolyticus*. Of these, 182 genes were significantly up-regulated and 331 genes were significantly down-regulated (**Figure 1B** and **Supplementary Table S3**). The DEGs in V82 were enriched in functional categories of multiple catabolic processes, phosphate ion transport, and oxidoreductase activity (**Figure 1C** and **Supplementary Table S4**).

In contrast, 118 genes, which accounted for only 2.53% of all genes in the bacterium, showed significantly differential expression in V82, including 42 up-regulated and 76 down-regulated genes that were enriched in the functional categories of glutamine and arginine metabolic processes, and oxidoreductase

activity (**Figure 1D**). Interestingly, most of the DEGs in V82 overlapped with those in VL8 (66.67% of up-regulated genes and 80.26% of down-regulated genes, **Figure 1B**), reflecting that most of the responses to cold stress in V82 should be similar to those in VL8.

The annotation of KEGG pathways also demonstrated the differences and similarities between the responses of strains VL8 and V82 to cold stress. There were more DEGs annotated to the pathway of the ATP-binding cassette (ABC) transporter in VL8 (**Figure 2A**), while more DEGs in V82 were annotated to the pathway of the biosynthesis of amino acids (**Figure 2B**). In addition, the DEGs identified in these two strains were commonly enriched in the pathways of carbon metabolism, arginine biosynthesis, pyruvate metabolism, and butanoate metabolism.

Moreover, the randomly selected DEGs showed significantly differential expression levels by qRT-PCR analysis that were consistent with the results of RNA-seq analysis, suggesting the reliability of the RNA-seq results (**Supplementary Figure S2**).

Global Changes at the Protein Levels in VL8 and V82 Under the Cold Stress and Their Correlation With Transcript Levels

The iTRAQ mass spectrometric analysis was performed on three replicates of the cold-treated VL8 and V82 experiments to identify the differences in protein levels. In total, 1539 proteins were verified with quantitative information in all three replicates. The cold stress resulted in 20 up-accumulated

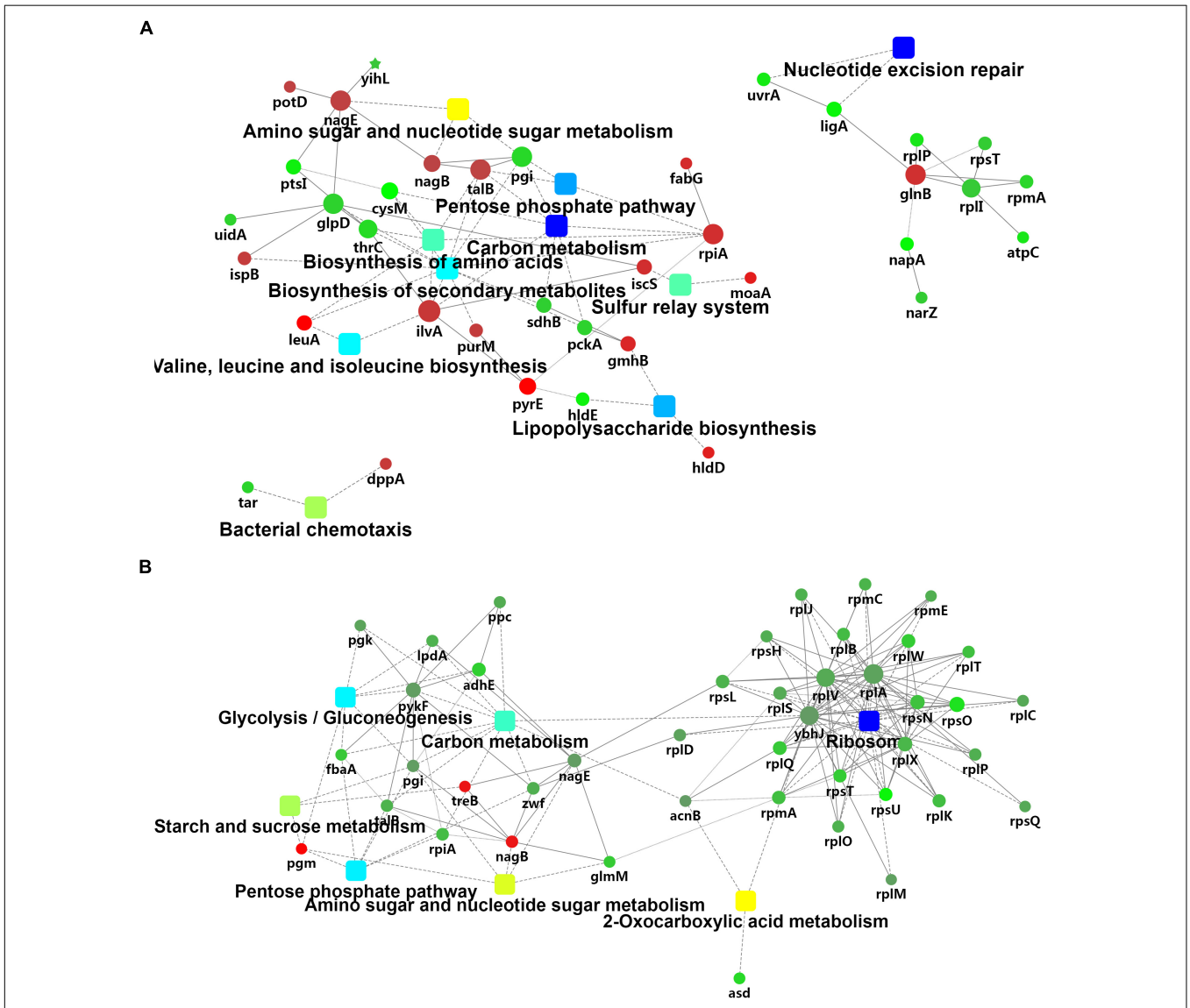

FIGURE 3 | Analyses of the iTRAQ data of two *V. parahaemolyticus* strains under cold stress. The comparison was performed on the 4°C (supplemented) to 37°C (control) in each strain. A network analysis was performed on these differentially-accumulated proteins from the comparison of VL8 **(A)** and V82 **(B)**.

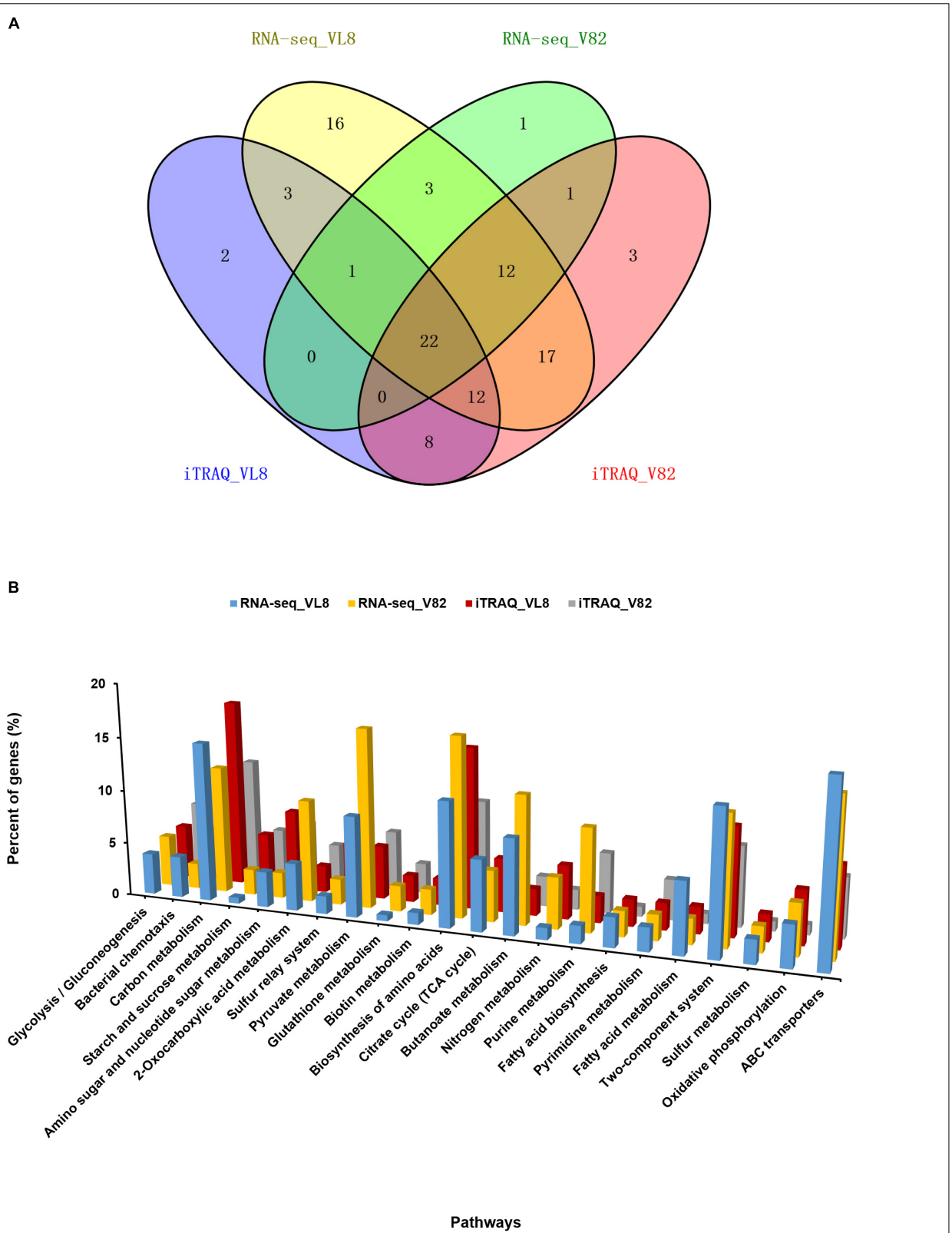

FIGURE 4 | Combined analyses of the RNA-seq and iTRAQ data of two *V. parahaemolyticus* strains under cold stress. **(A)** Venn diagrams of regulated pathways from RNA-seq and iTRAQ analyses from the comparison of strains VL8 and V82. **(B)** Details of 22 overlapping pathways identified in all RNA-seq and iTRAQ datasets. The Y-axis represented the percent of genes in all DEGs or differentially expressed proteins.

and 25 down-accumulated proteins in VL8, and 17 up-accumulated and 129 down- accumulated proteins in V82 (**Supplementary Tables S5**, **S6**). Cold stress induced distinct changes in carbon metabolism and the pentose phosphate pathway for both strains (**Figures 3A,B**). We also observed changes in protein clusters of nucleotide excision repair (**Figure 3A**) and ribosome (**Figure 3B**), which might indicate a response to prevent the misfolding of proteins under cold stress.

We then performed an integrated analysis of the iTRAQ and RNA-seq data sets. Overall, 38 and 42 overlapping pathways were found between the RNA-seq and iTRAQ data in VL8 and V82, respectively (**Figure 4A**). Moreover, a total of 22 pathways were found to be affected in all data sets, including some important

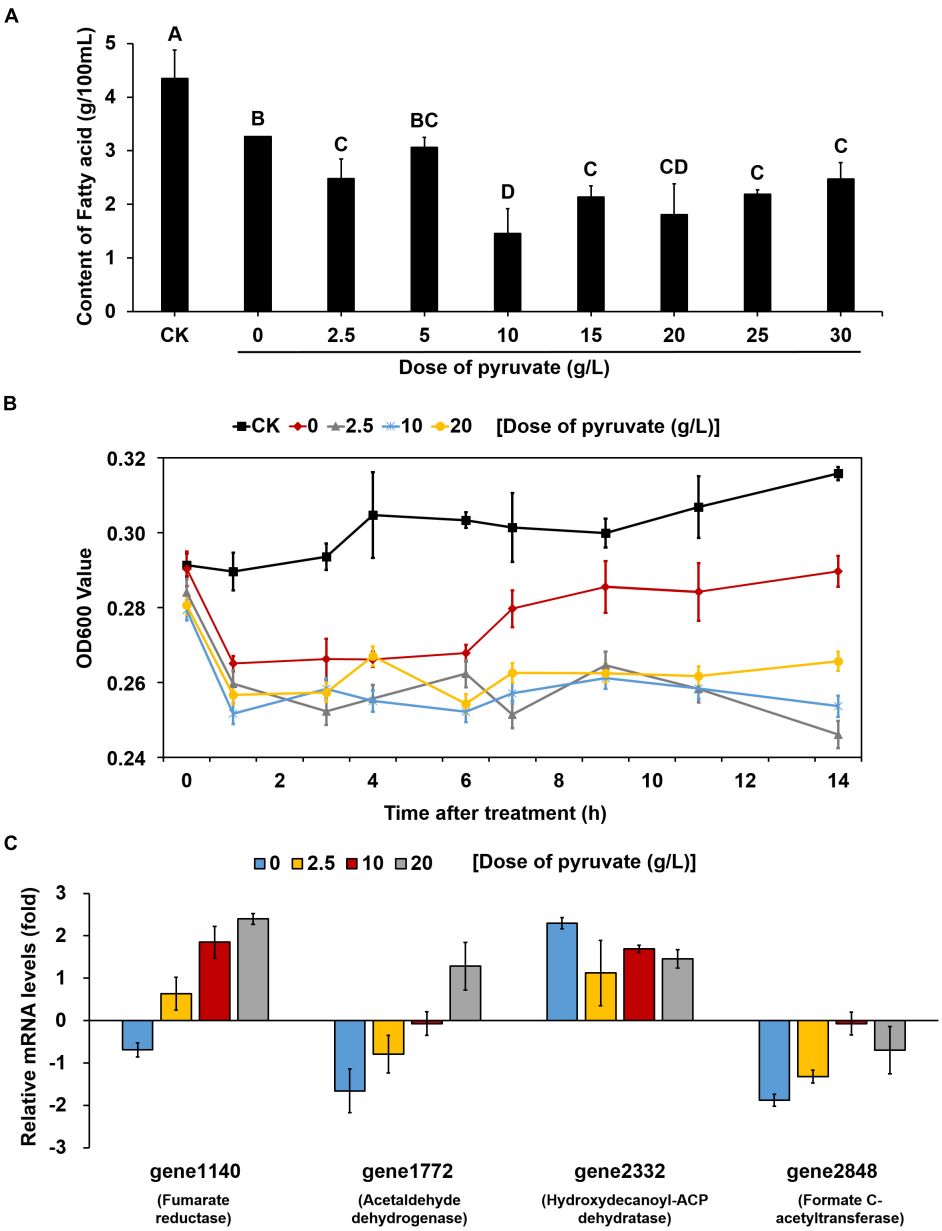

FIGURE 5 | The supplement of exogenous pyruvate reduced the accumulation of fatty acid and effect on *V. parahaemolyticus* growth at low temperature by reversing the expression patterns of key genes. **(A)** Changes in the content of total fatty acids in unit of bacteria supplemented with different doses of pyruvate at 4°C. CK represents bacteria grown at 37°C without any treatment. All bacteria were detected in the same OD value. The values sharing the same letter are not significantly different at $P < 0.05$ (least significant range tests). **(B)** Changes in the growth of bacteria supplemented with different doses of pyruvate at 4°C. CK represents bacteria grown at 37°C without any treatment. **(C)** Changes in the mRNA levels of key genes within pyruvate metabolism and fatty acid biosynthesis pathways of bacteria supplemented with different doses of pyruvate at 4°C. All data are normalized relative to the mRNA levels of bacteria grown at 37°C without any treatment. All values are mean of three biological replicates.

metabolic pathways such as carbon metabolism, biosynthesis of amino acids, and fatty acid metabolism (**Figure 4B** and **Supplementary Table S7**). Interestingly, the numbers of affected genes were relatively high in the pathways of pyruvate metabolism and ABC transporters, reflecting their important roles in the acclimation to cold of *V. parahaemolyticus*.

Decrease in Pyruvate Metabolism Confers Resistance to Cold Stress in *V. parahaemolyticus*

Consistent with the significant change detected in the pyruvate metabolic pathway in both VL8 and V82 under cold stress based on the integrated analysis, the KEGG mapping results demonstrated that the biosynthesis and utilization of pyruvate were significantly decreased (**Supplementary Figure S3**). Consequently, tricarboxylic acid (TCA) cycle pathway was also down-regulated (**Figure 5B**). Interestingly, the lower metabolism of pyruvate led to the promotion of fatty acid biosynthesis, resulting in suppression of fatty acid degradation (**Supplementary Figure S3**).

To clarify whether the up-regulation of fatty acid biosynthesis was caused by a decrease in pyruvate metabolism, different concentrations of pyruvate were added to the culture medium inoculated and maintained at 4°C. Compared with the cultures without pyruvate supplement, the fatty acid contents in almost all pyruvate supplement cultures (except for those supplemented with 5 g/L pyruvate) were significantly reduced (**Figure 5A**). We then measured the growth curves of cultures supplemented with three concentrations of pyruvate (2.5, 10, and 20 g/L) at 4°C, which were compared to those of cultures without pyruvate supplement at both 4 and 37°C. At physiological temperature (37°C), the bacteria grew gradually whereas growth was markedly suppressed at low temperature (4°C) (**Figure 5B**). The cultures without pyruvate supplement could overcome the cold stress over time and slowly resumed normal growth. However, the pyruvate-supplemented populations could barely recover growth throughout the experiment.

Quantitative reverse transcription-polymerase chain reaction analysis was conducted to further determine the changes in the expression of key genes involved in the corresponding pathways identified to be enriched under cold stress. Three genes in the pyruvate metabolism pathway, gene1140 (fumarate reductase), gene1772 (acetaldehyde dehydrogenase), and gene2848 (formate *C*-acetyltransferase), were significantly down-regulated under 4°C (**Figure 5C**). Notably, the OD600 values decreased for cultures at low temperature during the first 1 h. Confocal laser scanning microscopy images indicated that most bacteria died at 4°C compared to the culture at 37°C (**Supplementary Figure S4**). Thus, we inferred that the decrease in OD600 values were mainly attributed to cellular lysis of dead bacterial. However, the addition of pyruvate disrupted the down-regulation of these genes, and even elevated their mRNA levels. Similarly, the up-regulation of a key gene (gene2332, hydroxydecanoyl-ACP dehydratase) in the fatty acid biosynthesis pathway was also prevented to a certain degree by the pyruvate treatment. Collectively, these results suggested that cold stress induced the accumulation of fatty acids by reducing pyruvate metabolism, but that supplementation of exogenous pyruvate would disrupt this process (**Figure 6**).

DISCUSSION

In parallel with improvements in the standard of life, consumers are increasingly concerned with both the taste and nutritive value of their food. To meet this consumer demand, food

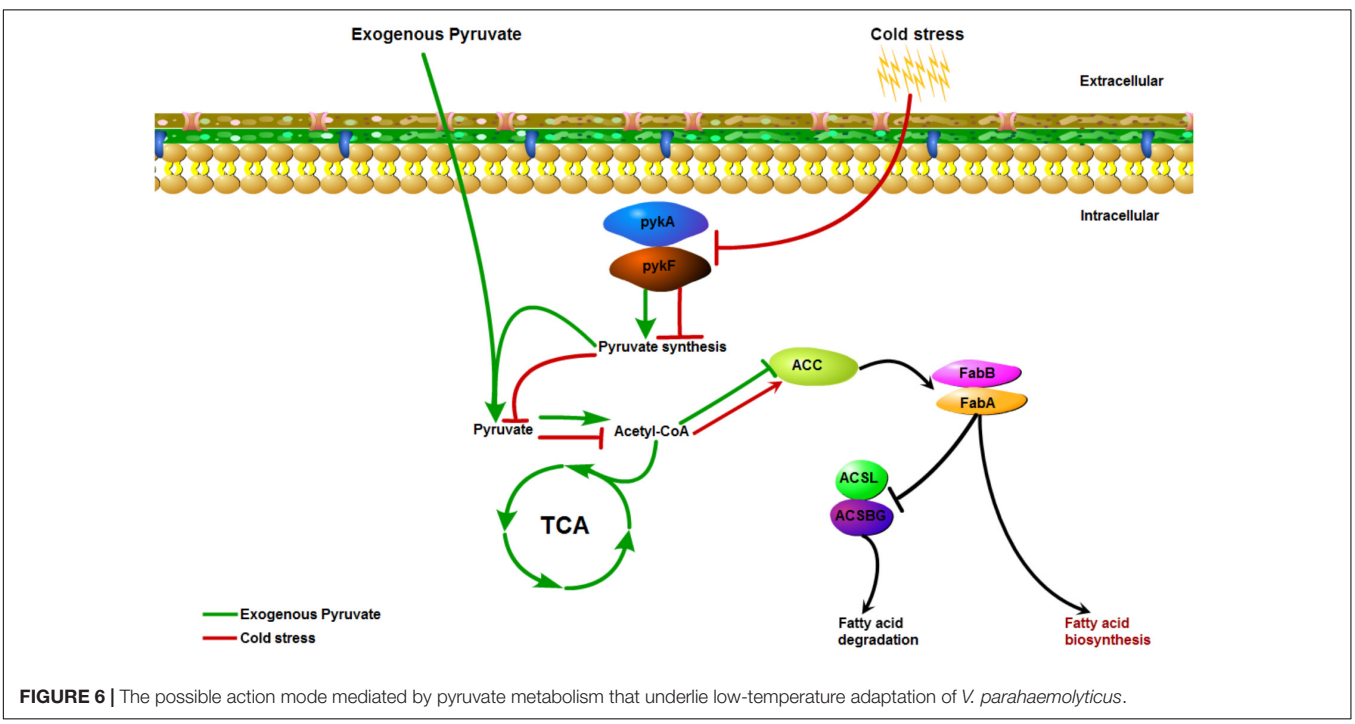

FIGURE 6 | The possible action mode mediated by pyruvate metabolism that underlie low-temperature adaptation of *V. parahaemolyticus*.

producers must continuously adjust processing methods and storage conditions to maintain the original taste and quality of foods (Ma, 2016). Post-harvest processing is particularly important for maintaining the quality and taste of seafood, and low-temperature storage is an essential aspect of this process so as to challenge the survival of *V. parahaemolyticus* given that its virulence decreases in a low-temperature environment, including a reduction in hemolysin and protease production to induce a cytotoxic effect (Mahoney et al., 2010). Indeed, microorganism fitness (growth and survival) has been shown to be significantly linked with temperature (Boonyawantang et al., 2012). Thus, to survive and adapt to changes of the outside environment, microorganisms including foodborne pathogens can undergo a series of changes in gene regulation to control relevant metabolic pathways to combat the negative effects of stress conditions (Azizoglu et al., 2009). Given that *V. parahaemolyticus* can clearly survive under the low-temperature storage conditions in seafood and cause foodborne illness, we assessed the global changes in transcript and protein levels of a clinical and a frozen food *V. parahaemolyticus* isolate at low temperature to determine the adaptation mechanism. This integrated analysis revealed several stimulus-response pathways that were induced under cold stress in both strains, including the commonly affected pathways of ABC transporters, pyruvate metabolism, and fatty acid biosynthesis. Although common patterns were detected in both isolates, there were many more unique DEGs identified in VL8, suggesting that the gene expression profile in the environmental strain was relatively more stable under cold stress, while the pathogenic strain would need to mobilize more gene resources to protect itself from the cold stress.

The ABC transporter proteins, also known as highly conserved in ATP-binding sites proteins (Higgins et al., 1986), are found in all domains of life, and are mainly involved in the uptake of nutrients and micronutrients, extrusion of building blocks, and drug resistance by exporting certain toxic substances outside of the cell (Cuthbertson et al., 2010; Locher, 2016). Similar to the present findings, ABC transporters were found to be significantly inhibited in *V. parahaemolyticus* isolates with a mutation in the CSP gene *cspA* to compensate for the deficiency and protect the bacterium from low temperature induced damage (Zhu et al., 2017). Another report showed that *V. parahaemolyticus* ABC transporters demonstrated notable variation in response to acid and toxicity stress (Nydam et al., 2014; Sun et al., 2014). Thus, our results confirm an important role of ABC transporter pathways in response to cold stress at both the transcriptome and proteome levels in *V. parahaemolyticus*, which have been shown to play an important role in low-temperature adaptation of many other bacteria (Allen et al., 2009).

Interestingly, the down-regulation of pyruvate metabolism and the up-regulation of fatty acid biosynthesis co-occurred in this bacterium under cold stress. Fatty acids are crucial metabolites that are present in almost all living organisms, which play essential roles in maintaining membrane integrity with a direct effect on some cellular processes such as environmental adaptation, cellular differentiation, DNA replication, and cell death (Mansilla et al., 2008; Garba et al., 2016). The accumulation of fatty acids has also been considered to confer an advantage to bacteria for growth under low temperature (Suutari and Laakso, 1994), and Mansilla et al. (2004) showed that bacteria could stringently control the production and modulation of fatty acids within varying temperatures to maintain membrane lipids in the correct physical state. Thus, changing the fatty acid composition is a common strategy for bacteria to overcome low-temperature pressure. For example, different kinds of fatty acids were shown to respond to cold stress in *Shewanella piezotolerans* strains (Wang et al., 2009), and multiple genes related to fatty acid metabolism were induced under cold exposure over time in a previous study of *V. parahaemolyticus* (Yang et al., 2009). Changes of lipids and lipid-like molecules in *V. parahaemolyticus* at low temperature were also observed at the metabolome level (Feng et al., 2016). Pyruvate, a small molecule that plays a central role in metabolism, is the final product of glycolysis and the starting substrate for the TCA cycle (Fink, 2003), also acting as a potent and effective reactive oxygen species scavenger to protect bacteria from oxidative stress (Karabeyoğlu et al., 2008). Pyruvic acid affects the metabolic rate of fatty acids, which in turn influences the TCA cycle (de Groot et al., 1995; Zhang et al., 2010).

Besides demonstrating a link to pyruvate metabolism and fatty acid biosynthesis in terms of gene and protein expression changes under cold stress, we found that direct supplementation of exogenous pyruvate to the culture medium could reduce the fatty acid content to suppress *V. parahaemolyticus* growth under low temperature. Based on these results, we inferred that reduction of pyruvate synthesis can decrease the energy metabolism in *V. parahaemolyticus* in the face of cold stress. However, the addition of pyruvate may transmit an error signal to activate the TCA cycle and intensify the utilization rate of fatty acids. Since the accumulation of fatty acids is a significant microbial cold tolerance adaptation, The down-regulation of fatty acid synthesis caused by exogenous pyruvate is a strategy that could induce the death of *V. parahaemolyticus* cells growth at low temperature and improve food safety. These findings provide a new method to control the growth of this pathogen on frozen aquatic products during transport by adjusting the concentration of pyruvic acid to decrease the survival rate of *V. parahaemolyticus* and reduce the potential of contamination.

CONCLUSION

This study represents the first investigation of foodborne and clinical *V. parahaemolyticus* isolates in response to low temperature using an integrated transcriptome and proteome analysis. We detected distinct global-level gene expression and protein accumulation profiles, revealing several potential key mechanisms for coping with cold stress, such as modulating the pathways of ABC transporters, pyruvate metabolism, and fatty acid biosynthesis. Moreover, pyruvate addition reduced the fatty acid biosynthesis to suppress *V. parahaemolyticus* growth at low temperature. Our results should facilitate further in-depth research of the cold stress resistance of *V. parahaemolyticus* to provide a potential strategy of controlling this seafood-borne pathogen.

AUTHOR CONTRIBUTIONS

TX and RP are the common first authors, finish the article experiment, and write the article together. QW give the idea and experiments support. JZ, TL, YL, JW, YD, MC, and JB help to finish the experiment on article.

FUNDING

Our work was supported by the Key Project of Natural Science Foundation of China (Grant No. 31730070), the Natural Science Foundation of Guangdong Province (Grant No. S2012030006235), and the Science and Technology Planning Project of Guangdong Province (Grant Nos. 2016A010105012 and 2017B020207007).

SUPPLEMENTARY MATERIAL

The Supplementary Material for this article can be found online at: https://www.frontiersin.org/articles/10.3389/fmicb.2019.00178/full#supplementary-material

FIGURE S1 | The growth curve of V82, VL8 at different temperature stages.

FIGURE S2 | Differentially expressed genes validated by qRT-PCR analysis.

FIGURE S3 | The important pathways affected by cold stress in *V. parahaemolyticus*, including pyruvate metabolism pathway **(A)**, citrate cycle (TCA cycle) pathway **(B)**, fatty acid biosynthesis pathway **(C)**, and fatty acid degradation pathway **(D)**. Red indicates that the gene is up-regulated at low temperature, while green indicates that the gene is down-regulated at low temperature.

FIGURE S4 | Laser confocal fluorescence microscopy indicating the status of bacteria supplied with different doses of pyruvate at 4°C. **(A)** Initial sample at 37°C without any treatment. **(B)** Sample at 37°C for 1 h. **(C)** Sample without pyruvate supplement at 4°C for 1 h. **(D)** Sample with 2.5 g/L pyruvate supplement at 4°C for 1 h. **(E)** Sample with 10 g/L pyruvate supplement at 4°C for 1 h. **(F)** Sample with 20 g/L pyruvate supplement at 4°C for 1 h. Green cells represent the alive bacteria, while red cells represent the dead bacteria.

TABLE S1 | Parameters used for database identification by ProteinPilo.

TABLE S2 | The primers used in qRT-PCR.

TABLE S3 | Differentially expressed genes in *V. parahaemolyticus* strain VL8 under cold stress.

TABLE S4 | Differentially expressed genes in *V. parahaemolyticus* strain V82 under cold stress.

TABLE S5 | Differentially accumulated proteins identified from VL8.

TABLE S6 | Differentially accumulated proteins identified from V82.

TABLE S7 | Details of 22 overlapping pathways identified in all RNA-seq and iTRAQ datasets.

REFERENCES

Allen, M. A., Lauro, F. M., Williams, T. J., Burg, D., Siddiqui, K. S., De, F. D., et al. (2009). The genome sequence of the psychrophilic archaeon, *Methanococcoides burtonii*: the role of genome evolution in cold adaptation. *Isme J.* 3, 1012–1035. doi: 10.1038/ismej.2009.45

Amato, P., and Christner, B. C. (2009). Energy metabolism response to low-temperature and frozen conditions in *Psychrobacter cryohalolentis*. *Appl. Environ. Microbiol.* 75, 711–718.

Azizoglu, R. O., Osborne, J., Wilson, S., and Kathariou, S. (2009). Role of growth temperature in freeze-thaw tolerance of *Listeria spp*. *Appl. Environ. Microbiol.* 75, 5315–5320. doi: 10.1128/AEM.00458-09

Boonyawantang, A., Mahakarnchanakul, W., Rachtanapun, C., and Boonsupthip, W. (2012). Behavior of pathogenic *Vibrio parahaemolyticus* in prawn in response to temperature in laboratory and factory. *Food Control* 26, 479–485.

Chen, T. Y., Kuo, S. H., Chen, S. T., and Hwang, D. F. (2016). Differential proteomics to explore the inhibitory effects of acidic, slightly acidic electrolysed water and sodium hypochlorite solution on *Vibrio parahaemolyticus*. *Food Chem.* 194, 529–537. doi: 10.1016/j.foodchem.2015.08.019

Cuthbertson, L., Kos, V., and Whitfield, C. (2010). ABC Transporters involved in export of cell surface glycoconjugates. *Microbiol. Mol. Biol. Rev.* 74, 341–362. doi: 10.1128/MMBR.00009-10

D'Amico, S., Collins, T., Marx, J. C., Feller, G., Gerday, C., and Gerday, C. (2006). Psychrophilic microorganisms: challenges for life. *Embo Rep.* 7, 385–389.

de Groot, M. J., Van Helden, M. A., De Jong, Y. F., Coumans, W. A., and Gj, V. D. V. (1995). The influence of lactate, pyruvate and glucose as exogenous substrates on free radical defense mechanisms in isolated rat hearts during ischaemia and reperfusion. *Mol. Cell. Biochem.* 146, 147–155.

Deng, C., Deng, Y., and Yi, J. (2017). Analysis of microbial food poisoning from 2010 to 2016 in Sanya city. *Hainan Med. J.* 28, 2723–2725.

Feng, B., Guo, Z., Zhang, W., Pan, Y., and Zhao, Y. (2016). Metabolome response to temperature-induced virulence gene expression in two genotypes of pathogenic *Vibrio parahaemolyticus*. *BMC Microbiol.* 16:75. doi: 10.1186/s12866-016-0688-5

Fink, M. P. (2003). Ethyl pyruvate: a novel anti-inflammatory agent. *Crit. Care Med.* 31, S51–S56.

Garba, L., Ali, M. S., Oslan, S. N., and Rahman, R. N. (2016). Heterologous expression of PA8FAD9 and functional characterization of a Δ9-fatty acid desaturase from a cold-tolerant *Pseudomonas* sp. A8. *Mol. Biotechnol.* 58, 718–728.

Graumann, P., and Marahiel, M. A. (1996). Some like it cold: response of microorganisms to cold shock. *Arch. Microbiol.* 166, 293–300.

Higgins, C. F., Hiles, I. D., Salmond, G. P., Gill, D. R., Downie, J. A., Evans, I. J., et al. (1986). A family of related ATP-binding subunits coupled to many distinct biological processes in bacteria. *Nature* 323, 448–450.

Horn, G., Hofweber, R., Kremer, W., and Kalbitzer, H. R. (2007). Structure and function of bacterial cold shock proteins. *Cell. Mol. Life Sci.* 64, 1457–1470.

Jiang, C., Li, Z., Zhang, L., Tian, Y., Dong, D., and Peng, Y. (2016). Significance of hyphae formation in virulence of Candida tropicalis and transcriptomic analysis of hyphal cells. *Microbiol. Res.* 192, 65–72. doi: 10.1016/j.micres.2016.06.003

Kanehisa, M., Araki, M., Goto, S., Hattori, M., Hirakawa, M., Itoh, M., et al. (2008). KEGG for linking genomes to life and the environment. *Nucleic Acids Res.* 36, D480–D484.

Karabeyoğlu, M., Unal, B., Bozkurt, B., Dolapçi, I., Bilgihan, A., Karabeyoğlu, I., et al. (2008). The effect of ethyl pyruvate on oxidative stress in intestine and bacterial translocation after thermal injury. *J. Surg. Res.* 144, 59–63.

Livak, K. J., and Schmittgen, T. D. (2012). Analysis of relative gene expression data using real-time quantitative PCR and the $2^{-\Delta\Delta C T}$ method. *Methods* 25, 402–408.

Locher, K. P. (2016). Mechanistic diversity in ATP-binding cassette (ABC) transporters. *Nat. Struct. Mol. Biol.* 23, 487–493. doi: 10.1038/nsmb.3216

Ma, Y. (2016). *Acid Tolerance Deputy Hemolytic Vibrio Biological Characteristics and the Analysis of Transcriptome and Proteome*. Shanghai: Shanghai Ocean University.

Mahoney, J. C., Gerding, M. J., Jones, S. H., and Whistler, C. A. (2010). Comparison of the pathogenic potentials of environmental and clinical *Vibrio parahaemolyticus* strains indicates a role for temperature regulation in virulence. *Appl. Environ. Microbiol.* 76, 7459–7465. doi: 10.1128/AEM.01450-10

Mansilla, M. C., Banchio, C. E., and de Mendoza, D. (2008). "Signalling pathways controlling fatty acid desaturation," in *Lipids in Health and Disease*, eds P. Quinn and X. Wang (Dordrecht: Springer), 71–99.

Mansilla, M. C., Cybulski, L. E., Albanesi, D., and De, M. D. (2004). Control of membrane lipid fluidity by molecular thermosensors. *J. Bacteriol.* 186, 6681–6688.

Nydam, S. D., Shah, D. H., and Call, D. R. (2014). Transcriptome analysis of*Vibrio parahaemolyticusin* type III secretion system 1 inducing conditions. *Front. Cell. Infect. Microbiol.* 4:1. doi: 10.3389/fcimb.2014.00001

Ross, P. L., Huang, Y. N., Marchese, J. N., Williamson, B., Parker, K., Hattan, S., et al. (2004). Multiplexed protein quantitation in Saccharomyces cerevisiae using amine-reactive isobaric tagging reagents. *Mol. Cell. Proteom.* 3, 1154–1169.

Samoĭlenko, A. M., Teplīnskiĭ, Y. V., and Tsyganovskiĭ, N. S. (2003). Adaptive and inflammatory immune responses in patients infected with strains of *Vibrio parahaemolyticus*. *J. Infect. Dis.* 187, 1085–1096.

Sun, H., Bi, R., Liu, P., Nolan, L. K., and Lamont, S. J. (2016). Combined analysis of primary lymphoid tissues' transcriptomic response to extra-intestinal *Escherichia coli* (ExPEC) infection. *Dev. Comp. Immunol.* 57, 99–106. doi: 10.1016/j.dci.2015.12.013

Sun, X., Liu, T., Peng, X., and Chen, L. (2014). Insights into *Vibrio parahaemolyticus* CHN25 response to artificial gastric fluid stress by transcriptomic analysis. *Int. J. Mol. Sci.* 15, 22539–22562. doi: 10.3390/ijms151222539

Suutari, M., and Laakso, S. (1994). Microbial fatty acids and thermal adaptation. *Crit. Rev. Microbiol.* 20, 285–328.

Szklarczyk, D., Morris, J. H., Cook, H., Kuhn, M., Wyder, S., Simonovic, M., et al. (2017). The STRING database in 2017: quality-controlled protein–protein association networks, made broadly accessible. *Nucleic Acids Res.* 45, D362–D368. doi: 10.1093/nar/gkw937

Trapnell, C., Roberts, A., Goff, L., Pertea, G., Kim, D., Kelley, D. R., et al. (2012). Differential gene and transcript expression analysis of RNA-seq experiments with TopHat and cufflinks. *Nat. Protoc.* 7, 562–578. doi: 10.1038/nprot.2012.016

Wang, F., Xiao, X. H., Gai, Y., and Wang, F. (2009). Role and regulation of fatty acid biosynthesis in the response of Shewanella piezotolerans WP3 to different temperatures and pressures. *J. Bacteriol.* 191, 2574–2584. doi: 10.1128/JB.00498-08

Wang, M., Zhao, X., Su, L., Xu, D., and Tai, J. (2016). Investigation and analysis of food poisoning caused by *Vibrio parahaemolyticus*. *Capital J. Public Health* 10, 272–275.

Wasinger, V. C., Cordwell, S. J., Cerpa-Poljak, A., Yan, J. X., Gooley, A. A., Wilkins, M. R., et al. (1995). Progress with gene-product mapping of the Mollicutes: *Mycoplasma genitalium*. *Electrophoresis* 16, 1090–1094.

Wiśniewski, J. R., Zougman, A., Nagaraj, N., and Mann, M. (2009). Universal sample preparation method for proteome analysis. *Nature methods* 6, 359–362. doi: 10.1038/nmeth.1322

Xie, T., Wu, Q., Zhang, J., Xu, X., and Cheng, J. (2017). Comparison of *Vibrio parahaemolyticus*, isolates from aquatic products and clinical by antibiotic susceptibility, virulence, and molecular characterisation. *Food Control* 71, 315–321.

Yang, L., Zhan, L., Han, H., Gao, H., Guo, Z., Qin, C., et al. (2010). The low-salt stimulon in *Vibrio parahaemolyticus*. *Int. J. Food Microbiol.* 137, 49–54. doi: 10.1016/j.ijfoodmicro.2009.11.006

Yang, L., Zhou, D., Liu, X., Han, H., Zhan, L., Guo, Z., et al. (2009). Cold-induced gene expression profiles of *Vibrio parahaemolyticus*: a time-course analysis. *Fems Microbiol. Lett.* 291, 50–58. doi: 10.1111/j.1574-6968.2008.01434.x

Zhang, D. Y., Zhang, Q., Shen, X. Z., and Chen, J. (2010). Effect of calcium pyruvate on fatty acid metabolism in rats. *Acta Nutrimenta Sinica* 32, 245–282.

Zhu, C., Sun, B., Liu, T., Zheng, H., Gu, W., Wei, H., et al. (2017). Genomic and transcriptomic analyses reveal distinct biological functions for cold shock proteins (VpaCspA and VpaCspD) in *Vibrio parahaemolyticus* CHN25 during low-temperature survival. *BMC Genomics* 18:436. doi: 10.1186/s12864-017-3784-5

Zhu, K., Bayles, D. O., Xiong, A., Jayaswal, R. K., and Wilkinson, B. J. (2005). Precursor and temperature modulation of fatty acid composition and growth of *Listeria monocytogenes* cold-sensitive mutants with transposon-interrupted branched-chain alpha-keto acid dehydrogenase. *Microbiology* 151, 615–623.

Conflict of Interest Statement: The authors declare that the research was conducted in the absence of any commercial or financial relationships that could be construed as a potential conflict of interest.

frontiers in Microbiology

ORIGINAL RESEARCH
published: 08 May 2019
doi: 10.3389/fmicb.2019.01045

Global Proteomic Analysis of the Resuscitation State of *Vibrio parahaemolyticus* Compared With the Normal and Viable but Non-culturable State

Qingping Zhong[1,2], Bin Wang[3], Jie Wang[1], Yufei Liu[1], Xiang Fang[1] and Zhenlin Liao[1]*

[1] Guangdong Provincial Key Laboratory of Food Quality and Safety, College of Food Science, South China Agricultural University, Guangzhou, China, [2] SCAU (Chaozhou) Food Institute Co. Ltd., Chaozhou, China, [3] Guangdong Scau Assets Management Co., Ltd., South China Agricultural University, Guangzhou, China

Vibrio parahaemolyticus is a common pathogen which has become a major concern of seafood products. The bacteria in the viable but non-culturable (VBNC) state are unable to form colonies on growth media, but under appropriate conditions they can regain culturability. In this study, *V. parahaemolyticus* was induced into VBNC state at low temperature and oligotrophic condition, and was resuscitated to culturable state. The aim of this study is to explore the comparative proteomic profiles of the resuscitation state compared with the VBNC state and the exponential phase of *V. parahaemolyticus* using isobaric tags for relative and absolute quantitation (iTRAQ) technique. The differentially expressed proteins (DEPs) were subjected to GO functional annotations and KEGG pathway analysis. The results indicated that a total of 429 proteins were identified as the significant DEPs in the resuscitation cells compared with the VBNC cells, including 330 up-regulated and 99 down-regulated DEPs. Meanwhile, the resuscitation cells displayed 25 up-regulated and 36 down-regulated DEPs (total of 61 DEPs) in comparison with the exponential phase cells. The remarkable DEPs including ribosomal proteins, ABC transporters, outer membrane proteins and flagellar proteins. GO annotation showed that the 429 DEPs were classified into 37 GO terms, of which 17 biological process (BP) terms, 9 cellular component (CC) terms and 11 molecular function (MF) terms. The up-regulated proteins presented in all GO terms except two terms of developmental process and reproduction. The 61 DEPs were assigned to 23 GO terms, the up- and down-regulated DEPs were both mainly involved in cellular process, establishment of localization, metabolic process and so on. KEGG pathway analysis revealed that the 429 DEPs were assigned to 35 KEGG pathways, and the pathways of ribosome, glyoxylate and dicarboxylate metabolism were significantly enriched. Moreover, the 61 DEPs located in 26 KEGG pathways, including the significantly enriched KEGG pathways of ABC transporters and two-component system. This study would contribute to a better understanding of the molecular mechanism underlying the resuscitation of the VBNC state of *V. parahaemolyticus*.

Keywords: *Vibrio parahaemolyticus*, viable but non-culturable state, resuscitation, proteome, differentially expressed proteins, iTRAQ

OPEN ACCESS

Edited by:
Maria Fiorella Mazzeo, Institute of Food Sciences, National Research Council (CNR-ISA), Italy

Reviewed by:
Divakar Sharma, Aligarh Muslim University, India
Jens Andre Hammerl, Bundesinstitut für Risikobewertung, Germany

****Correspondence:***
Qingping Zhong
zhongqp@scau.edu.cn

Specialty section:
This article was submitted to Food Microbiology, a section of the journal Frontiers in Microbiology

Received: *04 January 2019*
Accepted: *25 April 2019*
Published: *08 May 2019*

Citation:
Zhong Q, Wang B, Wang J, Liu Y, Fang X and Liao Z (2019) Global Proteomic Analysis of the Resuscitation State of Vibrio parahaemolyticus Compared With the Normal and Viable but Non-culturable State. Front. Microbiol. 10:1045. doi: 10.3389/fmicb.2019.01045

INTRODUCTION

Vibrio parahaemolyticus is a gram-negative marine bacterium which can be frequently found in coastal environments and a variety of seafood such as shrimp, prawns, oyster, clam, mussel, crab, and marine fish. It is a significant foodborne pathogen which is usually responsible for food poisoning and acute gastroenteritis (McLaughlin et al., 2005; Nair et al., 2007; Su and Liu, 2007; Yu et al., 2016). In recent years, *V. parahaemolyticus* is becoming the leading foodborne pathogen that leads to food poisoning in China and the United States, and the food poisoning outbreaks caused by *V. parahaemolyticus* have been spread all over the world including Asia, America, Europe, and Africa (Ansaruzzaman et al., 2005; McLaughlin et al., 2005; Drake et al., 2007; Nair et al., 2007; Wu et al., 2014; Xu et al., 2014).

Recently, the viable but non-culturable state (VBNC) of bacteria has attracted great attention and more than 85 species of bacteria have been demonstrated to be capable of entering the VBNC state (Li et al., 2014; Zhao et al., 2017). VBNC bacteria are unable to form colonies on conventional growth media, but are viable and maintain metabolic activity, which may constitute an unrecognized source of food contamination and infection (Oliver, 2005; Li et al., 2014). This state is a survival strategy adopted by some bacteria when they are exposed to adverse environmental conditions, but under favorable conditions they can resuscitate to culturable state and retain pathogenicity (Oliver, 2005, 2010; Bedard et al., 2014). Some studies indicated that the VBNC bacteria in food exhibited virulence after resuscitation in food model systems (Dinu and Bach, 2011; Ferro et al., 2018). Therefore, this state of pathogens has been considered as a significant food safety and public health concern (Li et al., 2014; Ferro et al., 2018).

Although *V. parahaemolyticus* has been reported to enter into VBNC state under harsh environmental stresses (Chen et al., 2009; Lai et al., 2009; Boonyawantang et al., 2012; Su et al., 2013; Yoon et al., 2017), and resuscitate upon exposure to appropriate conditions (Mizunoe et al., 2000; Wong, 2004; Coutard et al., 2007), the responses of the VBNC and resuscitation state of *V. parahaemolyticus* at the proteomic level have not been clarified, especially the protein expressions during the recovery phase remain unclear.

In recent years, a comprehensive protein profiling strategy named as isobaric tags for relative and absolute quantification (iTRAQ) has emerged as a powerful high-throughput proteomics method (Zieske et al., 2005; Wright et al., 2012). As for the iTRAQ-based research on *V. parahaemolyticus*, Yang et al. (2015) presented the proteomic profile of *V. parahaemolyticus* under different culture conditions, but only one iTRAQ-based study on the VBNC state of *V. parahaemolyticus* has been reported previously (Zhong et al., 2018). And there is no global proteomic analysis of the resuscitation state of *V. parahaemolyticus* compared with the normal or VBNC state. In the present study, the iTRAQ method was employed to analyze protein profiles of these three states of *V. parahaemolyticus*. The differentially expressed proteins (DEPs) were identified, and the functional interpretation of the DEPs was carried out. This study would contribute to broadening our understanding on the molecular mechanism underlying the resuscitation of the VBNC state of *V. parahaemolyticus*.

MATERIALS AND METHODS

Bacterial Strain and Culture Conditions

Vibrio parahaemolyticus ATCC17802 was obtained from Guangdong Culture Collection Centre of Microbiology (Guangdong, China). The strain was preserved in 10% (w/v) glycerol broth at −80°C and was refreshed twice on tryptic soy agar (TSA) plates containing 3.0% NaCl at 37°C. Then the strain with high activity was cultured into exponential phase in tryptic soy broth (TSB) containing 3.0% NaCl by keeping in a shaker incubator (120 rpm) at 37°C.

Induction of the VBNC State of *V. parahaemolyticus*

After being cultured overnight, the cells were harvested by centrifugation (Eppendorf, Hamburg, Germany) at 8,000 rpm for 5 min at 4°C, and rinsed twice with 3% NaCl solutions, then the cells were re-suspended in the sterile 3% NaCl at a final density of 10^7 CFU/mL which was determined by plate counting on 3.0% NaCl-TSA. The cells were kept at 4°C to be induced into the VBNC state. At each designated time points, the culturability and viability of the cells were analyzed, and the VBNC cells were conformed and enumerated as described previously (Liu et al., 2018). All the experiments were carried out in triplicate. The VBNC cells were collected by centrifugation at 10,000 rpm for 5 min for the following experiments.

Resuscitation of the VBNC Cells

The VBNC cells were collected by centrifugation at 8,000 rpm for 5 min at 4°C, and re-suspended by 9 mL TSB containing 1% Tween 80 (v/v). The cell suspension was incubated at 37°C for 24 h with shaking (120 rpm). Plate counts (on 3% NaCl TSA) were conducted to determine the resuscitation of the VBNC cells.

Protein Extraction, Digestion and Labeling With iTRAQ Reagents

Protein expression profile analysis was conducted for three samples which were exponential-phase cells (C sample), VBNC cells (V sample) and resuscitation cells (R sample). The cells were washed twice with cooled phosphate-buffered saline (PBS) and were centrifuged at 8,000 rpm for 5 min at 4°C. The collected cells were immediately stored at −80°C. Three biological replicates were used per sample. The bacterial cells were mixed with lysis solution (1% SDS, 200 mM DTT, protease inhibitor cocktail at a volume ratio of 1:100, 50 mM Tris–HCl, pH 8.8) at a ratio of 1:10, and incubated in ice-bath for 30 min, vortex-oscillated for 10 s every 10 min, then incubated at 100°C for 5 min. The mixture was centrifuged at 12,000 g, 4°C for 20 min. The supernatant was added with pre-cooled acetone at a ratio of 1:4. The proteins were precipitated overnight and centrifuged at 12,000 × *g*, 4°C for 20 min. The protein precipitate was mixed

with 90% acetone for 10 s and then centrifuged at 12,000 × *g*, 4°C for 20 min. The protein precipitate was dissolved in the protein lysis solution (1% SDS, 8 M urea, protease inhibitor cocktail at a volume ratio of 1:100), and the supernatant was obtained by centrifugation at 4°C for 30 min. The protein concentrations were determined using a BCA Assay Kit (Thermo Fisher Scientific, United States). The sample solution was added with TCEP at the final concentration of 10 mM, and incubated at 37°C for 60 min. Then iodoacetamide was added (40 mM), the reaction took place in the dark at room temperature for 40 min. The solution was mixed with pre-cooled acetone at a volume ratio of 1:6, and put at −20°C for 4 h. The precipitate was collected by centrifugation at 10,000 × *g* for 20 min, dissolved with 100 μL of 100 mM TEAB, and then digested with trypsin at the mass ratio of 25:1 overnight at 37°C. The peptide mixture was labeled with the 8-plex iTRAQ reagent according to the protocol provided by the manufacturer (AB Sciex, United States).

Chromatographic Separation and MS/MS Analysis

The labeled peptides were resuspended with loading buffer (water, adjusted to pH10 with ammonia and formic acid), separated by high pH reversed-phase liquid chromatography (RPLC) using an Acquity UPLC system (Waters, United States). The gradient elution was performed on C18 column (1.7 μm, 2.1 mm × 150 mm XBridge BEH300, Waters, United States) at a flow rate of 400 μL/min with the gradient increased from 0 to 100% B (B: acetonitrile) in 40 min. Twenty fractions were collected from each sample which were subsequently pooled resulting in ten total fractions per sample. Vacuum centrifugal concentration was performed using rotation vacuum concentration Christ RVC 2–25 (Christ, Germany).

Mass spectrometry analysis was conducted on a Q-Exactive mass spectrometer (Thermo Fisher Scientific, United States) that was coupled with EASY-nLC 1200 (Thermo Fisher Scientific, United States). The peptide mixture was loaded onto the C18-reversed phase column (5 μm, 75 μm × 25 cm, Thermo Fisher Scientific, United States) in 2% B (B: 0.1% formic acid in acetonitrile) and separated with a linear gradient increased from 2 to 80% B in 90 min at a flow rate of 300 nL/min. The Q-Exactive mass spectrometer was operated in the data-dependent mode to switch automatically between MS and MS/MS acquisition. Survey full-scan MS spectra (m/z 350-1300) were acquired with a mass resolution of 70 K, followed by twenty sequential high energy collisional dissociation (HCD) MS/MS scans with a resolution of 17.5 K. In all cases, one microscan was recorded using a dynamic exclusion period of 18 s. For MS/MS, Normalized collision energy was set at 30. Mass spectrometric analyses were performed in duplicate for each biological replicate.

Proteomic Analysis of the Differential Expression Proteins

The protein sequences of *V. parahaemolyticus* were downloaded from UniProt database[1]. The database searching was performed using Proteome Discoverer Software 2.1. Proteome discoverer database search parameters were showed in **Supplementary Table S1**. A threshold of 1% false discovery rate (FDR) was used to identify and quantify proteins, and one unique peptide was considered suitable for a reliable protein identification. The differential expression proteins (DEPs) in the resuscitation cells and control samples were identified, the fold change of each protein was calculated based on $\log_2$ value of the relative abundance between test and control samples. The p-value < 0.05 and fold change (FC) >1.50 or <0.67 were used as the threshold to define the significance of protein expression difference. Then DEPs were further subject to functional analysis according to the Gene Ontology (GO)[2] and KEGG pathway[3] databases, and were enriched into different functions with $p \leq 0.05$ as a threshold to determine the significant enrichment of DEPs.

RESULTS

Mass Spectrometric Identification of the Proteins, GO and KEGG Pathway Annotations

We applied ITRAQ technique to analyze comparative proteomic profiles, the total spectrum, identified spectrum, peptide number, protein number were showed in **Supplementary Table S1**. All the identified proteins were presented in detail in **Supplementary Table S2**, and were subjected to GO and KEGG annotations to understand the biological functions. The GO database contains three ontologies: biological process (BP), cellular component (CC), and molecular function (MF). A total of 2625 identified proteins were categorized into the three main categories, at 39 secondary levels, 174 third levels and 476 forth levels of GO terms. At secondary level, metabolic process, cell and catalytic activity were the most significant GO terms in BP, CC and MF, respectively. At level 4, macromolecule metabolic process, intracellular and anion binding were the most significant GO terms in BP, CC and MF, respectively (**Figure 1**). In addition, the top 20 pathways with the largest number of the identified proteins were presented in **Figure 2**. The pathways of two-component system, ABC transporters and purine metabolism had 116, 99 and 73 proteins, respectively.

Differentially Expressed Proteins (DEPs)

As the fold change >1.50 or <0.67 and p-value < 0.05 were used as the threshold to define the significance of protein expression difference, 429 proteins were identified as the significant DEPs in comparison with the resuscitation cells and the VBNC cells. Scatter plots were generated to visualize the distribution of expression variation of proteins (**Supplementary Figure S1**). Of the 429 DEPs, 330 were significantly up-regulated and 99 were down-regulated. Some DEPs were showed in **Tables 1**, **2**. Among the remarkably up-regulated proteins,

[1]http://www.uniprot.org/proteomes/UP000004323

[2]http://www.geneontology.org/

[3]http://www.genome.jp/kegg/

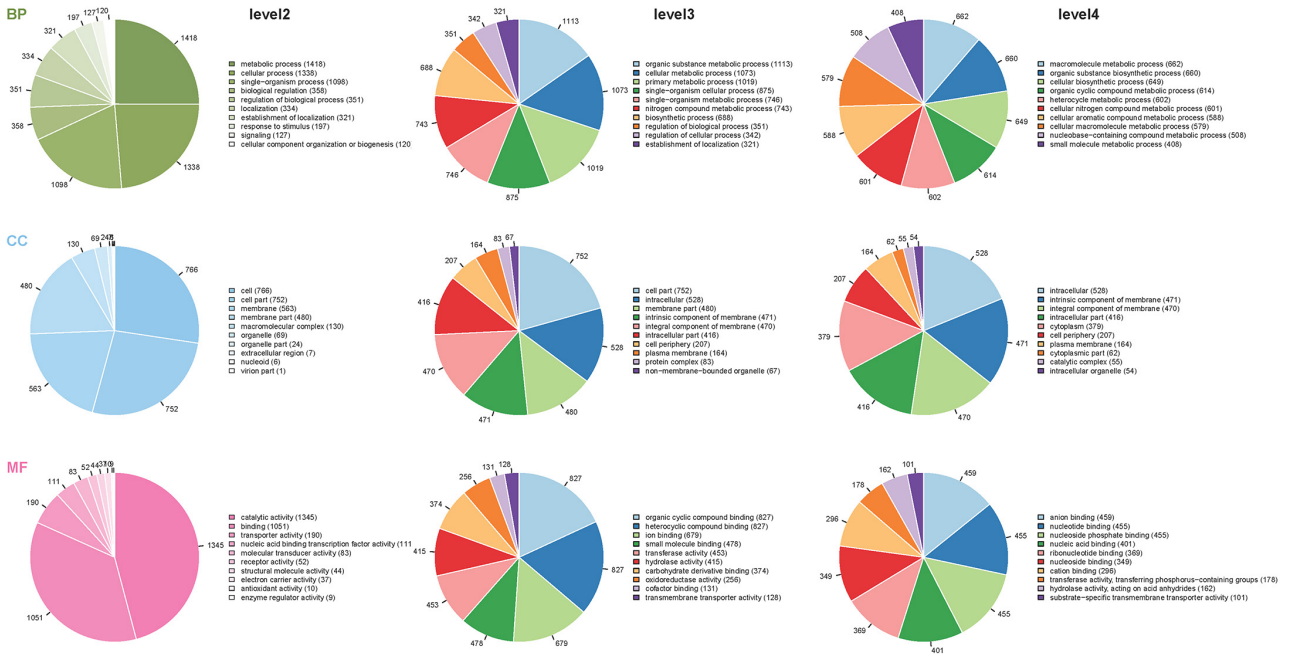

FIGURE 1 | Distribution of the proteins classified into different GO terms at the second, third and fourth levels. The different colors in pies represent different GO terms. The area is the relative proportion of proteins in each GO term. The nine pie charts were sorted by the three main categories, BP, biological processes; CC, cellular components, and MF, molecular function from up to down and level of second, third and forth from left to right. The descriptions of BP, CC, and MF are more detailed with the increase of level numbers.

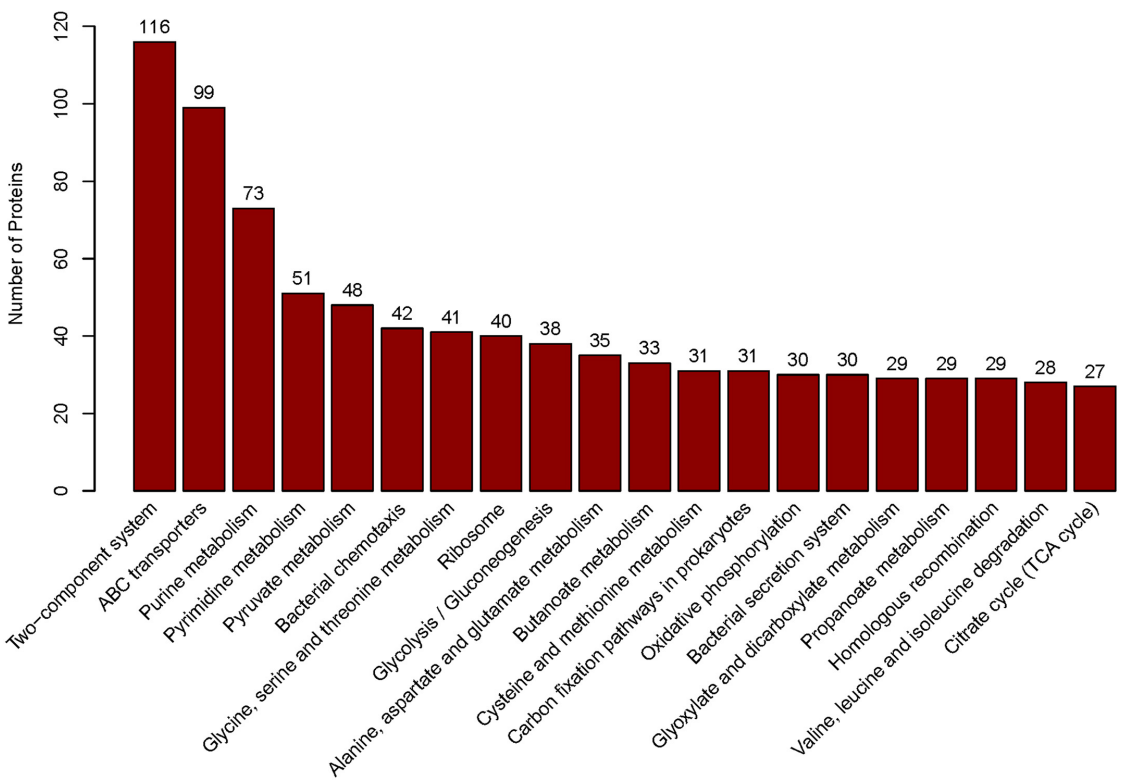

FIGURE 2 | The top 20 pathways. Those pathways were sorted by the protein numbers which annotated the corresponding pathway. Therefore, more annotated proteins involved in the pathway, the higher bar is.

TABLE 1 | Some significantly up-regulated proteins in the resuscitation cells compared with VBNC cells of *V. parahaemolyticus*.

Accession	Description	FC	log2FC	GO	KO	COG
A6B9I5	30S ribosomal protein S19 OS	6.575916	2.717192	GO:0003723; GO:0003735; GO:0005840; GO:0006412; GO:0015935; GO:0019843; GO:0030529	K02965	COG0185
A6AX32	Phosphate ABC transporter, periplasmic phosphate-binding protein OS	6.124724	2.614645	GO:0006810	K02040	COG0226
A6B9H4	50S ribosomal protein L24 OS	4.952381	2.308122	GO:0003723; GO:0003735; GO:0005622; GO:0005840; GO:0006412; GO:0019843; GO:0030529	K02895	COG0198
A6B9B5	50S ribosomal protein L17 OS	4.873684	2.285013	GO:0003735; GO:0005622; GO:0005840; GO:0006412; GO:0030529	K02879	COG0203
A6B883	Integration host factor subunit alpha OS	4.5672269	2.191318	GO:0003677; GO:0006310; GO:0006351; GO:0006355; GO:0006417	K04764	COG0776
A6B1K7	Twin-arginine translocation pathway signal OS	4.505689	2.171748	-	K07093	COG3211
A6BBF2	Ribosomal protein S7 (Fragment) OS	4.129496	2.045966	GO:0003723; GO:0003735; GO:0005840; GO:0006412; GO:0015935; GO:0019843; GO:0030529	K02992	COG0049
A6B646	Thioredoxin OS	3.590717	1.844272	GO:0005623; GO:0006662; GO:0015035; GO:0045454; GO:0055114	K03671	COG0526
A6BAY8	50S ribosomal protein L28 OS	3.504983	1.809408	GO:0003735; GO:0005622; GO:0005840; GO:0006412; GO:0030529	K02902	COG0227
A6B6K0	30S ribosomal protein S21 OS	3.487455	1.802175	GO:0003735; GO:0005622; GO:0005840; GO:0006412; GO:0030529	K02970	COG0828
A6B3T6	30S ribosomal protein S15 OS	3.479876	1.799036	GO:0003723; GO:0003735; GO:0005622; GO:0005840; GO:0006412; GO:0019843; GO:0030529	K02956	COG0184
A6B0V5	Proton/glutamate symporter OS	3.432071	1.77908	GO:0015293; GO:0016020; GO:0016021; GO:0055085	–	COG1301
A6B5K1	DNA-binding protein HU-beta OS	3.327703	1.734527	GO:0003677; GO:0030261	K05787	COG0776
A6AX92	Periplasmic maltose-binding protein OS	3.258359	1.704145	GO:0005215; GO:0005363; GO:0006810; GO:0015768	K10108	COG2182
A6B3L4	Pirin domain protein OS	3.127946	1.645216	–	K06911	COG1741
A6B3R6	DNA-binding protein OS	3.098160	1.631411	GO:0003677; GO:0005622; GO:0006355; GO:0046983	K03746	COG2916
A6B613	Polar flagellar FlgM OS	3.090032	1.6276218	GO:0045892	K02398	COG2747

the ribosomal proteins such as 30S ribosomal protein S19 OS (A6B9I5), 50S ribosomal protein L24 OS (A6B9H4), 50S ribosomal protein L17 OS (A6B9B5) and ribosomal protein S7 OS (A6BBF2) showed notable up regulation. Moreover, integration host factor subunit alpha OS (A6B883), twin-arginine translocation pathway signal OS (A6B1K7), and thioredoxin OS (A6B646) were over-expressed significantly (**Table 1**). In addition, some ABC transporters were significantly up-regulated, of which phosphate ABC transporter, periplasmic phosphate-binding protein OS (A6AX32); ABC transporter, periplasmic substrate-binding protein OS (A6B7T6) and ABC transporter substrate-binding protein (A6B1I7) expressed at much higher level, with the fold change of 6.1247, 2.8945, and 2.5739, respectively (**Table 1** and **Supplementary Table S3A**). The results revealed a significant up regulation of some important proteins in the resuscitation state, these could result in the increase of protein synthesis and some physiological activity. Of the down-regulated proteins (**Table 2**), TrkA-N domain protein OS (A6AX62), PhoH family protein OS (A6B7I9), outer membrane lipoprotein OS (A6BA68) and potassium uptake protein (A6AX63) were expressed at lower level in the resuscitation cells than in the VBNC cells. The detailed information of all the DEPs was listed in **Supplementary Table S3A**.

Compared with the exponential phase cells, the resuscitation cells displayed 61 significant DEPs, including 25 up-regulated and 36 down-regulated DEPs. Some notably DEPs were indicated in **Tables 3**, **4**. A few proteins presented at increased abundance in the resuscitation cells, such as phosphate ABC transporter

TABLE 2 | Some significantly down-regulated proteins in the resuscitation cells compared with VBNC cells of *V. parahaemolyticus*.

Accession	Description	FC	log2FC	GO	KO	COG
A6B843	Uncharacterized protein OS	0.251340	−1.99229	GO:0016020; GO:0016021	–	–
A6B5A3	Uncharacterized protein OS	0.332894	−1.58687	–	–	–
A6AX62	TrkA-N domain protein OS	0.355519	−1.492	GO:0006813; GO:0008324; GO:0098655	K03499	COG0569
A6B7I9	PhoH family protein OS	0.398355	−1.32787	GO:0005524	K07175	COG1875
A6B969	Uncharacterized protein OS	0.425146	−1.23397	GO:0008152; GO:0016491; GO:0055114	–	COG4230
A6BA68	Outer membrane lipoprotein OS	0.454938	−1.13626	GO:0019867	K06078	COG4238
A6AX63	Potassium uptake protein, TrkH family OS	0.462428	−1.1127	GO:0006812; GO:0008324; GO:0016020; GO:0016021; GO:0022820; GO:0055085; GO:0071805	K03498	COG0168
A6B4E2	ATP synthase C chain OS	0.473320	−1.07911	GO:0006810; GO:0006811; GO:0015078; GO:0015986; GO:0015991; GO:0015992; GO:0016020; GO:0016021; GO:0016787; GO:0033177; GO:0045263	K02110	COG0636
A6B2D1	Isochorismatase family protein OS	0.487431	−1.03673	GO:0003824; GO:0008152	–	COG1335

TABLE 3 | Some significantly up-regulated proteins in the resuscitation cells compared with exponential-phase cells of *V. parahaemolyticus*.

Accession	Description	FC	log2FC	GO	KO	COG
A6AX32	Phosphate ABC transporter, periplasmic phosphate-binding protein OS	5.549	2.472228	GO:0006810	K02040	COG0226
A6B4C7	Uncharacterized protein OS	4.118	2.041944	–	–	–
A6B1K7	Twin-arginine translocation pathway signal OS	3.564	1.833497	–	K07093	COG3211
A6B195	Outer membrane protein OS	2.205	1.140779	–	–	COG3203
A6B4Y1	Alkaline phosphatase OS	1.912	0.935082	GO:0003824; GO:0008152; GO:0016311; GO:0016791	K01077	COG1785
A6BCI2	P pilus assembly/Cpx signaling pathway, periplasmic inhibitor/zinc-resistance associated protein (Fragment) OS	1.904	0.929033	GO:0042597	K06006	COG3678
A6B7T6	ABC transporter, periplasmic substrate-binding protein OS	1.893	0.920674	GO:0006810	K02040	COG0226

(A6AX32), twin-arginine translocation pathway signal OS (A6B1K7), outer membrane protein OS (A6B195). The proteins displayed down-regulated were putative outer membrane porin protein locus of qsr prophage OS (A6B101), acetyl-CoA carboxylase, biotin carboxyl carrier protein OS (A6B7L0), ABC-type proline/glycine betaine transport system, periplasmic component OS (A6AZ90), and so on. The **Supplementary Table S3B** presented the detailed information of these DEPs.

GO Annotation and GO Enrichment of the Significant DEPs

The functional interpretation of the significant DEPs was carried out by GO annotation. During the reversion from the VBNC to the culturable state, 429 proteins were differentially expressed and classified into 37 GO terms (**Figure 3A**), of which 17 BP terms, 9 CC terms and 11 MF terms. The up-graduated proteins involved in all terms except two terms of developmental process and reproduction. In the BP ontology, the DEPs primarily associated with metabolic process (containing 189 up- and 40 down-regulated proteins), cellular process (174 up- and 34 down-regulated proteins), and single-organism process (120 up- and 41 down-regulated proteins). For the CC ontology, the DEPs located mainly in cell, cell part, membrane and organelle. According to GO annotation of MF, the DFPs were involved in catalytic activity (131 up- and 41 down-regulated proteins), binding (129 up- and 19 down-regulated proteins), and so on. In addition, only up-regulated proteins were associated with the 13 GO functional groups, including organelle, structural molecule activity, organelle part, and nucleic acid binding transcription factor activity, with 43, 40, 11, and 6 up-regulated proteins, respectively.

Compared with the exponential-phase cells, the 61 DEPs of the resuscitation cells were grouped into 23 GO terms (**Figure 3B**). The up- and down-graduated DEPs were both mainly involved in cellular process, establishment of localization, metabolic process, single-organism process, membrane, catalytic activity and so on. However, only one down-graduated DEP was associated with developmental process, negative regulation of biological process, signaling, cellular component organization or biogenesis, and structural molecule activity, respectively. The

TABLE 4 | Some significantly down-regulated proteins in the resuscitation cells compared with exponential-phase cells of *V. parahaemolyticus*.

Accession	Description	FC	log2FC	GO	KO	COG
A6B101	Putative outer membrane porin protein locus of qsr prophage OS	0.221	−2.17788	–	–	–
A6B7L0	Acetyl-CoA carboxylase, biotin carboxyl carrier protein OS	0.386	−1.37333	GO:0003989; GO:0006633; GO:0009317	K02160	COG0511
A6AZ90	ABC-type proline/glycine betaine transport system, periplasmic component OS	0.403	−1.31115	GO:0005215; GO:0006810; GO:0015871; GO:0033265; GO:0042597	K02002	COG2113
A6B8M3	Transport-associated OS	0.405	−1.30401	–	–	–
A6AZ88	NAD/NADP-dependent betaine aldehyde dehydrogenase OS	0.429	−1.22095	GO:0008152; GO:0008802; GO:0016491; GO:0016620; GO:0019285; GO:0046872; GO:0055114	K00130	COG1012
A6AZ92	Glycine betaine transport ATP-binding protein opuAA OS	0.432	−1.2109	GO:0000166; GO:0005524; GO:0015220; GO:0015418; GO:0015871; GO:0016787; GO:0016887; GO:0055052; GO:0055085	K02000	COG4175
A6AZ89	Oxygen-dependent choline dehydrogenase OS	0.452	−1.14561	GO:0008812; GO:0016491; GO:0016614; GO:0019285; GO:0050660; GO:0055114	K00108	COG2303
A6B3M1	Sodium/glutamate symporter OS	0.457	−1.12973	GO:0015501; GO:0015813; GO:0016020; GO:0016021; GO:0089711	K03312	COG0786

results indicated that the resuscitation cells recovered to high extent from the VBNC state.

The GO enrichment analysis of the DEPs could present the functional enrichment of the DEPs and clarify the difference of samples at the functional level. **Figure 4A** displayed GO enrichment results of the DEPs in the resuscitation cells versus VBNC cells. Many GO terms were enriched dramatically, for example in the BP ontology, ionotropic glutamate receptor signaling pathway, cell surface receptor signaling pathway, glutamate receptor signaling pathway, fatty acid oxidation, lipid oxidation and fatty acid beta-oxidation were notably enriched. For the CC ontology, many GO terms such as ribosome, intracellular non-membrane-bounded organelle, ribonucleoprotein complex, ribosomal subunit and small ribosomal subunit were enriched significantly. Moreover, the molecular functions such as rRNA binding, structural molecule activity, glutamate receptor activity, ligand-gated ion channel activity, transmembrane signaling receptor activity and acetyl-CoA C-acyltransferase activity were enriched dramatically. More detailed GO enrichment information of the DEPs was listed in **Supplementary Table S3C**.

In comparison with the exponential-phase cells, the GO enrichment analysis of the DEPs of the resuscitation cells were also conducted. The results showed that the significantly enriched GO terms were belong to BP and MF, such as glycine betaine metabolic process, glycine betaine biosynthetic process, amino-acid betaine metabolic process, choline metabolic process, modified amino acid transport, glycogen phosphorylase activity, aldehyde dehydrogenase (NAD) activity, oligopeptide transmembrane transporter activity, lysine decarboxylase activity and lipid kinase activity (**Figure 4B** and **Supplementary Table S3D**).

KEGG Pathway Analysis of the Significant DEPs

In addition to the functional GO annotation, KEGG pathway analysis were also conducted on the significant DEPs, in order to provide a comprehensive understanding on the protein profiles of the resuscitation cells of *V. parahaemolyticus*. After conversion from the VBNC to resuscitation state, 429 DEPs were found and assigned to 35 KEGG pathways (**Figure 5**), and a majority of the pathways related to metabolism (M), 3 pathways associated with human diseases (HD), 1 pathway for environmental information processing (EIP), 1 for genetic information processing (GIP). The KEGG pathways of ribosome, glyoxylate and dicarboxylate metabolism were significantly enriched. Ribosome was the most significant pathway with 39 up-regulated DEPs (**Figure 6**).

Compared with the exponential-phase cells, the DEPs of the resuscitation cells were assigned to 26 KEGG pathways, including 21 metabolism pathways (M), 2 human diseases pathways (HD), 2 environmental information processing (EIP) pathways, and 1 genetic information processing (GIP). The significantly enriched KEGG pathways including ABC transporters, and two-component system (**Figure 7**). ABC transporters was the most significant pathway with 2 up-regulated and 2 down-regulated DEPs (**Figure 8**).

DISCUSSION

Up to now, a number of studies have carried out on *V. parahaemolyticus* to reveal the behavior, entry into the VBNC state in response to various environmental conditions and resuscitation to culturable state when exposed to favorable

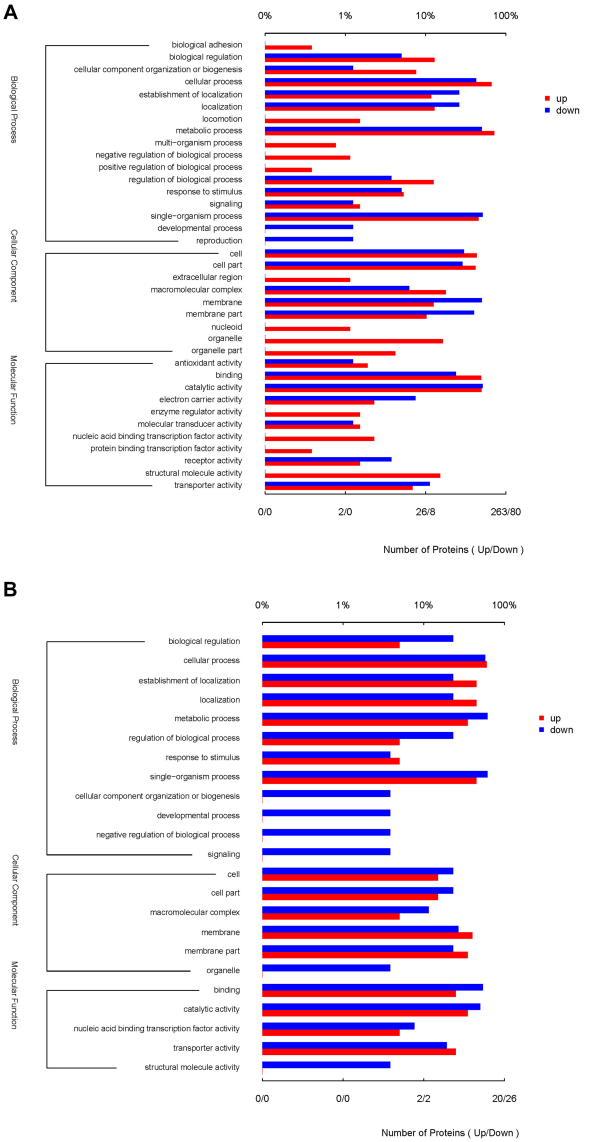

FIGURE 3 | GO terms of the significantly DEPs of the resuscitation cells compared with the VBNC **(A)** or exponential-phase **(B)** cells of *V. parahaemolyticus*. The red bars represented the up-regulated proteins, and blue bars for down-regulated proteins.

conditions, and characterize the biochemical properties of the VBNC state (Mizunoe et al., 2000; Wong, 2004; Coutard et al., 2007; Chen et al., 2009; Boonyawantang et al., 2012; Su et al., 2013; Yoon et al., 2017), as well as develop rapid detection methods (Zhong et al., 2016; Liu et al., 2018). However, little studies have reported to analyze the gene or protein expression profiles (Lai et al., 2009; Meng et al., 2015; Zhong et al., 2018). To our knowledge, there is no information concerning the comprehensive protein expression profile of the resuscitation state of *V. parahaemolyticus*.

In our study, the global comparative proteomic profiles of the resuscitation cells compared with the VBNC state and the exponential phase of *V. parahaemolyticus* were studied by iTRAQ technique. In the VBNC state, the levels of the proteins related to ribosome, rRNA binding and tRNA binding were reduced, and the transcription and translation were generally minimized (Zhong et al., 2018). In the present study, after transition from the VBNC to resuscitation state, almost all ribosomal proteins (39/40) were over-expressed notably (**Supplementary Table S3A**). Among them, some ribosomal proteins were the most distinguished DEPs (**Table 1**). These 30S and 50S ribosomal subunit proteins constitute ribosome and exhibit different functions in protein synthesis (Yang et al., 2015). Furthermore, GO terms related to ribosome were enriched remarkably (**Figure 4**). The KEGG pathway analysis also indicated that the pathway of "Ribosome" was the most significantly enriched pathway (**Figure 5**). This implicating the expression and synthesis of proteins were extensively enhanced to meet a greater requirement of cell growth.

The membrane proteins of bacteria play a crucial role during many cellular and physiological processes, involving in antibiotic efflux system, secretion system, transport, etc., ATP-binding cassette (ABC) transporters are multidomain integral membrane proteins that utilize the energy of ATP hydrolysis to translocate solutes across cellular membranes, and they form one of the largest of all protein families. Through the transport of molecules such as ions, sugars, amino acids, vitamins, peptides, polysaccharides, hormones, lipids and xenobiotics, ABC transporters play major roles in diverse cellular processes such as maintenance of osmotic homeostasis, nutrient uptake, resistance to xenotoxins, antigen processing, cell division, pathogenesis, cholesterol and lipid trafficking (Jones and George, 2004; Rees et al., 2009). In the present study, more than ten ABC transporters expressed at higher level in the resuscitation cells compared with the VBNC cells, and it is worth noting that the 3 top up-regulated ABC transporters (A6AX32, A6B7T6, and A6B1I7) also showed increased abundance compared with the normal cells (**Supplementary Tables S3A,B**). This suggested that the resuscitated bacterial cells accelerated the synthesis of ABC transporters and increased the *trans*-membrane transport function and the intra- and extra-cellular substance exchange, thereby promoting nutrient absorption and excretion of metabolic products. These key DEPs might be the potential regulatory proteins which deserve much more attention and further study.

In addition, we also observed that the resuscitation cells exhibited higher abundance of Type I secretion target GGXGXDXXX repeat (2 copies) domain protein OS (A6B7Z2) than the VBNC cells and normal cells, with the fold change of 2.252 and 1.732. Investigation of secretion systems is critical to understanding the virulence mechanisms of pathogens. The results also showed that cation/multidrug efflux pump OS (A6B3Y5) expressed at increased level (fold change 1.618) in the resuscitation cells compared with the VBNC cells. Drug efflux pumps can participate in drug resistance to multiple antimicrobials through export drugs, and play other roles in bacteria (Yang et al., 2015). As a result, the VBNC cells may

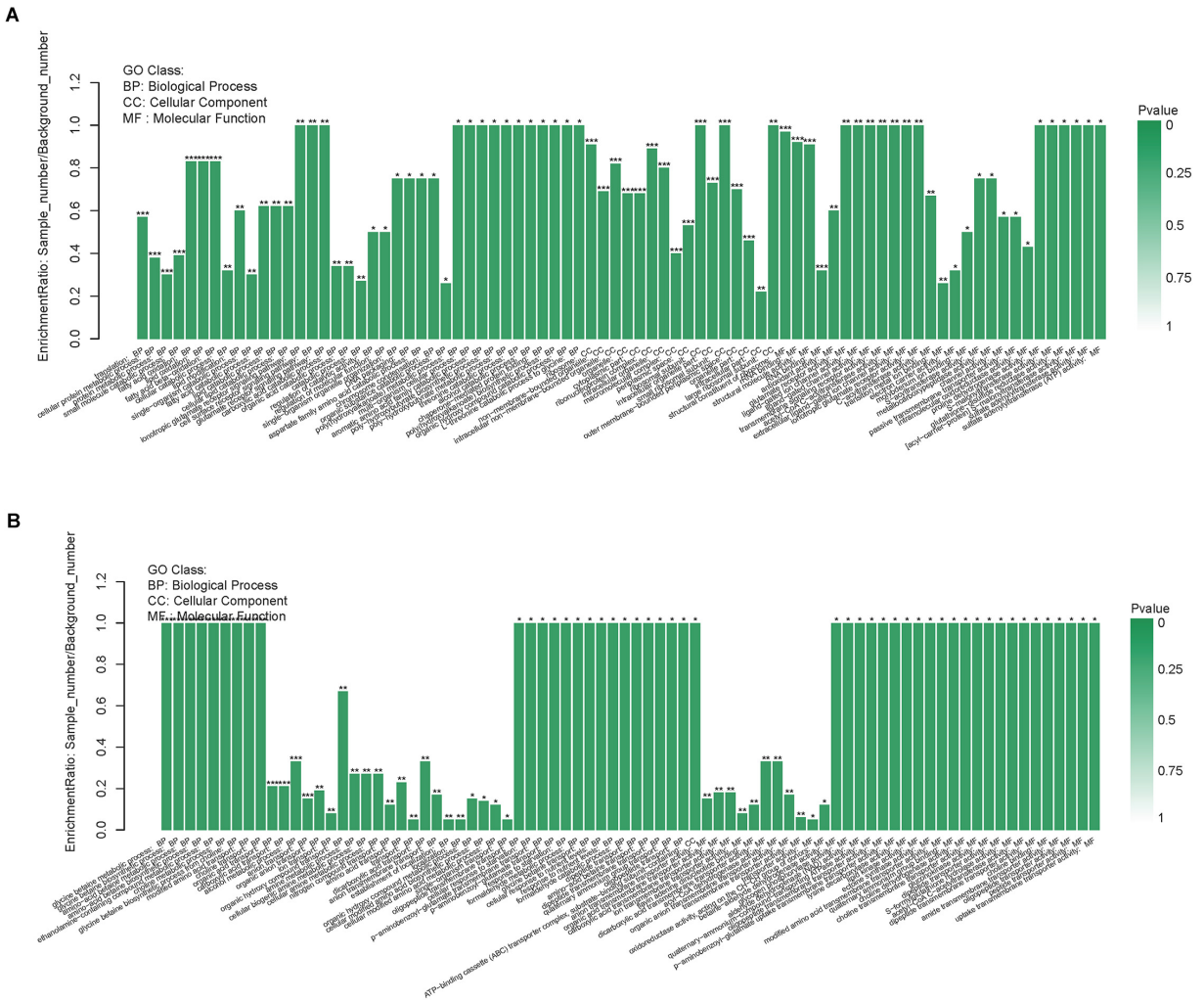

FIGURE 4 | GO enrichment of DEPs in the resuscitation cells compared with the VBNC cells **(A)** or the exponential-phase cells **(B)**. Each bar represented one GO term, which was marked ***$p < 0.001$, **$p < 0.01$, and *$p < 0.05$.

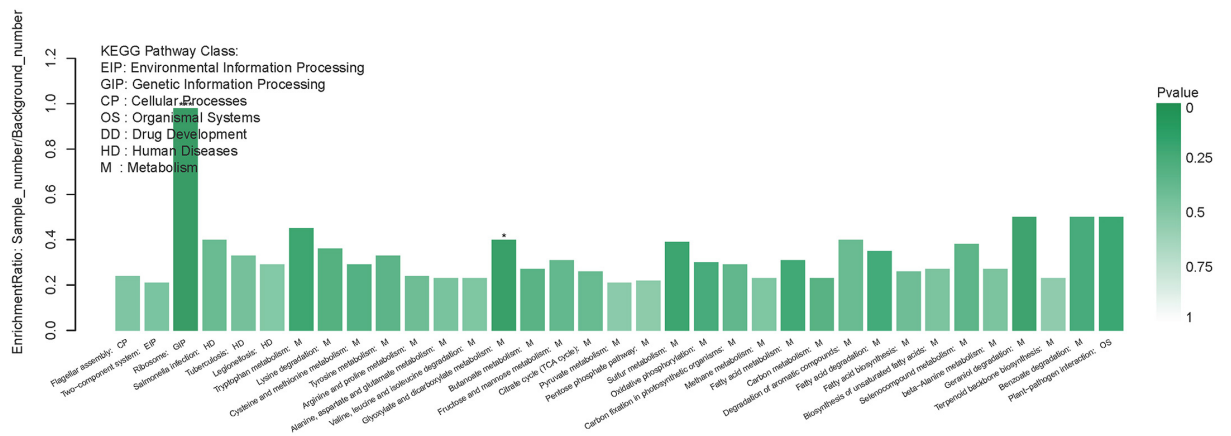

FIGURE 5 | KEGG pathway enrichment of DEPs in the resuscitation cells in comparison with the VBNC cells. Each bar represented one KEGG pathway. Pathway was marked ***$p < 0.001$ and *$p < 0.05$. Color of the bars was related to the *p*-value. Decreasing of the *p*-value was corresponded to the color from light to dark.

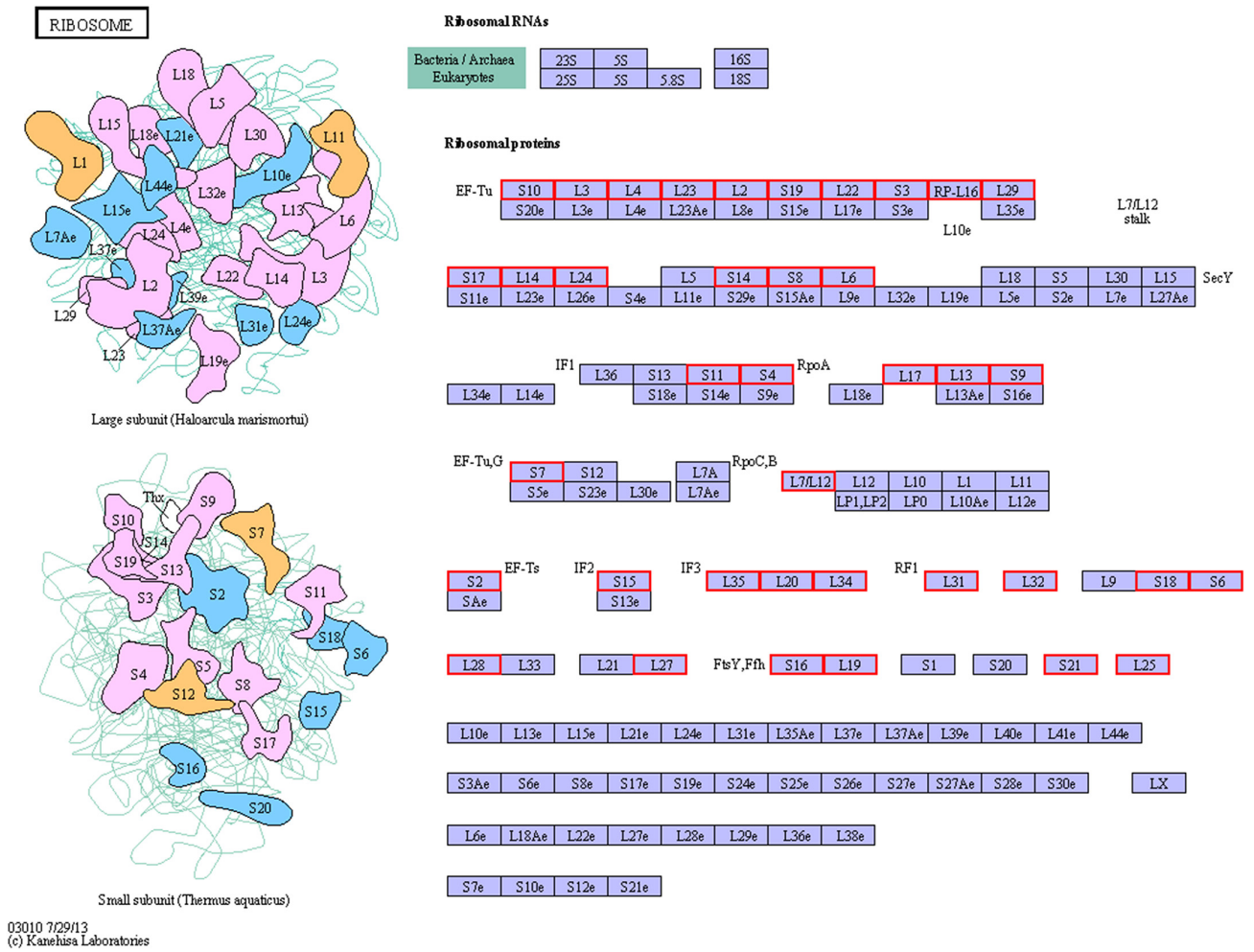

FIGURE 6 | KEGG pathway map of ribosome of the resuscitation cells compared with the VBNC cells. Proteins in blue block belonged to the experimental species. Up-regulated proteins were marked by red frames while down-regulated proteins were marked by green frames.

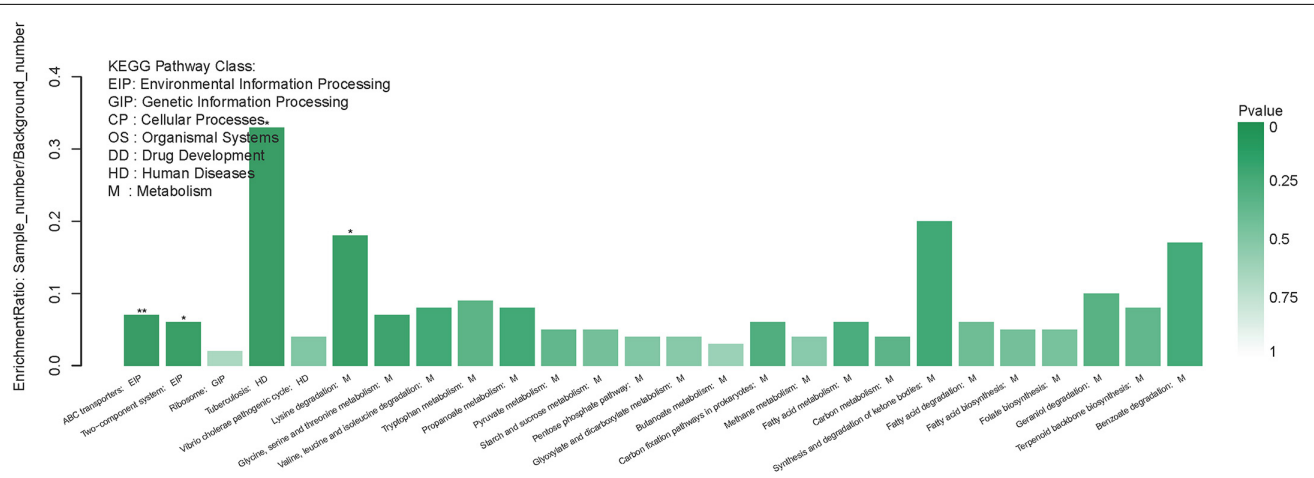

FIGURE 7 | KEGG pathway enrichment of DEPs in the resuscitation cells compared with the exponential-phase cells. Each bar represented one KEGG pathway. Pathway was marked $^{**}p < 0.01$ and $^{*}p < 0.05$. Color of the bars was related to the *p*-value. Decreasing of the *p*-value was corresponded to the color from light to dark.

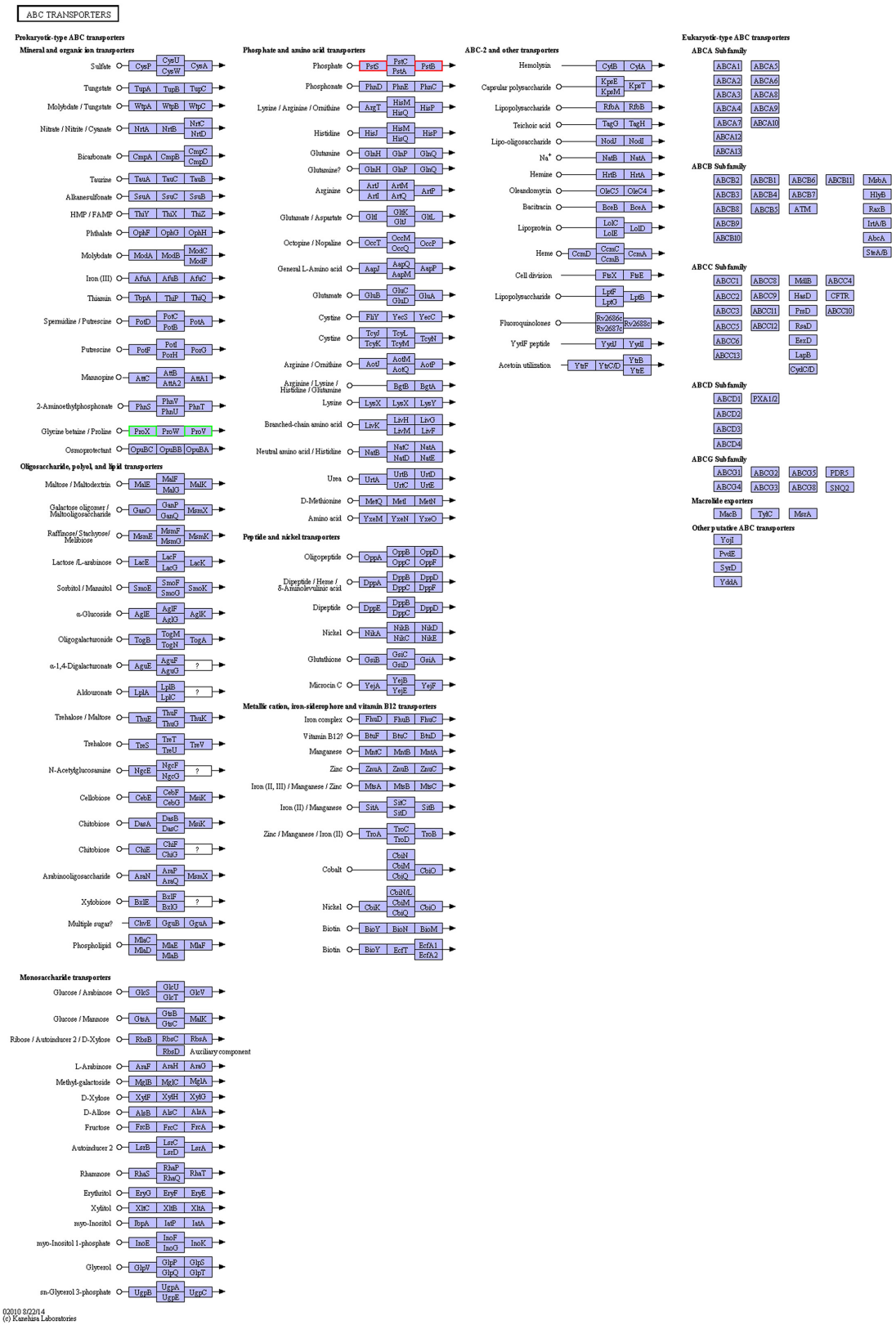

FIGURE 8 | KEGG pathway map of ABC transporters of the resuscitation cells compared with the exponential-phase cells. Proteins in blue block belonged to the experimental species. Up-regulated proteins were marked by red frames while down-regulated proteins were marked by green frames.

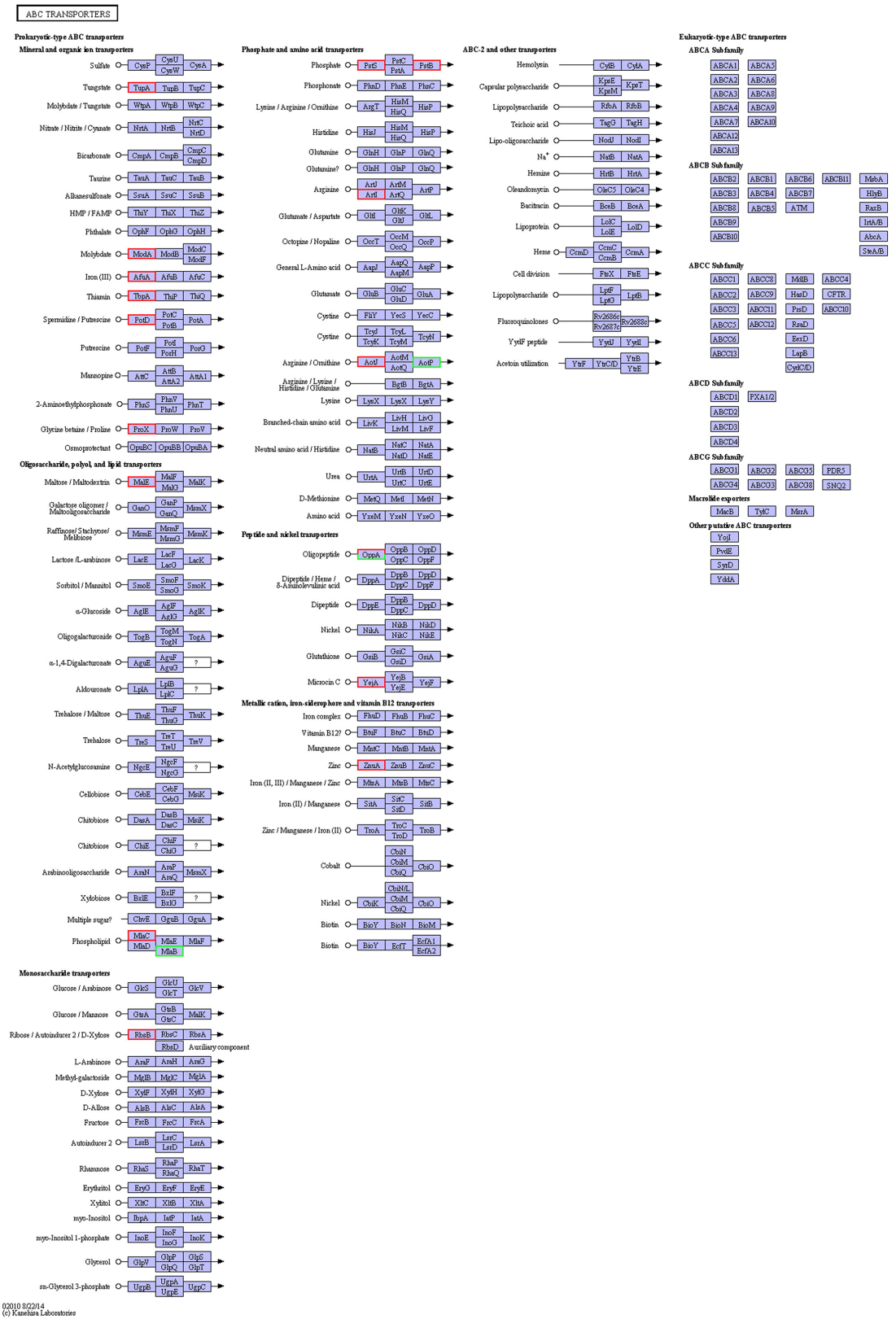

FIGURE 9 | KEGG pathway map of ABC transporters of the resuscitation cells compared with the VBNC cells. Proteins in blue block belonged to the experimental species. Up-regulated proteins were marked by red frames while down-regulated proteins were marked by green frames.

recover the pathogenicity and drug resistance after resuscitation which deserves much more attention.

The outer membrane proteins (OMPs) play key roles in adaptation to changes of external environments due to their location at the outermost area of the cell (Xu et al., 2005). The stressed environmental conditions may pose significant expression changes of OMPs during the VBNC state of bacteria (Xu et al., 2005; Abdallah et al., 2009, 2010; Parada et al., 2016; Zhong et al., 2018). Abdallah et al. (2010) indicated that *V. parahaemolyticus* modified the expression of certain OMPs (e.g., OmpW, OmpA, maltoporin) to respond to gamma irradiation exposure. In the present study, several OMPs were detected at lower abundance in the resuscitated cells, such as outer membrane protein OS (A6BA68); outer membrane porin, OprD family OS (A6B423); putative outer membrane protein, Ail and OmpX OS (A6B7X2); outer membrane protein OmpA OS (A6B0M6), with the fold change of 0.4549, 0.5506, 0.5679, and 0.5878, respectively. These DEPs perhaps were key players or regulators in the VBNC state, but after resuscitation their expression were down-regulated.

The flagellum is a key feature affecting the morphology, chemotaxis, behavior and survival of bacteria (Chilcott and Hughes, 2000). Movement is required for pathogenicity of *V. parahaemolyticus* (Perez-Acosta et al., 2018). Our previous study indicated that the proteins associated with the flagellum were remarkably down-regulated in the VBNC state, the motility decreased and the cells congregated in close proximity (Zhong et al., 2018). In the present study, 5 flagellar proteins were significantly up-regulated in the resuscitation cells, including polar flagellar FlgM OS (A6B613), polar flagellar FlgN OS (A6B614), and flagellin OS (A6B026). In addition, P pilus assembly/Cpx signaling pathway, periplasmic inhibitor/zinc-resistance associated protein (A6BCI2) displayed higher expression in the resuscitation cells than in the VBNC cells and normal cells. GO annotation results also demonstrated that the up-regulated DEPs were involved in the biological processes of locomotion and biological adhesion (**Figure 2**). Pilus contributes to the adhesion and is important for colonization of bacteria. Furthermore, up-regulating of flagellar proteins and adhesins improved the virulence of *V. parahaemolyticus* (Perez-Acosta et al., 2018). These notably up-regulated proteins were suggested to be the key elements which contribute to the normal viability and function of *V. parahaemolyticus*.

Based on the analysis of GO annotations and KEGG pathways, we found that the DEPs in the resuscitation cells were comprehensively up-regulated, which associated with cellular process, metabolic process, single-organism process, localization, membrane, catalytic activity, transporter activity, binding, and so on. Many GO terms were enriched dramatically, for example ionotropic glutamate receptor signaling pathway, cell surface receptor signaling pathway, fatty acid oxidation, rRNA binding, structural molecule activity, and transmembrane signaling receptor activity. Moreover, compared with normal cells, main up-regulated DEPs were related to cellular process, localization and membrane. The results indicated that the resuscitation cells recovered to high extent from the VBNC state. Furthermore, a majority of the KEGG pathways were related to metabolism. The pathways of ribosome and ABC transporters were the most significantly enriched pathways compared with the VBNC cells and the exponential-phase cells, respectively. These KEGG pathways were presented in **Figures 6**, **8**, **9**. These results confirmed that the resuscitated cells of *V. parahaemolyticus* increased the expression and synthesis of proteins extensively to support the cell functions and growth, and some proteins involved in ABC transporters, pilus, type I secretion system, etc., were over-expressed in comparison with the exponential-phase cells.

CONCLUSION

In conclusion, this study was carried out to explore the comparative proteomic profiles of the resuscitation state compared with the VBNC state and the exponential phase of *V. parahaemolyticus* using iTRAQ method. The results indicated that the DEPs in the resuscitation cells were comprehensively up-regulated, which involved in protein synthesis, *trans*-membrane transport, secretion system, movement, adhesion and other vital processes. The pathways of ribosome and ABC transporters were the most significantly enriched pathways. The remarkable DEPs such as ABC transporters, ribosomal proteins and flagellar proteins might be the potential regulatory proteins or biomarkers associated with the responses of *V. parahaemolyticus* during resuscitation from the VBNC state, and this study would help broaden our understanding of the mechanisms underlying the VBNC and resuscitation states of *V. parahaemolyticus*.

AUTHOR CONTRIBUTIONS

QZ analyzed the data and prepared the manuscript. JW contributed to manuscript discussion. BW and YL designed and performed the experiments. XF and ZL contributed to manuscript revision.

FUNDING

This study was supported by National Key R&D Program of China (Grant No. 2017YFC1601200), Natural Science Foundation of Guangdong Province (Grant No. 2017A030313146), and National Natural Science Foundation of China (Grant No. 31271956).

ACKNOWLEDGMENTS

We thank Shanghai Majorbio Bio-Pharm Technology Co., Ltd., for helping the iTRAQ experiments.

SUPPLEMENTARY MATERIAL

The Supplementary Material for this article can be found online at: https://www.frontiersin.org/articles/10.3389/fmicb.2019.01045/full#supplementary-material

FIGURE S1 | Scatter plot for DEPs of the resuscitation cells compared with the VBNC **(A)** or exponential-phase cells **(B)**. Each point represents a

particular protein. Red dots mean up-regulate proteins while green dots mean down-regulate proteins and gray ones for no significant differential expression proteins.

TABLE S1 | Proteome discoverer database search parameters.

TABLE S2 | Detail information of the identified proteins.

TABLE S3 | The DEPs and the GO enrichment information. **(A)** The DEPs of the resuscitation cells compared with the VBNC cells. **(B)** The DEPs of the resuscitation cells in comparison with the exponential-phase cells. **(C)** GO enrichment of the DEPs of the resuscitation cells compared with the VBNC cells. **(D)** GO enrichment of the DEPs of the resuscitation cells compared with the exponential-phase cells.

REFERENCES

Abdallah, F. B., Ellafi, A., Lagha, R., Bakhrouf, A., Namane, A., Rousselle, J. C., et al. (2010). Identification of outer membrane proteins of *Vibrio parahaemolyticus* and *Vibrio alginolyticus* altered in response to γ-irradiation or long-term starvation. *Res. Microbiol.* 161, 869–875. doi: 10.1016/j.resmic.2010.10.009

Abdallah, F. B., Kallel, H., and Bakhrouf, A. (2009). Enzymatic, outer membrane proteins and plasmid alterations of starved *Vibrio parahaemolyticus* and *Vibrio alginolyticus* cells in seawater. *Arch. Microbiol.* 191, 493–500. doi: 10.1007/s00203-009-0477-8

Ansaruzzaman, M., Lucas, M., Deen, J. L., Bhuiyan, N. A., Wang, X. Y., Safa, A., et al. (2005). Pandemic serovars (O3:K6 and O4:K68) of *Vibrio parahaemolyticus* associated with diarrhea in mozambique: spread of the pandemic into the African continent. *J. Clin. Microbiol.* 43, 2559–2562.

Bedard, E., Charron, D., Lalancette, C., Deziel, E., and Prevost, M. (2014). Recovery of *Pseudomonas aeruginosa* culturability following copper- and chlorine-induced stress. *FEMS Microbiol. Lett.* 356, 226–234. doi: 10.1111/1574-6968.12494

Boonyawantang, A., Mahakarnchanakul, W., Rachtanapun, C., and Boonsupthip, W. (2012). Behavior of pathogenic *Vibrio parahaemolyticus* in prawn in response to temperature in laboratory and factory. *Food Control.* 26, 479–485. doi: 10.1016/j.foodcont.2012.02.009

Chen, S. Y., Jane, W. N., Chen, Y. S., and Wong, H. C. (2009). Morphological changes of *Vibrio parahaemolyticus* under cold and starvation stresses. *Int. J. Food Microbiol.* 129, 157–165. doi: 10.1016/j.ijfoodmicro.2008.11.009

Chilcott, G. S., and Hughes, K. T. (2000). Coupling of flagellar gene expression to flagellar assembly in *Salmonella enterica* serovar typhimurium and *Escherichia coli*. *Microbiol. Mol. Biol. Rev.* 64, 694–708. doi: 10.1128/MMBR.64.4.694-708.2000

Coutard, F., Crassous, P., Droguet, M., Gobin, E., Colwell, R. R., Pommepuy, M., et al. (2007). Recovery in culture of viable but nonculturable *Vibrio parahaemolyticus*: regrowth or resuscitation? *ISME J.* 1, 111–120. doi: 10.1038/ismej.2007.1

Dinu, L. D., and Bach, S. (2011). Induction of viable but nonculturable *Escherichia coli* O157:H7 in the phyllosphere of lettuce: a food safety risk factor. *Appl. Environ. Microbiol.* 77, 8295–8302. doi: 10.1128/AEM.05020-11

Drake, S. L., DePaola, A., and Jaykus, L. A. (2007). An overview of *Vibrio vulnificus* and *Vibrio parahaemolyticus*. *Compr. Rev. Food Sci. Food* 6, 120–144. doi: 10.1111/j.1541-4337.2007.00022.x

Ferro, S., Amorico, T., and Deo, P. (2018). Role of food sanitising treatments in inducing the'viable but nonculturable'state of microorganisms. *Food Control.* 91, 321–329. doi: 10.1016/j.foodcont.2018.04.016

Jones, P. M., and George, A. M. (2004). The ABC transporter structure and mechanism perspectives on recent research. *CMLS Cell. Mol. Life Sci.* 61, 682–699. doi: 10.1007/s00018-003-3336-9

Lai, C. J., Chen, S. Y., Lin, I. H., Chang, C. H., and Wong, H. C. (2009). Change of protein profiles in the induction of the viable but nonculturable state of *Vibrio parahaemolyticus*. *Int. J. Food Microbiol.* 135, 118–124. doi: 10.1016/j.ijfoodmicro.2009.08.023

Li, L., Mendis, N., Trigui, H., Oliver, J. D., and Faucher, S. P. (2014). The importance of the viable but non-culturable state in human bacterial pathogens. *Front. Microbiol.* 5:258. doi: 10.3389/fmicb.2014.00258

Liu, Y. F., Zhong, Q. P., Wang, J., and Lei, S. W. (2018). Enumeration of *Vibrio parahaemolyticus* in VBNC state by PMA-combined real-time quantitative PCR coupled with confirmation of respiratory activity. *Food Control.* 91, 85–91. doi: 10.1016/j.foodcont.2018.03.037

McLaughlin, J. B., DePaola, A., Bopp, C. A., Martinek, K. A., Napolilli, N. P., Allison, C. G., et al. (2005). Outbreak of *Vibrio parahaemolyticus* gastroenteritis associated with Alaskan oysters. *N. Engl. J. Med.* 353, 1463–1470. doi: 10.1056/NEJMoa051594

Meng, L., Alter, T., Aho, T., and Huehn, S. (2015). Gene expression profiles of *Vibrio parahaemolyticus* in viable but non-culturable state. *FEMS Microbiol. Ecol.* 91:fiv035. doi: 10.1093/femsec/fiv035

Mizunoe, Y., Wai, S. N., Ishikawa, T., Takade, A., and Yoshida, S. I. (2000). Resuscitation of viable but nonculturable cells of *Vibrio parahaemolyticus* induced at low temperature under starvation. *FEMS. Microbiol. Lett.* 186, 115–120. doi: 10.1111/j.1574-6968.2000.tb09091.x

Nair, G. B., Ramamurthy, T., Bhattacharya, S. K., Dutta, B., Takeda, Y., and Sack, D. A. (2007). Global dissemination of *Vibrio parahaemolyticus* serotype O3:K6 and its serovariants. *Clin. Microbiol. Rev.* 20, 39–48. doi: 10.1128/CMR.00025-06

Oliver, J. D. (2005). The viable but nonculturable state in bacteria. *J. Microbiol.* 43, 93–100.

Oliver, J. D. (2010). Recent findings on the viable but nonculturable state in pathogenic bacteria. *FEMS Microbiol. Rev.* 34, 415–425. doi: 10.1111/j.1574-6976.2009.00200.x

Parada, C., Orruño, M., Kaberdin, V., Bravo, Z., Barcina, I., and Arana, I. (2016). Changes in the *Vibrio harveyi* cell envelope subproteome during permanence in cold seawater. *Microb. Ecol.* 72, 549–558. doi: 10.1007/s00248-016-0802-0

Perez-Acosta, J. A., Martınez-Porchas, M., Elizalde-Contreras, J. M., Leyva, J. M., Ruiz-May, E., Gollas-Galvan, T., et al. (2018). Proteomic profiling of integral membrane proteins. *Microbiol. Immunol.* 62, 14–23. doi: 10.1111/1348-0421.12556

Rees, D. C., Johnson, E., and Lewinson, O. (2009). ABC transporters: the power to change. *Nat. Rev. Mol. Cell Biol.* 10, 218–227. doi: 10.1038/nrm2646

Su, C. P., Jane, W. N., and Wong, H. C. (2013). Changes of ultrastructure and stress tolerance of *Vibrio parahaemolyticus* upon entering viable but nonculturable state. *Int. J. Food Microbiol.* 160, 360–366. doi: 10.1016/j.ijfoodmicro.2012.11.012

Su, Y. C., and Liu, C. C. (2007). *Vibrio parahaemolyticus*: a concern of seafood safety. *Food Microbiol.* 24, 549–558. doi: 10.1016/j.fm.2007.01.005

Wong, H. (2004). Resuscitation of viable but non-culturable *Vibrio parahaemolyticus* in a minimum salt medium. *FEMS Microbiol. Lett.* 233, 269–275. doi: 10.1016/j.femsle.2004.02.015

Wright, P. C., Noirel, J., Ow, S. Y., and Fazeli, A. (2012). A review of current proteomics technologies with a survey on their widespread use in reproductive biology investigations. *Theriogenology* 77, 738–765. doi: 10.1016/j.theriogenology.2011.11.012

Wu, Y. N., Wen, J., Ma, Y., Ma, X. C., and Chen, Y. (2014). Epidemiology of foodborne disease outbreaks caused by *Vibrio parahaemolyticus*, China, 2003-2008. *Food Control.* 46, 197–202. doi: 10.1016/j.foodcont.2014.05.023

Xu, C. G., Wang, S. Y., Ren, H. X., Lin, X. M., Wu, L. N., and Peng, X. X. (2005). Proteomic analysis on the expression of outer membrane proteins of *Vibrio alginolyticus* at different sodium concentrations. *Proteomics* 5, 3142–3152. doi: 10.1002/pmic.200401128

Xu, X. K., Wu, Q. P., Zhang, J. M., Cheng, J. H., Zhang, S. H., and Wu, K. (2014). Prevalence, pathogenicity, and serotypes of *Vibrio parahaemolyticus* in shrimp from Chinese retail markets. *Food Control.* 46, 81–85. doi: 10.1016/j.foodcont.2014.04.042

Yang, W. X., Ding, D. W., Zhang, C. D., Zhou, J., and Su, X. R. (2015). iTRAQ-based proteomic profiling of *Vibrio parahaemolyticus* under various culture conditions. *Proteome Sci.* 13:19. doi: 10.1186/s12953-015-0075-4

Yoon, J. H., Bae, Y. M., and Lee, S. Y. (2017). Effects of varying concentrations of sodium chloride and acidic conditions on the behavior of *Vibrio parahaemolyticus* and *Vibrio vulnificus* cold-starved in artificial sea water microcosms. *Food Sci. Biotechnol.* 26, 829–839. doi: 10.1007/s10068-017-0105-3

Yu, Q. Q., Niu, M. Y., Yu, M. Q., Liu, Y. H., Wang, D. P., and Shi, X. M. (2016). Prevalence and antimicrobial susceptibility of *Vibrio parahaemolyticus* isolated

from retail shellfish in Shanghai. *Food Control.* 60, 263–268. doi: 10.1016/j.foodcont.2015.08.005

Zhao, X. H., Zhong, J. L., Wei, C. J., Lin, C. W., and Ding, T. (2017). Current perspectives on viable but non-culturable state in foodborne pathogens. *Front. Microbiol.* 8:580. doi: 10.3389/fmicb.2017.00580

Zhong, Q. P., Tian, J., Wang, B., and Wang, L. (2016). PMA based real-time fluorescent LAMP for detection of *Vibrio parahaemolyticus* in viable but nonculturable state. *Food Control.* 63, 230–238. doi: 10.1016/j.foodcont.2015.11.043

Zhong, Q. P., Tian, J., Wang, J., Fang, X., and Liao, Z. L. (2018). iTRAQ-based proteomic analysis of the viable but nonculturable state of *Vibrio parahaemolyticus* ATCC 17802 induced by food preservative and low temperature. *Food Control.* 85, 369–375. doi: 10.1016/j.foodcont.2017.10.011

Zieske, L., Huang, Y., Ross, P., Pillai, S., Purkayastha, S., and Pappin, D. (2005). Protein complex and profiling studies using iTRAQ reagent technology. *Comp. Biochem. Phys. A* 141, S247–S248.

Conflict of Interest Statement: The authors declare that the research was conducted in the absence of any commercial or financial relationships that could be construed as a potential conflict of interest.

frontiers in Microbiology

ORIGINAL RESEARCH
published: 06 February 2019
doi: 10.3389/fmicb.2019.00094

Combined Transcriptome and Proteome Analysis of RpoS Regulon Reveals Its Role in Spoilage Potential of *Pseudomonas fluorescens*

Xiaoxiang Liu[1]*, *Jun Xu*[2], *Junli Zhu*[3], *Peng Du*[1] and *Aihua Sun*[1]*

[1] School of Basic Medical Sciences and Forensic Medicine, Hangzhou Medical College, Hangzhou, China, [2] Hangzhou Lin'an District People's Hospital, Hangzhou, China, [3] College of Food Science and Biotechnology, Zhejiang Gongshang University, Hangzhou, China

Microbial contamination is considered the main cause of food spoilage. *Pseudomonas fluorescens* is a typical spoilage bacterium contributing to a large extent to the spoilage process of proteinaceous foods. RpoS is known as an alternative sigma factor controlling stress resistance and virulence in many pathogens. Our previous work revealed that RpoS contributes to the spoilage activities of *P. fluorescens* by regulating resistance to different stress conditions, extracellular acylated homoserine lactone (AHL) levels, extracellular protease and total volatile basic nitrogen (TVB-N) production. However, RpoS-dependent genes in *P. fluorescens* remained undefined. RNA-seq transcriptomics analysis combined with quantitative proteomics analysis based on multiplexed isobaric tandem mass tag (TMT) labeling was performed in the *P. fluorescens* wild-type strain UK4 and its derivative carrying an *rpoS* mutation. A total of 375 differentially expressed coding sequences (DECs) and 212 differentially expressed proteins (DEPs) were identified. The DECs were further verified by qRT-PCR. The combined transcriptome and proteome analyses revealed the involvement of this regulator in several cellular processes, mainly including polysaccharide metabolism, intracellular secretion, extracellular structures, cell wall biogenesis, stress responses, and amino acid and biogenic amine metabolism, which may contribute to the biofilm formation, stress resistance, and spoilage activities of *P. fluorescens*. Moreover, we indeed observed that RpoS contributed to the production of the macrocolony biofilm's matrix. Our results provide insights into the regulatory network of RpoS and expand the knowledge about the role of RpoS in the functioning of *P. fluorescens* in food spoilage.

Keywords: transcriptome, proteome, RpoS, regulon, *Pseudomonas fluorescens*, food spoilage

OPEN ACCESS

Edited by:
Maria Fiorella Mazzeo, Istituto di Scienza dell'Alimentazione (ISA), Italy

Reviewed by:
Paola Roncada, Università degli Studi Magna Græcia di Catanzaro, Italy
Josselin Noirel, Conservatoire National des Arts et Métiers (CNAM), France

***Correspondence:**
Xiaoxiang Liu
liuxiaoxiang413@126.com
Aihua Sun
aihuasun@126.com

Specialty section:
This article was submitted to Food Microbiology, a section of the journal Frontiers in Microbiology

Received: *02 September 2018*
Accepted: *16 January 2019*
Published: *06 February 2019*

Citation:
Liu X, Xu J, Zhu J, Du P and Sun A (2019) Combined Transcriptome and Proteome Analysis of RpoS Regulon Reveals Its Role in Spoilage Potential of Pseudomonas fluorescens. Front. Microbiol. 10:94. doi: 10.3389/fmicb.2019.00094

INTRODUCTION

Most food products are highly perishable as they contain rich nutrient contents for microbial development. *Pseudomonas fluorescens* is a common spoilage microorganism in proteinaceous raw foods stored under aerobic refrigerated conditions, such as dairy products (Andreani et al., 2015), meat (Remenant et al., 2015), and seafoods (Xie et al., 2018). As a spoiler, *P. fluorescens* can produce ammonia, amine, ketones, aldehydes, esters, organic acids and non-H_2S sulfides with

spoilage off-odors and off-flavors (Ghaly et al., 2010). Moreover, it also causes spoilage by producing heat-stable lipases and proteases (Rajmohan et al., 2002), biofilms (Aswathanarayan and Vittal, 2014), biosurfactants (Mellor et al., 2011), siderophores (Liu et al., 2017), pigments (Andreani et al., 2014), and quorum-sensing signaling molecules (Liu et al., 2018). So far, the knowledge of regulatory mechanisms of bacterial spoilage is still very limited.

RpoS is an alternative sigma factor of RNA polymerase that was first described in *Escherichia coli* (Hengge-Aronis, 1999). Homologs of RpoS have also been characterized in the γ, β, and δ subclasses of *Proteobacteria* (Núñez et al., 2006; Dong and Schellhorn, 2010). A sigma factor is needed by the RNA core polymerase to recognize promoters and initiate transcription. In addition to housekeeping sigma factors controlling the transcription of the majority of genes, including essential genes, bacteria possess alternative sigma factors that recognize specific set of promoters (Schellhorn, 2014). RpoS is an alternative sigma factor induced in stationary growth phase and under stress conditions (Landini et al., 2014). Consequently, *rpoS* deficient mutants are sensitive to nutrient starvation, heat, osmolarity, acidic pH, oxidative stress, and are usually altered for virulence (Dong and Schellhorn, 2010). RpoS regulates the production of alginate, exotoxin A, and secreted proteases in *Pseudomonas aeruginosa* (Suh et al., 1999; Sonnleitner et al., 2003); the formation of virulence factor curli in *E. coli* (Mika and Hengge, 2014); the secretion of extracellular proteases and siderophores in *Burkholderia pseudomallei* (Wongtrakoongate et al., 2012); and the generation of flagella, exopolysaccharides, and biofilms in *Yersinia pseudotuberculosis* (Guan et al., 2015). The involvement of RpoS in stress resistance and virulence suggests that RpoS may play a key role in modulating the spoilage activity of *P. fluorescens* in food systems. Our previous work revealed that RpoS contributes to spoilage potential in *P. fluorescens* by regulating resistance to different stress conditions, extracellular AHL levels, extracellular proteases and TVB-N production (Liu et al., 2018). However, it remains unknown how many genes are regulated by this transcriptional regulator.

RpoS regulons have been characterized by microarrays in *E. coli* and *P. aeruginosa*. RpoS controls a large regulon consisting of 10% of the genome in the *E. coli* strain K12 in the stationary phase and under stress conditions (Patten et al., 2004; Dong and Schellhorn, 2009). In *P. aeruginosa*, 772 genes are regulated by RpoS in the stationary but not in the logarithmic growth phase, including over 40% of all genes controlled by quorum sensing (Schuster et al., 2004). In addition, the RpoS regulon of *B. pseudomallei* has been identified using a proteomics approach, and 70 differentially expressed proteins were identified (Osiriphun et al., 2009). RNA sequencing (RNA-seq) is an attractive method to monitor global transcriptomic changes, overcoming many defects of traditional DNA microarrays (Marioni et al., 2008). Proteomic sequencing is an important technique to explore changes in gene expression at protein levels. The latest protein quantitative analysis technology based on mass spectrometry (MS) and multiplexed isobaric TMT labeling is widely used (Ahrné et al., 2016; Han, 2017). Thus, combining the two techniques should substantially improve the global view of the regulatory roles of RpoS.

To better understand the role of RpoS in the spoilage activity of *P. fluorescens*, we combined transcriptome and proteome analyses in the *P. fluorescens* wild-type strain UK4 and the *rpoS* mutant in stationary phase to identify the RpoS regulon. We found that RpoS influenced the expression of a large number of CDSs at the mRNA and protein levels. The DECs were verified by quantitative real-time PCR (qRT-PCR). The function of the RpoS regulon was further analyzed by COG (cluster of orthologous groups) categorization, GO (gene ontology) enrichment, and KEGG (Kyoto encyclopedia of genes and genomes) enrichment. Our study revealed the large impact of RpoS on gene expression at the mRNA level and protein level, providing insights into the spoilage function of *rpoS* in *P. fluorescens*.

Abbreviations: AHL, Acylated homoserine lactone; COG, Cluster of orthologous groups; DECs, Differentially expressed coding sequences; DEPs, Differently expressed proteins; DTT, Dithiothreitol; EDTA, Ethylene diamine tetraacetic acid; FPKM, Fragments per kilobase of transcript sequence per millions base pairs sequenced; GO, Gene ontology; HPLC, high-performance liquid chromatography; KEGG, Kyoto encyclopedia of genes and genomes; MS, Mass spectrometry; NB, Nutrient broth; qRT-PCR, quantitative real-time PCR; RNA-seq, RNA sequencing; TEAB, Tetraethyl-ammonium bromide; TEM, Transmission electron microscopy; TMT, Tandem mass tag; UPLC, Ultra performance liquid chromatography.

MATERIALS AND METHODS

Bacterial Strains and Culture Conditions

The wild-type strain UK4 and the *rpoS* in-frame deletion mutant of *P. fluorescens* (Liu et al., 2018) were grown aerobically at 28°C with shaking at 220 rpm in nutrient broth (NB) medium, and growth was monitored spectrophotometrically at OD_{600}. Cultures were grown in triplicates and the bacterial cells at stationary-phase ($OD_{600} \approx 1.5$) were harvested by centrifugation at 7,000 g for 10 min, then frozen in liquid nitrogen immediately for RNA and protein isolation.

Illumina Library Preparation and RNA-seq

Three biological replicates were prepared for the wild-type strain and the *rpoS* mutant. The total RNA was isolated using an RNeasy Plant Mini Kit (Qiagen, Germany) and was treated with an RNase-Free DNase Set (Qiagen, Germany) to remove the contaminating DNA. The concentration and quality were determined using a NanoDrop spectrophotometer (Thermo, USA) and Agilent 2100 Bioanalyzer (Agilent, USA). Then, rRNA from the total RNAs was removed using a Ribo-Zero Magnetic Kit (Epicentre, USA) for Gram-negative bacteria as per the manufacturer's protocol. Fragmentation buffer was added to cleave the mRNA into short fragments. Strand-specific RNA sequencing libraries were constructed according to a modified deoxy-UTP (dUTP) strand-marking protocol as described previously (Borodina et al., 2011). Briefly, first strand cDNA was synthesized using random hexamer primers and M-MuLV Reverse Transcriptase (NEB, USA). Double-stranded cDNA was subsequently synthesized with dUTP incorporation into the second strand. Illumina TruSeq adaptors were ligated to the ends of the cDNA fragments, and then amplified with the adaptor primers according to the manufacturer's instructions

(Illumina, USA). The fragments were purified with an AMPure XP system (Beckman Coulter, USA) to select cDNA fragments of preferentially 150∼200 bp in length. Then the dUTP-marked strand was selectively degraded using USER enzyme (NEB, USA) and the remaining strand was amplified to produce a cDNA library suitable for sequencing. Following validation with the Agilent Bioanalyzer 2100 system (Agilent, USA), the cDNA library was sequenced on a flow cell using high-throughput 150-bp pair-end mode on an Illumina HiSeq 4000 platform (Illumina, USA).

Analysis of RNA-seq Data

The raw sequencing data of RNA-seq was deposited to the Short Reads Archive of NCBI with accession numbers SRP158301 (https://www.ncbi.nlm.nih.gov/sra/). Clean data (clean reads) were obtained by removing adapter-containing reads, higher N rate reads (N rates > 10%), and low-quality reads (50% bases with Q-score ≤ 5) from the raw data (raw reads) using in-house Perl scripts. At the same time, the Q20, Q30 and GC content of the clean reads were calculated. Of the clean reads, the Q20 and Q30 values were > 98 and 95%, respectively, showing that the data were of high quality (**Supplementary Table S1**). All downstream analyses were based on the high-quality clean data. Sequence alignment with the reference UK4 genome sequence (Dueholm et al., 2014) was conducted by Bowtie2-2.2.3 (Langmead and Salzberg, 2012). The software parameter mismatch was set to 2, and other parameters were default values. Subsequent analyses were based on the unique mapped reads. For gene expression analysis, HTSeq v0.6.1 was used to count the read numbers mapped to each gene. And then FPKM (Fragments Per Kilobase of transcript sequence per Millions base pairs sequenced) of each gene was calculated (Trapnell et al., 2012). The FPKM value was directly used for comparing differences in gene expression among samples, as this method removes effects caused by sequencing depth and gene length in calculating gene expression. The CDSs with FPKM > 1 were considered to be expressed. The software package DESeq R 1.18.0 was used to calculate the fold-change of transcripts and to screen all DECs (Wang et al., 2010). DESeq provides statistical routines for determining differential expression in digital CDS expression data using a model based on the negative binomial distribution. The resulting *p*-values were adjusted using Benjamini and Hochberg's approach for controlling the false discovery rate. The criteria of significant difference expression were $|\log_2$ fold change$| \geq 1$ and adjusted *p*-value (padj) ≤ 0.05. Putative operons analysis are based on chromosomal organization and similarity of transcript patterns. The criteria used to generate a list of potential operons were that every CDS within a gene cluster was in the same orientation, that every CDS had the same trend in differential expression, that the absolute transcript profiles of the candidate CDSs in an operon showed patterns similar to each other, and that the intergenic region between two adjacent CDSs was <250 bp (Schuster et al., 2004).

Protein Extraction and LC-MS/MS Analysis

Protein extraction and LC-MS/MS analysis were performed using the protocol described previously (Guerreiro et al., 2014; Peng et al., 2018) with a few modifications. Briefly, a sample was sonicated three times on ice in lysis buffer containing 8 M urea, 2 mM EDTA, 10 mM DTT, and 1% Protease Inhibitor Cocktail (Sigma-Aldrich, USA). After centrifugation at 20,000 g at 4°C for 10 min, the debris was removed, and the supernatant was precipitated with cold 15% trichloroacetic acid for 4 h at −20°C. After centrifugation at 4°C for 3 min, the obtained precipitate was washed with cold acetone three times. The protein precipitate was redissolved in buffer (8 M urea, 100 mM TEAB, pH 8.0), and the protein concentration in the supernatant was determined by a 2-D Quant kit (GE Healthcare, USA) according to the manufacturer's protocol. The protein solution was reduced with 5 mM DTT for 30 min at 56°C and alkylated with 11 mM iodoacetamide for 15 min at room temperature in the dark. For trypsin digestion, the protein sample was diluted with buffer (200 mM TEAB, < 2 M urea). Finally, trypsin was added to approximately 100 μg protein for each sample at an enzyme:protein ratio of 1:50 for the first overnight digestion and an enzyme:protein ratio of 1:100 for a second 4-h digestion. After trypsin digestion, peptides were desalted by a Strata X C18 SPE column (Phenomenex, USA) and vacuum-dried. The digested peptides were reconstituted in 1 M TEAB and were labeled using a 6-plex TMT kit (Thermo, USA) according to the manufacturer's instructions to perform protein quantitation. The peptides from the six samples of UK4 and the *rpoS* mutant were labeled with 126, 127, 128, 129, 130, and 131 TMT reagents, respectively. Each sample was mixed and then fractionated using high pH reverse-phase HPLC with an Agilent 300 Extend C18 column (5 μm particles, 4.6 mm inner diameter, 250 mm length). Briefly, peptides were first separated with a gradient of 2–60% acetonitrile in 10 mM ammonium bicarbonate (pH 9.0) over 80 min into 80 fractions. Then, the peptides were combined into 18 fractions and dried by vacuum centrifugation. For LC-MS/MS analysis, peptides were dissolved in 0.1% formic acid, and loaded onto a reversed-phase pre-column directly (Acclaim PepMap 100, Thermo, USA). Peptide separation was carried out using a reversed-phase analytical column (Acclaim PepMap RSLC, Thermo, USA). The gradient was comprised of an increase from 5 to 25% of solvent B (0.1% formic acid in 98% acetonitrile) over 26 min, 25–40% over 8 min, 80% over 3 min, then held at 80% for the last 3 min, all at a constant flow rate of 350 nl/min on an EASY-nLC 1000 UPLC system (Thermo, USA). The peptides were subjected to nanoelectrospray ionization followed by tandem MS in Q Exactive (Thermo, USA) coupled online to the UPLC. Intact peptides were detected in the orbitrap at a resolution of 70,000. Peptides were selected for MS/MS using Normalized Collision Energy (NCE) setting as 28. Ion fragments were detected in the orbitrap at a resolution of 17,500. Three biological replicates for each strain were used for proteomic analyses.

Proteomics Data Processing

The MS proteomics data was deposited to the ProteomeXchange Consortium with the dataset identifier PXD010845 (https://www.ebi.ac.uk/pride/archive/). The MS/MS data was processed using MaxQuant with the integrated Andromeda search engine (v.1.5.2.8). Tandem mass spectra were searched against the

genome database of *P. fluorescens* UK4 containing 5321 proteins in GenBank (https://www.ncbi.nlm.nih.gov/genome/150?genome_assembly_id=204445). Trypsin was chosen as cleavage specificity allowing up to two missing cleavages. Carbamidomethyl on Cys was specified as a fixed modification, while oxidation on Met and acetylation on protein N-term were specified as variable modifications. Mass error was set to 10 ppm for precursor ions and 0.02 Da for fragment ions. For protein quantitation, protein quantitative ratios were weighted and normalized relative to the median ratio in Mascot (http://www.matrixscience.com). Only proteins with significant quantitative ratios between the two strains ($p < 0.05$) and with fold changes >1.2 or <0.83 were considered to be differentially expressed (Ning et al., 2018).

qRT-PCR

To confirm the RNA-Seq results, 30 DECs from the RNA-Seq analysis were selected, and qRT-PCR was carried out to verify the expression changes of these 30 DECs. The qRT-PCRs were performed with RNA samples used for RNA-seq. The total RNA was reverse transcribed to single-stranded cDNA using a hexamer primer and SuperScript III First-Strand Synthesis SuperMix (Invitrogen, USA). Quantitative real-time PCR was performed on a CFX384 Touch Real-Time PCR Detection System (Bio-Rad, USA) using Power SYBR1 Green PCR Master Mix (Applied Biosystems, USA) according to the manufacturers' instructions. Gene-specific primers are listed in **Supplementary Table S2**, and the 16S rRNA gene was used as the internal control to normalize mRNA abundance between samples (Leneveu-Jenvrin et al., 2015). PCR was performed according to the following steps (two-step PCR amplification procedure): 1 min at 95°C, 40 cycles of 15 s at 95°C, and 25 s at 63°C. Melting curve analysis of amplification products was performed to evaluate the specificity of the amplification. The relative expression was calculated using the $2^{-\Delta\Delta Ct}$ method (Livak and Schmittgen, 2001). Samples were run in triplicate, and the experiments were repeated at least three times.

COG Categorization

Function description of DECs and DEPs was performed according to a *P. fluorescens* UK4 genome annotation (http://www.pseudomonas.com/) and relative reports. COG functional categories for the DECs and DEPs were conducted according to the NCBI COG database (http://www.ncbi.nlm.nih.gov/COG/) and the function descriptions.

GO and KEGG Enrichment Analysis

The GO and KEGG pathway annotations for DECs and DEPs were performed using the UniProt-GOA database (http://www.ebi.ac.uk/GOA/) and KEGG database (http://www.kegg.jp/kegg/pathway.html). A two-tailed Fisher's exact test was employed to test the enrichment of the DECs and DEPs against all identified genes and proteins. Corrections for multiple hypothesis testing were carried out using standard false discovery rate control methods. GO and KEGG pathways with $p < 0.05$ were considered significant.

Transmission Electron Microscopy (TEM) of Macrocolony Biofilm

The wild-type strain UK4 and the *rpoS* mutant were grown overnight in liquid NB medium under aeration at 28°C. A total of 5 μl of the overnight cultures was spotted on Congo red plates (1% tryptone, 1% agar, 20 μg/ml Congo red, and 10 μg/ml Coomassie brilliant blue G250) (Friedman and Kolter, 2004). Plates incubated at 28°C for up to 7 days were used to judge colony morphology and color. For TEM, the macrocolonies were scraped from the agar plates (without Congo red and Coomassie brilliant blue G250) gently and were fixed with 2.5% glutaraldehyde for 2 h at room temperature, then the macrocolonies were postfixed, dehydrated, embedded in TAAB resin, ultrathin sectioned, and stained according to the protocol previously described (Zhang et al., 2012). The macrocolony biofilms were observed under a transmission electron microscope (Hitachi H-600, Japan).

RESULTS

Overview of Transcriptomic and Proteomic Data

Our previous studies suggested that RpoS plays a global regulatory role in the stress resistance, quorum sensing and spoilage potential of *P. fluorescens*. In the present study, as a further step to investigate the regulatory role of RpoS, we applied combined transcriptome and proteome analyses to establish the set of CDSs or proteins belonging to the RpoS regulon. We compared *P. fluorescens* wild-type strain UK4 with its derivative, the *rpoS* mutant, which has a 705 bp segment deletion inside the *rpoS* coding region (Liu et al., 2018). For transcriptome analysis, three RNA-Seq libraries were prepared for each strain grown to the stationary phase under the same conditions. After filtering through the raw reads, there were on average 17,442,829 clean reads for UK4 and 18,902,146 for the mutant, giving rise to an average 2.62 G and 2.84 G of total clean bases, respectively (**Supplementary Table S1**). The clean reads of the *P. fluorescens* transcriptome were mapped to the genome sequence of UK4. The unique mapped rates to the genome were at least 97.7% in all samples (**Supplementary Table S3**). In the genome of UK4, 98.90% of CDSs were quantified. All the detailed data of the CDSs from RNA-seq are shown in **Supplementary Table S4**. For proteome analysis, a total of 135,890 spectra generated from 3 biological replicates of UK4 and the *rpoS* mutant were analyzed using the Andromeda search engine. There were 35,804 spectra matched with proteins of UK4, comprising 19,399 peptides and 19,345 unique peptides. Finally, 2730 protein were identified, among which 2,559 proteins were quantified. The detailed information of protein MS data are shown in **Supplementary Table S5**.

Identification of DECs and DEPs

At the mRNA level, a total of 372 DECs were identified using the statistical criteria ($|\log_2$ fold change$| \geq 1$, padj ≤ 0.05). Among these DECs, 352 were significantly downregulated and 20 were significantly upregulated in the *rpoS* mutant

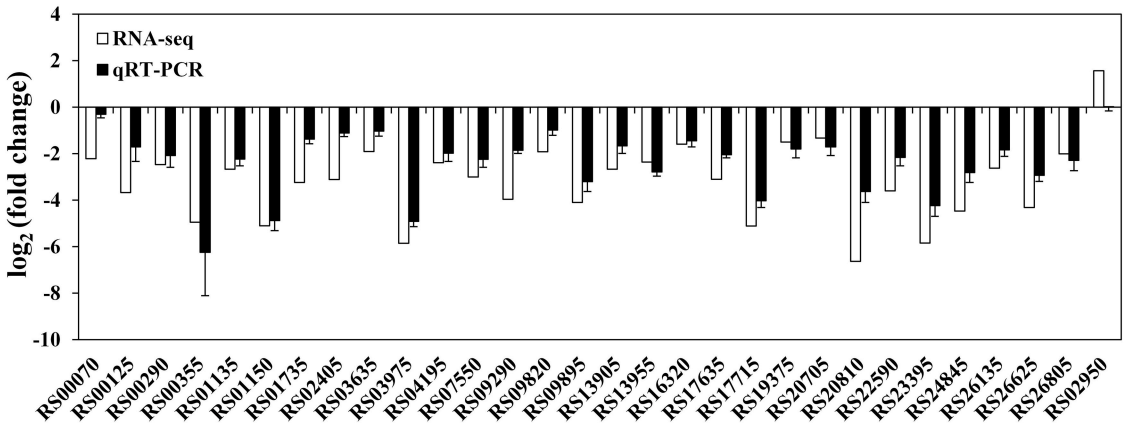

FIGURE 1 | Validation of RNA-seq data using qRT-PCR. White bars represent RNA-seq data, while the black bars represent mean values of $\log_2$ (fold change) observed for the *rpoS* mutant samples vs. the wild-type samples. The qRT-PCR results are the mean of three biological replicates with three technical replicates for each gene. Error bars represent standard deviation.

compared to the wild-type strain (**Supplementary Figure S1**), and 155 DECs were found to be organized in 50 supposed operons. The CDS locus tags, putative operon organization, readcounts, $\log_2$ (fold change), padj, CDS product descriptions, COG protein categories, and GO and KEGG annotations of the DECs are provided in **Supplementary Table S6**. To validate the data generated from the RNA-seq experiment, 29 downregulated and 1 upregulated CDSs were randomly selected from the DECs to verify their expression by qRT-PCR. The qRT-PCR results agreed with RNA-seq data, except for CDS RS02950 (**Figure 1**), indicating that our RNA-seq results are reliable.

At protein levels, proteins with significant quantitative ratios between the *rpoS* mutant and the wild-type strain ($p < 0.05$) and with fold changes > 1.2 or < 0.83 were considered as DEPs. In brief, a total of 212 DEPs were identified, of which, 140 proteins were downregulated in the *rpoS* mutant, and 72 proteins were upregulated (**Supplementary Figure S2**; **Supplementary Table S7**).

The relationship between the transcriptome and proteome data were further analyzed. The 372 DECs and 212 DEPs identified were used to perform correlation analysis, and a total of 99 candidates were obtained in the overlap of transcriptome and proteome datasets (**Figure 2**; **Supplementary Table S8**). The 99 DEPs (46.7% of the total DEPs) were consistent with the tendency of the change in abundance of the mRNA. In general, in both bacteria and eukaryotes, mRNA formation is only partially correlated with protein synthesis (Maier et al., 2011; Vogel and Marcotte, 2012; Lv et al., 2017). Maybe it is because the RNA-seq detection is much more sensitive than proteome determination, or because of post-transcriptional, translational and protein degradation regulation (Maier et al., 2009; Zhang et al., 2018). Thus, we can obtain useful insight that is otherwise impossible to obtain from individual analysis of mRNA or protein expressions by combing analysis of transcriptomic and proteomic data (Oshone et al., 2017).

Functional Analysis of DECs and DEPs

The DECs and DEPs were classified using their functional annotations in GenBank or through homology with protein functions determined from the COG database (**Figure 2**). COG functional analysis assigned DECs and DEPs to 22 predicted pathways. According to the number of the DECs and DEPs, except for groups with function unknown (COG S) and general function prediction only (COG R), the top 5 groups were related to signal transduction mechanisms (COG T), carbohydrate transport and metabolism (COG G), amino acid transport and metabolism (COG E), transcription (COG K), and inorganic ion transport and metabolism (COG P).

The DECs and DEPs were combined, and GO enrichment analysis was performed (**Supplementary Table S9**). The significantly enriched GO functions are shown in **Figure 3**. At the biological process level, the DECs and DEPs were mainly involved in the phosphorelay signal transduction system, cell communication, response to stimulus, polysaccharide metabolic process, and protein secretion. At the molecular function level, the DECs and DEPs were mainly enriched in transferase activity transferring hexosyl groups, oxidoreductase activity acting on peroxide as an acceptor, and hydrolase activity hydrolyzing O-glycosyl compounds.

Additionally, the transcriptome and proteome datasets were also used for KEGG pathway enrichment analysis. All the DECs and DEPs were combined and were significantly enriched in six pathways, including biofilm formation, starch and sucrose metabolism, two-component system, oxidative phosphorylation, sulfur metabolism, and amino sugar and nucleotide sugar metabolism (**Figure 4**; **Supplementary Table S10**). In addition, the combined DECs and DEPs were divided into six categories according to their protein-mRNA regulation types (**Figure 5**; **Supplementary Table S10**). In the cluster with protein and mRNA both downregulated in the mutant, the significantly enriched pathways were biofilm formation, two-component system and amino sugar and nucleotide sugar metabolism. In

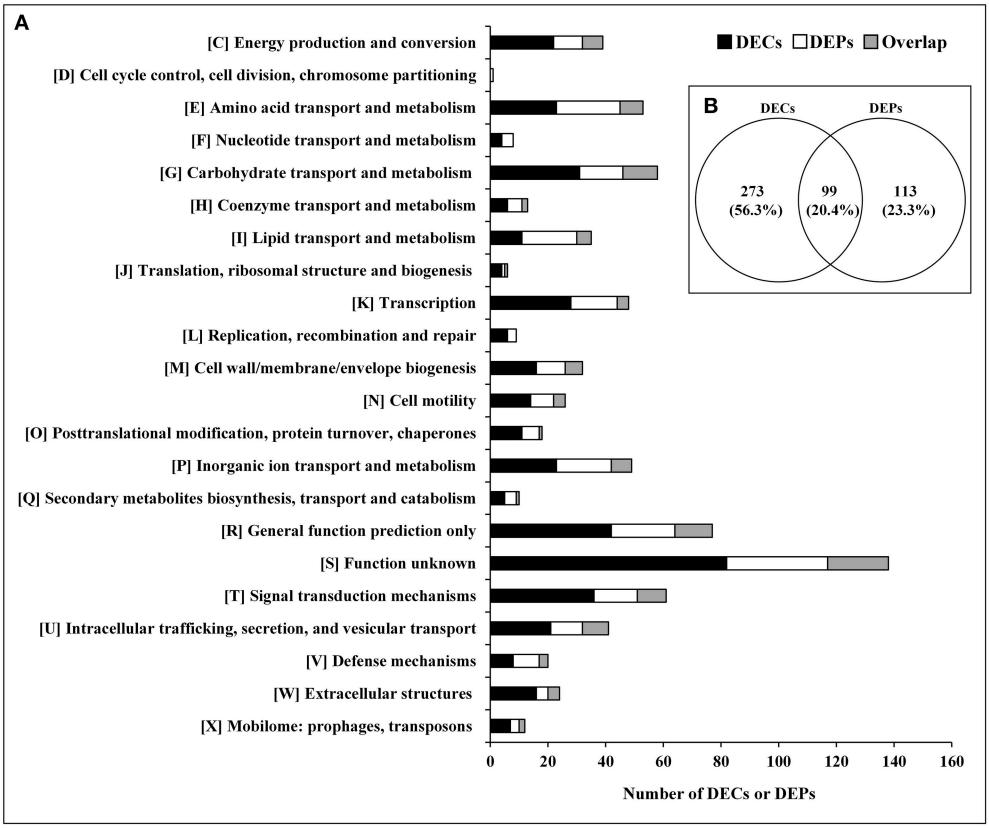

FIGURE 2 | DECs and DEPs in the *rpoS* mutant in relation to the wild-type strain UK4. **(A)** Classification of the DECs, DEPs, and their overlap into individual functional groups (COGs C-X). **(B)** Venn diagram of DECs and DEPs. This figure was drawn using Venny 2.0 (http://bioinfogp.cnb.csic.es/tools/venny/index.html).

the cluster with protein and mRNA both upregulated, only the pathway ABC transporters were significantly enriched. In the cluster with only protein downregulated, the functions were mainly enriched in benzoate degradation, glutathione metabolism, beta-alanine metabolism, and quorum sensing. In the cluster with only protein upregulated, the two pathways, sulfur metabolism and biofilm formation, were significantly enriched. In the cluster with only mRNA downregulated, the functions were mainly enriched in starch and sucrose metabolism, biofilm formation, oxidative phosphorylation, two-component system and cationic antimicrobial peptide resistance. In the cluster with only mRNA upregulated, the functions were mainly involved in sulfur metabolism and ABC transporters.

Effects of *rpoS* Mutation on Macrocolony Biofilm Formation

Macrocolony biofilms that form on nutrient-providing semi-solid agar plates reflect the conditions of biofilms that grow on decaying organic materials such as soil or human food. We compared macrocolony biofilms of the *rpoS* mutant and the wild-type. Macrocolonies of the strains were grown for 3–7 d at 28°C on agar plates containing Congo red. Seven-day-old macrocolony are shown in **Figure 6**. The wild-type strains formed red and wrinkled macrocolonies whereas the *rpoS* mutant macrocolonies were pale pink and smooth. In addition, we used TEM to visualize the macrocolonies at the cellular level. Although both colonies of the wild-type and the mutant contained rod-shaped cells, it was apparent that the wild-type cells were embedded in an extracellular matrix that formed basket-like networks whereas the extracellular matrix of the mutant cells was disordered and of lower content than the wild-type. These results suggest that RpoS is involved in the production of the biofilm matrix.

DISCUSSION

Our previous work showed that the spoilage activities of *P. fluorescens* were regulated by RpoS. To better understand its network, mechanisms, and association with spoilage activities, we report here for the first time, the initial characterization of the RpoS regulon in an important spoilage bacterium *P. fluorescens*, via combined transcriptomic and proteomic analyses. In this section, we discuss the most interesting pathways regulated by RpoS. The representative DECs and DEPs are listed in **Table 1**.

Transcription Factors and Signal Transduction

According to the COG functional category, except for the CDSs categorized as COG S or COG R, Group K and

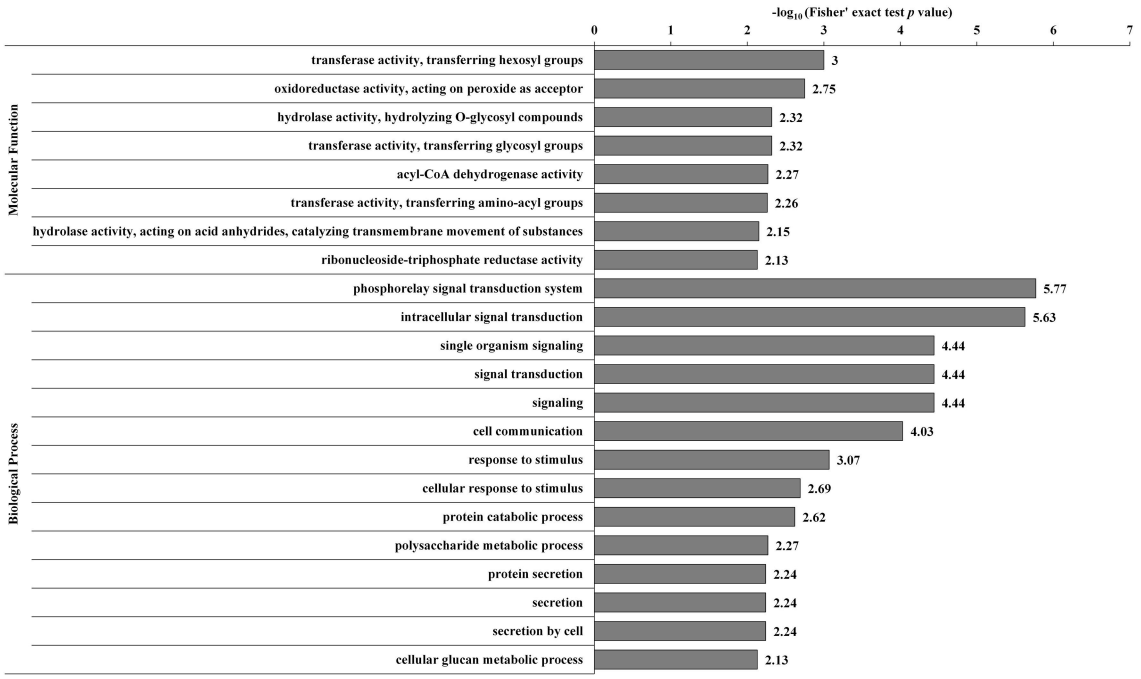

FIGURE 3 | GO-based enrichment analysis of the combined DECs and DEPs. GO categories significantly enriched ($p < 0.05$) are shown in the figure.

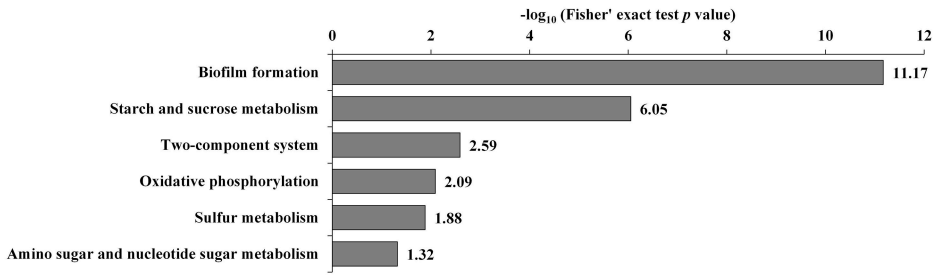

FIGURE 4 | KEGG pathway enrichment analysis of the combined DECs and DEPs. KEGG pathways significantly enriched ($p < 0.05$) are shown in the figure.

Group T were the two top groups (**Figure 2**). The GO and KEGG analyses also showed that signal transduction and two-component system were significantly enriched (**Figures 3**, **4**), and most of these CDSs were downregulated at the mRNA and protein levels in the *rpoS* mutant. As shown in **Table 1**, the operon RS01140-35 encoding homologs of the quorum-sensing system RhlR-RhlI was significantly downregulated in the *rpoS* mutant. This agrees with our previous result that RpoS positively regulates AHL synthesis (Liu et al., 2018). The adjacent operon RS01150-45 (*rhlAB*) that is involved in rhamnolipid biosurfactant synthesis, was also positively regulated by RpoS. In *P. aeruginosa*, RhlR-RhlI regulates the *rhlAB* operon and affects rhamnolipid biosurfactant synthesis (Reis et al., 2011). Biosurfactants can play an important role in the bacterial spoilage process. *P. fluorescens* leads to the spoilage of aerobically stored chicken meat by producing biosurfactants that can make nutrients more freely available and providing the strains producing them with a competitive advantage (Mellor et al., 2011). The operon RS10680-50 (*wspABCDEFR*), coding for a chemosensory system, and the regulation proteins RsmA, HsbA, and HsbR have all been observed to regulate biofilm formation of *P. aeruginosa* (Hickman et al., 2005; Hsu et al., 2008; Irie et al., 2010). RpoS also positively regulates the response regulator NtrC of the two-component system NtrB-NtrC, which is involved in nitrogen metabolism. In *P. fluorescens* SBW25, deletion of *ntrC* eliminates the degradation and the utilization of 28 nitrogen substrates (Zhang and Rainey, 2008). Several regulators related to stress resistance are regulated by RpoS, such as BasR and RpoE (Haines-Menges et al., 2014; Rubin et al., 2015). In addition, many CDSs coding for protein kinases and diguanylate cyclase/phosphodiesterase were downregulated in the *rpoS* mutant, and these enzymes may play an important role in signal transduction. Accordingly, RpoS is a global regulator showing direct or indirect control

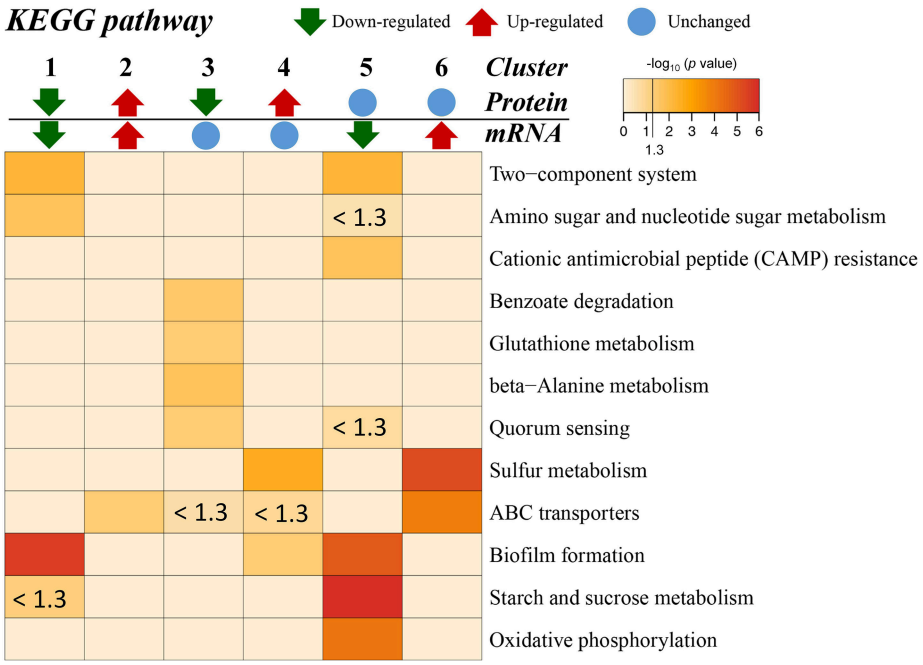

FIGURE 5 | KEGG pathway enrichment for different categories based on protein-mRNA regulation types. 1, the cluster with protein and mRNA both downregulated in the mutant; 2, the cluster with protein and mRNA both upregulated in the mutant; 3, the cluster with only protein downregulated in the mutant; 4, the cluster with only protein upregulated in the mutant; 5, the cluster with only mRNA downregulated in the mutant; 6, the cluster with only mRNA upregulated in the mutant. The pathways with $p < 0.05$ [$-\log_{10}(p) > 1.3$] are considered significant. The color intensity presents the enrichment level as shown in the bar of $-\log_{10}(p)$. The deep red color codes represent the remarkable enriched pathways. The pale yellow in background represents there is no enrichment in the corresponding pathway.

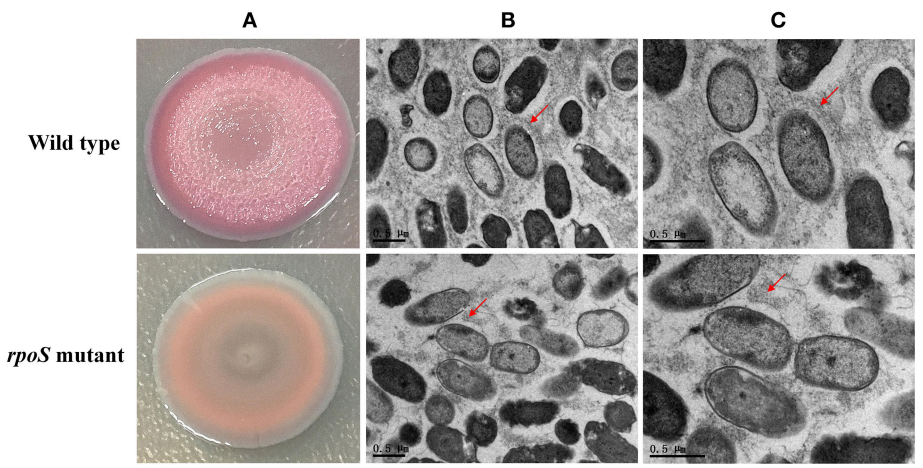

FIGURE 6 | Macrocolony biofilm properties of the *rpoS* mutant in comparison to the wild-type. **(A)** Macrocolony morphology of the wild-type and the *rpoS* mutant grown on Congo red and Coomassie brilliant blue plates for 7 days. **(B,C)** Transmission electron micrographs of the macrocolony biofilms at ×11,500 and ×20,500 magnification. Matrix materials surrounding the cells are marked with red arrows.

of many secondary transcription factors and signal transducing proteins.

Polysaccharide Metabolism

According to the COG analysis and GO enrichment analysis, a large part of DECs and DEPs were involved in the synthesis of various polysaccharides. There was a large operon, RS00125-070, that showed strong downregulation in the *rpoS* mutant at the mRNA and protein levels (**Table 1**). This operon is homologous to the *psl* operon of *P. aeruginosa*, a locus encoding a potential exopolysaccharide that is essential for biofilm formation (Jackson et al., 2004). The operon contained

12 co-transcribed CDSs. Among the 12 CDSs, 8 CDSs were enriched in the biofilm pathway of *P. aeruginosa* (**Figure 4**; **Supplementary Table S10**). As shown in **Figure 6**, *P. fluorescens* UK4 formed red and wrinkled macrocolony biofilms on agar plates containing Congo red, whereas the *rpoS* mutant did not. Congo red binds extracellular matrix components of bacteria, such as polysaccharides and amyloid adhesins (Larsen et al., 2007; Irie et al., 2010). Moreover, the results of TEM showed that most cells of UK4 macrocolony biofilms were surrounded by extracellular matrix, which was more disordered and much less than in the *rpoS* mutant. Similar to the present results, Irie et al. (2010) found that RpoS is a positive transcriptional regulator of *psl* gene expression in *P. aeruginosa* PAO1, and Psl overproduction confers rugose and red small colony variant morphology on Congo red plates. In *E. coli*, RpoS regulates the formation of wrinkled and red macrocolony biofilms on Congo red plates by controlling the production of cellulose and curli fibers (Mika and Hengge, 2014). Our results suggest that RpoS possibly regulates the formation of macrocolony biofilm by positively regulating the expression of *psl* genes coding for polysaccharide synthesis in *P. fluorescens*. Bacteria in biofilms are generally well-protected against environmental stress, and consequently, they are extremely difficult to detect and eradicate in food processing environments.

In addition, several CDSs and proteins were significantly enriched in the starch and sucrose metabolism pathway (**Figures 4**, **5**). They are associated with glycogen and trehalose metabolism, and are mainly located in two tandem operons, RS03630-55 and RS03680-70. These DECs were downregulated in the *rpoS* mutant, suggesting that RpoS positively regulated glycogen and trehalose metabolism. These results were similar to a previous report showing that RpoS regulates the expression of the carbon storage genes for the biosynthesis and degradation of glycogen and the osmoprotectant trehalose in *Salmonella* (Lévi-Meyrueis et al., 2014). Glycogen and trehalose are two important storage metabolites, and their amounts change in response to a number of environmental stresses, such as osmotic, oxidative, and cold stress (Dalmasso et al., 2012; Kobayashi et al., 2015). Additionally, the glycogen biosynthesis enzymes GlgC, GlgA, and GlgP have been observed to play key roles in the formation of biofilms in *E. coli*. Stress resistance and biofilm formation are important factors for the spoilage activities of bacteria (Van Houdt and Michiels, 2010). Thus, RpoS might regulate spoilage activities by controlling polysaccharide synthesis in *P. fluorescens*.

Intracellular Secretion and Extracellular Structures

Two tandem operons, RS20810-20775 and RS20815-20825, related to pilus formation, were notably downregulated in the *rpoS* mutant at the mRNA and protein levels (**Table 1**). The operon RS20810-775 contains 8 CDSs, including 2 CDSs coding for proteins RcpC and RcpA, 5 CDSs coding for TadZ, TadA, TadB, TadC, and TadD, and 1 coding for a hypothetical protein. The other operon RS20815-25 contains 3 CDSs, among which RS20815 and RS20825 code for Flp family type IVb pilins, and RS20820 codes for a response regulator. The homologs of the two operons are both required for the formation of adhesive Flp pili in *Aggregatibacter actinomycetemcomitans* (Clock et al., 2008). In addition, RS03975 codes for a β-barrel membrane pore, which is analogous to the *Pseudomonas* FapF protein involved in the transport of amyloid-like fimbriae monomers (Rouse et al., 2018). The *fapF* gene belongs to the operon *fapABCDEF* related to amyloid-like fimbriae formation (Zeng et al., 2015). However, according to our results, only the *fapF* gene of the operon was regulated by RpoS, suggesting that *fapF* may have an independent promoter. Flp pili and amyloid-like fimbriae have been reported to be essential for adherence, colonization, and biofilm formation in many bacteria (de Bentzmann et al., 2006; Romero et al., 2010; Stenvang et al., 2016), and they may also contribute to macrocolony biofilm formation in addition to exopolysaccharide in *P. fluorescens*. Pilus formation is likely another factor responsible for the spoilage activity of *P. fluorescens*.

Cell Wall Biogenesis

Several genes associated with cell wall biogenesis were differentially expressed in the analyzed strains (**Figure 2**). In the functional group (COG M), RS02640, RS26590 and the operon RS09290-325 were remarkably downregulated in the *rpoS* mutant at the mRNA and protein levels. RS02640 codes for an LPS O-antigen chain length determinant protein, and RS26590 codes for a glycosyl transferase involved in cell wall biosynthesis. It is noteworthy that in operon RS09290-315 there were 5 CDSs enriched in the cationic antimicrobial peptide (CAMP) resistance pathway (**Figure 5**; **Supplementary Table S10**). The five CDSs code for homologs of ArnA, ArnC, ArnD, ArnE, and ArnT in *E. coli*, which contribute to the biosynthesis of UDP-L-Ara4FN and transfer of the L-Ara4N moiety to lipid A (Breazeale et al., 2005). In *E. coli* and *Salmonella typhimurium*, the addition of L-Ara4N groups to lipid A under the control of the transcription factor BasR (PmrA) is required for maintaining resistance to certain cationic antimicrobial peptides (Yan et al., 2007; Rubin et al., 2015). This agrees with our result showing that the expression of the *basR* (*pmrA*) gene was also downregulated in the *rpoS* mutant (**Table 1**). The expression of CDSs with functions related to cell wall synthesis and maintenance is involved in resistance to external stresses that damage the cell envelope (Liu et al., 2017). Our results indicate that RpoS might contribute to the formation of resistance to cell wall stress conditions.

Stress Responses

As expected, many of the identified downregulated CDSs and proteins were those that are important for stress response. For example, the *rpoS* mutation resulted in decreased expression of CDSs coding for antioxidant enzymes (AhpC, KatE, OsmC), RND transporters (TriABC, CzcAB), and other stress related proteins (PcoAB, UspA) (**Table 1**). RpoS controls the antioxidant enzymes that are also observed in *E. coli*, *Salmonella*, and *B. pseudomallei* (Dong and Schellhorn, 2009; Osiriphun et al., 2009; Lévi-Meyrueis et al., 2014). Levels of reactive oxygen species can increase when bacteria are exposed to certain types of environmental stresses, such as heat, ethanol, ultraviolet

TABLE 1 | Representative CDSs differentially expressed in the *rpoS* mutant and the wild-type strain UK4 at the mRNA and protein levels.

Locus tag[a]	Protein accession	Function description	mRNA Δ*rpoS*/UK4 ratio (adjusted *p*-value)[b]	Protein Δ*rpoS*/UK4 ratio (*p*-value)[c]	Regulation type (mRNA/protein)[d]
TRANSCRIPTION FACTORS AND SIGNAL TRANSDUCTION					
HZ99_RS01135	WP_038440714.1	Acyl-homoserine-lactone synthase RhlI	0.157 (2.51E-12)	–	Down/–
HZ99_RS01140	WP_038440716.1	Transcriptional regulator RhlR	0.192 (2.38E-10)	–	Down/–
HZ99_RS01145	WP_038440719.1	Rhamnosyltransferase chain B, RhlB	0.034 (1.36E-24)	–	Down/–
HZ99_RS01150	WP_038440722.1	Rhamnosyltransferase 1 subunit A, RhlA	0.029 (3.31E-19)	–	Down/–
HZ99_RS01735	WP_038440888.1	LuxR family transcriptional regulator	0.106 (1.78E-04)	–	Down/–
HZ99_RS01825	WP_038440917.1	RNA polymerase sigma factor	0.176 (4.49E-05)	–	Down/–
HZ99_RS03980	WP_038441499.1	Fis family transcriptional regulator	0.083 (4.47E-05)	–	Down/–
HZ99_RS09360	WP_038442561.1	DNA-binding transcriptional regulator BasR (PmrA)	0.232 (7.59E-08)	–	Down/–
HZ99_RS09580	WP_003178872.1	Carbon storage regulator RsmA	0.262 (6.78E-07)	–	Down/–
HZ99_RS09820	WP_038442724.1	RNA polymerase subunit sigma-24, RpoE	0.265 (4.04E-02)	–	Down/–
HZ99_RS09895	WP_038442747.1	Methyl-accepting chemotaxis protein	0.058 (1.43E-03)	0.291 (4.20E-05)	Down/Down
HZ99_RS10650	WP_038442895.1	Diguanylate cyclase response regulator WspR	0.329 (6.95E-03)	–	Down/–
HZ99_RS10655	WP_038442896.1	Chemotaxis-specific methylesterase WspF	0.280 (1.11E-06)	0.746 (3.24E-02)	Down / Down
HZ99_RS10660	WP_038442897.1	Chemotaxis sensor/effector fusion protein WspE	0.301 (3.33E-04)	–	Down/–
HZ99_RS10665	WP_038442898.1	Chemotaxis protein WspD	0.321 (7.73E-03)	–	Down/–
HZ99_RS10670	WP_038442899.1	Chemotaxis protein WspC	0.306 (2.22E-02)	–	Down/–
HZ99_RS10675	WP_038442901.1	Chemotaxis protein WspB	0.292 (2.76E-04)	–	Down/–
HZ99_RS10680	WP_038442902.1	Chemotaxis transducer WspA	0.251 (1.05E-04)	0.812 (6.07E-03)	Down/Down
HZ99_RS14415	WP_017739508.1	PrkA family serine protein kinase	0.014 (3.29E-16)	0.097 (2.78E-04)	Down/Down
HZ99_RS14470	WP_038443829.1	Bifunctional diguanylate cyclase/phosphodiesterase	0.044 (2.50E-09)	–	Down/–
HZ99_RS15265	WP_038444050.1	ArsR family transcriptional regulator	–	0.578 (2.84E-03)	–/Down
HZ99_RS16305	WP_038444414.1	DNA-binding response regulator	0.512 (1.97E-02)	0.795 (9.15E-03)	Down/Down
HZ99_RS19375	WP_038445316.1	Two-component system response regulator NtrC	0.354 (2.64E-04)	0.759 (1.09E-02)	Down/Down
HZ99_RS20755	WP_038445694.1	PAS domain-containing sensor histidine kinase	0.037 (1.74E-09)	–	Down/–
HZ99_RS20770	WP_038445699.1	DNA-binding response regulator CitB	0.129 (2.11E-07)	0.574 (2.15E-03)	Down/Down
HZ99_RS23975	WP_038446534.1	Bifunctional diguanylate cyclase/phosphodiesterase	0.073 (9.68E-06)	–	Down/–
HZ99_RS24460	WP_038446651.1	RNA polymerase sigma-H factor AlgU	–	1.458 (1.78E-02)	-/Up
HZ99_RS25335	WP_038446976.1	Anti-anti-sigma factor HsbA	0.087 (1.88E-04)	0.182 (4.82E-05)	Down/Down
HZ99_RS25340	WP_038446978.1	HptB-dependent secretion and biofilm regulator HsbR	0.090 (2.23E-03)	–	–
HZ99_RS25765	WP_038447108.1	Methyl-accepting chemotaxis protein	–	0.565 (2.85E-03)	–/Down
POLYSACCHARIDE METABOLISM					
HZ99_RS00070	WP_038440366.1	Polysaccharide biosynthesis protein PslL	0.215 (2.35E-08)	–	Down/–
HZ99_RS00075	WP_038440367.1	Acyltransferase	0.169 (2.82E-11)	–	Down/–
HZ99_RS00080	WP_038440369.1	Polysaccharide biosynthesis protein PslJ	0.161 (1.58E-11)	–	Down/–
HZ99_RS00085	WP_038440370.1	Polysaccharide biosynthesis protein PslI	0.127 (4.49E-14)	0.619 (1.95E-02)	Down/Down
HZ99_RS00090	WP_038440371.1	Polysaccharide biosynthesis protein PslH	0.136 (1.51E-13)	–	Down/–
HZ99_RS00095	WP_038440372.1	Polysaccharide biosynthesis protein pslG	0.098 (6.06E-18)	0.577 (1.43E-02)	Down/Down
HZ99_RS00100	WP_038440373.1	Polysaccharide biosynthesis protein PslF	0.117 (2.05E-13)	0.684 (1.25E-02)	Down/Down
HZ99_RS00105	WP_038440374.1	Polysaccharide biosynthesis protein PslE	0.102 (1.81E-16)	0.590 (4.52E-03)	Down/Down
HZ99_RS00110	WP_038440375.1	Polysaccharide biosynthesis protein PslD	0.085 (6.34E-17)	–	Down/–
HZ99_RS00115	WP_038440377.1	Polysaccharide biosynthesis protein PslC	0.092 (2.69E-16)	0.526 (1.20E-03)	Down/Down
HZ99_RS00120	WP_038440378.1	Polysaccharide biosynthesis protein PslB	0.107 (9.57E-14)	0.593 (2.05E-02)	Down/Down
HZ99_RS00125	WP_038440379.1	Polysaccharide biosynthesis protein PslA	0.078 (3.34E-16)	–	Down/–
HZ99_RS03630	WP_038441389.1	Glycogen synthase GlgA	0.355 (1.23E-04)	–	Down/–
HZ99_RS03635	WP_038441390.1	Malto-oligosyltrehalose trehalohydrolase TreZ	0.266 (7.44E-06)	–	Down/–
HZ99_RS03640	WP_038441391.1	4-alpha-glucanotransferase MalQ	0.405 (2.76E-03)	–	Down/–
HZ99_RS03645	WP_038441393.1	Malto-oligosyltrehalose synthase TreY	0.234 (1.78E-07)	–	Down/–
HZ99_RS03650	WP_038441395.1	Hypothetical protein	0.365 (1.87E-03)	–	Down/–

(Continued)

TABLE 1 | Continued

Locus tag[a]	Protein accession	Function description	mRNA Δ*rpoS*/UK4 ratio (adjusted *p*-value)[b]	Protein Δ*rpoS*/UK4 ratio (*p*-value)[c]	Regulation type (mRNA/protein)[d]
HZ99_RS03655	WP_038441396.1	Glycogen debranching enzyme GlgX	0.299 (2.46E-05)	0.747 (4.89E-02)	Down/Down
HZ99_RS03670	WP_038441402.1	1,4-alpha-glucan branching protein GlgB	0.210 (1.57E-07)	–	Down/–
HZ99_RS03675	WP_038441404.1	Maltose alpha-D-glucosyltransferase TreS	0.298 (1.60E-05)	–	Down/–
HZ99_RS03680	WP_038441406.1	Alpha-1,4-glucan—maltose-1-phosphate maltosyltransferase GlgE	0.247 (6.95E-07)	–	
HZ99_RS10715	WP_038442912.1	Phosphoethanolamine transferase OpgE	0.237 (2.95E-02)	0.553 (1.08E-02)	Down/Down
HZ99_RS19405	WP_038445324.1	Maltodextrin phosphorylase GlgP	0.190 (1.31E-09)	0.553 (5.91E-03)	Down/Down
HZ99_RS23185	WP_038446334.1	Trehalose permease IIC protein		0.554(5.91E-03)	–/Down
INTRACELLULAR SECRETION AND EXTRACELLULAR STRUCTURES					
HZ99_RS00355	WP_080727762.1	Type V secretory pathway, adhesin AidA	0.032 (3.29E-03)	-	Down/–
HZ99_RS03975	WP_008603564.1	FapF	0.017 (3.21E-08)	0.468 (2.66E-04)	Down/Down
HZ99_RS20775	WP_038445702.1	Hypothetical protein	0.029 (6.35E-15)	–	Down/–
HZ99_RS20780	WP_038445704.1	Type II secretion system protein TadD	0.018 (8.12E-10)	–	Down/–
HZ99_RS20785	WP_038445705.1	Pilus assembly protein TadC	0.021 (2.26E-09)	–	Down/–
HZ99_RS20790	WP_038445707.1	Flp pilus assembly protein TadB	0.022 (5.07E-09)	–	Down/–
HZ99_RS20795	WP_038445708.1	ATPase TadA	0.020 (4.85E-11)	0.100 (5.84E-04)	Down/Down
HZ99_RS20800	WP_038445709.1	Flp pilus assembly protein TadZ	0.016 (3.03E-11)	0.216 (2.83E-03)	Down/Down
HZ99_RS20805	WP_038445710.1	Type II/III secretion system protein RcpA	0.017 (2.35E-08)	–	Down/–
HZ99_RS20810	WP_038445713.1	Flp pilus assembly protein RcpC	0.010 (1.38E-14)	0.217 (1.61E-03)	Down/Down
HZ99_RS20815	WP_038445716.1	Flp family type IVb pilin	0.040 (9.64E-13)	–	Down/–
HZ99_RS20820	WP_038445718.1	Response regulator	0.043 (7.89E-12)	–	Down/–
HZ99_RS20825	WP_038445719.1	Flp family type IVb pilin	0.059 (6.93E-15)	–	Down/–
HZ99_RS20830	WP_038445722.1	Hemolysin activation/secretion protein FhaC	0.017 (6.11E-10)	0.380 (1.97E-03)	Down/Down
HZ99_RS21155	WP_024015038.1	Type II secretory pathway, component ExeA (predicted ATPase)	0.088 (2.31E-11)	0.201 (3.09E-04)	Down/Down
HZ99_RS24960	WP_038446836.1	HlyD family type I secretion periplasmic adaptor subunit	0.073 (2.27E-09)	–	Down/–
HZ99_RS24965	WP_038448190.1	Type I secretion system permease/ATPase	0.085 (7.92E-11)	–	Down/–
HZ99_RS24970	WP_038446837.1	Type I secretion outer membrane protein, TolC family	0.019 (1.61E-04)	0.310 (2.86E-04)	Down/Down
CELL WALL BIOGENESIS					
HZ99_RS02640	WP_038441173.1	LPS O-antigen chain length determinant protein	0.297 (3.08E-06)	0.800 (3.04E-02)	Down/Down
HZ99_RS09290	WP_038442547.1	UDP 4-amino-4-deoxy-L-arabinose aminotransferase	0.064 (8.84E-04)	–	Down/–
HZ99_RS09295	WP_038442548.1	UDP 4-deoxy-4-formamido-L-arabinose transferase ArnC	0.040 (2.47E-04)	–	Down/–
HZ99_RS09300	WP_038442549.1	Bifunctional UDP-glucuronic acid oxidase/UDP-4-amino-4-deoxy-L-arabinose formyltransferase ArnA	0.087 (2.13E-03)	0.202 (1.00E-03)	Down/Down
HZ99_RS09305	WP_038442550.1	4-deoxy-4-formamido-L-arabinose-phosphoundecaprenol deformylase ArnD	0.069 (1.15E-06)	–	Down/–
HZ99_RS09310	WP_038442551.1	4-amino-4-deoxy-L-arabinose transferase ArnT	0.069 (5.68E-04)	–	Down/–
HZ99_RS09315	WP_038442552.1	4-amino-4-deoxy-L-arabinose-phospho-UDP flippase ArnE	0.175 (4.61E-02)	–	Down/–
HZ99_RS09325	WP_038442554.1	UDP-glucose 6-dehydrogenase	0.100 (4.32E-06)	0.442 (3.52E-03)	Down/Down
HZ99_RS26590	WP_038447400.1	Glycosyl transferase	–	0.443 (1.87E-02)	–/Down
STRESS RESPONSES					
HZ99_RS02240	WP_038441046.1	Peroxiredoxin AhpC	–	0.809 (2.96E-02)	–/Down
HZ99_RS13955	WP_038443738.1	Catalase KatE	0.194 (5.59E-05)	0.469 (2.68E-03)	Down/Down
HZ99_RS16790	WP_028618516.1	GlsB/YeaQ/YmgE family stress response membrane protein	0.165 (2.28E-04)	–	Down/–
HZ99_RS17150	WP_038444652.1	RND divalent metal cation efflux transporter CzcA	0.379 (2.52E-04)	–	Down/–
HZ99_RS17155	WP_019334917.1	RND divalent metal cation efflux membrane fusion protein CzcB precursor	0.293 (3.53E-02)	–	Down/–
HZ99_RS17205	WP_038444665.1	Copper resistance protein A precursor PcoA	0.185 (9.81E-03)	0.621 (1.29E-03)	Down/Down

(Continued)

TABLE 1 | Continued

Locus tag[a]	Protein accession	Function description	mRNA Δ*rpoS*/UK4 ratio (adjusted *p*-value)[b]	Protein Δ*rpoS*/UK4 ratio (*p*-value)[c]	Regulation type (mRNA/protein)[d]
HZ99_RS17210	WP_038444668.1	Copper resistance protein B precursor PcoB	0.195 (3.68E-02)	0.757 (2.90E-02)	Down/Down
HZ99_RS17635	WP_038444793.1	Peroxiredoxin OsmC	0.116 (1.73E-06)	0.251 (4.43E-03)	Down/Down
HZ99_RS18120	WP_038444941.1	Multidrug export protein EmrA	0.156 (4.07E-11)	–	Down/–
HZ99_RS18555	WP_038445116.1	RND triclosan efflux membrane fusion protein, TriA	0.210 (1.11E-02)	–	Down/–
HZ99_RS18560	WP_038445117.1	RND triclosan efflux membrane fusion protein, TriB	0.235 (1.13E-03)	0.550 (1.04E-02)	Down/Down
HZ99_RS18565	WP_038445119.1	RND triclosan efflux membrane fusion protein, TriC	0.184 (4.00E-04)	–	Down/–
HZ99_RS22450	WP_038446132.1	Glutathione peroxidase	–	0.763 (0.00123)	–/Down
HZ99_RS26805	WP_029298005.1	Universal stress protein UspA	0.248 (1.72E-07)	–	Down/–
AMINO ACID AND BIOGENIC AMINE METABOLISM					
HZ99_RS02405	WP_038441100.1	Spermidine synthase	0.115 (1.56E-05)	–	Down/–
HZ99_RS04195	WP_038441535.1	Lysine decarboxylase	0.191 (1.23E-05)	–	Down/–
HZ99_RS06735	WP_038441955.1	Methionine gamma-lyase	–	0.482 (8.69E-03)	–/Down
HZ99_RS07550	WP_038442095.1	Agmatine deiminase	0.125 (6.06E-07)	–	Down/–
HZ99_RS10175	WP_038442810.1	Arginine deiminase	–	0.797 (7.34E-03)	–/Down
HZ99_RS10185	WP_038442812.1	Carbamate kinase ArcC	0.468 (4.14E-02)	0.803 (2.35E-03)	Down/Down
HZ99_RS14340	WP_038443794.1	Spermidine/putrescine ABC transporter substrate-binding protein	–	0.524 (2.47E-02)	–/Down
HZ99_RS14900	WP_038443918.1	Glycine cleavage system protein R	0.194 (9.81E-05)	0.391 (9.62E-03)	Down/Down
HZ99_RS15270	WP_038444052.1	Methionine adenosyltransferase	0.482 (1.05E-02)	0.580 (1.57E-03)	Down/Down
HZ99_RS20705	WP_038445679.1	Arginine decarboxylase SpeA	0.397 (4.55E-04)	0.821 (1.61E-02)	Down/Down
HZ99_RS22590	WP_038446180.1	Glu/Leu/Phe/Val dehydrogenase	0.083 (2.60E-10)	0.293 (3.62E-04)	Down/Down
HZ99_RS26135	WP_038447234.1	Spermidine/putrescine ABC transporter ATP-binding protein	0.163 (3.69E-04)	–	Down/–
HZ99_RS26140	WP_029292823.1	ABC-type spermidine/putrescine transport system, permease component II	0.169 (1.39E-02)	–	Down/–
HZ99_RS26155	WP_038447240.1	Spermidine/putrescine-binding periplasmic protein	0.110 (1.70E-02)	0.461 (8.83E-03)	Down/Down
OXIDATIVE PHOSPHORYLATION					
HZ99_RS17715	WP_038444813.1	Cytochrome b559 subunit alpha	0.029 (1.72E-07)	0.194 (9.29E-05)	Down/Down
HZ99_RS17720	WP_038444815.1	Cytochrome c oxidase subunit I	0.035 (1.81E-03)	–	Down/–
HZ99_RS17725	WP_038444816.1	Cytochrome c oxidase assembly protein	0.032 (9.73E-04)	–	Down/–
HZ99_RS17730	WP_038444818.1	Cytochrome c oxidase subunit III	0.044 (2.36E-04)	–	Down/–
HZ99_RS17740	WP_038444821.1	Cytochrome oxidase biogenesis protein Surf1,facilitates heme A insertion	0.026 (2.98E-07)	–	Down/–
HZ99_RS17745	WP_038448109.1	Hypothetical protein	0.042 (7.68E-06)	–	Down/–
HZ99_RS17750	WP_038444822.1	Cytochrome b561	0.051 (4.43E-05)	–	Down/–
HZ99_RS17755	WP_038444823.1	Protoheme IX farnesyltransferase	0.044 (4.04E-04)	–	Down/–
HZ99_RS23395	WP_038446389.1	NADH:flavin oxidoreductase/NADH oxidase	0.017 (4.36E-07)	0.275 (5.50E-06)	Down/Down
SULFUR METABOLISM					
HZ99_RS15945	WP_003213899.1	Transporter	6.011 (3.59E-04)		Up/–
HZ99_RS15950	WP_038444290.1	Aliphatic sulfonates ABC transporter ATP-binding protein SsuB	5.495 (5.07E-04)		Up/–
HZ99_RS15955	WP_038444293.1	Alkanesulfonate transporter permease subunit SsuC	4.988 (3.08E-02)		Up/–
HZ99_RS18395	WP_038445051.1	Sulfate-binding protein precursor	-	1.394 (4.14E-02)	–/Up
HZ99_RS18400	WP_032856532.1	Sulfate ABC transporter permease subunit CysT	2.407 (1.39E-02)		Up/–
HZ99_RS18410	WP_038445056.1	Sulfate ABC transporter ATP-binding protein CysA	2.391 (6.81E-03)		Up/–
HZ99_RS18930	WP_038445174.1	Taurine dioxygenase TauD	2.522 (2.42E-02)		Up/–
HZ99_RS18940	WP_038445178.1	Taurine transporter ATP-binding subunit TauB	–	1.597 (2.31E-04)	–/Up
HZ99_RS18945	WP_038445179.1	Taurine ABC transporter substrate-binding protein TauA	–	1.319 (2.97E-02)	–/Up
HZ99_RS27240	WP_038447698.1	Methanesulfonate sulfonatase MsuD	–	1.447 (6.49E-03)	–/Up

[a] *CDSs belonging to a putative operon are marked with a box.*

[b,c,d] *The symbol "–" indicates that the expression of the gene was not detected or was not significantly different between the rpoS mutant and wild-type.*

radiation, or antibiotics, and the oxidative injury to cells can be reduced by increased antioxidant enzyme activities (Liu et al., 2012; El-Halfawy and Valvano, 2014). The Resistance-Nodulation-Cell Division (RND) transporters mainly contribute to resistance to antimicrobial agents (Venter et al., 2015). The RND pump expression is regulated in response to external stress factors such as reactive oxygen species, membrane damaging agents or ribosome blocking substances (Dreier and Ruggerone, 2015). The copper resistance proteins PcoA and PcoB contribute to copper resistance in *E. coli* and *Pseudomonas* (Chihomvu et al., 2015). The universal stress protein UspA is involved in oxidative stress defense, and the induction of the UspA protein is independent of RpoS in *E. coli* (Kim et al., 2012). However, our results indicated that the expression of UspA was positively regulated by RpoS at the mRNA level in *P. fluorescens*. Our previous work indicated that RpoS affects the resistance of *P. fluorescens* to several stress conditions (Liu et al., 2018). Taken together, RpoS may regulate the resistance of *P. fluorescens* to the stress conditions by controlling the expression of these stress-related CDSs and proteins.

Amino Acid and Biogenic Amine Metabolism

Microbial growth and metabolism are a major cause of food spoilage that produces ammonia and biogenic amines such as putrescine, histamine, and cadaverine with unpleasant and unacceptable off-flavors (Ghaly et al., 2010). In the *rpoS* mutant of *P. fluorescens*, the expression of a large group of CDSs related to amino acid transport and metabolism (COG E) was significantly downregulated at the mRNA and protein levels (**Figure 2**). Many of these CDSs are involved in producing ammonia and biogenic amines, and typical DECs and DEPs are shown in **Table 1**. RS06735, RS07550, RS10175, RS14900, and RS22590 encode proteins related to the generation of ammonia, while RS02405, RS04195, RS07550, and RS20705 code for enzymes resulting in the production of spermidine, cadaverine, N-carbamoylputrescine, and agmatine, respectively. In addition, RS14340, RS26135, RS26140, and RS26155 code for proteins involved in the transport of spermidine or putrescine. Similarly, RpoS activates genes for transport and degradation of amino acids in *P. aeruginosa*, *Salmonella*, and *E. coli* (Schuster et al., 2004; Dong and Schellhorn, 2009; Lévi-Meyrueis et al., 2014). Our previous study showed that the *rpoS* mutant of *P. fluorescens* significantly reduces TVB-N production in sterilized salmon juice (Liu et al., 2018), which might be caused by downregulating the expression of CDSs related to the production of ammonia and biogenic amines in the mutant. So RpoS may play an important role in the spoilage potential of *P. fluorescens* by controlling the expression of CDSs related to amino acid and biogenic amine metabolism.

Oxidative Phosphorylation

The KEGG analyses showed that 10 downregulated CDSs and 1 upregulated CDS were enriched in the oxidative phosphorylation pathway (**Figure 4**; **Supplementary Table S10**). It is worthy to note that two tandem operons, RS17715-30 and RS17740-55, that code for proteins contributing to the respiratory chain were notably downregulated in the *rpoS* mutant at the mRNA and protein levels. Consistent with this, RpoS also positively regulates CDSs coding for cytochrome c oxidase in *P. aeruginosa* and *Geobacter sulfurreducens* (Schuster et al., 2004; Núñez et al., 2006). Lindqvist et al. (2000) indicated that the respiratory oxidases can protect *E. coli* K12 from oxidative stress. However, negative effects of RpoS on the respiratory chain have been observed in *Salmonella* (Lévi-Meyrueis et al., 2014). The effects of RpoS on oxidative phosphorylation are species-dependent.

Sulfur Metabolism

As mentioned above, RpoS mainly functions as a positive regulator. Only a small portion of CDSs were negatively regulated by RpoS, and most of these negatively regulated CDSs showed a smaller change in expression levels compared to the positively regulated CDSs at both the mRNA and protein levels (**Supplementary Tables S6, S7**). However, according to the KEGG enrichment analyses, the CDSs enriched in sulfur metabolism were all negatively regulated by RpoS and are all related to the utilization of sulfonate and sulfate. As a sigma factor, negative control showed by RpoS is likely to be an indirect regulation, probably resulting from sigma factor competition (Farewell et al., 1998).

CONCLUSIONS

In this study, the RpoS regulon was identified by a combined transcriptome and proteome analysis of *P. fluorescens* wild-type strain UK4 and its *rpoS* mutant in the stationary phase. This analysis showed that RpoS regulated the expression of a large set of CDSs at the mRNA and protein levels, mainly including those related to polysaccharide metabolism, intracellular secretion and extracellular structures, cell wall biogenesis, stress responses, ammonia, and biogenic amine metabolism. These cell processes may contribute to biofilm formation, stress resistance and spoilage activities of *P. fluorescens*, and may be also regulated by the transcription factors and signal transduction dependent on RpoS. In addition, several other pathways, such as oxidative phosphorylation, sulfur metabolism and so on, were also affected by RpoS, showing the roles of RpoS in cell processes are diverse. The present findings expand our knowledge about the regulatory mechanisms of bacterial spoilage. RpoS and the pathways regulated by RpoS may be used as potential targets for new food preservative screening, or as molecular markers in assessment of microbial food safety and food quality.

AUTHOR CONTRIBUTIONS

XL conceived and designed the experiments, carried out the experiments, analyzed the data and wrote the manuscript. JX, JZ, and PD participated in performing experiments, and analyzing and interpreting the data. AS participated in designing the experiments, analyzing the data, and revising the manuscript.

XL and AS supervised the project as co-correspondence. All the authors have read and approved the final version of the manuscript.

FUNDING

This work was funded by the National Natural Science Foundation of China (No. 31501581), and the Zhejiang Provincial Program for the Cultivation of High-level Innovative Health Talents (2016-63). We thank LetPub (www.letpub.com) for its linguistic assistance during the preparation of this manuscript.

SUPPLEMENTARY MATERIAL

The Supplementary Material for this article can be found online at: https://www.frontiersin.org/articles/10.3389/fmicb.2019.00094/full#supplementary-material

REFERENCES

Ahrné, E., Glatter, T., Viganò, C., Schubert, C.v., Nigg, E. A., and Schmidt, A. (2016). Evaluation and improvement of quantification accuracy in isobaric mass tag-based protein quantification experiments. *J. Proteome Res.* 15, 2537–2547. doi: 10.1021/acs.jproteome.6b00066

Andreani, N. A., Carraro, L., Martino, M. E., Fondi, M., Fasolato, L., Miotto, G., et al. (2015). A genomic and transcriptomic approach to investigate the blue pigment phenotype in *Pseudomonas fluorescens*. *Int. J. Food Microbiol.* 213, 88–98. doi: 10.1016/j.ijfoodmicro.2015.05.024

Andreani, N. A., Martino, M. E., Fasolato, L., Carraro, L., Montemurro, F., Mioni, R., et al. (2014). Tracking the blue: a MLST approach to characterise the *Pseudomonas fluorescens* group. *Food Microbiol.* 39, 116–126. doi: 10.1016/j.fm.2013.11.012

Aswathanarayan, J. B., and Vittal, R. R. (2014). Attachment and biofilm formation of *Pseudomonas fluorescens*, PSD4 isolated from a dairy processing line. *Food Sci. Biotechnol.* 23, 1903–1910. doi: 10.1007/s10068-014-0260-8

Borodina, T., Adjaye, J., and Sultan, M. (2011). A strand-specific library preparation protocol for RNA sequencing. *Meth. Enzymol.* 500, 79–98. doi: 10.1016/B978-0-12-385118-5.00005-0

Breazeale, S. D., Ribeiro, A. A., McClerren, A. L., and Raetz, C. R. (2005). A formyltransferase required for polymyxin resistance in *Escherichia coli* and the modification of lipid A with 4-Amino-4-deoxy-L-arabinose. Identification and function of UDP-4-deoxy-4-formamido-L-arabinose. *J. Biol. Chem.* 280, 14154–14167. doi: 10.1074/jbc.M414265200

Chihomvu, P., Stegmann, P., and Pillay, M. (2015). Characterization and structure prediction of partial length protein sequences of pcoA, pcoR and chrB genes from heavy metal resistant bacteria from the Klip River, South Africa. *Int. J. Mol. Sci.* 16, 7352–7374. doi: 10.3390/ijms16047352

Clock, S. A., Planet, P. J., Perez, B. A., and Figurski, D. H. (2008). Outer membrane components of the Tad (tight adherence) secreton of *Aggregatibacter actinomycetemcomitans*. *J. Bacteriol.* 190, 980–990. doi: 10.1128/JB.01347-07

Dalmasso, M., Aubert, J., Even, S., Falentin, H., Maillard, M. B., Parayre, S., et al. (2012). Accumulation of intracellular glycogen and trehalose by *Propionibacterium freudenreichii* under conditions mimicking cheese ripening in the cold. *Appl. Environ. Microbiol.* 78, 6357–6364. doi: 10.1128/AEM.00561-12

de Bentzmann, S., Aurouze, M., Ball, G., and Filloux, A. (2006). FppA, a novel *Pseudomonas aeruginosa* prepilin peptidase involved in assembly of type IVb pili. *J. Bacteriol.* 188, 4851–4860. doi: 10.1128/JB.00345-06

Dong, T., and Schellhorn, H. E. (2009). Global effect of RpoS on gene expression in pathogenic *Escherichia coli* O157:H7 strain EDL933. *BMC Genomics*. 10:349. doi: 10.1186/1471-2164-10-349

Dong, T., and Schellhorn, H. E. (2010). Role of RpoS in virulence of pathogens. *Infect. Immun.* 78, 887–897. doi: 10.1128/IAI.00882-09

Dreier, J., and Ruggerone, P. (2015). Interaction of antibacterial compounds with RND efflux pumps in *Pseudomonas aeruginosa*. *Front. Microbiol.* 6:660. doi: 10.3389/fmicb.2015.00660

Dueholm, M. S., Danielsen, H. N., and Nielsen, P. H. (2014). Complete genome sequence of *Pseudomonas* sp. UK4, a model organism for studies of functional amyloids in *Pseudomonas*. *Genome Announc.* 2:e00898–14. doi: 10.1128/genomeA.00898-14

El-Halfawy, O. M., and Valvano, M. A. (2014). Putrescine reduces antibiotic-induced oxidative stress as a mechanism of modulation of antibiotic resistance in *Burkholderia cenocepacia*. *Antimicrob. Agents Chemother.* 58, 4162–4171. doi: 10.1128/AAC.02649-14

Farewell, A., Kvint, K., and Nyström, T. (1998). Negative regulation by RpoS: a case of sigma factor competition. *Mol. Microbiol.* 29, 1039–1051. doi: 10.1046/j.1365-2958.1998.00990.x

Friedman, L., and Kolter, R. (2004). Genes involved in matrix formation in *Pseudomonas aeruginosa* PA14 biofilms. *Mol. Microbiol.* 51, 675–690. doi: 10.1046/j.1365-2958.2003.03877.x

Ghaly, A. E., Dave, D., Budge, S., and Brooks, M. S. (2010). Fish spoilage mechanisms and preservation Techniques: review. *Am. J. Appl. Sci.* 7, 859–877. doi: 10.3844/ajassp.2010.859.877

Guan, J., Xiao, X., Xu, S., Gao, F., Wang, J., Wang, T., et al. (2015). Roles of RpoS in *Yersinia pseudotuberculosis* stress survival, motility, biofilm formation and type VI secretion system expression. *J. Microbiol.* 53, 633–642. doi: 10.1007/s12275-015-0099-6

Guerreiro, A. C., Benevento, M., Lehmann, R., van Breukelen, B., Post, H., Giansanti, P., et al. (2014). Daily rhythms in the cyanobacterium *Synechococcus elongatus* probed by high-resolution mass spectrometry-based proteomics reveals a small defined set of cyclic proteins. *Mol. Cell. Proteomics* 13, 2042–2055. doi: 10.1074/mcp.M113.035840

Haines-Menges, B., Whitaker, W. B., and Boyd, E. F. (2014). Alternative sigma factor RpoE is important for *Vibrio parahaemolyticus* cell envelope stress response and intestinal colonization. *Infect. Immun.* 82, 3667–3677. doi: 10.1128/IAI.01854-14

Han, M. J. (2017). Comprehensive analysis of proteomic differences between *Escherichia coli* K-12 and B strains using multiplexed isobaric tandem mass tag (TMT) labeling. *J. Microbiol. Biotechnol.* 27, 2028–2036. doi: 10.4014/jmb.1708.08024

Hengge-Aronis, R. (1999). Interplay of global regulators and cell physiology in the general stress response of *Escherichia coli*. *Curr. Opin. Microbiol.* 2, 148–152. doi: 10.1016/S1369-5274(99)80026-5

Hickman, J. W., Tifrea, D. F., and Harwood, C. S. (2005). A chemosensory system that regulates biofilm formation through modulation of cyclic diguanylate levels. *Proc. Natl. Acad. Sci. U.S.A.* 102, 14422–14427. doi: 10.1073/pnas.0507170102

Hsu, J. L., Chen, H. C., Peng, H. L., and Chang, H. Y. (2008). Characterization of the histidine-containing phosphotransfer protein B-mediated multistep phosphorelay system in *Pseudomonas aeruginosa* PAO1. *J. Biol. Chem.* 283, 9933–9944. doi: 10.1074/jbc.M708836200

Irie, Y., Starkey, M., Edwards, A. N., Wozniak, D. J., Romeo, T., and Parsek, M. R. (2010). *Pseudomonas aeruginosa* biofilm matrix polysaccharide Psl is regulated transcriptionally by RpoS and post-transcriptionally by RsmA. *Mol. Microbiol.* 78, 158–172. doi: 10.1111/j.1365-2958.2010.07320.x

Jackson, K. D., Starkey, M., Kremer, S., Parsek, M. R., and Wozniak, D. J. (2004). Identification of *psl*, a locus encoding a potential exopolysaccharide that is essential for *Pseudomonas aeruginosa* PAO1 biofilm formation. *J. Bacteriol.* 186, 4466–4475. doi: 10.1128/JB.186.14.4466-4475.2004

Kim, H., Goo, E., Kang, Y., Kim, J., and Hwang, I. (2012). Regulation of universal stress protein genes by quorum sensing and RpoS in *Burkholderia glumae*. *J. Bacteriol.* 194, 982–992. doi: 10.1128/JB.06396-11

Kobayashi, Y., Iwata, H., Yoshida, J., Ogihara, J., Kato, J., and Kasumi, T. (2015). Metabolic correlation between polyol and energy-storing carbohydrate under

osmotic and oxidative stress condition in *Moniliella megachiliensis*. *J. Biosci. Bioeng.* 120, 405–410. doi: 10.1016/j.jbiosc.2015.02.014

Landini, P., Egli, T., Wolf, J., and Lacour, S. (2014). sigmaS, a major player in the response to environmental stresses in *Escherichia coli*: role, regulation and mechanisms of promoter recognition. *Environ. Microbiol. Rep.* 6, 1–13. doi: 10.1111/1758-2229.12112

Langmead, B., and Salzberg, S. L. (2012). Fast gapped-read alignment with Bowtie 2. *Nat. Methods* 9, 357–359. doi: 10.1038/nmeth.1923

Larsen, P., Nielsen, J. L., Dueholm, M. S., Wetzel, R., Otzen, D., and Nielsen, P. H. (2007). Amyloid adhesins are abundant in natural biofilms. *Environ. Microbiol.* 9, 3077–3090. doi: 10.1111/j.1462-2920.2007.01418.x

Leneveu-Jenvrin, C., Bouffartigues, E., Maillot, O., Cornelis, P., Feuilloley, M. G., Connil, N., et al (2015). Expression of the translocator protein (TSPO) from *Pseudomonas fluorescens* Pf0-1 requires the stress regulatory sigma factors AlgU and RpoH. *Front Microbiol.* 6:1023. doi: 10.3389/fmicb.2015.01023

Lévi-Meyrueis, C., Monteil, V., Sismeiro, O., Dillies, M. A., Monot, M., Jagla, B., et al. (2014). Expanding the RpoS/σS-network by RNA sequencing and identification of σS-controlled small RNAs in *Salmonella*. *PLoS ONE* 9:e96918. doi: 10.1371/journal.pone.0096918. eCollection 2014

Lindqvist, A., Membrillo-Hernandez, J., Poole, R. K., and Cook, G. M. (2000). Roles of respiratory oxidases in protecting *Escherichia coli* K12 from oxidative stress. *Antonie Van Leeuwenhoek*. 78, 23–31. doi: 10.1023/A:1002779201379

Liu, X., Ji, L., Wang, X., Li, J., Zhu, J., and Sun, A. (2018). Role of RpoS in stress resistance, quorum sensing and spoilage potential of *Pseudomonas fluorescens*. *Int. J. Food Microbiol.* 270, 31–38. doi: 10.1016/j.ijfoodmicro.2018.02.011

Liu, X., Li, J., Yang, Y., and Chen, X. (2012). Exposure of *Pseudomonas aeruginosa* to green tea polyphenols enhances the tolerance to various environmental stresses. *World J. Microbiol. Biotechnol.* 28, 3373–3380. doi: 10.1007/s11274-012-1149-4

Liu, X., Shen, B., Du, P., Wang, N., Wang, J., Li, J., et al. (2017). Transcriptomic analysis of the response of *Pseudomonas fluorescens* to epigallocatechin gallate by RNA-seq. *PLoS ONE* 12:e0177938. doi: 10.1371/journal.pone.0177938. eCollection 2017

Livak, K. J., and Schmittgen, T. D. (2001). Analysis of relative gene expression data using real-time quantitative PCR and the 2(-Delta Delta C(T)) Method. *Methods* 25, 402–408. doi: 10.1006/meth.2001.1262

Lv, L. X., Yan, R., Shi, H. Y., Shi, D., Fang, D. Q., Jiang, H. Y., et al. (2017). Integrated transcriptomic and proteomic analysis of the bile stress response in probiotic *Lactobacillus salivarius* LI01. *J. Proteomics* 150, 216–229. doi: 10.1016/j.jprot.2016.08.021

Maier, T., Güell, M., and Serrano, L. (2009). Correlation of mRNA and protein in complex biological samples. *FEBS Lett.* 583, 3966–3973. doi: 10.1016/j.febslet.2009.10.036

Maier, T., Schmidt, A., Güell, M., Kühner, S., Gavin, A. C., Aebersold, R., et al. (2011). Quantification of mRNA and protein and integration with protein turnover in a bacterium. *Mol. Syst. Biol.* 7, 511–522. doi: 10.1038/msb.2011.38

Marioni, J. C., Mason, C. E., Mane, S. M., Stephens, M., and Gilad, Y. (2008). RNA-seq: an assessment of technical reproducibility and comparison with gene expression arrays. *Genome Res.* 18, 1509–1517. doi: 10.1101/gr.079558.108

Mellor, G. E., Bentley, J. A., and Dykes, G. A. (2011). Evidence for a role of biosurfactants produced by *Pseudomonas fluorescens* in the spoilage of fresh aerobically stored chicken meat. *Food Microbiol.* 28, 1101–1104. doi: 10.1016/j.fm.2011.02.003

Mika, F., and Hengge, R. (2014). Small RNAs in the control of RpoS, CsgD, and biofilm architecture of *Escherichia coli*. *RNA Biol.* 11, 494–507. doi: 10.4161/rna.28867

Ning, L. N., Zhang, T., Chu, J., Qu, N., Lin, L., Fang, Y. Y., et al. (2018). Gender-related hippocampal proteomics study from young rats after chronic unpredicted mild stress exposure. *Mol. Neurobiol.* 55, 835–850. doi: 10.1007/s12035-016-0352-y

Núñez, C., Esteve-Núñez, A., Giometti, C., Tollaksen, S., Khare, T., Lin, W., et al. (2006). DNA microarray and proteomic analyses of the RpoS regulon in *Geobacter sulfurreducens*. *J. Bacteriol.* 188, 2792–2800. doi: 10.1128/JB.188.8.2792-2800.2006

Oshone, R., Ngom, M., Chu, F., Mansour, S., Sy, M. O., Champion, A., et al. (2017). Genomic, transcriptomic, and proteomic approaches towards understanding the molecular mechanisms of salt tolerance in *Frankia* strains isolated from *Casuarina* trees. *BMC Genomics* 18, 633–653. doi: 10.1186/s12864-017-4056-0

Osiriphun, Y., Wongtrakoongate, P., Sanongkiet, S., Suriyaphol, P., Thongboonkerd, V., and Tungpradabkul, S. (2009). Identification and characterization of RpoS regulon and RpoS-dependent promoters in *Burkholderia pseudomallei*. *J. Proteome Res.* 8, 3118–3131. doi: 10.1021/pr900066h

Patten, C. L., Kirchhof, M. G., Schertzberg, M. R., Morton, R. A., and Schellhorn, H. E. (2004). Microarray analysis of RpoS-mediated gene expression in *Escherichia coli* K-12. *Mol. Genet. Genomics* 272, 580–591. doi: 10.1007/s00438-004-1089-2

Peng, J. X., He, P. P., Wei, P. Y., Zhang, B., Zhao, Y. Z., Li, Q. Y., et al. (2018). Proteomic responses under cold stress reveal unique cold tolerance mechanisms in the pacific white shrimp (*Litopenaeus vannamei*). *Front. Physiol.* 9:1399. doi: 10.3389/fphys.2018.01399

Rajmohan, S., Dodd, C. E., and Waites, W. M. (2002). Enzymes from isolates of *Pseudomonas fluorescens* involved in food spoilage. *J. Appl. Microbiol.* 93, 205–213. doi: 10.1046/j.1365-2672.2002.01674.x

Reis, R. S., Pereira, A. G., Neves, B. C., and Freire, D. M. (2011). Gene regulation of rhamnolipid production in *Pseudomonas aeruginosa*–a review. *Bioresour. Technol.* 102, 6377–6384. doi: 10.1016/j.biortech.2011.03.074

Remenant, B., Jaffrès, E., Dousset, X., Pilet, M. F., and Zagorec, M. (2015). Bacterial spoilers of food: behavior, fitness and functional properties. *Food Microbiol.* 45:45–53. doi: 10.1016/j.fm.2014.03.009

Romero, D., Aguilar, C., Losick, R., and Kolter, R. (2010). Amyloid fibers provide structural integrity to *Bacillus subtilis* biofilms. *Proc. Natl. Acad. Sci. U.S.A.* 107, 2230–2234. doi: 10.1073/pnas.0910560107

Rouse, S. L., Stylianou, F., Wu, H. Y. G., Berry, J. L., Sewell, L., Morgan, R. M. L., et al. (2018). The FapF amyloid secretion transporter possesses an atypical asymmetric coiled coil. *J. Mol. Biol.* 430, 3863–3871. doi: 10.1016/j.jmb.2018.06.007

Rubin, E. J., Herrera, C. M., Crofts, A. A., and Trent, M. S. (2015). PmrD is required for modifications to *Escherichia coli* endotoxin that promote antimicrobial resistance. *Antimicrob. Agents Chemother.* 59, 2051–2061. doi: 10.1128/AAC.05052-14

Schellhorn, H. E. (2014). Elucidating the function of the RpoS regulon. *Future Microbiol.* 9, 497–507. doi: 10.2217/fmb.14.9

Schuster, M., Hawkins, A. C., Harwood, C. S., and Greenberg, E. P. (2004). The *Pseudomonas aeruginosa* RpoS regulon and its relationship to quorum sensing. *Mol. Microbiol.* 51, 973–985. doi: 10.1046/j.1365-2958.2003.03886.x

Sonnleitner, E., Hagens, S., Rosenau, F., Wilhelm, S., Habel, A., Jäger, K. E., et al. (2003). Reduced virulence of a hfq mutant of *Pseudomonas aeruginosa* O1. *Microb. Pathog.* 35, 217–228. doi: 10.1016/S0882-4010(03)00149-9

Stenvang, M., Dueholm, M. S., Vad, B. S., Seviour, T., Zeng, G., Geifman-Shochat, S., et al. (2016). Epigallocatechin gallate remodels overexpressed functional amyloids in *Pseudomonas aeruginosa* and increases biofilm susceptibility to antibiotic treatment. *J. Biol. Chem.* 291, 26540–26553. doi: 10.1074/jbc.M116.739953

Suh, S. J., Silo-Suh, L., Woods, D. E., Hassett, D. J., West, S. E., and Ohman, D. E. (1999). Effect of *rpoS* mutation on the stress response and expression of virulence factors in *Pseudomonas aeruginosa*. *J. Bacteriol.* 181, 3890–3897.

Trapnell, C., Roberts, A., Goff, L., Pertea, G., Kim, D., Kelley, D. R., et al. (2012). Differential gene and transcript expression analysis of RNA-seq experiments with TopHat and Cufflinks. *Nat. Protoc.* 7, 562–578. doi: 10.1038/nprot.2012.016

Van Houdt, R., and Michiels, C. W. (2010). Biofilm formation and the food industry, a focus on the bacterial outer surface. *J. Appl. Microbiol.* 109, 1117–1131. doi: 10.1111/j.1365-2672.2010.04756.x

Venter, H., Mowla, R., Ohene-Agyei, T., and Ma, S. (2015). RND-type drug efflux pumps from Gram-negative bacteria: molecular mechanism and inhibition. *Front. Microbiol.* 6:377. doi: 10.3389/fmicb.2015.00377. eCollection 2015.

Vogel, C., and Marcotte, E. M. (2012). Insights into the regulation of protein abundance from proteomic and transcriptomic analyses. *Nat. Rev. Genet.* 13, 227–232. doi: 10.1038/nrg3185

Wang, L., Feng, Z., Wang, X., Wang, X., and Zhang, X. (2010). DEGseq: an R package for identifying differentially expressed genes from RNA-seq data. *Bioinformatics* 26, 136–138. doi: 10.1093/bioinformatics/btp612

Wongtrakoongate, P., Tumapa, S., and Tungpradabkul, S. (2012). Regulation of a quorum sensing system by stationary phase sigma factor RpoS and their co-regulation of target genes in *Burkholderia pseudomallei*. *Microbiol. Immunol.* 56, 281–294. doi: 10.1111/j.1348-0421.2012.00447.x

Xie, J., Zhang, Z., Yang, S. P., Cheng, Y., and Qian, Y. F. (2018). Study on the spoilage potential of *Pseudomonas fluorescens* on salmon stored at different temperatures. *J. Food Sci. Technol.* 55, 217–225. doi: 10.1007/s13197-017-2916-x

Yan, A., Guan, Z., and Raetz, C. R. (2007). An undecaprenyl phosphate-aminoarabinose flippase required for polymyxin resistance in *Escherichia coli*. *J. Biol. Chem.* 282, 36077–36089. doi: 10.1074/jbc.M706172200

Zeng, G., Vad, B. S., Dueholm, M. S., Christiansen, G., Nilsson, M., Tolker-Nielsen, T., et al. (2015). Functional bacterial amyloid increases *Pseudomonas* biofilm hydrophobicity and stiffness. *Front. Microbiol.* 6:1099. doi: 10.3389/fmicb.2015.01099. eCollection 2015

Zhang, L., Zhang, C., Ojcius, D. M., Sun, D., Zhao, J., Lin, X., et al. (2012). The mammalian cell entry (Mce) protein of pathogenic *Leptospira* species is responsible for RGD motif-dependent infection of cells and animals. *Mol. Microbiol.* 83, 1006–1023. doi: 10.1111/j.1365-2958.2012.07985.x

Zhang, X. X., and Rainey, P. B. (2008). Dual involvement of CbrAB and NtrBC in the regulation of histidine utilization in *Pseudomonas fluorescens* SBW25. *Genetics* 178, 185–195. doi: 10.1534/genetics.107.081984

Zhang, Y., Burkhardt, D. H., Rouskin, S., Li, G. W., Weissman, J. S., and Gross, C. A. (2018). A stress response that monitors and regulates mRNA structure is central to cold shock adaptation. *Mol. Cell.* 70, 274–286. doi: 10.1016/j.molcel.2018.02.035

Conflict of Interest Statement: The authors declare that the research was conducted in the absence of any commercial or financial relationships that could be construed as a potential conflict of interest.

frontiers in Microbiology

ORIGINAL RESEARCH
published: 04 December 2018
doi: 10.3389/fmicb.2018.03032

Surface Immunoproteomics Reveals Potential Biomarkers in *Alicyclobacillus acidoterrestris*

Yiheng Shi[1,2,3], *Tianli Yue*[1,2,3], *Yipei Zhang*[1,2,3], *Jianping Wei*[1,2,3] *and Yahong Yuan*[1,2,3]*

[1] College of Food Science and Engineering, Northwest A&F University, Yangling, China, [2] Laboratory of Quality and Safety Risk Assessment for Agro-Products, Ministry of Agriculture, Yangling, China, [3] National Engineering Research Center of Agriculture Integration Test, Yangling, China

Alicyclobacillus acidoterrestris is a major putrefying bacterium that can cause pecuniary losses in the global juice industry. Current detection approaches are time-consuming and exhibit reduced specificity and sensitivity. In this study, an immunoproteomic approach was utilized to identify specific biomarkers from *A. acidoterrestris* for the development of new detection methods. Cell surface-associated proteins were extracted and separated by 2-D (two-dimensional) gel electrophoresis. Immunogenic proteins were detected by Western blot analysis using antisera against *A. acidoterrestris*. Twenty-two protein spots exhibiting immunogenicity were excised and eighteen of the associated spots were successfully identified by matrix-assisted laser desorption/ionization time-of-flight tandem mass spectrometry (MALDI-TOF/TOF MS). These proteins were observed to be involved in energy and carbohydrate metabolism, transmembrane transport, response to oxidative stress, polypeptide biosynthesis, and molecule binding activity. This is the first report detailing the identification of cell surface-associated antigens of *A. acidoterrestris*. The identified immunogenic proteins could serve as potential targets for the development of novel detection methods.

Keywords: immunoproteomics, immunogenic proteins, *Alicyclobacillus acidoterrestris*, cell surface proteins, biomarkers

OPEN ACCESS

Edited by:
Sergio Uzzau,
University of Sassari, Italy

Reviewed by:
Nurul-Syakima Ab Mutalib,
UKM Medical Molecular Biology Institute (UMBI), Malaysia
Adriana Gielbert,
Animal and Plant Health Agency, United Kingdom

***Correspondence:**
Yahong Yuan
yyh324@126.com

Specialty section:
This article was submitted to Food Microbiology, a section of the journal Frontiers in Microbiology

Received: *12 July 2018*
Accepted: *23 November 2018*
Published: *04 December 2018*

Citation:
Shi Y, Yue T, Zhang Y, Wei J and Yuan Y (2018) Surface Immunoproteomics Reveals Potential Biomarkers in Alicyclobacillus acidoterrestris. Front. Microbiol. 9:3032. doi: 10.3389/fmicb.2018.03032

INTRODUCTION

Alicyclobacillus acidoterrestris is a thermo-acidophilic, aerobic, spore-forming, Gram-positive bacterium which is capable of growing at a temperature range of 25–60°C, and a pH range of 2.5–6.0 (Chang et al., 2013). The spores that are produced by *A. acidoterrestris* can germinate and grow at pH < 4 and are capable of resisting heat treatment at 90°C for 16 to 23 min, a more stringent heat treatment regimen than the conventional pasteurization treatments used in juice processing (Steyn et al., 2011; Celenk and Ayse Handan, 2015). *A. acidoterrestris* can use vanillin and tyrosine as precursors in the synthesis of guaiacol, an organic compound that emits a "phenolic" odor (Uchida and Silva, 2017). The latter compound triggers spoilage of fruit juices and acidic beverages, resulting in significant economic losses to the juice industry (Oteiza et al., 2015; Fernandez et al., 2017). According to a survey conducted by the European Fruit Juice Association (AIJN) in 2005, about 45% of the 68 fruit processing industries experienced *Alicyclobacillus* related problems, including 33% undergoing problems more than once (Steyn et al., 2011). Current detection methods are either labor-intensive and time-consuming or highly technique-requiring (Chang and Kang, 2004;

Concina et al., 2010; Pérez-Cacho et al., 2011; Wang et al., 2012). Although immunoassays have been developed for many years, the effectiveness of immunoassays largely depends on the quality of antibody. Bacteria with high homology could express similar antigens especially in gram-positive bacteria that teichoic-acid could serve as an important surface antigen in all species (Pasquina et al., 2013). So, finding species-specific biomarkers and preparing their corresponding antibodies could lead to the development of more accurate methods for the detection of *A. acidoterrestris*.

As a combination of immunology and proteomics, immunoproteomics has been successfully utilized in pathogenic microorganism for revealing the pathogenesis and elucidating novel diagnostic biomarkers (Hernandez-Haro et al., 2015; Ray et al., 2016; Chen et al., 2018). Thus, immunoproteomics can be used as a preliminary step for specific antibody and immunoassay development to facilitate the detection of foodborne microbiology accurately and rapidly possible (Xiong et al., 2012; Rasmussen et al., 2016). However, up until now limited research has been performed to investigate the use of this technique in detecting non-pathogenic bacteria capable of contaminating food matrices and products.

For most bacteria, the cell wall proteins are often exposed at the surface and exhibit strain specificity (Yu et al., 2012). Thus, based on these properties, cell surface exposed proteins have already served as drug targets and for vaccine and pathogen-specific immunoassay techniques development (Rodriguez-Ortega et al., 2006). The aim of this study was to resolve the cell wall proteins of *A. acidoterrestris* using an immunoproteomics approach to find species-specific biomarkers for immunodetection of this bacterium. Type strain *A. acidoterrestris* DSM3923 was used in this research. Cell wall proteins were extracted and separated by 2-D gel electrophoresis. Protein spots on gels exhibiting immunogenicity were identified and these proteins were chosen as biomarkers for future immunoassay development. We expect that we can monitor the *A. acidoterrestris* in real time from orchard to table in the future based on our findings. Therefore, it could reduce or prevent economic losses to the juice industry resulting from spoilage caused by metabolic products of *A. acidoterrestris.*

MATERIALS AND METHODS

Ethics Statement

This study was carried out in accordance with the recommendations of the Animal Ethics Procedures and Guidelines of the People's Republic of China. All efforts were exerted to minimize the suffering of animals. The animal experiments were approved by the Ethics Committee of Northwest A&F University.

Strain and Growth Conditions

Alicyclobacillus acidoterrestris DSM 3923 used in this study was purchased from the Deutsche Sammlung von Mikroorganismen und Zellkulturen (DSMZ) and stored at −80°C. The culture was grown in AAM broth (Yamazaki et al., 1996) with some modifications (yeast extract 2.0 g, glucose 2.0 g, $(NH_4)_2SO_4$ 0.4 g, $MgSO_47H_2O$ 1.0 g, KH_2PO_4 1.2 g, $CaCl_2$ 0.38 g, distilled water 1000 mL, pH 4.0) on a shaker at 45°C.

Preparation of Immunized Sera

Antisera against whole *A. acidoterrestris* DSM 3923 cells were obtained by immunizing rabbits as previously described (Wang et al., 2012). Briefly, two New Zealand white male rabbits (Xi'an Jiaotong University Health Science Center, China) were subcutaneously immunized with formaldehyde-inactivated *A. acidoterrestris* DSM 3923 at a dose of 1×10^8 CFU/rabbit mixed with an equal volume of Freund's complete adjuvant (Sigma, United States). Four booster immunizations were administered every 2 weeks using the same concentration of bacterial cells mixed with Freund's incomplete adjuvant (Sigma, United States). One week after the final booster immunization, the rabbits were anesthetized with absolute ether and sacrificed to collect blood samples. The blood samples were incubated at 37°C for 1–2 h followed by overnight incubation at 4°C. The samples were subsequently centrifuged at 4500 *g* for 15–20 min at 4°C and the sera were collected and divided into 1 mL-aliquots and stored at −20°C until further required. Next, the isolated antisera were purified by MabSelect SuRe (GE Healthcare, United States) and stored at −20°C until further required.

Preparation of Cell Wall Proteins

Cell wall proteins from *A. acidoterrestris* DSM 3923 were isolated according to a method (with some modifications) published by Siegel et al. (1981). Briefly, *A. acidoterrestris* cells grown to the log phase (OD600 = 0.5) were harvested by centrifugation at 10,000 *g* for 10 min at 4°C. The cells were subsequently washed three times with PBS (137 mM NaCl, 2.7 mM KCl, 10 mM Na_2HPO_4, 2 mM KH_2PO_4) to remove the excess culture medium. The resultant pellets were suspended in extraction buffer (30 mM Tris–HCl (pH 7.5), 3 mM $MgCl_2$, 25% sucrose, 125 U/mL mutanolysin, 400 U/mL lysozyme) containing a protease inhibitor cocktail (Roche, Switzerland) and incubated at 37°C for 90 min. The protoplast fraction was removed by centrifugation at 10,000 *g* for 10 min at 4°C and the supernatant containing the cell wall proteins was collected and filtered through a 0.22 μm R.C membrane. The cell wall proteins were precipitated using trichloroacetic acid (TCA)/acetone (Wu et al., 2014). Prechilled (-20°C) 10% TCA/acetone containing 0.1% Dithiothreitol (DTT) was added to the resultant supernatant. Proteins were allowed to precipitate for 1 h at −20°C. The precipitate was washed three times with cold (−20°C) acetone containing 0.1% DTT to remove TCA. The final pellet was air-dried and solubilized in rehydration buffer [7 M urea, 2 M thiourea, 4% (w/v) CHAPS, 65 mM DTT and 0.2% (v/v) Bio-Lyte pH range 3–10 (Bio-Rad, United States)]. Protein concentration was determined by the Bradford assay.

2-D Gel Electrophoresis

For the first dimension, isoelectric focusing (IEF) was performed in a PROTEAN™ IEF cell (Bio-Rad, United States). Cell wall protein samples (approximately 400 μg each) were suspended in rehydration buffer containing 0.001% (w/v) bromophenol blue and loaded onto the IEF focusing tray with ReadyStrip™

IPG Strips (17 cm, pH 4–7). The samples were subsequently rehydrated overnight (12 h) at 20°C, and 50 V. IEF was carried out using the following conditions: 250 V for 30 min, 1000 V for 1 h, 8500 V for 5 h and final focusing at 8500 V for a total of 60,000 Vh. The current was limited to 50 μA per IPG strip, and the temperature was kept at 20°C for all of the focusing steps. After the IEF, the strip was equilibrated for 15 min with 5 mL of equilibration buffer (6 M urea, 2% (w/v) SDS, 0.375 M Tris-HCl (pH 8.8), 20% (v/v) glycerol) containing 2% (w/v) DTT and another 15 min in the same buffer containing 2.5% iodoacetamide. Finally, the IPG strip was dipped into running buffer (25 mM Tris base, 192 mM glycine, 0.1% (w/v) SDS, pH 8.3), positioned on top of a 12% polyacrylamide gel and sealed in place with 0.5% agarose. The second-dimension electrophoresis was carried out in PROTEAN II XL Cell (Bio-Rad, United States). The resultant gel was run at 10 mA for 30 min and 25 mA until the bromophenol dye reached the bottom of the gel. Following electrophoresis, the gel was stained using Coomassie Brilliant Blue G-250 and scanned using a GS-800™ Calibrated Densitometer (Bio-Rad, United States). Three independent replicates were performed for each experiment.

Immunoblot Analysis

Proteins in the gel were transferred onto a 0.45 μm Immobilon-P polyvinylidene difluoride (PVDF) membrane (Merck Millipore, United States) using a Trans-Blot®SD Semi-Dry Electrophoretic Transfer Cell (Bio-Rad, United States) at 25 V for 30 min with transfer buffer (25 mM Tris base, 192 mM glycine, 0.02% (w/v) SDS, 20% (v/v) methanol). Next, the membrane was rinsed three times with TBST (20 mM Tris base, 137 mM NaCl, 0.1% Tween-20, pH 7.5) for 5 min and blocked with 5% skimmed milk in TBST for 2 h at room temperature. The membrane was subsequently incubated with 1:2000 diluted antisera at 4°C overnight. Next, the membrane was rinsed five times with TBST for 8 min and incubated with a 1:10000 dilution of goat anti-rabbit IgG horseradish peroxidase (HRP)-conjugated secondary antibody (Jackson, United States) for 1 h at room temperature. Finally, the membrane was washed five times with TBST for 8 min and the excess buffer was dried with filter paper. Immunoreactive spots on the membrane were detected by chemiluminescence (Pierce™ ECL Western Blotting Substrate, Thermo Scientific, United States) according to the manufacturer's instructions. The blot was visualized using a ChemiDo™ XRS+ system (Bio-Rad, United States).

In-Gel Digestion

In-gel digestion was performed as previously described (Shevchenko et al., 1996) with some modifications. Briefly, immunoreactive protein spots were selected and manually excised from stained gels. The gel spots were destained with 30% acetonitrile (ACN) containing 100 mM NH_4HCO_3 and dehydrated in 100% ACN. The liquid phase was removed. The gel pieces were completely dried in a vacuum centrifuge. Next, the gel pieces were reswollen with 10 ng/μL sequencing-grade trypsin at 4°C for 30 min; the pieces were subsequently incubated at 37°C overnight (approximately 20 h). Excess trypsin solution was removed and peptides were extracted three times with 60% ACN containing 0.1% trifluoroacetic acid (TFA). Then the extracts were pooled and lyophilized.

MALDI-TOF/TOF MS Analysis

The lyophilized peptides were dissolved in 20% acetonitrile. The samples (1 μL each) were spotted on a MALDI target plate and allowed to air-dry. Next, 0.5 μL of matrix (5 mg/mL α-cyano-4-hydroxycinnamic acid diluted in 0.1% TFA and 50% ACN) were mixed with dried peptides and allowed to air-dry. Sample analysis was carried out using a 4800 Plus MALDI-TOF/TOF MS Analyzer (Applied Biosystems, United States) in positive ion reflector mode with 2 kV accelerating voltage and 355 nm Nd:YAG laser source. Positive ion mode and automatic acquisition mode were used for data collection. A peptide mass fingerprint (PMF) in the 800–4000 Da range was generated. Peaks with a signal-to-noise ratio greater than 50 were selected for MS/MS analysis using a collision energy of 2 kV.

Bioinformatics Analysis

Data searches were performed using MASCOT 2.2 (Matrix Science, United Kingdom) and Global Proteome Server Explorer (Applied Biosystems) protein identification. The parameters were set as follows: UniProt database, and species restriction to *A. acidoterrestris*; Enzyme, Trypsin; Fixed modifications, Carbamidomethyl (C)s; Dynamical modifications, Oxidation (M); Peptide Mass Tolerance, ± 100 ppm; Fragment Mass Tolerance, ± 0.4 Da; Peptide Charge State, 1+; Max Missed Cleavages, 1. GPS software-reported protein scores with confidence intervals (C.I.%) greater than 95% were considered as successful identifications for proteins. Protein–protein interaction was performed using STRING [version 10.5[1] (Szklarczyk et al., 2017)] and the protein network was constructed.

SDS–PAGE and Western Blot Analysis of Identified Proteins

Eight identified antigens, namely, GADPH, Polyamine aminopropyl transferase, Succinate-CoA ligase [ADP-forming] subunit alpha, EF-Tu, 6PGD, Hypothetical protein N007_04435, SOD, AhpC were chosen for antigenicity veridiction. Genomic DNA of DSM 3923 were extracted by QIAamp DNA Mini Kit (Qiagen, Germany) following manufacturer's instruction. PCR reactions were performed using T100™ Thermal Cycler (Bio-Rad, United States). The PCR products were purified by Gel Extraction Kit (Omega BIO-TEK, United States) before cloned into pET-28a (+) and pET-32a (+) vectors (Novagen, Germany). The constructs were sequenced by ABI 3730XL. Recombinant plasmids were transformed into *E. coli* BL21 (DE3) (Invitrogen™, United States) competent cells for expression. The recombinant proteins were purified by Ni-NTA His Bind Resin (Merck Millipore, United States) and examined by 12% SDS–PAGE. Western blot was performed as described above, apart from the transfer parameters which were changed from 25 V for 30 min into 15 V for 15 min.

[1]https://string-db.org/

RESULTS

2-D Gel Electrophoresis Map of Cell Wall Proteins of *A. acidoterrestris* DSM 3923

Cell wall proteins of *A. acidoterrestris* were extracted using enzymolysis and separated by 2-D gel electrophoresis. A total of more than 200 spots in the gel were clearly observed with a molecular mass range from 10 to 75 kDa and pH range from 4 to 7 as shown in **Figure 1A**. Protein spots were evenly scattered and most of them showed in small light dots. High abundance proteins (big spots) were predominantly distributed in the 10–35 kDa range and low abundance proteins (small spots) in the 35–75 kDa range.

Immunoblot Analysis of Cell Wall Proteins of *A. acidoterrestris* DSM 3923

Cell wall extracts of *A. acidoterrestris* DSM 3923 separated by 2-D gel electrophoresis were blotted onto a PVDF membrane and visualized using chemiluminescence. **Figure 1B** shows that a large number of protein spots reacted with the antisera and the strongest reactors were mainly in the 15–35 kDa range. This analysis also indicated that, compared with the 2-D map, highly abundant proteins reacted strongly with antisera while those proteins that were less prevalent reacted with the antisera in a less intense fashion. Furthermore, several intense reaction spots that were not observed clearly on the gel were detected by Western blot, indicating that some proteins that were expressed at reduced levels but were exposed on the cell surface could potently stimulate host immune response (Wang et al., 2013).

Identification of Cell Wall Protein Immunogens in *A. acidoterrestris* DSM 3923

Twenty-two immunoreactive spots recognized by antisera that correlated with relatively high abundance protein spots in the Coomassie-stained gel were picked for MALDI-TOF/TOF MS identification. All twenty-two immunoreactive spots were excised from the gel and eighteen spots were successfully identified (**Table 1**). Of the eighteen spots, eight were characterized as three kinds of hypothetical protein (N007_00440, N007_08970, N007_04435). Two spots were identified as the elongation factor Tu (EF-Tu), and the rest were classified as metabolic enzymes (**Table 2**). These proteins were mainly involved in transmembrane transport of matter, carbohydrate and energy metabolic process, chain elongation in polypeptide synthesis, maintaining redox homeostasis in respond to oxidative stress, and cell growth (**Figure 2A** and **Table 2**). Among the identified antigens, two were newly found in our study that never been reported in the previous researches. Five were identified as "common antigen" and the rest five were classified into "antigen been reported" (**Figure 2B** and **Table 2**). To further understand the property and correlation of immunogenic proteins, Protein–protein interaction prediction was performed using online database STRING. **Figure 3** shows that seven proteins which involved in glycometabolism and oxidative stress could interact with each other. The three hypothetical proteins include two newly identified antigens showed no relationship with others.

Validation of Antigenic Property of Recombinant Cell Wall Proteins

To further evaluate the potential as biomarkers of the identified proteins, eight proteins were cloned and expressed in *E. coli* BL21 (DE3) cell. **Figure 4A** confirms that the recombinant proteins were successfully expressed. The molecule mass of recombinant proteins matched the data of MS analysis. Western blot demonstrates that the eight proteins could be recognized by anti-*A. acidoterrestris* antisera (**Figure 4B**).

DISCUSSION

Alicyclobacillus acidoterrestris is a thermo-acidophilic bacterial species that is capable of surviving conventional pasteurization

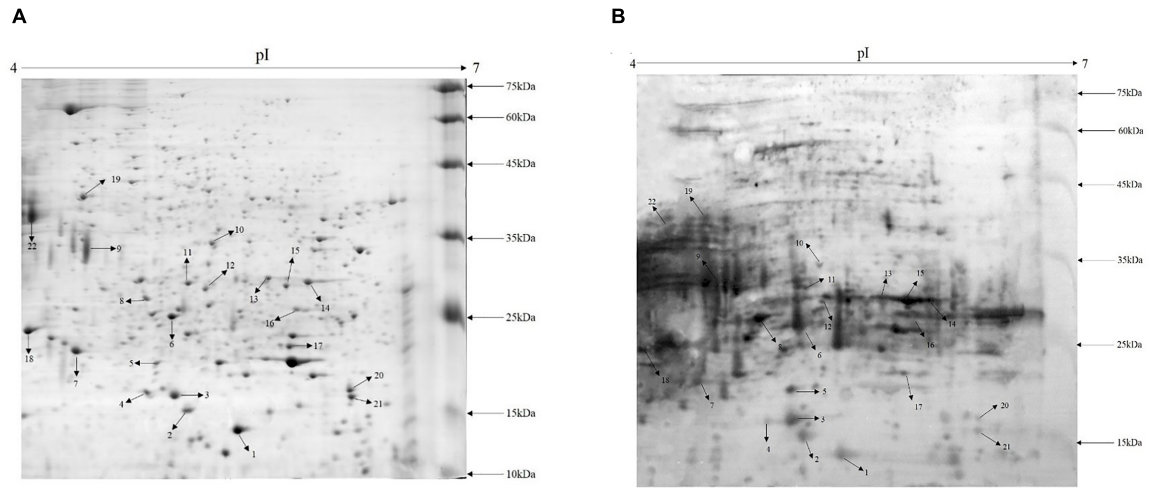

FIGURE 1 | Proteome map and immunoblot profile of cell wall proteins of *A. acidoterrestris*. **(A)** 2-D map of cell wall proteins; **(B)** immunoblot analysis of cell wall proteins.

TABLE 1 | Immunoreactive proteins in *A. acidoterrestris* cell wall identified by MALDI-TOF MS.

Spot no.	Protein name	Accession no.	Gene	Theoretical Mr (kDa)/pI	Protein score	Matched pep.	Coverage %
1	Hypothetical protein N007_00440	T0C5G8	N007_00440	63753/4.64	209	7	19.44
2	Probable thiol peroxidase	T0CJI3	tpx	18634.5/5.23	317	17	87.21
4	Elongation factor Tu	T0D867	tuf	43353/5.09	409	13	38.48
5	Alkyl hydroperoxide reductase subunit C	T0CIG8	N007_20450	20796.5/4.93	367	11	64.71
6	Elongation factor Tu	T0D867	tuf	43353/5.09	596	15	42.78
9	Hypothetical protein N007_08970	T0BYX4	N007_08970	114313.8/4.01	188	8	7.05
10	Malate dehydrogenase	T0BTR2	mdh	33360.7/5.2	381	17	72.12
11	Hypothetical protein N007_04435	T0C6H1	N007_04435	32737.6/5.18	499	14	56.56
12	Succinate-CoA ligase [ADP-forming] subunit alpha	T0C0Z3	sucD	31636.3/5.37	469	15	50.66
13	Polyamine aminopropyl transferase	T0DMQ2	speE	31094.8/5.52	308	16	65.7
14	Hypothetical protein N007_08970	T0BYX4	N007_08970	114313.8/4.01	183	6	4.87
16	Hypothetical protein N007_08970	T0BYX4	N007_08970	114313.8/4.01	129	6	4.7
17	Glyceraldehyde-3-phosphate dehydrogenase	T0BM94	gapA	35675.5/5.78	103	11	35.33
18	Hypothetical protein N007_00440	T0C5G8	N007_00440	63753/4.64	174	9	49.2
19	Hypothetical protein N007_00440	T0C5G8	N007_00440	63753/4.64	142	9	67.38
20	Superoxide dismutase	T0D4I3	N007_10430	22299.1/5.66	280	11	65.35
21	6-Phosphogluconate dehydrogenase	T0CYB3	N007_01705	32612.2/5.57	384	12	41.95
22	Hypothetical protein N007_08970	T0BYX4	N007_08970	114313.8/4.01	117	7	5.48

TABLE 2 | Summary of immunoreactive protein spots from *A. acidoterrestris* cell wall extracts.

Spot no.	Characterization	Potential function	Description
1, 18, 19	Hypothetical protein N007_00440	Transmembrane transport	Antigen been reported
9, 14, 16, 22	Hypothetical protein N007_08970	Unknown	Newly identified antigen
4, 6	Elongation factor Tu	Polypeptide synthesis	Common antigen
2	Probable thiol peroxidase	Respond to oxidative stress	Antigen been reported
5	Alkyl hydroperoxide reductase subunit C	Respond to oxidative stress	Antigen been reported
10	Malate dehydrogenase	Carbohydrate and energy metabolic	Common antigen
11	Hypothetical protein N007_04435	Catalyzing oxidation-reduction reaction	Newly identified antigen
12	Succinate-CoA ligase [ADP-forming] subunit alpha	Carbohydrate and energy metabolic	Antigen been reported
13	Polyamine aminopropyl transferase	Cell growth	Antigen been reported
17	Glyceraldehyde-3-phosphate dehydrogenase	Carbohydrate and energy metabolic	Common antigen
20	Superoxide dismutase	Respond to oxidative stress	Common antigen
21	6-Phosphogluconate dehydrogenase	Carbohydrate and energy metabolic	Common antigen

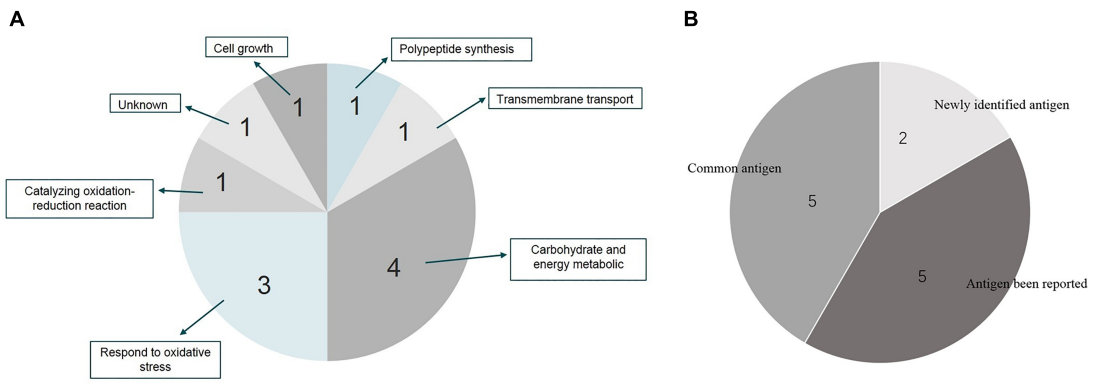

FIGURE 2 | Distribution and function summary of identified antigens from *A. acidoterrestris* cell wall. **(A)** Function characterization of identified antigens; **(B)** antigen description of identified proteins.

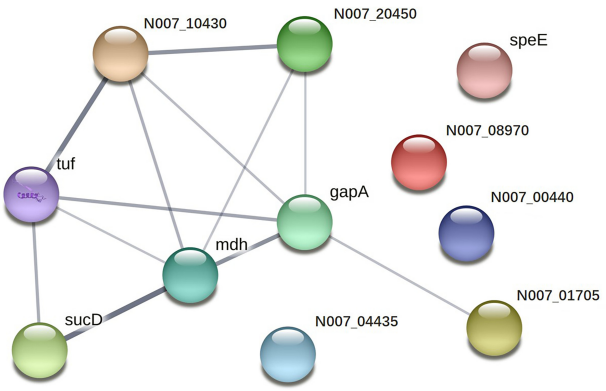

FIGURE 3 | Protein–protein interaction network of immunoreactive proteins.

procedures for fruit juices and acidic products. The presence of this bacterium results in product spoilage and economic losses (dos Anjos et al., 2016). However, existing detection methods used to identify this microorganism are not without problems (Chang et al., 2013). It has previously been suggested that bacterial cell wall-associated proteins could serve as potential diagnostic candidates for detection. However, the surface proteome of *A. acidoterrestris* cells has yet to be elucidated. Hence, in the present study, we utilized 2-D gel electrophoresis followed by Western blotting to elucidate new biomarkers for *A. acidoterrestris*.

The use of two kinds of cell wall hydrolases, lysozyme and mutanolysin, in the extraction of cell wall proteins, has facilitated the release proteins attached to the cell wall, thereby giving a more complete picture of the proteome. **Figure 1A** shows most of protein spots are small and faint, while only a few are large and of high intensity. In gram-positive bacteria, cell walls mainly contain peptidoglycan and teichoic acid,with less than 10% of the exported proteins covalently attached to the bacterial cell wall (Siegel et al., 2016). Thus, the cell wall proteome indicates that most proteins are expressed at low levels. However, a large number of spots could elicit strong reactions against the antisera including many spots which were not clearly observed on the gel. Overall, the data show that the cell wall proteins of *A. acidoterrestris* were successfully extracted and had a high affinity to the antisera. While these proteins were present at low levels, they were sufficiently exposed on the surface to elicit a strong antibody response (from the rabbits) (Wang et al., 2013).

Among the eighteen spots that were successfully identified, three proteins (Hypothetical protein N007_00440, Hypothetical protein N007_08970, Elongation factor Tu) were identified from two or more spots. The presence of the same protein in multiple spots was also observed in the proteomic study of *Sporothrix schenckii* (Messias et al., 2015). The existence of natural isoforms, post-translational modifications, or differential methods of sample preparation might explain these divergences (Wang et al., 2013).

Five of the identified proteins were recognized as "common antigen," as these proteins have been widely reported in pathogenic bacteria. Typically, 6-phosphogluconate dehydrogenase (6PGD) (spot 21), glyceraldehyde-3-phosphate dehydrogenase (GAPDH) (spot 17) and malate dehydrogenase (MDH) (spot 10) which play a key role in the carbohydrate and energy metabolic pathway so that they can catalyze different substrates to maintain normal function of bacteria (Rendina et al., 1984; Sirover, 1997; Musrati et al., 1998). Consequently, these proteins are the most active in the cellular metabolism and have been identified as immunogenic proteins in many pathogenic bacteria (Severin et al., 2007; Wang et al., 2013; Elfaham et al., 2017). Superoxide dismutase (SOD) (spot 20) were also recognized by the antisera. It can convert superoxide (O_2^-) radicals into either ordinary molecular oxygen (O_2) or hydrogen peroxide (H_2O_2) to protect cells from oxidative stress and contributes to the survival of some pathogenic bacteria *in vivo* (Zhang et al., 1991). Thus, it has served as important biomarker in *Cronobacter sakazakii* (Wang et al., 2013). Notably, Elongation factor Tu (EF-Tu) (spot 4, 6) were also identified in our study. This protein is mainly involved in chain elongation during polypeptide synthesis which could bind and transport of aminoacyl-tRNA to the ribosome and interact with GTP in the catalysis of GTP into GDP (Caldas et al., 1998). It is widely distributed in bacteria and has been identified as immunogen

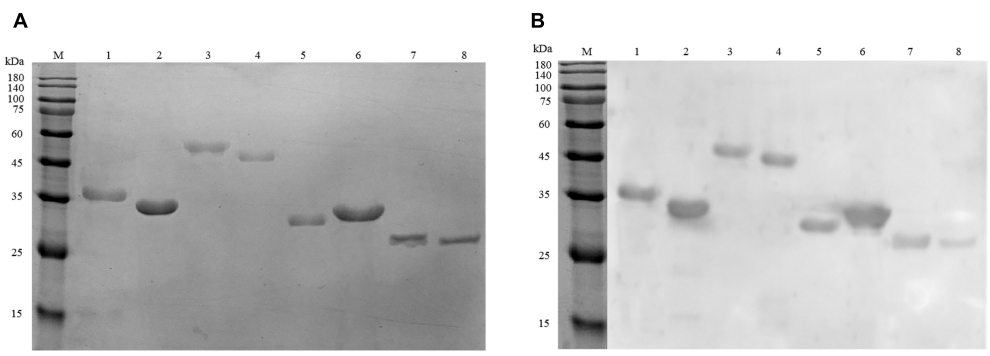

FIGURE 4 | Analysis of recombinant antigen proteins. **(A)** SDS–PAGE of eight purified recombinant proteins. **(B)** Immunoreactivity analysis of recombinant proteins using anti-*A. acidoterrestris* polyclonal antibody. Lanes: M, pre-stain protein molecular weight marker (kDa). 1–8: GADPH, polyamine aminopropyl transferase, succinate-CoA ligase [ADP-forming] subunit alpha, EF-Tu, 6PGD, hypothetical protein N007_04435, SOD, AhpC.

in many microorganisms (Fowsantear et al., 2014; Casas et al., 2017).

Five proteins were classified as "antigen been reported," which means that these proteins have been identified as antigen candidates and served as biomarkers in diagnosis of pathogens in other studies (Stent et al., 2012; Kim et al., 2014; Gomes et al., 2016). These proteins also participate in the metabolic pathway to regulate the function of bacteria. Thiol peroxidase and alkyl hydroperoxide reductase subunit C (AhpC) (spot 5) reduce hydrogen peroxide and peroxynitrite to maintain homeostasis of bacteria and protect cell from oxidative damage (Delaunay et al., 2002; Zuo et al., 2014). They have been identified as important immunogens and vaccine candidates of *Helicobacter pylori* (Stent et al., 2012) and anthrax (Kim et al., 2014), respectively. Succinate-CoA ligase [ADP-forming] (spot 12), also named Succinyl-CoA synthetase, functions in substrate-level phosphorylation in the citric acid cycle (TCA), catalyzing succinate, CoA and ATP or GTP into Succinyl-CoA, phosphate and ADP or GDP, respectively. It has been suggested that this enzyme is a potential antigenic target that could be utilized for the development of a novel diagnostic approach for pathogenic bacterium detection *Bartonella bacilliformis* (Gomes et al., 2016). Moreover, an ATP-binding cassette (ABC) transporter substrate-binding protein analog, hypothetical protein N007_00440 (spot 1, 18, and 19) was recognized as an immunoreactive protein. This protein is mainly involved in transmembrane transport process and is capable of binding substrates outside of the cell and delivering them into cell (Schneider and Hunke, 1998). Members of this family are also involved in the antigen presentation and bacterial pathogenesis and were able to be used as targets to facilitate the detection of pathogenic bacteria (Rodriguez-Ortega et al., 2006; Chen et al., 2018). Polyamine aminopropyl transferase (spot 13) is involved in the first step of the sub-pathway of polyamine biosynthesis which is mainly function in the growth and function of a normal cell (Wallace et al., 2003; Belda-Palazon et al., 2012).

Two proteins were newly identified as immunogens. Protein spots 9, 14, 16, and 22 were identified as the same protein, hypothetical protein N007_08970. This protein was first identified and reported in our research. The structural property and functional information have not been clearly elucidated in any research up to now. Furthermore, homologs from other organisms eliciting immunoreactions have yet to be reported. Hypothetical protein N007_04435 (spot 11) was also first identified as a novel antigen in our study and predicted to be similar to aldo–keto reductases which are involved in the catalysis of a diverse range of substrates, including aliphatic and aromatic aldehydes, monosaccharides, steroids, prostaglandins, polycyclic aromatic hydrocarbons, and isoflavonoids (Hyndman et al., 2003). As for hypothetical protein N007_04435 (spot 11), homologs from other organisms eliciting similar immunoreactions have yet to be elucidated. However, Aldo–keto reductases have been described as therapeutic drug targets (Jez et al., 1997). Our present work demonstrates that this protein is easily recognizable by antibodies. The results support that these proteins are excellent candidates as biomarkers for the detection of *A. acidoterrestris*. The fact that no interaction partners were identified for either N007_08970 or N007_04435 (**Figure 3**), illustrates their novelty as antigens from a different perspective.

CONCLUSION

This is the first study to report the occurrence of specific antigens in the cell surface of *A. acidoterrestris*, a species that causes fruit juice contamination leading to significant economic losses. Hypothetical protein N007_08970 and Hypothetical protein N007_04435 are two antigens that were first identified as part of this study. The other antigens that were identified as part of this study are homologs of antigens reported in pathogenic species and could also act as biomarkers. We believe that the species-specific antigens identified in this study may be important in the development of methods for the accurate detection of *A. acidoterrestris* in fruit juices.

GADPH, polyamine aminopropyl transferase, succinate-CoA ligase [ADP-forming] subunit alpha, EF-Tu, 6PGD, hypothetical protein N007_04435, SOD and AhpC were selected to express as recombinant in *E. coli* to further evaluate the potential as molecular biomarkers for detection or antibody development. All selected proteins could react with antisera against *A. acidoterrestris*. This demonstrates that these proteins are suitable targets for future development of an immunological detection method for *A. acidoterrestris*.

AUTHOR CONTRIBUTIONS

YS conceived and designed the experiments, analyzed the data, and wrote the manuscript. YS and YZ conducted the experiments. YY and TY supervised all work. YS, JW, YY, and TY revised the manuscript.

FUNDING

This work was supported by the National Natural Science Foundation of China (31671866), the Scientific and Technology Cooperation Project in Hong Kong, Macau, and Taiwan of China (2015DFT30130), the Shaanxi Special Project of China (2016KTCQ03-12), and the National Basic Research Program of China (2013FY113400).

ACKNOWLEDGMENTS

The authors thank Shanghai Hoogen Biotechnology Co., Ltd., for their technical help.

SUPPLEMENTARY MATERIAL

The Supplementary Material for this article can be found online at: https://www.frontiersin.org/articles/10.3389/fmicb.2018.03032/full#supplementary-material

REFERENCES

Belda-Palazon, B., Ruiz, L., Marti, E., Tarraga, S., Tiburcio, A. F., Culianez, F., et al. (2012). Aminopropyl transferases involved in polyamine biosynthesis localize preferentially in the nucleus of plant cells. *PLoS One* 7:e46907. doi: 10.1371/journal.pone.0046907

Caldas, T. D., El Yaagoubi, A., and Richarme, G. (1998). Chaperone properties of bacterial elongation factor EF-Tu. *J. Biol. Chem.* 273, 11478–11482. doi: 10.1074/jbc.273.19.11478

Casas, V., Rodriguez-Asiain, A., Pinto-Llorente, R., Vadillo, S., Carrascal, M., and Abian, J. (2017). *Brachyspira hyodysenteriae* and *B. pilosicoli* proteins recognized by sera of challenged pigs. *Front. Microbiol.* 8:723. doi: 10.3389/fmicb.2017.00723

Celenk, M., and Ayse Handan, B. (2015). Effects of pomegranate and pomegranate-apple blend juices on the growth characteristics of *Alicyclobacillus acidoterrestris* DSM 3922 type strain vegetative cells and spores. *Int. J. Food Microbiol.* 200, 52–56. doi: 10.1016/j.ijfoodmicro.2015.01.019

Chang, S. S., and Kang, D. H. (2004). *Alicyclobacillus* spp. in the fruit juice industry: history, characteristics, and current isolation/detection procedures. *Crit. Rev. Microbiol.* 30, 55–74. doi: 10.1080/10408410490435089

Chang, S. S., Park, S. H., and Kang, D. H. (2013). Development of novel agar media for isolating guaiacol producing *Alicyclobacillus* spp. *Int. J. Food Microbiol.* 164, 1–6. doi: 10.1016/j.ijfoodmicro.2013.03.015

Chen, S., Hao, H., Zhao, P., Ji, W., Li, M., Liu, Y., et al. (2018). Differential immunoreactivity to bovine convalescent serum between mycoplasma bovis biofilms and planktonic cells revealed by comparative immunoproteomic analysis. *Front. Microbiol.* 9:379. doi: 10.3389/fmicb.2018.00379

Concina, I., Bornsek, M., Baccelliere, S., Falasconi, M., Gobbi, E., and Sberveglieri, G. (2010). *Alicyclobacillus* spp detection in soft drinks by electronic nose. *Food Res. Int.* 43, 2108–2114. doi: 10.1016/j.foodres.2010.07.012

Delaunay, A., Pflieger, D., Barrault, M. B., Vinh, J., and Toledano, M. B. (2002). A thiol peroxidase is an H2O2 receptor and redox-transducer in gene activation. *Cell* 111, 471–481. doi: 10.1016/S0092-8674(02)01048-6

dos Anjos, M. M., da Silva, A. A., de Pascoli, I. C., Mikcha, J. M., Machinski, M. Jr., Peralta, R. M., et al. (2016). Antibacterial activity of papain and bromelain on *Alicyclobacillus* spp. *Int. J. Food Microbiol.* 216, 121–126. doi: 10.1016/j.ijfoodmicro.2015.10.007

Elfaham, M. H., Eissa, M. M., Igetei, J. E., Amer, E. I., Liddell, S., Elazzouni, M. Z., et al. (2017). Treatment of *Schistosoma mansoni* with miltefosine in vitro enhances serological recognition of defined worm surface antigens. *PLoS Negl. Trop. Dis.* 11:e0005853. doi: 10.1371/journal.pntd.0005853

Fernandez, P., Antonio Gabaldon, J., and Jesus Periago, M. (2017). Detection and quantification of *Alicyclobacillus acidoterrestris* by electrical impedance in apple juice. *Food Microbiol.* 68, 34–40. doi: 10.1016/j.fm.2017.06.016

Fowsantear, W., Argo, E., Pattinson, C., and Cash, P. (2014). Comparative proteomics of *Helicobacter* species: the discrimination of gastric and enterohepatic *Helicobacter* species. *J. Proteomics* 97, 245–255. doi: 10.1016/j.jprot.2013.07.016

Gomes, C., Palma, N., Pons, M. J., Magallon-Tejada, A., Sandoval, I., Tinco-Valdez, C., et al. (2016). Succinyl-CoA synthetase: new antigen candidate of *Bartonella bacilliformis*. *PLoS Negl. Trop. Dis.* 10:e0004989. doi: 10.1371/journal.pntd.0004989

Hernandez-Haro, C., Llopis, S., Molina, M., Monteoliva, L., and Gil, C. (2015). Immunoproteomic profiling of *Saccharomyces cerevisiae* systemic infection in a murine model. *J. Proteomics* 112, 14–26. doi: 10.1016/j.jprot.2014.08.008

Hyndman, D., Bauman, D. R., Heredia, V. V., and Penning, T. M. (2003). The aldo-keto reductase superfamily homepage. *Chem. Biol. Interact* 143-144, 621–631. doi: 10.1016/S0009-2797(02)00193-X

Jez, J. M., Bennett, M. J., Schlegel, B. P., Lewis, M., and Penning, T. M. (1997). Comparative anatomy of the aldo-keto reductase superfamily. *Biochem. J.* 326(Pt 3), 625–636. doi: 10.1042/bj3260625

Kim, Y. H., Kim, K. A., Kim, Y. R., Choi, M. K., Kim, H. K., Choi, K. J., et al. (2014). Immunoproteomically identified GBAA_0345, alkyl hydroperoxide reductase subunit C is a potential target for multivalent anthrax vaccine. *Proteomics* 14, 93–104. doi: 10.1002/pmic.201200495

Messias, R. A., Kubitschek-Barreira, P. H., Ferreira, F. G., de Almeida, S. R., Lopes-Bezerra, L. M., and de Camargo, Z. P. (2015). Immunoproteomic analysis reveals a convergent humoral response signature in the *Sporothrix schenckii* complex. *J. Proteomics* 115, 8–22. doi: 10.1016/j.jprot.2014.11.013

Musrati, R. A., Kollarova, M., Mernik, N., and Mikulasova, D. (1998). Malate dehydrogenase: distribution, function and properties. *Gen. Physiol. Biophys.* 17, 193–210.

Oteiza, J. M., Soto, S., Alvarenga, V. O., Sant'Ana, A. S., and Gianuzzi, L. (2015). Fate of *Alicyclobacillus* spp. in enrichment broth and in juice concentrates. *Int. J. Food Microbiol.* 210, 73–78. doi: 10.1016/j.ijfoodmicro.2015.05.021

Pasquina, L. W., Maria, J. P. S., and Walker, S. (2013). Teichoic acid biosynthesis as an antibiotic target. *Curr. Opin. Microbiol.* 16, 531–537. doi: 10.1016/j.mib.2013.06.014

Pérez-Cacho, P. R., Danyluk, M. D., and Rouseff, R. (2011). GC–MS quantification and sensory thresholds of guaiacol in orange juice and its correlation with *Alicyclobacillus* spp. *Food Chem.* 129, 45–50. doi: 10.1016/j.foodchem.2011.04.014

Rasmussen, K. J., Mattsson, A. H., Pilely, K., Asferg, C. A., Ciofu, O., Vitved, L., et al. (2016). Proteome-wide antigen discovery of novel protective vaccine candidates against *Staphylococcus aureus* infection. *Vaccine* 34, 4602–4609. doi: 10.1016/j.vaccine.2016.07.016

Ray, A., Kinch, L. N., Santos, M. D. S., Grishin, N. V., Orth, K., and Salomon, D. (2016). Proteomics analysis reveals previously uncharacterized virulence factors in *Vibrio proteolyticus*. *mBio* 7:e01077-16. doi: 10.1128/mBio.01077-16

Rendina, A. R., Hermes, J. D., and Cleland, W. W. (1984). Use of multiple isotope effects to study the mechanism of 6-phosphogluconate dehydrogenase. *Biochemistry* 23, 6257–6262. doi: 10.1021/bi00320a056

Rodriguez-Ortega, M. J., Norais, N., Bensi, G., Liberatori, S., Capo, S., Mora, M., et al. (2006). Characterization and identification of vaccine candidate proteins through analysis of the group A Streptococcus surface proteome. *Nat. Biotechnol.* 24, 191–197. doi: 10.1038/nbt1179

Schneider, E., and Hunke, S. (1998). ATP-binding-cassette (ABC) transport systems: functional and structural aspects of the ATP-hydrolyzing subunits/domains. *FEMS Microbiol. Rev.* 22, 1–20. doi: 10.1111/j.1574-6976.1998.tb00358.x

Severin, A., Nickbarg, E., Wooters, J., Quazi, S. A., Matsuka, Y. V., Murphy, E., et al. (2007). Proteomic analysis and identification of Streptococcus pyogenes surface-associated proteins. *J. Bacteriol.* 189, 1514–1522. doi: 10.1128/JB.01132-06

Shevchenko, A., Wilm, M., Vorm, O., and Mann, M. (1996). Mass spectrometric sequencing of proteins silver-stained polyacrylamide gels. *Anal. Chem.* 68, 850–858. doi: 10.1021/ac950914h

Siegel, J. L., Hurst, S. F., Liberman, E. S., Coleman, S. E., and Bleiweis, A. S. (1981). Mutanolysin-induced spheroplasts of Streptococcus mutants are true protoplasts. *Infect. Immun.* 31, 808–815.

Siegel, S. D., Liu, J., and Ton-That, H. (2016). Biogenesis of the Gram-positive bacterial cell envelope. *Curr. Opin. Microbiol.* 34, 31–37. doi: 10.1016/j.mib.2016.07.015

Sirover, M. A. (1997). Role of the glycolytic protein, glyceraldehyde-3-phosphate dehydrogenase, in normal cell function and in cell pathology. *J. Cell. Biochem.* 66, 133–140. doi: 10.1002/(SICI)1097-4644(19970801)66:2<133::AID-JCB1>3.0.CO;2-R

Stent, A., Every, A. L., Ng, G. Z., Chionh, Y. T., Ong, L. S., Edwards, S. J., et al. (2012). *Helicobacter pylori* thiolperoxidase as a protective antigen in single- and multi-component vaccines. *Vaccine* 30, 7214–7220. doi: 10.1016/j.vaccine.2012.10.022

Steyn, C. E., Cameron, M., and Witthuhn, R. C. (2011). Occurrence of *Alicyclobacillus* in the fruit processing environment–a review. *Int. J. Food Microbiol.* 147, 1–11. doi: 10.1016/j.ijfoodmicro.2011.03.004

Szklarczyk, D., Morris, J. H., Cook, H., Kuhn, M., Wyder, S., Simonovic, M., et al. (2017). The STRING database in 2017: quality-controlled protein-protein association networks, made broadly accessible. *Nucleic Acids Res.* 45, D362–D368. doi: 10.1093/nar/gkw937

Uchida, R., and Silva, F. V. M. (2017). *Alicyclobacillus acidoterrestris* spore inactivation by high pressure combined with mild heat: modeling the effects of temperature and soluble solids. *Food Control* 73, 426–432. doi: 10.1016/j.foodcont.2016.08.034

Wallace, H. M., Fraser, A. V., and Hughes, A. (2003). A perspective of polyamine metabolism. *Biochem. J.* 376(Pt 1), 1–14. doi: 10.1042/BJ20031327

Wang, J., Du, X. J., Lu, X. N., and Wang, S. (2013). Immunoproteomic identification of immunogenic proteins in *Cronobacter sakazakii* strain BAA-894. *Appl. Microbiol. Biotechnol.* 97, 2077–2091. doi: 10.1007/s00253-013-4720-5

Wang, Z., Yue, T., Yuan, Y., Cai, R., Guo, C., Wang, X., et al. (2012). Development of polyclonal antibody-based indirect enzyme-linked immunosorbent assay for the detection of Alicyclobacillus strains in apple juice. *J. Food Sci.* 77, M643–M649. doi: 10.1111/j.1750-3841.2012.02961.x

Wu, X., Xiong, E., Wang, W., Scali, M., and Cresti, M. (2014). Universal sample preparation method integrating trichloroacetic acid/acetone precipitation with phenol extraction for crop proteomic analysis. *Nat. Protoc.* 9, 362–374. doi: 10.1038/nprot.2014.022

Xiong, X., Wang, X., Wen, B., Graves, S., and Stenos, J. (2012). Potential serodiagnostic markers for Q fever identified in *Coxiella burnetii* by immunoproteomic and protein microarray approaches. *BMC Microbiol.* 12:35. doi: 10.1186/1471-2180-12-35

Yamazaki, K., Teduka, H., and Shinano, H. (1996). Isolation and identification of *Alicyclobacillus acidoterrestris* from acidic beverages. *Biosci. Biotechnol. Biochem.* 60, 543–545. doi: 10.1271/bbb.60.543

Yu, T., Xu, X., Peng, Y., Luo, Y., and Yang, K. (2012). Cell wall proteome of *Clostridium thermocellum* and detection of glycoproteins. *Microbiol. Res.* 167, 364–371. doi: 10.1016/j.micres.2012.02.006

Zhang, Y., Lathigra, R., Garbe, T., Catty, D., and Young, D. (1991). Genetic analysis of superoxide dismutase, the 23 kilodalton antigen of Mycobacterium tuberculosis. *Mol. Microbiol.* 5, 381–391. doi: 10.1111/j.1365-2958.1991.tb02120.x

Zuo, F., Yu, R., Khaskheli, G. B., Ma, H., Chen, L., Zeng, Z., et al. (2014). Homologous overexpression of alkyl hydroperoxide reductase subunit C (ahpC) protects *Bifidobacterium longum* strain NCC2705 from oxidative stress. *Res Microbiol* 165, 581–589. doi: 10.1016/j.resmic.2014.05.040

Conflict of Interest Statement: The authors declare that the research was conducted in the absence of any commercial or financial relationships that could be construed as a potential conflict of interest.

frontiers in Nutrition

ORIGINAL RESEARCH
published: 17 May 2019
doi: 10.3389/fnut.2019.00071

Detailed Soluble Proteome Analyses of a Dairy-Isolated *Enterococcus faecalis*: A Possible Approach to Assess Food Safety and Potential Probiotic Value

Simona Cirrincione[1†], Bernd Neumann[2†], Daniela Zühlke[2], Katharina Riedel[2‡] and Enrica Pessione[1‡]*

[1] Department of Life Sciences and Systems Biology, Univerity of Torino, Turin, Italy, [2] Department for Microbial Physiology and Molecular Biology, University of Greifswald, Greifswald, Germany

Enterococci are common inhabitants of the gastrointestinal tracts of humans and animals and thanks to their capability to tolerate different environmental conditions and their high rates of gene transfer, they are able to colonize various ecological niches, as food matrices. *Enterococcus faecalis* bacteria are defined as controversial microorganisms. From one side they are used as food starters, bio-control agents and probiotics to improve human or animal health. From the other side, in the last two decades enterococci have emerged as important nosocomial pathogens, because bearing high-level of resistance to antibiotics and several putative virulence factors. In this study, the soluble proteome quantitation data (LC-MS/MS) of the food-isolated strain *E. faecalis* D27 (dairy-isolate) was compared with the soluble proteome quantitation data of the pathogenic *E. faecalis* UW3114 (urinary tract infection isolate) and with the one of the health promoting strain *E. faecalis* Symbioflor1, respectively. The comparison of cytosolic protein expression profiles highlighted statistically significant changes in the abundance of proteins mainly involved in specific metabolic pathways, nutrient transport, stress response, and cell wall modulation. Moreover, especially in the dairy isolate and the clinical isolate, several proteins with potential pathogenic implications were found, such as serine proteases, von Willebrand factor, serine hydrolase with beta lactamase activity, efflux transporter, and proteins involved in horizontal gene transfer. The analysis of the extracellular proteome provided interesting results concerning proteins involved in bacterial communication, such as pheromones and conjugative elements and also proteins able to interact with human components. The phenotypic characterization evaluating (i) biofilm formation (ii) hemolytic activity on blood agar plates (iii) protease activity (iv) gelatinase (v) antibiotic resistance pattern, enabled us to elucidate the risks associated with the poor characterized foodborne *E. faecalis* D27.

Keywords: foodborne bacteria, gel-free proteomics, virulence, antibiotic resistance, host interaction

OPEN ACCESS

Edited by:
Maria Fiorella Mazzeo, National Research Council (CNR-ISA), Italy

Reviewed by:
Helge Holo, Norwegian University of Life Sciences, Norway
Victor Ladero, Spanish National Research Council (CSIC), Spain

****Correspondence:***
Simona Cirrincione
simona.cirrincione@ispa.cnr.it

†Present Address:
Simona Cirrincione, CNR-ISPA, Grugliasco, Italy
Bernd Neumann, Robert Koch Institute, Wernigerode Branch, Wernigerode, Germany

‡These authors have contributed equally to this work

Specialty section:
This article was submitted to Food Microbiology, a section of the journal Frontiers in Nutrition

Received: *26 November 2018*
Accepted: *26 April 2019*
Published: *17 May 2019*

Citation:
Cirrincione S, Neumann B, Zühlke D, Riedel K and Pessione E (2019) Detailed Soluble Proteome Analyses of a Dairy-Isolated Enterococcus faecalis: A Possible Approach to Assess Food Safety and Potential Probiotic Value. Front. Nutr. 6:71. doi: 10.3389/fnut.2019.00071

INTRODUCTION

Enterococci are ubiquitous gram-positive bacteria that can be found in various ecosystems, ranging from soil, surface waters, plants, the gastrointestinal tract (GIT) of animals and humans as well as in foods. Enterococci also emerged as important pathogens, since they are one of the major cause of both nosocomial and outpatient-associated infections (1), including clinical manifestations such as urinary tract infections, endocarditis, primary bacteremia and meningitis (2).

In the last decades, enterococci were widely studied because they have intrinsic (absence of target, impermeability, absence of uptake mechanism) and, often, acquired (antibiotic degrading or modifying enzymes) resistance to antibiotics (3, 4). Generally, intrinsic/natural resistance is chromosomally-encoded and therefore non-transmissible, whereas acquired resistance can be plasmid-mediated and hence transmissible by genetic recombination (5). An increasing number of multidrug resistant enterococci has been detected as the predominant microbiota under antibiotic pressure, predisposing hospitalized patients to severe infections and mortality (6).Some virulence factors and antibiotic resistances determinants are carried on mobile genetic elements (MGE) (7), supporting the theory of enterococci as reservoir for antibiotic resistance determinants found in pathogens (8, 9). A large number of reports has focused on the presence or absence of virulence determinants in enterococcal isolates from different origins (food and living being) (10, 11). In particular, the higher incidence in clinical isolated enterococci of genetic elements encoding for virulence factors indicate that these genes enhance their ability to colonize humans, increasing the infection level, as suggested by virulence studies on bacterial mutants in animal models (12).

Within enterococci species, whereas *E. faecium* harbors more antibiotic resistance traits, *E. faecalis* shows a higher potential for virulence, because it synthesizes many proteins that facilitate interaction with environmental (both biotic and abiotic) surfaces, biofilm formation and host colonization (13, 14). Some of these proteins, such as aggregation substance, cytolysin, enterococcal surface protein, gelatinase and protease, are considered to be potential virulence factors (15, 16).

Enterococcus faecalis appears to be typically associated with the human GIT (17) and it is one of the first lactic acid bacteria (LAB) to colonize the intestine of the newborn (18). In healthy human GIT, this bacterium is harmless and present in low abundance, however it can cause life-threatening infections during antibiotic-induced dysbiosis (19). *E. faecalis* is usually carried by food, due to its widespread distribution in the environment. In particular it is often isolated from food of animal origin such as meat (20), milk (21), and cheese (22). Its presence may indicate a natural contamination during manufacturing processes, in some cases as a consequence of fecal contamination caused by poor hygiene (23). Otherwise, *E. faecalis* is used as starter culture (24) to carry out fermentative processes, indeed it plays an important role in cheese ripening and aroma development. However, some authors have reported the presence of antimicrobial resistance and virulence determinants in enterococci found in foods, including cheeses (25, 26). Therefore, a food contaminating *E. faecalis* could represent a possible intermediate vehicle for the transmission of pathogenic traits. In this case, bacteria could act as vectors for the dissemination of antibiotic resistance determinants and virulence factors via the food chain to the consumer, a risk that has so far been poorly addressed (27–29). Actually, it has been observed that human gut enterococci are probably acquired from food since they possess the same antibiotypes and toxinogenic profiles than cattle-, pig-, and sheep- isolated enterococci (30).

Despite the risks associated to *E. faecalis* have led to define these bacteria as controversial (31) they are currently present not only in fermented food but even used as health supplements and probiotics by the pharmaceutical industry. Enterococcal probiotics are usually utilized as "food supplements" in the form of encapsulated or lyophilized pharmaceutical preparations (32). This choice is partly motivated by the lower acid resistance of enterococci compared to lactococci and lactobacilli, that render them less suitable to survive the gastric pH transit. These bacteria are thus ingested in high number to achieve functional or probiotic effects especially for treatment of diseases such as irritable bowel syndrome, diarrhea, antibiotic associated diarrhea, or for health improvement such as cholesterol levels lowering or immune regulation (33, 34).

For all these reasons (possible pathogenicity/virulence determinants or transferable antibiotic resistance characters), a careful selection of *E. faecalis* strains for food supplementation should be done and a constant monitoring on new food-isolated enterococcal strains is required to limit the propagation of virtually harmful microorganism. However, evaluating these risks only by genome analysis of strains is limiting since gene function annotation is based just on sequence homologies with genes present in databanks. Therefore, some evidences should be validated by functional investigations as well as by studying bacterial protein profiles and separately analyze sub-proteomes.

In this view, the present study intended to characterize *Enterococcus faecalis* D27, isolated from cheese, with the specific aim to elucidate if this strain harbors pathogenic traits or rather reveals probiotic features. For this reason, we also examine both a pathogenic (clinically isolated) and a probiotic strain belonging to the same species, to understand the similarities and differences among all the three strains by comparing phenotypic traits, proteomic, and biochemical profiles.

MATERIALS AND METHODS

Bacterial Strains and Cultured Condition

In this study three strains of *Enterococcus faecalis* (present in our collection), with different origin were investigated: D27 (isolated from an artisanal cheese), Symbioflor 1 (commercial probiotic strain) and UW3114 (clinical isolated strain, bearing the pathogenicity island of *E.faecalis* MMH594) (35). All strains were maintained in BHI medium (Oxoid, Munich, Germany) at −20°C in 0.5 mL aliquots with 0.5 mL 40% v/v glycerol. For both proteome analyses and phenotypical assays three biological replicates were performed. Bacterial cultures were grown in the BHI medium at 37°C with slight agitation (180 rpm). Culture supernatants (extracellular proteome) and cells

(cytosolic proteome) were recovered by centrifugation (10,000xg, 10 min, 4°C) from the same bacterial culture in the early stationary growth phase.

Sample Preparation for Proteomic Analyses

Cytosolic Proteins

The intracellular protein extract was obtained as previously described by Zühlke et al. (36). Briefly, cell pellet was washed with TE buffer and lysed by glass beads (diameter: 0.1–0.11 mm) using a Precellys 24 Homogenizator (Peq Lab, Erlangen, Germany).In-solution digestion of protein extracts with trypsin was done according to the method described previously (37). Proteins were dissolved in 50 mM TEAB/0.1% RapiGest™ SF (Waters, Milford, MA, USA), reduced with TCEP (tris-(2-carboxyethyl)phosphine hydrochloride, Invitrogen, Carlsbad, CA, USA) for 45 min at 60°C and alkylated with iodoacetamide (Sigma, Steinheim, Germany) for 15 min at room temperature. Proteins were digested with 0.5 mg trypsin in a 1:200 ratio (Promega, Madison, MA, USA) for 6 h under gentle agitation at 37°C. Desalting of peptides was achieved using a standard protocol (38). For absolute quantification, a tryptic digest of yeast alcohol dehydrogenase (ADH1, Waters, USA) was added into the samples to final concentration of 50 fmol/μL.

Extracellular Proteins

The extracellular protein extract was obtained as previously describe by Lassek et al. (39). Briefly, 10% TCA were added to the cell free supernatant and incubated o/n at 4°C. Samples were centrifuged (10,000 x g, 1 h, 4°C). Protein pellet was washed with 70% ethanol (in the last step 96% ethanol was used). After drying using a vacuum centrifuge (Concentrator plus, Eppendorf) proteins were resuspended in 8M urea/2M thiourea buffer and centrifuged (16,000 x g, 10 min, RT) to recovery the supernatant. Proteins were separated using a Criterion™ TGX™ precast gel (4–20%, 12+2 Well Comb, 45 μL, 1 mm) (Biorad, Hercules, CA, USA), fitting with Mini Protean II-Apparatus (140 V for 75 min, in glycine running buffer). The digestion of the extracellular proteins was performed as described by Lassek et al. (39). Briefly, the excised gel pieces, from SDS-PAGE, were destained using 50% (v/v) methanol in 100 mM NH_4HCO_3. Gel pieces were dehydrated and modified trypsin (sequencing grade, Promega, Fitchburg, WI) was added to a final ratio of 1:10 (trypsin/sample) in 50 mM Tris/HCl, pH 7.5, and the sample incubated at 37°C overnight. Peptides were iteratively extracted from the gel using an ultrasonic bath for 15 min.

The protein concentration of both intracellular and extracellular extracts was determined using Roti Nanoquant (Roth, Germany) according to the manufacturer's instructions.

MS Analysis

Cytosolic Proteins

The separation of the peptide mixture from intracellular proteins was performed using a nanoACQUITY™ UPLC™ system (Waters, USA) following the protocol described by Zühlke et al. (36). The obtained data were searched against a randomized *E. faecalis* OG1RF database (NCBI, version 2015-09-01) with added laboratory contaminants and yeast ADH1 sequence and sequences from the proteins encoded by the pathogenicity island of *E. faecalis* MMH594 (5,490 entries). For positive protein identification the following criteria had to be met: 1 fragment ion matched per peptide, 5 fragment ions matched per protein, 1 peptide matched per protein; 2 missed cleavages allowed, primary digest reagent: trypsin, fixed modification: carbamidom ethylation C (+57.0215), variable modifications: deamidation N, Q (+0.9840), oxidation M (+15.9949), pyrrolidonecarboxy lacid N-TERM (−27.9949). The protein false discovery rate (FDR) was set to 5%. For the final analyses, only identifications based on at least two peptides were considered. A protein had to be identified in at least two out of three technical replicates per biological replicate. In addition, for the final analysis protein had to be present in two out of three biological replicates per time point, which reduced FDR on protein level to <0.7%.

Extracellular Proteins

Peptide mixtures resulting from in-gel tryptic cleavage were separated by RP chromatography using an EASY-nLC (ThermoFisher Scientific, Waltham, USA). Fractionated peptides were loaded onto the analytical column at a flow rate of 700 nL min−1 in 100% buffer A (0.1% acetic acid) and separated using a binary 87-min gradient from 5 to 35% of buffer B (0.1% acetic acid in acetonitrile) at a constant flow rate of 300 nL min−1. The EASY-nLC was coupled to an LTQ Orbitrap mass spectrometer (Thermo Fisher Scientific, Waltham, MA, USA). After a full survey scan in the Orbitrap (m/z range from 300 to 2,000, resolution 30,000, lock mass option-enabled [lock mass 445.120025)] MS/MS experiments in the LTQ XL were performed for the six most abundant precursor ions (CID). Unassigned charge states and singly charged ions were excluded from fragmentation; dynamic exclusion was enabled after 30 s. For protein identification, spectra were searched against a database of *E. faecalis* OG1RF (NCBI, version 2015-09-01) containing sequences of all predicted proteins from its genome, including reverse sequences and sequences of common laboratory contaminants and sequences from the proteins encoded by the pathogenicity island of *E. faecalis* MMH594 (5488 entries). Database searches using Sorcerer SEQUEST (version v. 27 rev. 11, Thermo Scientific) and Scaffold 4.4.1 (Proteome Software, Portland, OR, USA) as well as statistical analysis was done as described earlier (40).

Quantification Methods for Proteome Analysis of *E. faecalis* Strains

Cytosolic Proteins

The protocol that was used for the extraction of cytosolic proteins does not involve any steps that might lead to loss of proteins and is compatible with downstream in-solution digestion of proteins. For this reason, the label-free LC-IMSE approach was chosen for identification and quantification of proteins to reliably determine the abundances of cytosolic proteins. In particular,

the absolute quantitative data were obtained by applying a LC-IMSE approach in combination with the Hi3 quantification method (41, 42).

Extracellular Proteins

Extraction of extracellular proteins is based on precipitation and subsequent solubilization of proteins in a buffer that is not compatible with in-solution digestion. Therefore, separation by SDS-PAGE and in-gel digestion of proteins was applied, allowing to obtain reliable quantitative results based on relative spectral abundances. Relative quantitative data were obtained using a label-free LC-MS/MS approach and using normalized spectral counts (NSAF) for quantification of identified proteins (43). In this approach, the spectral counts of a protein are divided by its length and normalized to the sum of spectral counts/length in a given analysis.

Database Deposition and Graphic Representation of Data

The mass spectrometry proteomics data have been sent to the Proteome Xchange Consortium via the PRIDE partner repository (44) with the dataset identifier PXD011701 for the intracellular proteins and identifier PXD011660 for the extracellular proteins. For functional prediction and classification of both cytosolic and extracellular proteins, the analysis pipeline Prophane was used (40, 45) and Voronoi treemaps were generated using Paver (Decodon, Greifswald, Germany; http://www.decodon.com/paver/). Thanks to the Voronoi treemaps, it is possible to visualize the bacterial proteome, grouping the proteins according to their function, sub-function or specific protein name (the functional prediction is based on TIGRFAMS and Cluster of orthologous groups (COG).

Phenotypic Analyses

The *E. faecalis* isolates were analyzed for activity of different known virulence factors namely, biofilm formation, gelatinase, protease, and hemolytic activity.

Protease Assay

The assay was performed on the cell-free supernatant as described by Pessione et al. (16), using Azocasein solution (1% Azocasein, 50 mMTris-HCl, pH 7.5, 5 mM EDTA) instead of Azoalbumin.

Gelatinase Assay

The assay was performed on the cell-free supernatant as described by Pessione et al. (16). Briefly, 4 ml aliquots of a solution of 3% (p/v) gelatine in 50 mM pH 7.3 Tris-HCl were distributed in 15 ml tubes. At room temperature gelatin solution appears to be liquid, while at 4°C it becomes solid. The tubes were incubated at 4°C for 1 h to evaluate the ability of solution to solidify and then incubated at 37°C to bring it at the liquid state again. Four hundred microliters of the concentrated bacterial extracellular extracts were added to the liquid solutions and the mixtures were incubated 2 h at 37°C, the optimum for gelatinase activity. After that, they were incubated overnight at 4°C to allow to gelatin to solidify again if gelatinase was not present in the extracellular extracts.

Hemolytic Assay

Cells from a liquid culture were plated on Columbia Agar base (Oxoid, Munich, Germany) plates enriched with 5% defibrinated horse blood (TCS Biosciences, Botolph Claydon, UK). The hemolytic activity was checked after 48 h examining the cultures for signs of β-hemolysis (clear zones around colonies), α-hemolysis (green zones around colonies), γ-hemolysis (no sign of hemolysis).

Biofilm Formation

In vitro biofilm formation was investigated as described by Laverede Gomez et al. (35) with slight modification. Bacterial cells from exponential growth phase were incubated for 48 h at 37°C in 96-well microliter plates. The planktonic culture was removed and the biofilm (placed on the bottom of the well) was washed with PBS and stained with crystal violet solution (Roth, Karlsruhe, Germany). The absorbance at $OD_{595nm}$of the 99.8% ethanol used to destain the biofilm was measured. The biofilm formation was determined as $OD600_{nm}/OD595_{nm}$ (ratio between culture and destaining solution absorbance).

Determination of Antimicrobial Susceptibility

The three strains were tested for susceptibility to 18 antibiotics, including different antibiotic classes such as aminoglycosides and glycopeptides, using the broth microdilution method according to DIN58940 (46). The following antibiotics were used: penicillin, ampicillin, gentamycin, streptomycin, vancomycin, teicoplanin, daptomycin, clindamycin, erythromycin, ciprofloxacin, moxifloxacin, tetracycline, tigecycline, rifampicin, linezolid, mupirocin, chloramphenicol, and trimethoprim/sulfamethoxazole. The test was performed according to EUCAST breakpoints definitions (v 8.1) or to ECOFF (epidemiological cut-off) values when no breakpoints were defined (www.eucast.org). As a quality control, also the *E. faecalis* ATCC29212 was tested in this experiment, as recommended by EUCAST guidelines.

RESULTS

The extracellular and intracellular proteomic profiles of the food-isolate *Enterococcus faecalis* D27 (from now referred to as D27) were compared to the profiles of the probiotic *E. faecalis* Symbioflor 1 (from now referred to as Symb1) and the pathogenic *E. faecalis* UW3114 (from now referred to as UW3114), in order to assess the potential risks and benefits associated to the not well-characterized *E. faecalis* D27. Phenotypic aspects connected to virulence/pathogenesis were also investigated.

Gel-free Proteomic Analyses

In order to highlight the proteins directly or partially related to pathogenicity possible present in each of the three investigated strains, the (NCBI) database of *E. faecalis* OG1RF was used for protein identification. Moreover, to identify proteins encoded by the pathogenicity island (PAI) of UW3114 the

database also contained the sequences of the PAI of strain MH594, since many of the proteins encoded by this PAI were also found on the PAI of UW3114 (35). Only proteins present in at least two of the three biological replicates, were considered for comparative analysis. The proteomic pattern obtained for the food strain D27, was compared to those of the probiotic strain Symb1 and the clinical isolate UW3114 separately. This approach allowed to establish: (i) which proteins are expressed by both matched bacteria but in different amounts and (ii) which proteins belong to the so called on/off proteins, that are synthesized by one strain but not by the other.

In the intracellular compartment of D27, Symb1, and UW3114 we identified 889, 883, and 860 proteins, respectively (**Tables S1**, **S2**). The classification of intracellular proteins in functional groups reveals similar profiles among the three strains (**Figure 1**), including proteins involved in: (I) protein synthesis, (II) energy metabolism (III) metabolism (metabolite transport and energy conversion), (IV) protein fate and (IV) poorly characterized proteins. The most striking difference is the presence of the high-abundant protein Gls24-like protein Ef0055 in strain UW3114, located on the pathogenicity island. In the secretome we identified 440, 370 and 253 proteins for D27, Symb1, and UW3114, respectively (**Tables S3**, **S4**). Only proteins with extracellular, cell wall, cell membrane or unknown sub-localization in the localization prediction by pSortb (version 3.0.2) were considered for the discussion.

Comparison Food/Probiotic

Concerning the cytosolic compartment, 794 shared proteins (88 % of the identified proteins), between D27 and Symb1, were identified by mass spectrometry analysis (**Table S1**). **Figure 2A** shows a general overview on the different proteins amount in D27 in comparison to Symb1 (color variation in a scale from red, abundant in D27 to blue, abundant in Symb1). Quantitative differences were detected, especially for proteins involved in metabolism, cell envelope, information storage and processing. Interestingly, the "poorly characterized" protein area comprises a high number of significant differentially expressed proteins (**Figure 2A**).

The proteins that are more abundant in D27 as compared to Symb1 are 37 and, among them the conserved protein UCP028846 (18.27 fold change - OG1RF_11419), tagatose-biphosphate aldolase (11.95 fold change - OG1RF_10434), 1-phosphofructokinase (7.70 fold change - OG1RF_10431), exonuclease SbcC (6.88 fold change - OG1RF_12058) and glycosil hydrolase (6.05 fold change - OG1RF_12425) show the highest fold change values. For what concern the 95 proteins present in D27 and absent in Symb1, are worth mentioning the hemolysin (OG1RF_10438) and the penicillin-binding protein 1B (OG1RF_11450) (**Table S1**).

D27 and Symb1 share 344 extracellular proteins that represent about the 90% of the identified proteins. The Voronoi treemap (**Figure 2B**) provides an overview of the differentially expressed proteins between the two strains according to the quantitative data [based on the normalized spectrum abundance factors (NSAF)]. As suggested by the graphic visualization, most of the common proteins show a comparable level in two strains considered. Forty proteins are more abundant in D27 as compared Symb1, showing fold changes ranging between 5.63 and 2.05, most belonging to membrane transporters and cell-wall biosynthetic enzymes. The proteins present in D27 and absent in Symb1 are 95, where the gelatinase (OG1RF_11526) is the most interesting identified protein (**Table S3**).

Comparison Food/Pathogen

The cytosolic identified proteins shared by the dairy-isolate D27 and the clinical isolate UW3114 are 769, corresponding to the 87% of the total identified proteins (**Table S2**). As noticed previously, comparing D27 and Symb1, most of the proteins were assigned to the functional groups of metabolism-involved, cell envelope, information storage/processing and poorly characterized proteins (**Figure 3A**). The proteins more abundant in D27, as compared to UW3114, are 43 (**Table S2**) and among them the aldehyde-alcohol dehydrogenase (9.47 fold change - OG1RF_10627), phosphoglycerate mutase (5.50 fold change - OG1RF_12264), formate acetyltransferase (5.30 fold change - OG1RF_11329), 2-dehydropantoate 2-reductase (5.20 fold change - OG1RF_11367), uracil phosphoribosyltransferase (5.14 fold change - OG1RF_11432) show the highest fold change values. For what concern the 120 proteins present in D27 and absent in UW3114, are worth mentioning the hemolysin A (OG1RF_10716) and the β-lactamase (OG1RF_11969).

In the extracellular compartment of the D27 and UW3114, 226 proteins expressed by both strains were found (**Table S4**). The Voronoi treemap (**Figure 3B**) outlines how most of the proteins (red cells) are more abundant in the food isolate compared to the clinical strain. In particular, 116 proteins were more abundant in D27 compared to UW3114, showing fold change ranging between 21.06 and 2.01 (**Table S4**). Besides membrane transporters and cell-wall biosynthetic enzymes are worth mentioning a penicillin-binding protein C (13.75 fold-change - OG1RF_10724) and a β-lactamase (6.98 fold-change - OG1RF_11219). The different protein profiles between strains, indicated by the high fold change variation of the common proteins, is also supported by the presence of 212 proteins only identified in D27 and absent in UW3114 (**Table S4**). Among these, the most interesting are: choloylglycine hydrolase (AAM75246.1_39), efflux transporter (RND family - OG1RF_10301), PFL4705 family integrating conjugative element protein (OG1RF_12168) and chitin-binding protein (OG1RF_12499) (**Table S4**).

Phenotypic Tests

Evaluation of Enzymatic Activities Related to Pathogenicity

Protease and hemolysis were evaluated in the three strains in study, being the most common enzymatic activities associated to virulence, and the results are reported in **Figure 4**. As shown in **Figure 4A**, the strain UW3114 displays a 2-fold more intense protease activity than the food-isolate D27. As respect to the probiotic, no comparison can be done since

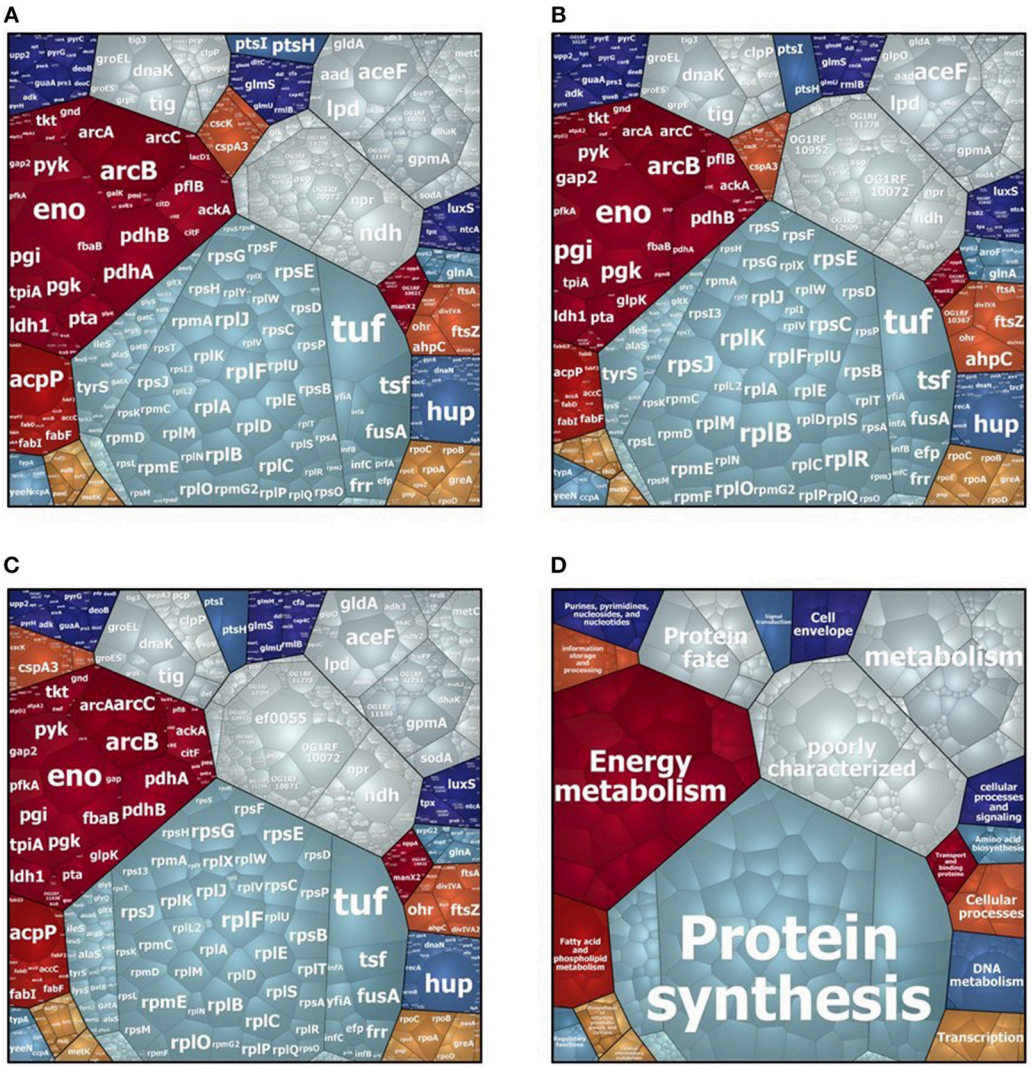

FIGURE 1 | Voronoi treemap visualization of cytosolic proteins of *E. faecalis* D27 **(A)**, *E. faecalis* Symbioflor 1 **(B)** and *E. faecalis* UW3114 **(C)**. Each protein is represented by a small cell, proteins are clustered according to their functional classification, cell-size correlates with protein abundance. **(D)** Represents functional organization of proteins.

for the latter measured absorbance values were negative. Concerning hemolysis, only the clinical isolate UW3114 shows hemolytic activity, against horse blood cells, where a β-hemolysis pattern (formation of clear halos) was observed (**Figure 4B**). Concerning gelatinase all the three strains were negative (data not shown).

Biofilm Formation

The ability to produce extracellular matrix was evaluated by growing bacteria on an abiotic solid surface, to allow biofilm formation. Although the three strains were able to secrete extracellular polymeric substances, biofilm quantification (using crystal violet staining) demonstrated that for the clinical strain biofilm is 8-fold more abundant than for Symb1 and 4-fold more than for D27 (**Figure 5**).

Antibiotic-Resistance Profiles

To get general insights in the antibiotics susceptibilities and resistances of the analyzed *E. faecalis* strains, 18 different antibiotics were tested and the results reported in **Table 1**. All the three isolates showed species-specific resistance to mupirocin (MUP) and also to clindamycin (CLI). These results were expected in enterococci, and confirmed by the test on the reference strain *E. faecalis* ATCC29212. None of the isolates showed resistance to glycopeptide compounds (vancomycin and teicoplanin) or to penicillin antibiotics (penicillin and ampicillin). Both the probiotic and the dairy-isolated strain D27 showed to be susceptible to 16 analyzed antibiotics. Conversely, the clinical isolate UW3114 was found to be resistant to 8 antibiotics, among which erythromycin. Erythromycin-resistance is ascribable

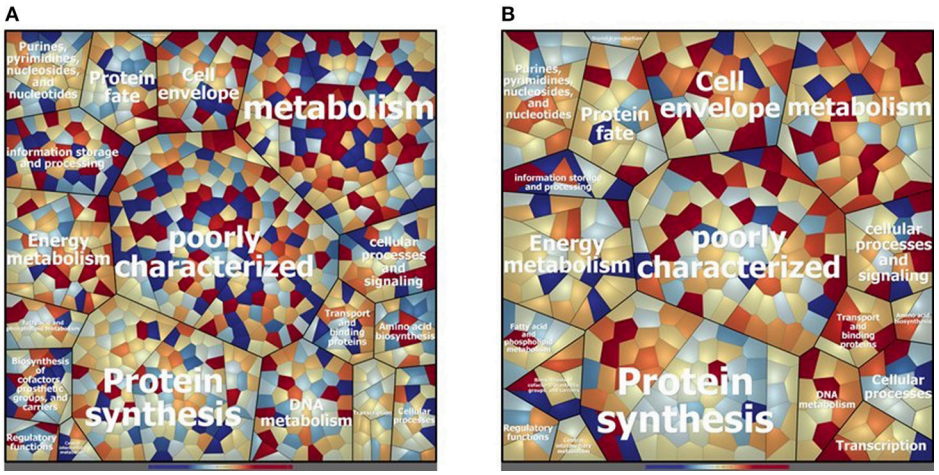

FIGURE 2 | Voronoi treemap visualization depicting the different protein pattern of *E. faecalis* D27 and *E. faecalis* Symbioflor 1 in the cytosolic **(A)** and extracellular **(B)** compartment. The proteins are grouped according to their predicted functional classification. Variation of relative protein amounts are indicated by color: red indicates higher amount in D27, blue higher abundance in Symbioflor 1.

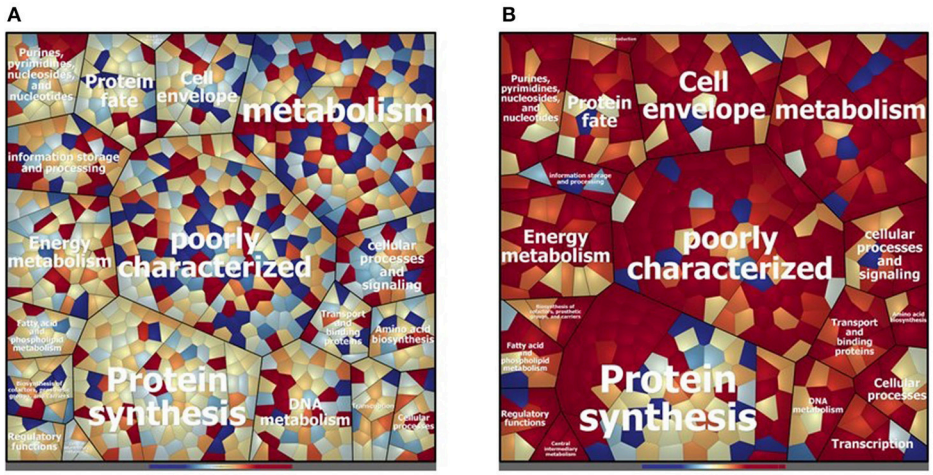

FIGURE 3 | Voronoi treemap visualization depicting the different protein pattern of *E. faecalis* D27 and *E. faecalis* UW3114 in the cytosolic **(A)** and extracellular **(B)** compartment. The proteins are grouped according to their predicted functional classification. Variation of relative protein amounts are indicated by color: red indicates higher amount in D27, blue higher abundance in UW3114.

to the presence of the PAI, as described before by Laverde Gomez (35).

DISCUSSION

Establishing the safety of a food-isolated strain is of primary importance especially when the controversial species *E. faecalis* is concerned. Actually, enterococci are not generally regarded as safe (GRAS) by e.g., the FDA. Proteomics is a valuable strategy to detect virulence characters. Furthermore, comparison with clearly recognized pathogenic and probiotic bacteria is an added value to highlight differences useful to classify the food-isolated strains as safe.

The *E. faecalis* in study D27 was compared to a clinical isolate UW3114 and to a commercialized probiotic Symb1. Several proteins display a significant fold-change as compared to the other two enterococci or are exclusively present in the food isolate. Of these, some are worth discussion because of their implication in pathogenicity, antibiotic resistance, gene transfer and possible human-host interaction.

Proteins Involved (or Possibly Involved) in Pathogenicity

Several proteins connected with pathogenic traits are expressed by the dairy-isolate D27. The protein named "secreted antigen" was found to be a serine protease by database search (BLAST

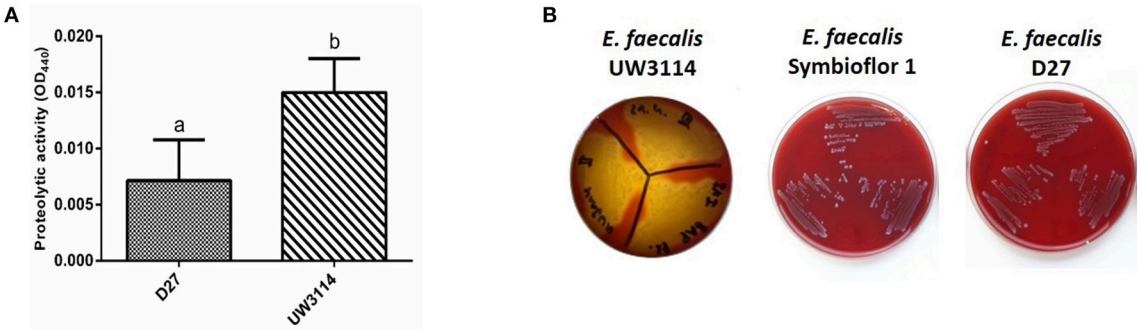

FIGURE 4 | (A) proteolytic activity, measured as optical density (OD) at 440 nm, in *E. faecalis* D27 and *E. faecalis* UW3114; **(B)** hemolytic activity of *E. faecalis* UW3114, Symbioflor 1 and D27 tested on horse blood agar plates. Only *E. faecalis* UW3114 shows β-hemolytic activity.

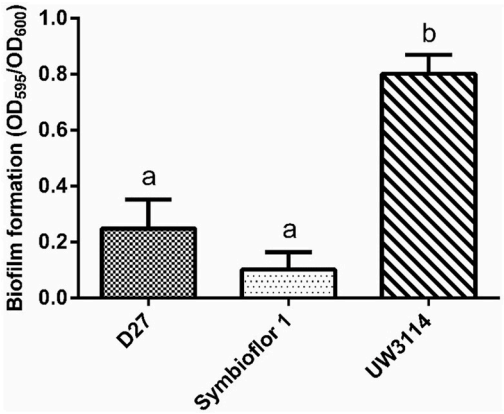

FIGURE 5 | biofilm quantification after crystal violet staining. The amount of biofilm produced by *E. faecalis* D27, *E. faecalis* Symbioflor 1, and *E. faecalis* UW3114 is proportional to the ratio between the crystal violet OD value (595) and culture OD value (600).

comparison with *E. faecalis* strains). The serine protease HtrA (OG1RF_12305) was expressed by both D27 and UW3114, however it was 2-fold more abundant in the clinical isolate. In the secretome, a different serine protease SprE (OG1RF_11525) was detected only in the hospital-isolated strain UW3114. Although D27 does not express SprE, another serine protease with pathogenic implications was found, the S41A family carboxy-terminal peptidase (OG1RF_11392). It has been reported that, in a murine sepsis model, disease caused by a S41-deficient mutant of *S. aureus* was less severe than that caused by the WT strain; this result demonstrates the role of these proteins in Gram-positive pathogenicity (47). A further proteolytic enzyme found in both D27 and UW3114 secretome is gelatinase (OG1RF_11526), one among the most important virulence factors in *E. faecalis*. The presence of genes for gelatinase E (GelE) and serine protease V8 (SprE) is usually considered a marker to identify potential pathogenic strains (48). However, it was already observed that a cheese-isolated *E. faecalis* strain does not show gelatinase or protease activity when submitted to phenotypic tests, even if possessing the abovementioned genes (16). This phenomenon was also observed in strains D27 and UW3114, where the presence of gelatinase enzyme does not support gelatinase activity. Two different types of hemolysins were present: hemolysin (OG1RF_10438) and hemolysin A (OG1RF_10716). D27 expresses both enzymes, whereas both the probiotic and the clinical strains express only one of them. However, the clinical isolate is the only strain showing β-hemolysis *in vitro,* as expected (**Figure 4B**). Actually, it is long time established that the presence of the *cyl* operon is indispensable but not sufficient for the hemolytic activity, since different enzymes are involved and a proteolytic cleavage is required for protein activation (49). The influence of environmental factors on gene expression is a well-known phenomenon. For Enterococcus, the effect of multiple external factors on pathogenic character expression has been described since 1998 (50).

Finally, a LemA family protein (OG1RF_10353) was found in D27 and UW3114, with less than 2-fold change in abundance. This protein family was well characterized in the *Pseudomonas* genus, where it was identified as a transmembrane histidine protein kinase (HPK) sensor-regulators, involved in lesion formation in the host (51).

Proteins Involved in Antibiotic Resistance

As a general rule, it has to be highlighted that in Enterococci, antibiotic resistance is based upon three main mechanisms: (a) intrinsic or natural resistance (b) acquired resistance and (c) tolerance. The intrinsic resistance is a genus-related feature and it is generally linked to insensitivity of the bacterial cell to the antibiotic molecules either through absence of the uptake mechanism (5), or to a modification of the antibiotic targets such as the PBPs (penicillin binding proteins) (52) or to efflux systems (53). Discovered in the 1980 (54) and referred to also as "intrinsic insensitivity" it is the main cause of the difficulty of treating enterococcal infections (55). The acquired resistance, on the contrary, is often based upon production of enzymes modifying or degrading the antibacterial molecule and it is transmissible by genetic recombination. Hence, this last mechanism is more dangerous since it can allow spread of the resistance character among strains (5).

Two classes of proteins were found that could confer antibiotic resistance to the *E. faecalis* strains under investigation: the

TABLE 1 | Antibiotic susceptibility (green) and resistance (red) of the three tested strains of *E. faecalis*, D27, UW3114, and Symbioflor 1, and the quality control strain *E. faecalis* ATCC29212, as recommended by EUCAST guidelines.

	D27	UW3114	Symbioflor1	ATCC29212
PEN	2	8	4	2
AMP	2	4	4	2
GEN	≤64	512	≤64	≤64
STR	≤128	2,048	≤128	≤128
VAN	2	2	4	4
TPL	≤1	≤1	≤1	≤1
DAP	≤2	≤2	≤2	≤2
CLI	>8	>8	8	8
ERY	≤1	>16	≤1	≤1
CIP	≤2	32	≤2	≤2
MFL	≤0.125	>2	≤0.125	0.25
LNZ	≤2	≤2	≤2	≤2
TET	≤0.5	>16	≤0.5	>16
TGC	≤0.063	≤0.063	≤0.063	≤0.063
RAM	2	≤1	4	≤1
SXT	≤0.032	≤0.032	≤0.032	≤0.032
CMP	8	8	8	8
MUP	>32	>32	>32	>32

PEN, penicillin; AMP, ampicillin; GEN, gentamycin; STR, streptomycin; VAN, vancomycin; TPL, teicoplanin; DAP, daptomycin; CLI, clindamycin; ERY, erythromycin; CIP, ciprofloxacin; MFL, moxifloxacin; LNZ, linezolid; TET, tetracycline; TGC, tigecycline; RAM, rifampicin; SXT, trimethoprim/sulfamethoxazole; CMP, chloramphenicol; MUP, mupirocin.

true resistance marker β-lactamase and the penicillin-binding proteins (PBPs) that can be involved in resistance if a mutation in their sequence occurs. The three strains show to possess a heterogeneous set of these proteins.

As far as the membrane-located PBPs are concerned, their relative abundance evaluation has the limitation of a low reliability, because the extraction procedure could not have been homogeneous in the three samples analyzed. PBPs (e.g., PBP2B, PBP3, PBP4, PBP5) are involved in the peptidoglycan formation. However, it was observed that the presence of a high molecular weight variant of PBP5 decreased susceptibility of *E. faecium* to ampicillin and other β-lactams (56, 57). In *E. faecalis,* resistance to both imipenem and ampicillin due to amino acid mutation (520 and 605 residues) in the PBP4 was observed (58). In the cytosolic proteome of the studied strains, the PBP1A (OG1RF_10925) seems 2.5-fold more abundant in D27 compared to Symb1; the PBP1B (OG1RF_11450) is exclusively expressed by D27; the PBPC (OG1RF_10724) was found in large amount in D27, compared to the other two strains. Furthermore, extracellular proteins identification in the food strain confirmed the presence of PBPs, with some differences respect the cytosolic compartment. PBP1A that in the cytosol was found more abundant in D27 compared to Symb1, in the extracellular compartment appears to be more abundant in the probiotic strain. Therefore, it seems that this abundance is rather due to compartmentalization than to higher gene expression.

Three different β-lactamases were found, both in the intra- and extra-cellular proteomes. Two of them are metallo-hydrolases, one exclusively expressed in Symb1 (OG1RF_10969) and the other (OG1RF_11863) 2.5-fold more abundant in the clinical isolate compared to the food-isolate; the last is a serine-hydrolase (OG1RF_11969) exclusively expressed in D27. The antibiotic inactivation based on hydrolytic activity is mostly effective when applied to β-lactam antibiotics. In particular, there are two main molecular strategies employed by β-lactamases to hydrolytically cleave the β-lactam ring of penicillins and cephalosporins: through the action of an active site Ser-nucleophile, or through activation of water via a Zn^{2+} center (59). As reported in the literature, the proteins described above are responsible for insensitivity to β-lactam antibiotics in enterococci (60). Furthermore, this type of resistance seems to be transmissible (5).

The identification of a high variety of proteins, possibly involved in resistance, found in the proteomes of the three strains in study, suggests that resistance events could occur also in the probiotic and the dairy-isolate that share a similar antibiotitype. Actually, probiotics were already described as harboring resistance traits (61). However, in spite of these protein profiles, the antibiotic susceptibility testing revealed a general sensitivity pattern toward beta-lactams in all the three strains considered (**Table 1**). As far as the PBPs are concerned, it is possible that they are active and not mutated forms as those described in *E faecalis* by Ono (58). Regarding beta lactamases, it is possible to hypothesize that the expression of these proteins is a condition necessary but not sufficient to engender resistance, suggesting that other factors can play a role in the occurrence of resistant phenotypes.

As far as the food-borne *Enterococcus* D27 is concerned, an efflux transporter (RND family - OG1RF_10301) has also been found. Efflux pumps, responsible either of multidrug resistance mechanisms or of single antibiotic extrusion, have been described in LAB as well (62). In the strain D27 this efflux system could be involved in the clindamycin resistance pattern observed (**Table 1**), whereas the resistance to mupirocin observed seems to be due to other mechanisms as it has long been established (63). On the other hand, both these resistances are present in all the three strain considered, suggesting that they can be based upon an intrinsic resistance mechanism as frequently described for Enterococci (55).

Proteins Involved in Horizontal Gene Transfer

The PFL4705 family integrating conjugative element protein (OG1RF_12168) was found both in the food-isolate D27 and in the probiotic strain Symb1, with comparable expression levels. Often, virulence determinants are acquired as mobile elements during gene transfer processes also mediated by this protein and these genetic exchanges are frequent between *E. faecalis* strains (35, 64).The second interesting protein more expressed by D27, is the pheromone cAM373 (OG1RF_11130). It was characterized also in *S. aureus* and corresponds to a

heptapeptide (AIFILAS) located within the C-termini of the signal sequences of putative pre-lipoproteins. This hydrophobic, linear peptide molecule acts as signals that facilitate the conjugative transfer of a specific category of plasmids referred to as pheromone-responsive plasmids (65). This specific type of inducible plasmid represents an important mechanism for dissemination of antibiotic resistance and virulence among *Enterococcus* strains (66). These findings also suggest that the food ecosystem is a suitable environment for favoring cell-to-cell communication.

In the extracellular fraction, a second pheromone, cAD1 (OG1RF_12509), more expressed by the dairy-isolate, was found. In *E. faecalis,* this octapeptide sex pheromone was identified as responsible of an induced mating response by donors carrying the hemolysin plasmid pAD1 or related elements (67). This result, although expected for the clinical isolate is surprising for the food strain that generally do not need to acquire hemolysins in its ecological niche.

Proteins Involved in Human Host/Environment Interactions

The von Willebrand factor (vWF) type A domain protein (OG1RF_10869) is an example of potential pathogenicity-associated protein more expressed in the secretome by the food-isolate strain compared to the probiotic and clinical isolates (fold-change 2.21 and 2.16, respectively). vWF is a huge multimeric protein, well-characterized in humans, where it triggers platelet adhesion in areas of vascular damage. In particular, the domain A1 mediates platelet adhesion under flow in areas of vessel injury through the platelet glycoprotein Ibα (GPIbα) (68). Most prokaryotic vWF domains have not been investigated in detail, however, Konto-Ghiorghi et al. (69) showed that the GBS PilA tip pilin vWF domain was important for pilus-mediated bacterial adhesion to human alveolar and intestinal epithelial cells *in vitro*. The last newsworthy evidence is the variety of lipoproteins produced by the dairy-isolate. Even if the function and the localization is still unknown for most of them it is well-recognized that lipoproteins in Gram-positive bacteria represent about the 25% of the surface associated proteins, which could play a major role in bacterial virulence processes (70).

Among up-regulated proteins in D27, choloylglycine hydrolase (AAM75246.1_39) represents an interesting enzyme since it catalyzes the initial "gateway" reaction in the bacterial metabolism of CBAs (conjugated bile acids). The reaction consists in a deconjugation of CBAs to liberate free primary bile acids (BAs; cholic acid or chenodeoxycholic acid) and amino acids (71). CBAs have been suggested to repress bacterial growth in the small intestine by means of direct antimicrobial effects, up-regulation of host mucosal defenses, or synergistic action of both mechanisms (72). The expression of this enzyme by the food-isolate can increase the ability of the strain to survive to CBAs action in the gut, thus enhancing the probiotic potential of D27. This is partly expected, because Enterococci generally display a high degree of resistance to bile salts (73). Considering that, all the three strains share the presence of several proteins involved in mucosa and mucus adhesion (e.g., enolase, EFTu, EFTs, DnaK, Clp, GroEL, chitin-binding protein) (74, 75), it is possible to hypothesize that the foodborne D27 can also share the same attitude to persist in the human host by adhering to the gut mucosa. However, D27 ability to form biofilm, although higher than Symb1, is four-fold lower than the one observed in the pathogenic UW3114.

CONCLUSION

The results obtained in the present investigation comparing a food-isolated *E. faecalis* D27 with a patented probiotic and a pathogenic isolate, underline that there is the need of a detailed typing of strains, either employed in food fermentation or foodborne contaminants, to avoid risks of virulence dissemination.

The probiotic strain *E. faecalis* Symbioflor 1, although bearing some resistance traits, possess several proteins that support its role as a probiotic, namely involved in stress response, that are of primary importance both for the shelf-life of the probiotic preparation and for bacterial survival in the human gastro-intestinal tract. The clinical isolate *E. faecalis* UW3114 was the only strain synthesizing some of the ascertained virulence determinants such as the serine protease SprE and displaying the highest levels of antibiotic resistance included aminoglycosides. All these results were expected.

As far as the foodborne isolate is concerned, *E. faecalis* D27 besides showing a high metabolic activity (confirmed by the up-regulation of several proteins involved in hydrolysis, energy metabolism, and nutrient transport) also displays some proteins whose function could be hazardous. Among these, antibiotic resistance factors (although not all expressed in the tested conditions) and horizontal gene transfer involved proteins (PFL4705 family integrating conjugative element), are a clear evidence that recombination events (both in food and in the GIT) can cause antibiotic resistance spread. Other possible virulence factors are the vWF type A domain protein, and some proteases involved in pathogenicity, like the serine protease HtrA, the S41A family carboxy-terminal peptidase and LemA. On the other hand, the presence in D27 of a high number of proteolytic enzymes is probably linked to the advantage of possessing proteases in a food matrix like cheese that is very rich in proteins. It is worth to highlight that single approaches for typing bacteria to find pathogenicity factors all have the limitation of considering characters (genes or proteins) that not always are disclosed.

Considering the heterogeneous habitat in which food microorganisms live, modifications of their proteomic patterns can also occur both by interaction with other bacteria (genetic exchanges) and during contact with the host. The results obtained in the present investigation are far to be exhaustive since new genes and proteins involved in pathogenesis in different *E. faecalis* strains are repeatedly reported in the literature. However, taken together, these data demonstrate the importance of carefully and periodically characterize food-isolated enterococcal strains to ascertain their safety before employing them for human consumption. In this context, in parallel to genetic analysis, complementing gel-free proteomics (especially the

analyses concerning secreted "marker-factors") and phenotypic tests proved to be a valuable tool to assess these features.

AUTHOR CONTRIBUTIONS

All authors listed have made a substantial, direct and intellectual contribution to the work, and approved it for publication.

ACKNOWLEDGMENTS

We are grateful to Dirk Albrecht for helping with the mass spectrometry analyses, to Jörg Bernhardt for assistance in data visualization, Guido Werner from the Robert Koch Institute for providing the strain UW3114 and Carola Fleige for technical assistance. SC benefitted of Erasmus program for 4 months staying in the Department for Microbial Physiology and Molecular Biology of Greifswald University.

SUPPLEMENTARY MATERIAL

The Supplementary Material for this article can be found online at: https://www.frontiersin.org/articles/10.3389/fnut.2019.00071/full#supplementary-material

Table S1 | The table includes the cytosolic proteins identified in at least two of the three biological replicates of *E. faecalis* D27 and *E. faecalis* Symbioflor 1 and the proteins found only in one *E. faecalis* strain and absent (off) in the other strain. The fold-change is given by the ratio between the average of the protein abundance (fmol/ng) in *E. faecalis* D27 and the average of the protein abundance (fmol/ng) in *E. faecalis* Symbioflor 1. Accession, protein name, description, localization (obtained by pSortb), main role and subrole are reported to give information on the protein function. For each protein, the abundance (fmol/ng) for all the biological replicates, as well as the average of the abundance are reported for both *E. faecalis* D27 and *E. faecalis* Symbioflor 1. The Repcount refers to the number of technical replicates in which the protein was identified.

Table S2 | The table includes the cytosolic proteins identified in at least two of the three biological replicates of *E. faecalis* D27 and *E. faecalis* UW3114 and the proteins found only in one *E. faecalis* strain and absent (off) in the other strain. The fold-change is given by the ratio between the average of the relative abundance (fmol/ng) in *E. faecalis* D27 and the average of the relative abundance (fmol/ng) in *E. faecalis* UW3114. Accession, protein name, description, localization (obtained by pSortb), main role and subrole are reported to give information on the protein function. For each protein, the abundance (fmol/ng) for all the biological replicates, as well as the average of the abundance are reported for both *E. faecalis* D27 and *E. faecalis* UW3114. The Repcount refers to the number of technical replicates in which the protein was identified.

Table S3 | The table includes the secreted proteins identified in at least two of the three biological replicates of *E. faecalis* D27 and *E. faecalis* Symbioflor 1 and the proteins found only in one *E. faecalis* strain and absent (off) in the other strain. The fold-change is given by the ratio between the average of the abundance [normalized spectral abundance factor (NSAF)] in *E. faecalis* D27 and the average of the abundance (NSAF) in *E. faecalis* Symbioflor 1. Accession, protein name, description, localization (obtained by pSortb), main role and subrole are reported to give information on the protein function. For each protein, the abundance (NSAF) for all the biological replicates are reported for both *E. faecalis* D27 and *E. faecalis* Symbioflor 1.

Table S4 | The table includes the secreted proteins identified in at least two of the three biological replicates of *E. faecalis* D27 and *E. faecalis* UW3114 and the proteins found only in one of *E. faecalis* strain and absent (off) in the other strain. The fold-change is given by the ratio between the average of the abundance [normalized spectral abundance factor (NSAF)] in *E. faecalis* D27 and the average of the abundance (NSAF) in *E. faecalis* UW3114. Accession, protein name, description, localization (obtained by pSortb), main role and subrole are reported to give information on the protein function. For each protein, the abundance (NSAF) for all the biological replicates are reported for both *E. faecalis* D27 and *E. faecalis* UW3114.

REFERENCES

1. Arias CA, Murray BE. Emergence and management of drug-resistant enterococcal infections, microbial drug resistance, future medicine. *Exp Rev Anti Infect Ther.* (2008) 6:637–55. doi: 10.1586/14787210.6.5.637
2. Schaberg DR, Culver DH, Gaynes RP. Major trends in the microbial etiology of nosocomial infection. *Am J Med.* (1991) 91:S72–5. doi: 10.1016/0002-9343(91)90346-Y
3. Mathur S, Singh R. Antibiotic resistance in food lactic acid bacteria—a review. *Int J Food Microbiol.* (2005) 105:281–95. doi: 10.1016/J.IJFOODMICRO.2005.03.008
4. Nam HM, Lim SK, Moon JS, Kang HM, Kim JM, Jang KC, et al. Antimicrobial resistance of enterococci isolated from mastitic bovine milk samples in Korea. *Zoonoses Public Health.* (2010) 57: e59–64. doi: 10.1111/j.1863-2378.2009.01307.x
5. Argyri AA, Zoumpopoulou G, Karatzas KAG, Tsakalidou E, Nychas GJE, Panagou EZ, et al. Selection of potential probiotic lactic acid bacteria from fermented olives by *in vitro* tests. *Food Microbiol.* (2013) 33:282–91. doi: 10.1016/j.fm.2012.10.005
6. Miller WR, Munita JM, Arias CA. Mechanisms of antibiotic resistance in enterococci. *Expert Rev Anti Infect Ther*. (2014) 12:1221–36. doi: 10.1586/14787210.2014.956092
7. Hegstad K, Mikalsen T, Coque TM, Werner G, Sundsfjord A. Mobile genetic elements and their contribution to the emergence of antimicrobial resistant *Enterococcus faecalis* and *Enterococcus faecium*. *Clin Microbiol Infect.* (2010) 16:541–54. doi: 10.1111/j.1469-0691.2010.03226.x
8. Levy SB, Bonnie M. Antibacterial resistance worldwide: causes, challenges and responses. *Nat Med.* (2004) 10:S122–9. doi: 10.1038/nm1145
9. Salyers AA, Shoemaker NB. Resistance gene transfer in anaerobes: new insights, new problems. *Clin Infect Dis.* (1996) 23 (Suppl. 1):S36–43. doi: 10.1017/s0950268812000635
10. Eaton T, Gasson M. Molecular screening of enterococcus virulance determinants and potential for genetic exchange between food and medical isolates. *Appl Environ Microbiol.* (2001) 67:1628–35. doi: 10.1128/AEM.67.4.1628
11. Mannu L, Paba A, Daga E, Comunian R, Zanetti S, Duprè I, et al. Comparison of the incidence of virulence determinants and antibiotic resistance between *Enterococcus faecium* strains of dairy, animal and clinical origin. *Int. J. Food Microbiol.* (2003) 88:291–304. doi: 10.1016/S0168-1605(03)00191-0
12. Shankar N, Lockatell CV, Baghdayan AS, Drachenberg C, Gilmore MS, Johnson DE. Role of Enterococcus faecalis surface protein esp in the pathogenesis of ascending urinary tract *Infection*. (2001) 69:4366–72. doi: 10.1128/IAI.69.7.4366
13. Daw K, Baghdayan AS, Awasthi S, Shankar N. Biofilm and planktonic Enterococcus faecalis elicit different responses from host phagocytes *in vitro*. *FEMS Immunol Med Microbiol.* (2012) 65:270–82. doi: 10.1111/j.1574-695X.2012.00944.x
14. Klein G. Taxonomy, ecology and antibiotic resistance of enterococci from food and the gastro-intestinal tract. *Int J Food Microbiol.* (2003) 88:123–31. doi: 10.1016/S0168-1605(03)00175-2
15. Kayaoglu G, Ömürlü H, Akca G, Gürel M, Gençay Ö, Sorkun K, et al. Antibacterial activity of propolis versus conventional endodontic disinfectants against *Enterococcus faecalis* in infected dentinal tubules. *J Endod.* (2011) 37:376–381. doi: 10.1016/J.JOEN.2010.11.024

16. Pessione A, Lamberti C, Cocolin L, Campolongo S, Grunau A, Giubergia S, et al. Different protein expression profiles in cheese and clinical isolates of *Enterococcus faecalis* revealed by proteomic analysis. *Proteomics.* (2012) 12:431–47. doi: 10.1002/pmic.201100468
17. Abriouel H, Omar N, Ben M, López RL, Grande MJ, Martínez-Viedma P, et al. Comparative analysis of genetic diversity and incidence of virulence factors and antibiotic resistance among enterococcal populations from raw fruit and vegetable foods, water and soil, and clinical samples. *Int J Food Microbiol.* (2008) 123:38–49. doi: 10.1016/J.IJFOODMICRO.2007.11.067
18. Vachee A, Drider D, Silvain A, Al Atya AK, Ravallec R, Drider-Hadiouche K. Probiotic potential of *Enterococcus faecalis* strains isolated from meconium. *Front Microbiol.* (2015) 6:227. doi: 10.3389/fmicb.2015.00227
19. Shepard BD, Gilmore MS. Antibiotic-resistant enterococci: the mechanisms and dynamics of drug introduction and resistance. *Microbes Infect.* (2002) 4:215–24. doi: 10.1016/S1286-4579(01)01530-1
20. Tyson GH, Nyirabahizi E, Crarey E, Kabera C, Lam C, Rice-Trujillo C, et al. Prevalence and antimicrobial resistance of Enterococci isolated from retail meats in the United States, 2002-2014. *Appl Environ Microbiol.* (2017) 84:AEM.01902–01917. doi: 10.1128/AEM.01902-17
21. Jiménez E, Ladero V, Chico I, Maldonado-Barragán A, López M, Martín V, et al. Antibiotic resistance, virulence determinants and production of biogenic amines among enterococci from ovine, feline, canine, porcine and human milk. *BMC Microbiol.* (2013) 13:288. doi: 10.1186/1471-2180-13-288
22. Peters J, Mac K, Wichmann-Schauer H, Klein G, Ellerbroek L. Species distribution and antibiotic resistance patterns of enterococci isolated from food of animal origin in Germany. *Int J Food Microbiol.* (2003) 88:311–4. doi: 10.1016/S0168-1605(03)00193-4
23. Švec P, Franz CMAP. *The Family Enterococcaceae.* (2014). doi: 10.1002/9781118655252.part3
24. Giraffa G. Functionality of enterococci in dairy products. *Int J Food Microbiol.* (2003) 88:215–22. doi: 10.1016/S0168-1605(03)00183-1
25. Hammad AM, Hassan HA, Shimamoto T. Prevalence, antibiotic resistance and virulence of *Enterococcus.* spp. in Egyptian fresh raw milk cheese. *Food Control.* (2015) 50:815–20. doi: 10.1016/J.FOODCONT.2014.10.020
26. Koluman A, Akan LS, Çakiroglu FP. Occurrence and antimicrobial resistance of enterococci in retail foods. *Food Control.* (2009) 20:281–3. doi: 10.1016/J.FOODCONT.2008.05.007
27. Agersø Y, Lester CH, Porsbo LJ, Ørsted I, Emborg HD, Olsen KEP, et al. Vancomycin-resistant *Enterococcus faecalis* isolates from a Danish patient and two healthy human volunteers are possibly related to isolates from imported turkey meat. *J. Antimicrob. Chemother.* (2008) 62:844–5. doi: 10.1093/jac/dkn271
28. Gaglio R, Couto N, Marques C, de Fatima Silva Lopes M, Moschetti G, Pomba C, et al. Evaluation of antimicrobial resistance and virulence of enterococci from equipment surfaces, raw materials, and traditional cheeses. *Int J Food Microbiol.* (2016) 236:107–14. doi: 10.1016/J.IJFOODMICRO.2016.07.020
29. Jacobsen L, Wilcks A, Hammer K, Huys G, Gevers D, Andersen SR. Horizontal transfer of tet(M) and erm(B) resistance plasmids from food strains of *Lactobacillus plantarum* to *Enterococcus faecalis* JH2-2 in the gastrointestinal tract of gnotobiotic rats. *FEMS Microbiol Ecol.* (2007) 59:158–66. doi: 10.1111/j.1574-6941.2006.00212.x
30. Ramos S, Igrejas G, Rodrigues J, Capelo-Martinez J-L, Poeta P. Genetic characterisation of antibiotic resistance and virulence factors in vanA-containing enterococci from cattle, sheep and pigs subsequent to the discontinuation of the use of avoparcin. *Vet J.* (2012) 193:301–3. doi: 10.1016/J.TVJL.2011.12.007
31. Domann E, Hain T, Ghai R, Billion A, Kuenne C, Zimmermann K, et al. Comparative genomic analysis for the presence of potential enterococcal virulence factors in the probiotic *Enterococcus faecalis* strain Symbioflor 1. *Int J Med Microbiol.* (2007) 297:533–9. doi: 10.1016/j.ijmm.2007.02.008
32. Franz CMAP, Huch M, Abriouel H, Holzapfel W, Gálvez A. Enterococci as probiotics and their implications in food safety. *Int J Food Microbiol.* (2011) 151:125–40. doi: 10.1016/j.ijfoodmicro.2011.08.014
33. Parvez S, Malik KA, Ah Kang S, Kim HY. Probiotics and their fermented food products are beneficial for health. *J Appl Microbiol.* (2006) 100:1171–85. doi: 10.1111/j.1365-2672.2006.02963.x
34. Tuohy KM, Probert HM, Smejkal CW, Gibson GR. Using probiotics and prebiotics to improve gut health. *Drug Discov Today.* (2003) 8:692–700. doi: 10.1016/S1359-6446(03)02746-6
35. Laverde Gomez JA, Hendrickx APA, Willems RJ, Top J, Sava I, Huebner J, et al. Intra- and interspecies genomic transfer of the Enterococcus faecalis pathogenicity Island. *PLoS ONE.* (2011) 6:16720. doi: 10.1371/journal.pone.0016720
36. Zühlke D, Dörries K, Bernhardt J, Maaß S, Muntel J, Liebscher V, et al. Costs of life-Dynamics of the protein inventory of Staphylococcus aureus during anaerobiosis. *Sci. Rep.* (2016) 6:1–13. doi: 10.1038/srep28172
37. Muntel J, Hecker M, Becher D. An exclusion list based label-free proteome quantification approach using an LTQ Orbitrap. *Rapid Commun Mass Spectrom.* (2012) 26:701–9. doi: 10.1002/rcm.6147
38. Rappsilber J, Mann M, Ishihama Y. Protocol for micro-purification, enrichment, pre-fractionation and storage of peptides for proteomics using StageTips. *Nat Protoc.* (2007) 2:1896–906. doi: 10.1038/nprot.2007.261
39. Lassek C, Berger A, Zühlke D, Wittmann C, Riedel K. Proteome and carbon flux analysis of *Pseudomonas aeruginosa* clinical isolates from different infection sites. *Proteomics.* (2016) 16:1381–5. doi: 10.1002/pmic.201500228
40. López-Mondéjar R, Zühlke D, Becher D, Riedel K, Baldrian P. Cellulose and hemicellulose decomposition by forest soil bacteria proceeds by the action of structurally variable enzymatic systems. *Sci Rep.* (2016) 6:1–12. doi: 10.1038/srep25279
41. Silva JC, Denny R, Dorschel CA, Gorenstein M, Kass IJ, Li GZ, et al. Quantitative proteomic analysis by accurate mass retention time pairs. *Anal Chem.* (2005) 77:2187–200. doi: 10.1021/ac048455k
42. Silva JC, Gorenstein MV, Li G-Z, Vissers JPC, Geromanos SJ. Absolute quantification of proteins by LCMSE: a virtue of parallel MS acquisition. *Mol Cell Proteomics.* (2005) 5:144–56. doi: 10.1074/mcp.M500230-MCP200
43. Zhang Y, Wen Z, Washburn MP, Florens L. Refinements to proteome quantitation based on spectral counting: how to deal with peptides shared by multiple proteins. *Anal Chem.* (2010) 82:2272–81. doi: 10.1021/ac9023999
44. Deutsch EW, Csordas A, Sun Z, Jarnuczak A, Perez-Riverol Y, Ternent T, et al. The ProteomeXchange consortium in 2017: Supporting the cultural change in proteomics public data deposition. *Nucleic Acids Res.* (2017) 45:D1100–6. doi: 10.1093/nar/gkw936
45. Schneider T, Schmid E, de Castro JV, Cardinale M, Eberl L, Grube M, et al. Structure and function of the symbiosis partners of the lung lichen (Lobaria pulmonaria L. Hoffm.) analyzed by metaproteomics. *Proteomics.* (2011) 11:2752–6.
46. Deutsches Institut für Normung. *DIN 58940-7 (Standard Draft): Medical Microbiology–Susceptibility Testing of Microbial Pathogens toAntimicrobial Agents–Part 7: Determination of the Minimum Bactericidal Concentration (MBC) by Means of the Microbouillon Dilution Method.* Berlin: Beuth (2008).
47. Carroll RK, Rivera FE, Cavaco CK, Johnson GM, Martin D, Shaw LN. The lone S41 family C-terminal processing protease in Staphylococcus aureus is localized to the cell wall and contributes to virulence. *Microbiol.* (2014) 160:1737–48. doi: 10.1099/mic.0.079798-0
48. Thurlow LR, Thomas VC, Narayanan S, Olson S, Fleming SD, Hancock LE. Gelatinase contributes to the pathogenesis of endocarditis caused by *Enterococcus faecalis*. *Infect Immun.* (2010) 78:4936–43. doi: 10.1128/IAI.01118-09
49. Semedo T, Almeida Santos M, Martins P, Silva Lopes MF, Figueiredeo Marques JJ, Teneiro R, et al. Comparative study using type strains and clinical and food isolated to examine hemolytic activity and ocurrente of the cyl operon in enterococci. *J Clin Microbiol.* (2003) 41:2569–76. doi: 10.1128/JCM.41.6.2569-2576.2003
50. Dupont H, Montravers P, Mohler J, Carbon C. Disparate findings on the role of virulence factors of *Enterococcus faecalis* in mouse and rat models of peritonitis. *Infect Immun.* (1998) 66:2570–75.
51. Rich JJ, Kinscherf TG, Kitten T, Willis DK. Genetic evidence that the gacA gene encodes the cognate response regulator for the lemA sensor in *Pseudomonas syringae*. *J Bacteriol.* (1994) 176:7468–75. doi: 10.1128/jb.176.24.7468-7475.1994
52. Williamson R, Le Bouguenec C, Gutmann L, Horaud T. One or two low affinity penicillin-binding proteins may be responsible for the range of susceptibility of *Enterococcus faecium* to benzylpenicillin. *J Gen Microbiol.* (1985) 131:1933–40. doi: 10.1099/00221287-131-8-1933

53. Lynch C, Courvalin P, Nikaido H. Active efflux of antimicrobial agents in wild-type strains of Enterococci. *Antimicrob. Agents Chemother.* (1997) 41:869–71.
54. Brown DFJ, Reynolds PE. Intrinsic resistance to /3-lactam antibiotics in *Staphylococcus aureus*. (1980) 122:275–8.
55. Hollenbeck BL, Rice LB. Intrinsic and acquired resistance mechanisms in enterococcus. *Virulence.* (2012) 3:421–33. doi: 10.4161/viru.21282
56. Galloway-Peña JR, Nallapareddy SR, Arias CA, Eliopoulos GM, Murray BE. Analysis of clonality and antibiotic resistance among early clinical isolates of *Enterococcus faecium* in the United States. *J Infect Dis.* (2009) 200:1566–73. doi: 10.1086/644790
57. Montealegre MC, Roh H, Rae M, Davlieva MG, Singh KV, Shamoo Y, et al. Differential Penicillin-Binding Protein 5 (PBP5) levels in the *Enterococcus faecium* clades with different levels of ampicillin resistance. *Antimicrob Chemother. Chemother.* (2017) 61:1–10. doi: 10.1128/AAC.02034-16
58. Ono S, Muratani T, Matsumoto T. Mechanisms of resistance to imipenem and ampicillin in *Enterococcus faecalis*. *Antimicrob Agents Chemother.* (2005) 49:2954–8. doi: 10.1128/AAC.49.7.2954-2958.2005
59. Wright GD. Bacterial resistance to antibiotics: enzymatic degradation and modification. *Adv Drug Deliv Rev.* (2005) 57:1451–70. doi: 10.1016/j.addr.2005.04.002
60. Fontana R, Canepari P, Lleò MM, Satta G. Mechanisms of resistance of enterococci to beta-lactam antibiotics. *Eur J Clin Microbiol Infect Dis.* (1990) 9:103–5.
61. Temmerman R, Pot B, Huys G, Swings J. Identification and antibiotic susceptibility of bacterial isolates from probiotic products. *Int J Food Microbiol.* (2003) 81:1–10. doi: 10.1016/S0168-1605(02)00162-9
62. Wacher-Rodarte M, del C, Trejo-Muñúzuri TP, Montiel-Aguirre JF, Drago-Serrano ME, Gutiérrez-Lucas RL, et al. Antibiotic resistance and multidrug-resistant efflux pumps expression in lactic acid bacteria isolated from pozol, a nonalcoholic Mayan maize fermented beverage. *Food Sci Nutr.* (2016) 4:423–30. doi: 10.1002/fsn3.304
63. Cookson BD. The emergence of mupirocin resistance: a challenge to infection control and antibiotic prescribing practice. *J Antimicrob Chemother.* (1998) 41:11–8.
64. Ruiz-Garbajosa P, Bonten MJM, Robinson DA, Top J, Nallapareddy SR, Torres C, et al. Multilocus sequence typing scheme for *Enterococcus faecalis* reveals hospital-adapted genetic complexes in a background of high rates of recombination. *J Clin Microbiol.* (2006) 44:2220–8. doi: 10.1128/JCM.02596-05
65. Dunny GM, Leonard BAB. Cell-cell communication in gram-positive bacteria. *Annu Rev Microbiol.* (1997) 51:527–64. doi: 10.1146/annurev.micro.51.1.527
66. Fisher K, Phillips C. The ecology, epidemiology and virulence of Enterococcus. *Microbiology.* (2009) 155:1749–57. doi: 10.1099/mic.0.026385-0
67. An FY, Sulavik MC, Clewell DB. Identification and characterization of a determinant (eep) on the *Enterococcus faecalis* chromosome that is involved in production of the peptide sex pheromone. *J Bacteriol.* (1999) 81:5915–21.
68. Posch S, Aponte-Santamaría C, Schwarzl R, Karner A, Radtke M, Gräter F, et al. Mutual A domain interactions in the force sensing protein von Willebrand factor. *J Struct Biol.* (2017) 197:57–64. doi: 10.1016/J.JSB.2016.04.012
69. Konto-Ghiorghi Y, Mairey E, Mallet A, Duménil G, Caliot E, Trieu-Cuot P, et al. Dual role for pilus in adherence to epithelial cells and biofilm formation in *Streptococcus agalactiae*. *PLoS Pathog.* (2009) 5:e1000422. doi: 10.1371/journal.ppat.1000422
70. Reffuveille F, Leneveu C, Chevalier S, Auffray Y, Rincé A. Lipoproteins of Enterococcus faecalis: Bioinformatic identification, expression analysis and relation to virulence. *Microbiology.* (2011) 157:3001–13. doi: 10.1099/mic.0.053314-0
71. Jones BV, Begley M, Hill C, Gahan CGM, Marchesi JR. Functional and comparative metagenomic analysis of bile salt hydrolase activity in the human gut microbiome. *Proc Natl Acad Sci USA.* (2008) 105:13580–5. doi: 10.1073/pnas.0804437105
72. Begley M, Hill C, Gahan CGM. Bile salt hydrolase activity in Probiotics. *Appl Environ Microbiol.* (2006) 72:1729–38. doi: 10.1128/AEM.72.3.1729
73. Le Breton Y, Mazé A, Hartke A, Lemarinier S, Auffray Y, Rincé A. Isolation and characterization of bile salts-sensitive mutants of *Enterococcus faecalis*. *Curr Microbiol.* (2002) 45:434–9. doi: 10.1007/s00284-002-3714-9
74. Genovese F, Coïsson JD, Majumder A, Pessione A, Svensson B, Jacobsen S, et al. An exoproteome approach to monitor safety of a cheese-isolated *Lactococcus lactis*. *Food Res Int.* (2013) 54:1072–9. doi: 10.1016/J.FOODRES.2012.12.017
75. Sánchez B, Urdaci MC, Margolles A. Extracellular proteins secreted by probiotic bacteria as mediators of effects that promote mucosa-bacteria interactions. *Microbiology.* (2010) 156:3232–42. doi: 10.1099/mic.0.044057-0

Conflict of Interest Statement: The authors declare that the research was conducted in the absence of any commercial or financial relationships that could be construed as a potential conflict of interest.

frontiers in Nutrition

MINI REVIEW
published: 24 April 2019
doi: 10.3389/fnut.2019.00052

Proteomics for the Investigation of Surface-Exposed Proteins in Probiotics

Rosa Anna Siciliano[1]*, *Rosa Lippolis*[2] and *Maria Fiorella Mazzeo*[1]

[1] Institute of Food Sciences, National Research Council (CNR-ISA), Avellino, Italy, [2] Institute of Biomembranes, Bioenergetics and Molecular Biotechnologies, National Research Council (CNR-IBIOM), Bari, Italy

Probiotics are commensal microorganisms that are present in the intestinal tract and in many fermented foods and positively affect human health, promoting digestion and uptake of dietary nutrients, strengthening intestinal barrier function, modulating immune response, and enhancing antagonism toward pathogens. The proteosurfaceome, i.e., the complex set of proteins present on the bacterial surface, is directly involved as leading actor in the dynamic communication between bacteria and host. In the last decade, the biological relevance of surface-exposed proteins prompted research activities exploiting the potentiality of proteomics to define the complex network of proteins that are involved in the molecular mechanisms at the basis of the adaptation to gastrointestinal environment and the probiotic effects. These studies also took advantages of the recent technological improvements in proteomics, mass spectrometry and bioinformatics that triggered the development of *ad hoc* designed innovative strategies to characterize the bacterial proteosurfaceome. This mini-review is aimed at describing the key role of proteomics in depicting the cell wall protein architecture and the involvement of surface-exposed proteins in the intimate and dynamic molecular dialogue between probiotics and intestinal epithelial and immune cells.

Keywords: proteomics, probiotics, proteosurfaceome, surface-exposed proteins, S-layer proteins, moonlighting proteins, immunomodulation

OPEN ACCESS

Edited by:
Fernanda Mozzi, CONICET Centro de Referencia para Lactobacilos (CERELA), Argentina

Reviewed by:
Silvina Graciela Fadda, CONICET Centro de Referencia para Lactobacilos (CERELA), Argentina
Maria de los Angeles Serradell, National Council for Scientific and Technical Research (CONICET), Argentina

***Correspondence:**
Rosa Anna Siciliano
rsiciliano@isa.cnr.it

Specialty section:
This article was submitted to Food Microbiology, a section of the journal Frontiers in Nutrition

Received: *25 February 2019*
Accepted: *05 April 2019*
Published: *24 April 2019*

Citation:
Siciliano RA, Lippolis R and Mazzeo MF (2019) Proteomics for the Investigation of Surface-Exposed Proteins in Probiotics. Front. Nutr. 6:52. doi: 10.3389/fnut.2019.00052

INTRODUCTION

Probiotics are commensal microorganisms that are present in the intestinal tract and in many fermented foods, and are defined as "live microorganisms that, when administered in adequate amounts, confer a health benefit on the host" (1). Most probiotics are Gram-positive bacteria, mainly lactic acid bacteria (LAB), and Bifidobacteria (2). More recently, *Propionibacterium freudenreichii*, a beneficial bacterium traditionally used as a cheese ripening starter, has been recognized to exhibit probiotic abilities, some of these due to the production of nutraceuticals and beneficial metabolites (3). The mechanisms by which probiotics positively affect human health include promotion of digestion and uptake of dietary nutrients, strengthening of intestinal barrier function, modulation of immune response and enhancement of antagonism toward pathogens, either by producing antimicrobial compounds or through competition for mucosal binding sites (4, 5).

Surface-exposed proteins constitute the first-line of contact between bacteria and host being leading actors in this complex interplay as they directly interact with epithelial and immune cells (6). This interaction could lead to the inhibition or activation of key signaling pathways in the intestinal cells involving nuclear factor-κB (NFκB) and mitogen-activated protein kinases (MAPKs), and influencing the regulation of downstream pathways such as the secretion of cytokines (chemokines and interleukins) responsible for the immunomodulation or antibacterial peptides (defensins). The activation of these cascades prompts physiological modifications (increase of mucin secretion, changes in the surface properties, rearrangement of the tight junctions, etc.) and changes in genetic expression that could affect cell proliferation and survival (7–9).

The in-depth analysis of the proteosurfaceome, defined as "the proteinaceous subset of the surfaceome found at the cell wall and totally or partially exposed on the external side of the cell membrane," represents a crucial point to elucidate molecular mechanisms underlying host/probiotic crosstalk (10, 11). In general, sorting of bacterial proteins to the cell surface is governed by the presence or absence of signal peptides which direct them to the protein export machinery thus allowing their migration to bacterial surface, and surface-retention domains responsible for their anchoring to cell wall or cytoplasmic membrane (12). Surface proteins can be mainly divided in four groups: (i) proteins anchored to the cytoplasmic membrane by hydrophobic transmembrane domain(s) (integral membrane proteins, IMP), (ii) lipoproteins which are covalently attached to membrane lipids after cleavage of a signal peptide by signal peptidase II, (iii) proteins containing C-terminal LPXTG-like motif and covalently attached to peptidoglycan by sortases, and (iv) non-covalently bound proteins which are associated to the cell wall through weak interactions (van der Waals forces, hydrogen or ion bonds) taking advantage of conserved structural domains (LysM proteins, WXL proteins, GW proteins, proteins with choline binding domains). Some bacteria can also show supramolecular structures, formed by the assembly of specific protein subunits on the cell envelope, such as flagella, mainly involved in cell motility, and pili or fimbriae, mainly involved in cell adhesion, aggregation, and immunomodulation (10, 11, 13). Furthermore, in several bacterial species (*Lactobacillus acidophilus, Lactobacillus helveticus, P. freudenreichii*, etc.) the outermost constituent of the cell wall is represented by a S-layer that is a semiporous proteinaceous crystalline array composed of self-assembling (glyco)protein subunits called S-layer proteins (SLPs) which act as a scaffold for non-covalently attached secreted proteins (also named S-layer associated proteins, SLAPs). SLPs are involved in several processes including maintaining cell shape, acting as molecular sieves, serving as binding sites, protecting against environmental stresses and mediating bacterial adhesion and gut immune response (14, 15). Noteworthy, cytoplasmic housekeeping proteins (metabolic enzymes, molecular chaperones, translational elongation factors, ribosomal proteins, etc.) have been identified in bacterial surface proteomes. Such proteins, defined as anchorless proteins or moonlighting proteins, display different, seemingly unrelated, functions in different cell locations, and lack any extra-cytoplasmic sorting sequence or binding domain, so that non-canonical secretion pathways have been hypothesized (16, 17).

Subcellular localization of bacterial proteins has been postulated by several bioinformatics tools mainly based on predictive algorithms. The most widely used tools are PSORTb v3.0 server that allows to obtain subcellular localization prediction on the basis of a multi-component approach including different modules such as SCL-BLAST for homology-based prediction, HMMTOP transmembrane helix prediction tool and a signal peptide identification tool (18, 19) and SignalP server, that predicts the presence and location of signal peptide cleavage sites in amino acid sequences from prokaryotes and eukaryotes (20). Prediction of transmembrane-spanning domains (helices) in IMP could be carried out by TMHMM v2.0 (21). Prediction of non-classically secreted proteins (such as moonlighting proteins) could be achieved by SecretomeP server (22) and MoonProt (23).

In the last decades, proteomics significantly contributed to depict an overall picture of the proteosurfeoceome through the identification of hundreds of proteins in a single analysis. In fact, this approach provided direct information on protein localization and topology, thus corroborating the bioinformatics prediction with experimental evidence, and allowed the identification of moonlighthing proteins, "unexpectedly" present on cell surface. More importantly, as the proteosurfaceome is a highly dynamic entity, tightly modulated by the host/bacteria molecular dialogue, proteomics represent the most suitable tool to monitor the wide reorganization of the surface proteins induced by either gastro intestinal tract (GIT) environment or other growth conditions, that could modulate the probiotic functionalities.

However, the proteomic analysis of these proteins proved to be a challenging task due to their low abundance and hydrophobicity. First generation proteomic strategies integrated protein extraction from subcellular fractions, two dimensional electrophoresis (2-DE) and mass spectrometry, i.e., Matrix Assisted Laser Desorption Ionization—Time of Flight Mass Spectrometry (MALDI-TOF-MS) or nano-liquid chromatography coupled to tandem mass spectrometry (LC-MS/MS) and usually led to the identification of a limited number of surface proteins as these are hardly amenable to 2-DE analysis. The need to overcome these experimental drawbacks successively prompted the design of sophisticated strategies that selectively targeted surface proteins either by proteases digestion (shaving procedures) or biotin labeling (protein biotinylation procedures) of intact cells (24). These approaches exploited technological advancements in mass spectrometry and proteomics that allowed the development of gel-free proteomic strategies (also named shotgun proteomics) based on the direct analysis of peptides obtained from the tryptic digestion of the entire proteome by LC-MS/MS and Ge-LC-MS/MS approaches that include a preliminary SDS-PAGE fractionation step of the extracted proteins (25) (**Figure 1**).

This mini-review is aimed at describing both methods applied in the last years to define the bacterial proteosurfaceome and proteomic studies that significantly contributed in depicting the

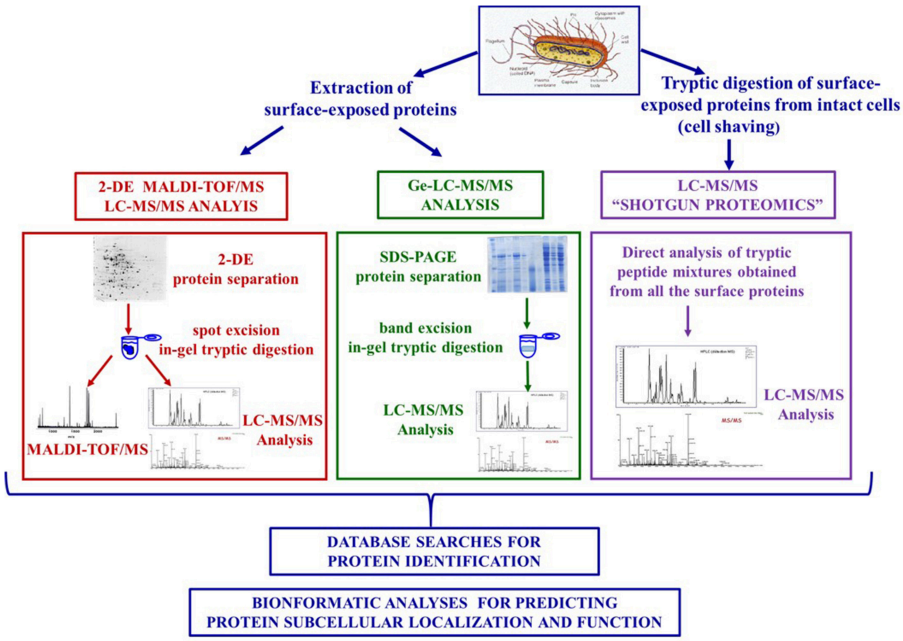

FIGURE 1 | Proteomic strategies generally applied in the analysis of surface-exposed proteins.

cell wall protein architecture and the involvement of surface-exposed proteins in the intimate and dynamic molecular dialogue between probiotics and host.

PROTEOMIC METHODS FOR THE ANALYIS OF SURFACE-EXPOSED PROTEINS

Protocols for Surface Protein Extraction

The analysis of surface proteins of Gram positive bacteria takes advantage of the cell envelope structure consisting of a cross-linked peptidoglycan layer. Cell wall degradation of intact cells is carried out for a short time (30–60 min) using enzymes such as lysozyme, mutanolysin (glycosidases), and/or lysostaphin (endopeptidase) in a buffer containing protease inhibitors and high sugar concentrations to create an osmotic pressure in order to maintain protoplast integrity and prevent contamination of cytoplasmic proteins. Surface proteins contained in the supernatants are recovered by centrifugation, precipitated, separated by 2-DE, and identified by mass spectrometry (26–29) (**Figure 1**). Denaturating agents (urea, guanidine-HCl, SDS buffers) have been also used to extract non-covalently bound surface proteins. Different protocols tailored to specific bacterial features have been proposed to ameliorate protein recovery and mass spectrometric analyses (26, 30, 31).

Surface proteins from S-layer forming bacteria are usually extracted using 5 M lithium chloride (LiCl) solutions thus breaking the hydrogen bonds that stabilize these supramolecular structures (32). More recently, a modified LiCl extraction protocol has been set up by Johnson et al. (33) to specifically separate the highly abundant SLPs from the less abundant SLAPs, exploiting their different solubility in 1 M LiCl solution, and applied to study SLAPs isolated from different probiotic bacteria (34–36).

As to Gram negative bacteria, classical methods for the extraction of surface exposed proteins take into account the peculiar features of their cell-envelope and include the subfractionation of outer membrane, cytoplasmic membrane and periplasmic proteins. Commonly, inner and outer membrane vesicles are prepared by lysozyme-EDTA lysis or French press lysis of bacteria, separated by density centrifugation using a sucrose gradient and analyzed by proteomics (37, 38).

Cell Shaving Strategy

The concept underlying this innovative strategy is that, regardless of anchoring mechanisms, surface exposed protein fragments can be selectively released through a limited proteolytic digestion step carried out on intact bacterial cells. The "shaved" peptides can be then separated from the whole cells by centrifugation and analyzed by shotgun proteomics thus achieving protein identification (39). Trypsin is the proteolytic enzyme more often used in these experiments, as lysine and arginine residues are widely represented in protein sequences and often easily accessible to the enzyme (**Figures 1**,**2A**).

In order to rule out osmotic shock and contamination of cytoplasmic proteins, bacterial cells are suspended in an isotonic buffer (obtained through the addition of sucrose or arabinose) and protease digestion is carried out for a short time (15–30 min) to preserve cell integrity. However, the limited proteolysis could produce high molecular weight protein fragments which are not amenable for LC-MS/MS analyses and a further extensive tryptic digestion step (18 hs) carried out on the shaved peptides has been included in optimized protocols (40, 41).

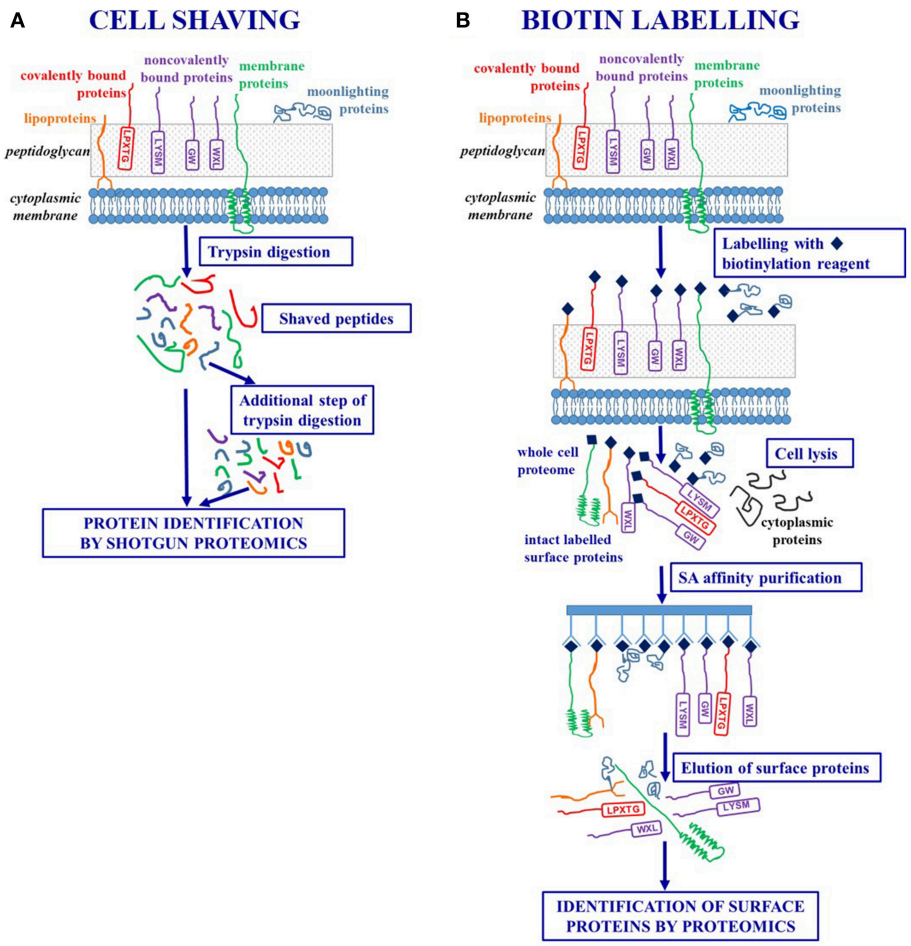

FIGURE 2 | Workflows of *ad hoc* designed strategies for selectively targeting surface-exposed proteins. **(A)** Cell shaving strategies based on a limited proteolytic digestion step of intact bacterial cells in order to release surface exposed protein fragments. **(B)** Labeling strategies based on biotinylation of surface-exposed proteins of intact bacterial cells in order to achieve their purification by affinity chromatography.

The cell shaving approach allows a comprehensive description of the bacterial proteosurfaceome and, as trypsin molecules could diffuse into the cell wall and interact with membrane and cell wall embedded proteins, a single experiment can provide the simultaneous identification of IMP, lipoproteins, LPXTG-proteins, non-covalently bound proteins, moonlighting proteins (40). Moreover, as the procedure selectively identifies peptides generated from surface-exposed domains, this methodology can contribute to refine the protein topology derived from bioinformatics by matching prediction and experimental data (39).

The method was conceived to identify potential targets of drugs and novel candidates for vaccines, and applied to study *Streptococcus pyogenes*, leading to the identification of 68 surface-associated proteins, one of which was validated in mice as a potential vaccine candidate (39, 42).

This protocol is particularly suitable for the analysis of Gram positive bacteria, due to their thick and rigid cell wall that is less prone to lysis during treatments, and comprehensive proteomic studies have been performed on several probiotics including *Lactococcus lactis* (43), *Bifidobacterium animalis* (44), *Lactobacillus rhamnosus* (45), *P. freudenreichii* (46, 47), and food pathogens like *Staphylococcus aureus* (48–50) and *Listeria monocytogenes* (51, 52). On the other hand, the cell shaving method has been applied for the analysis of surface proteins of Gram negative bacteria such as *Escherichia coli* (53) and *Salmonella enterica* (54), even if their cell envelope can be more easily damaged thus causing cytoplasmic protein contamination.

Labeling of Surface-Exposed Proteins

These approaches rely on labeling strategies that specifically target surface proteins of intact bacterial cells. A first approach is based on the labeling of surface-exposed proteins with fluorescent CyDye reagents. After the labeling step, a complete cell lysis is carried out and the proteins are separated by 2-DE. Labeled surface proteins are highlighted by fluorescence imaging and identified using mass spectrometry (46, 55) (**Figure 1**).

A more sophisticated approach uses *ad hoc* designed biotin containing reagents to target surface proteins and suitably exploits the highly specific and stable non-covalent interaction between avidin [or the bacterial protein streptavidin (SA)] and biotin (56). As the biotinylation reagents can penetrate the peptidoglycan structure, proteins that are buried within the cell wall can be labeled. After a cell lysis step, labeled surface proteins are separated from non-labeled cytoplasmic proteins by SA affinity chromatography. The intact surface proteins thus purified could be identified using both classical proteomic approaches (including 2-DE) and Ge-LC-MS/MS or shotgun proteomics (27, 57–59) (**Figures 1**,**2B**).

The chemical features of the labeling reagent have a crucial role in this protocol. The biotin moiety is at the basis of the affinity purification step and several spacers can be linked to the valeric acid carboxylic group of biotin and carry functional groups (such as N-hydroxysuccinimide, NHS) that covalently link to primary amino groups of proteins (ε-amino group of lysine residues and N-terminal α-amine group) (60).

The elution of biotinylated proteins from SA-coated resin could be severely hampered by the high stability of the biotin-SA complex. To overcome this problem, cleavable spacers that include a disulphide bridge in their structure have been introduced thus allowing to easily and completely elute the biotinylated proteins by using reducing reagents such as dithiotreitol. Sulpho-NHS-SS-biotin is nowadays the most commonly used reagent in proteomic studies. The negative charge of sulphonate group present on the NHS ring makes this molecule water soluble and unable to cross the cell membrane thus drastically reducing the contamination of cytoplasmic proteins (60).

This method is suitable to study the proteosurfaceome of both Gram-positive and Gram-negative bacteria but, unfortunately, up to now, it has been mainly applied to analyze the surface proteins of pathogens such as *S. aureus* (27, 57, 61), *L. monocytogenes* (52), *E. coli* (62). We can foresee that in the near future, this strategy will be also applied to the characterization of the proteosurfaceome of probiotics thus contributing to the advancement of knowledge in this field.

PROTEOMICS FOR STUDYING SURFACE-EXPOSED PROTEINS IN PROBIOTICS

The high biological relevance of surface-exposed proteins in the dynamic crosstalk between bacteria and their environment prompted the design of dedicated proteomic strategies useful for investigating the molecular mechanisms of adaptation to GIT environment, adhesion, colonization, and immunomodulation, key features for the probiotic action (63–65). First studies on this topic, integrating proteomics and biochemical assays, confirmed the presence of moonlighting proteins on the surface of Lactobacilli and Bifidobacteria and their ability to bind extracellular matrix components (plasminogen, fibronectin, mucin) and adhere to GIT (28, 66–72). More recently, a comparative proteomic study performed on potentially probiotic strains of *Lactobacillus pentosus* led to identify moonlighting proteins in the cell-wall proteome and to correlate their abundance level to strain specific adhesion capacities to mucus (73).

Importantly, the adaptation to GIT can enhanced probiotic features as, for instance, bile stress can be a signal of gut entry for bacteria, which triggers the re-organization of the surface protein pattern resulting in improved adhesion ability in the new niche. In fact, the abundance of surface-exposed Clp proteins (ClpB, ClpE), chaperone (DnaK), and enzymes involved in carbohydrate metabolism was enhanced in *L. rhamnosus* GG after exposure to bile stress. The abundance of some of these enzymes increased in the proteosurfaceome but not in the proteome, thus suggesting a sort of protein relocalization triggered by bile (55). Changes in the expression profile of moonlighting proteins (in particular ribosomal proteins and glycolytic enzymes) promoted by bile were also observed in *B. animalis* subsp. *lactis* and *B. longum* (29, 74).

Several factors supplied with diets such as plant polyphenols (resveratrol, ferulic acid, etc.) and prebiotic carbohydrates (raffinose, fructooligosaccharides, etc.) could influence the surface protein profile of probiotics. These molecules improved the adhesive capabilities to mucin and HT-29 cells of *L. acidophilus* NCFM probably by modulating biosynthesis and/or secretion of moonlighting proteins (75–77).

Proteomics also contributed to assess that the surface protein pattern is strain specific. In fact, a trypsin shaving approach applied to compare the proteosurfaceomes of *L. rhamnosus* GG and the closely related dairy strain Lc705, led to the identification of 102 and 198 proteins anchored to the surface trough different mechanisms (IMP, LPXTG proteins, lipoproteins, C-term and N-Term anchored proteins and moonlighting proteins). Strain specific differences were mainly associated to moonlighting proteins and could be related to the adaptation to their ecological niches and probiotic functions (response to bile, hydrolysis of casein, immunostimulation, pathogen exclusion) (45). In addition, SpaC and SpaA proteins, involved in the assembly of pilus structures, were identified only in the proteome of GG and related to adhesion properties and prolonged residence in the GIT of this strain compared to Lc705 (78).

Similarly, a pilin-like protein was identified in a *L. lactis* strain able to adhere to Caco-2 cells and the synthesis of pili was confirmed by immunoblotting detection and electron and atomic force microscopy observations (43). Several proteins potentially involved in adhesion, including the pilus structure proteins FimA and FimB, were also identified in a *B. animalis* ssp *lactis* strain (44).

S-layer proteins (SLPs) and S-layer associated proteins (SLAPs) have a key role in GIT adaptation and immunomodulation processes, as highlighted by functional studies integrated by proteomics. First studies performed on *L. acidophilus* NCFM, a S-layer forming microorganism, showed the involvement of the main SLP (SlpA) in adhesion to Caco2 cells (79) and dendritic cells (DCs) immunomodulation (80). Recently, using an optimized extraction protocol, 37 SLAPs of L. *acidophilus* NCFM were identified and most of them were predicted to be extracellular proteins while only four proteins

were potentially moonlighting proteins. The protein SLAP LBA1029 contributed to a pro-inflammatory response in murine DCs (inducing the expression of TNF-α), thus indicating that SLAPs may impart immunological properties to microbes (33). The surface-exposed proteins of *L. acidophilus* NCFM were also characterized by Celebioglu and Svensson (35), leading to the identification of a higher number of moonlighting proteins. In addition, a quantitative proteomic study performed using more sophisticated mass spectrometric approaches, defined a detailed catalog of the *L. acidophilus* NCFM surface proteins containing 276 SLAPs and demonstrated that the cell surface proteome was modulated by growth phase. This feature could be exploited to optimize probiotic actions and enhance their delivery, persistence, and general efficacy (36).

The presence or absence of the S-layer has a clear impact on the composition and complexity of proteosurfaceome of different lactobacilli. In fact, a proteomic study led to identify numerous SLAPs in proteosurfaceome of S-layer-forming strains of *L. acidophilus, L. helveticus, L. crispatus, L. amylovorus, and L. gallinarum*. On the other hand, the few proteins isolated with LiCl treatment of the non-S-layer forming strains of *L. delbrueckii subsp. bulgaricus and L. casei* were mostly intracellular proteins, likely presented extracellularly due to cell lysis in stationary phase. These findings also confirmed the role of SLAPs as integral components of S-layer (34).

Recently surface proteins from *P. freudenreichii*, a S-layer forming bacterium, have been characterized by using three complementary proteomic methods (guanidine hydrochloride extraction, cell shaving and fluorescent labeling with CyDye coupled to mass spectrometric analyses) and their ability in enhancing the production of the anti-inflammatory cytokines IL6 and IL10 by human immune cells was assessed (46). Furthermore, a study combining comparative genomics, transcriptomics and surface proteomics, coupled with gene inactivation, was performed on 23 strains of *P. freudenreichii* with different anti-inflammatory potential. Results evidenced the involvement of SlpB and SlpE in the release of IL10 by human immune cells and demonstrated that different combinations of surface and cytoplasmic proteins, depending on the strain, exerted a pleiotropic effect on the anti-inflammatory properties (47). Finally, do Carmo et al. demonstrated a direct role of SlpB in the adhesion to HT-29 cells and reported that the inactivation of *slpB* gene caused profound modifications in whole cell and surface proteomes as well as bacterial stress tolerance (81, 82).

The reported achievements clearly assess the ability of proteomics in investigating the structural features of different classes of surface proteins and its role in elucidating the mechanisms of bacteria/host interaction.

CONCLUDING REMARKS

In the past few years, proteomics proved to be the method of choice to investigate surface architecture of bacteria cells, contributing to define protein location and topology, and to deal with the extremely dynamic and constantly renewing nature of proteosurfaceome that is deeply affected by the environment. The exploitation of technological innovations in proteomics and mass spectrometry has improved the knowledge in the probiotics field. This review displays the essential role of proteomics in the elucidation of the molecular mechanisms of the probiotic action and the identification of key actors of the probiotics/host molecular dialogue, thus potentially providing new tools for selecting strains with specific healthy promoting functions. Future research perspectives should include the analysis of post-translational modifications of surface proteins (glycoproteomics, phosphoproteomics, etc.), and the investigation of their effects in the interaction with host epithelial cells.

AUTHOR CONTRIBUTIONS

All authors listed have made a substantial, direct and intellectual contribution to the work, and approved it for publication.

REFERENCES

1. Hill C, Guarner F, Reid G, Gibson GR, Merenstein DJ, Pot B, et al. Expert consensus document. The International Scientific Association for Probiotics and Prebiotics consensus statement on the scope and appropriate use of the term probiotic. *Nat Rev Gastroenterol Hepatol.* (2014) 11:506–14. doi: 10.1038/nrgastro.2014.66
2. Marco ML, Pavan S, Kleerebezem M. Towards understanding molecular modes of probiotic action. *Curr Opin Biotechnol.* (2006) 17:204–10. doi: 10.1016/j.copbio.2006.02.005
3. Rabah H, do Carmo FLR, Jan G. Dairy propionibacteria: versatile probiotics. *Microorganisms.* (2017) 5:24. doi: 10.3390/microorganisms5020024
4. Bron PA, van Baarlen P, Kleerebezem M. Emerging molecular insights into the interaction between probiotics and the host intestinal mucosa. *Nat Rev Microbiol.* (2012) 10:66–78. doi: 10.1038/nrmicro2690
5. Lebeer S, Bron PA, Marco ML, Van Pijkeren JP, O'Connell Motherway M, Hill C, et al. Identification of probiotic effector molecules: present state and future perspectives. *Curr Opin Biotechnol.* (2018) 49:217–23. doi: 10.1016/j.copbio.2017.10.007
6. Ruiz L, Hevia A, Bernardo D, Margolles A, Sánchez B. Extracellular molecular effectors mediating probiotic attributes. *FEMS Microbiol Lett.* (2014) 359:1–11. doi: 10.1111/1574-6968.12576
7. Lebeer S, Vanderleyden J, De Keersmaecker SC. Host interactions of probiotic bacterial surface molecules: comparison with commensals and pathogens. *Nat Rev Microbiol.* (2010) 8:171–84. doi: 10.1038/nrmicro2297
8. Sánchez B, Urdaci MC, Margolles A. Extracellular proteins secreted by probiotic bacteria as mediators of effects that promote mucosa-bacteria interactions. *Microbiology.* (2010) 156:3232–42. doi: 10.1099/mic.0.044057-0
9. Hevia A, Delgado S, Sánchez B, Margolles A. Molecular players involved in the interaction between beneficial bacteria and the immune system. *Front Microbiol.* (2015) 6:1285. doi: 10.3389/fmicb.2015.01285
10. Desvaux M, Dumas E, Chafsey I, Hébraud M. Protein cell surface display in Gram-positive bacteria: from single protein to macromolecular protein structure. *FEMS Microbiol Lett.* (2006) 256:1–15. doi: 10.1111/j.1574-6968.2006.00122.x
11. Desvaux M, Candela T, Serror P. Surfaceome and proteosurfaceome in parietal monoderm bacteria: focus on protein cell-surface display. *Front Microbiol.* (2018) 9:100. doi: 10.3389/fmicb.2018.00100

12. Scott JR, Barnett TC. Surface proteins of gram-positive bacteria and how they get there. *Annu Rev Microbiol.* (2006) 60:397–423. doi: 10.1146/annurev.micro.60.080805.142256
13. Kleerebezem M, Hols P, Bernard E, Rolain T, Zhou M, Siezen RJ, et al. The extracellular biology of the lactobacilli. *FEMS Microbiol Rev.* (2010) 34:199–230. doi: 10.1111/j.1574-6976.2010.00208.x
14. Hynönen U, Palva A. *Lactobacillus* surface layer proteins: structure, function and applications. *Appl Microbiol Biotechnol.* (2013) 97:5225–43. doi: 10.1007/s00253-013-4962-2
15. do Carmo FLR, Rabah H, De Oliveira Carvalho RD, Gaucher F, Cordeiro BF, da Silva SH, et al. Extractable bacterial surface proteins in probiotic-host interaction. *Front. Microbiol.* (2018) 9:645. doi: 10.3389/fmicb.2018.00645
16. Wang W, Jeffery CJ. An analysis of surface proteomics results reveals novel candidates for intracellular/surface moonlighting proteins in bacteria. *Mol Biosyst.* (2016) 12:1420–31. doi: 10.1039/c5mb00550g
17. Jeffery CJ. Protein moonlighting: what is it, and why is it important? *Philos Trans R Soc Lond B Biol Sci.* (2018) 373:20160523. doi: 10.1098/rstb.2016.0523
18. Gardy JL, Brinkman FS. Methods for predicting bacterial protein subcellular localization. *Nat Rev Microbiol.* (2006) 4:741–51. doi: 10.1038/nrmicro1494
19. Yu NY, Wagner JR, Laird MR, Melli G, Rey S, Lo R, et al. PSORTb 3.0: improved protein subcellular localization prediction with refined localization subcategories and predictive capabilities for all prokaryotes. *Bioinformatics.* (2010) 26:1608–15. doi: 10.1093/bioinformatics/btq249
20. Petersen TN, Brunak S, von Heijne G, Nielsen H. SignalP 4.0: discriminating signal peptides from transmembrane regions. *Nat Methods.* (2011) 8:785–6. doi: 10.1038/nmeth.1701
21. Krogh A, Larsson B, von Heijne G, Sonnhammer EL. Predicting transmembrane protein topology with a hidden Markov model: application to complete genomes. *J Mol Biol.* (2001) 305:567–80. doi: 10.1006/jmbi.2000.4315
22. Bendtsen JD, Kiemer L, Fausbøll A, Brunak S. Non-classical protein secretion in bacteria. *BMC Microbiol.* (2005) 5:58. doi: 10.1186/1471-2180-5-58
23. Chen C, Zabad S, Liu H, Wang W, Jeffery C. MoonProt 2.0: an expansion and update of the moonlighting proteins database. *Nucleic Acids Res.* (2018) 46:D640–4. doi: 10.1093/nar/gkx1043
24. Solis N, Cordwell SJ. Current methodologies for proteomics of bacterial surface-exposed and cell envelope proteins. *Proteomics.* (2011) 11:3169–89. doi: 10.1002/pmic.201000808
25. Aebersold R, Mann M. Mass spectrometry-based proteomics. *Nature.* (2003) 422:198–207. doi: 10.1038/nature01511
26. Nandakumar R, Nandakumar MP, Marten MR, Ross JM. Proteome analysis of membrane and cell wall associated proteins from *Staphylococcus aureus*. *J Proteome Res.* (2005) 4:250–7. doi: 10.1021/pr049866k
27. Gatlin CL, Pieper R, Huang ST, Mongodin E, Gebregeorgis E, Parmar PP, et al. Proteomic profiling of cell envelope-associated proteins from *Staphylococcus aureus*. *Proteomics.* (2006) 6:1530–49. doi: 10.1002/pmic.200500253
28. Izquierdo E, Horvatovich P, Marchioni E, Aoude-Werner D, Sanz Y, Ennahar S. 2-DE and MS analysis of key proteins in the adhesion of *Lactobacillus plantarum*, a first step toward early selection of probiotics based on bacterial biomarkers. *Electrophoresis.* (2009) 30:949–56. doi: 10.1002/elps.200800399
29. Ruiz L, Couté Y, Sánchez B, de los Reyes-Gavilán CG, Sanchez JC, Margolles A. The cell-envelope proteome of *Bifidobacterium longum* in an *in vitro* bile environment. *Microbiology.* (2009) 155:957–67. doi: 10.1099/mic.0.024273-0
30. Sánchez B, Bressollier P, Chaignepain S, Schmitter JM, Urdaci MC. Identification of surface-associated proteins in the probiotic bacterium *Lactobacillus rhamnosus* GG. *Int Dairy J.* (2009) 19:85–8. doi: 10.1016/j.idairyj.2008.09.005
31. Tiong HK, Hartson S, Muriana PM. Comparison of five methods for direct extraction of surface proteins from *Listeria monocytogenes* for proteomic analysis by orbitrap mass spectrometry. *J Microbiol Methods.* (2015) 110:54–60. doi: 10.1016/j.mimet.2015.01.004
32. Sleytr UB, Schuster B, Egelseer EM, Pum D. S-layers: principles and applications. *FEMS Microbiol Rev.* (2014) 38:823–64. doi: 10.1111/1574-6976.12063
33. Johnson B, Selle K, O'Flaherty S, Goh YJ, Klaenhammer T. Identification of extracellular surface-layer associated proteins in *Lactobacillus acidophilus* NCFM. *Microbiology.* (2013) 159:2269–82. doi: 10.1099/mic.0.070755-0
34. Johnson BR, Hymes J, Sanozky-Dawes R, Henriksen ED, Barrangou R, Klaenhammer TR. Conserved S-layer-associated proteins revealed by exoproteomic survey of S-layer-forming lactobacilli. *Appl Environ Microbiol.* (2016) 82:134–45. doi: 10.1128/AEM.01968-15
35. Celebioglu HU, Svensson B. Exo- and surface proteomes of the probiotic bacterium *Lactobacillus acidophilus* NCFM. *Proteomics.* (2017) 17:1700019. doi: 10.1002/pmic.201700019
36. Klotz C, O'Flaherty S, Goh YJ, Barrangou R. Investigating the effect of growth phase on the surface-layer associated proteome of *Lactobacillus acidophilus* using quantitative proteomics. *Front Microbiol.* (2017) 8:2174. doi: 10.3389/fmicb.2017.02174
37. Weiner JH, Li L. Proteome of the *Escherichia coli* envelope and technological challenges in membrane proteome analysis. *Biochim Biophys Acta.* (2008) 1778:1698–713. doi: 10.1016/j.bbamem.2007.07.020
38. Thein M, Sauer G, Paramasivam N, Grin I, Linke D. Efficient subfractionation of gram-negative bacteria for proteomics studies. *J Proteome Res.* (2010) 9:6135–47. doi: 10.1021/pr1002438
39. Rodríguez-Ortega MJ, Norais N, Bensi G, Liberatori S, Capo S, Mora M, et al. Characterization and identification of vaccine candidate proteins through analysis of the group A *Streptococcus* surface proteome. *Nat Biotechnol.* (2006) 24:191–7. doi: 10.1038/nbt1179
40. Tjalsma H, Lambooy L, Hermans PW, Swinkels DW. Shedding and shaving: disclosure of proteomic expressions on a bacterial face. *Proteomics.* (2008) 8:1415–28. doi: 10.1002/pmic.200700550
41. Olaya-Abril A, Gómez-Gascón L, Jiménez-Munguía I, Obando I, Rodríguez-Ortega MJ. Another turn of the screw in shaving Gram-positive bacteria: optimization of proteomics surface protein identification in *Streptococcus pneumoniae*. *J Proteomics.* (2012) 75:3733–46. doi: 10.1016/j.jprot.2012.04.037
42. Doro F, Liberatori S, Rodríguez-Ortega MJ, Rinaudo CD, Rosini R, Mora M, et al. Surfome analysis as a fast track to vaccine discovery: identification of a novel protective antigen for Group B *Streptococcus* hypervirulent strain COH1. *Mol Cell Proteomics.* (2009) 8:1728–37. doi: 10.1074/mcp.M800486-MCP200
43. Meyrand M, Guillot A, Goin M, Furlan S, Armalyte J, Kulakauskas S, et al. Surface proteome analysis of a natural isolate of *Lactococcus lactis* reveals the presence of pili able to bind human intestinal epithelial cells. *Mol Cell Proteomics.* (2013) 12:3935–47. doi: 10.1074/mcp.M113.029066
44. Zhu D, Sun Y, Liu F, Li A, Yang L, Meng XC. Identification of surface-associated proteins of *Bifidobacterium animalis* ssp. *lactis* KLDS 2.0603 by enzymatic shaving. *J Dairy Sci.* (2016) 99:5155–72. doi: 10.3168/jds.2015-10581
45. Espino E, Koskenniemi K, Mato-Rodriguez L, Nyman TA, Reunanen J, Koponen J, et al. Uncovering surface-exposed antigens of *Lactobacillus rhamnosus* by cell shaving proteomics and two-dimensional immunoblotting. *J Proteome Res.* (2015) 14:1010–24. doi: 10.1021/pr501041a
46. Le Maréchal C, Peton V, Plé C, Vroland C, Jardin J, Briard-Bion V, et al. Surface proteins of *Propionibacterium freudenreichii* are involved in its anti-inflammatory properties. *J Proteomics.* (2015) 113:447–61. doi: 10.1016/j.jprot.2014.07.018
47. Deutsch SM, Mariadassou M, Nicolas P, Parayre S, Le Guellec R, Chuat V, et al. Identification of proteins involved in the anti-inflammatory properties of *Propionibacterium freudenreichii* by means of a multi-strain study. *Sci Rep.* (2017) 7:46409. doi: 10.1038/srep46409
48. Solis N, Larsen MR, Cordwell SJ. Improved accuracy of cell surface shaving proteomics in *Staphylococcus aureus* using a false-positive control. *Proteomics.* (2010) 10:2037–49. doi: 10.1002/pmic.200900564
49. Solis N, Parker BL, Kwong SM, Robinson G, Firth N, Cordwell SJ. *Staphylococcus aureus* surface proteins involved in adaptation to oxacillin identified using a novel cell shaving approach. *J Proteome Res.* (2014) 13:2954–72. doi: 10.1021/pr500107p
50. Monteiro R, Hébraud M, Chafsey I, Chambon C, Viala D, Torres C, et al. Surfaceome and exoproteome of a clinical sequence type 398 methicillin resistant *Staphylococcus aureus* strain. *Biochem Biophys Rep.* (2015) 3:7–13. doi: 10.1016/j.bbrep.2015.07.004
51. Zhang CX, Creskey MC, Cyr TD, Brooks B, Huang H, Pagotto F, et al. Proteomic identification of *Listeria monocytogenes* surface-associated proteins. *Proteomics.* (2013) 13:3040–5. doi: 10.1002/pmic.201200449

52. Esbelin J, Santos T, Ribière C, Desvaux M, Viala D, Chambon C, et al. Comparison of three methods for cell surface proteome extraction of *Listeria monocytogenes* biofilms. *OMICS.* (2018) 22:779–87. doi: 10.1089/omi.2018.0144
53. Walters MS, Mobley HL. Identification of uropathogenic *Escherichia coli* surface proteins by shotgun proteomics. *J Microbiol Methods.* (2009) 78:131–5. doi: 10.1016/j.mimet.2009.04.013
54. Fagerquist CK, Zaragoza WJ. Proteolytic surface-shaving and serotype-dependent expression of SPI-1 invasion proteins in *Salmonella enterica* subspecies *enterica*. *Front Nutr.* (2018) 5:124. doi: 10.3389/fnut.2018.00124
55. Koskenniemi K, Laakso K, Koponen J, Kankainen M, Greco D, Auvinen P, et al. Proteomics and transcriptomics characterization of bile stress response in probiotic *Lactobacillus rhamnosus* GG. *Mol. Cell Proteomics.* (2011) 10:M110.002741. doi: 10.1074/mcp.M110.002741
56. Scheurer SB, Roesli C, Neri D, Elia G. A comparison of different biotinylation reagents, tryptic digestion procedures, and mass spectrometric techniques for 2-D peptide mapping of membrane proteins. *Proteomics.* (2005) 5:3035–9. doi: 10.1002/pmic.200402069
57. Hempel K, Pané-Farré J, Otto A, Sievers S, Hecker M, Becher D. Quantitative cell surface proteome profiling for SigB-dependent protein expression in the human pathogen *Staphylococcus aureus* via biotinylation approach. *J. Proteome Res.* (2010) 9:1579–90. doi: 10.1021/pr901143a
58. Bonn F, Maaß S, van Dijl JM. Enrichment of cell surface-associated proteins in Gram-positive bacteria by biotinylation or trypsin shaving for mass spectrometry analysis. *Methods Mol Biol.* (2018) 1841:35–43. doi: 10.1007/978-1-4939-8695-8_4
59. Elia G. Cell surface protein biotinylation for SDS-PAGE analysis. *Methods Mol Biol.* (2019) 1855:449–59. doi: 10.1007/978-1-4939-8793-1_37
60. Elia G. Biotinylation reagents for the study of cell surface proteins. *Proteomics.* (2008) 8:4012–24. doi: 10.1002/pmic.200800097
61. Moche M, Schlüter R, Bernhardt J, Plate K, Riedel K, Hecker M, et al. Time-resolved analysis of cytosolic and surface-associated proteins of *Staphylococcus aureus* HG001 under planktonic and biofilm conditions. *J Proteome Res.* (2015) 14:3804–22. doi: 10.1021/acs.jproteome.5b00148
62. Monteiro R, Chafsey I, Leroy S, Chambon C, Hébraud M, Livrelli V, et al. Differential biotin labelling of the cell envelope proteins in lipopolysaccharidic diderm bacteria: exploring the proteosurfaceome of *Escherichia coli* using sulfo-NHS-SS-biotin and sulfo-NHS-PEG4-bismannose-SS-biotin. *J Proteomics.* (2018) 181:16–23. doi: 10.1016/j.jprot.2018.03.026.
63. Siciliano RA, Mazzeo MF. Molecular mechanisms of probiotic action: a proteomic perspective. *Curr Opin Microbiol.* (2012) 15:390–6. doi: 10.1016/j.mib.2012.03.006
64. De Angelis M, Calasso M, Cavallo N, Di Cagno R, Gobbetti M. Functional proteomics within the genus *Lactobacillus*. *Proteomics.* (2016) 16:946–62. doi: 10.1002/pmic.201500117
65. Ruiz L, Hidalgo C, Blanco-Míguez A, Lourenço A, Sánchez B, Margolles A. Tackling probiotic and gut microbiota functionality through proteomics. *J Proteomics.* (2016) 147:28–39. doi: 10.1016/j.jprot.2016.03.023
66. Granato D, Bergonzelli GE, Pridmore RD, Marvin L, Rouvet M, Corthésy-Theulaz IE. Cell surface-associated elongation factor Tu mediates the attachment of *Lactobacillus johnsonii* NCC533 (La1) to human intestinal cells and mucins. *Infect Immun.* (2004) 72:2160–9. doi: 10.1128/IAI.72.4.2160-2169.2004
67. Bergonzelli GE, Granato D, Pridmore RD, Marvin-Guy LF, Donnicola D, Corthésy-Theulaz IE. GroEL of *Lactobacillus johnsonii* La1 (NCC 533) is cell surface associated: potential role in interactions with the host and the gastric pathogen *Helicobacter pylori*. *Infect Immun.* (2006) 74:425–34. doi: 10.1128/IAI.74.1.425-434.2006
68. Candela M, Bergmann S, Vici M, Vitali B, Turroni S, Eikmanns BJ, et al. Binding of human plasminogen to *Bifidobacterium*. *J Bacteriol.* (2007) 189:5929–36. doi: 10.1128/JB.00159-07
69. Siciliano RA, Cacace G, Mazzeo MF, Morelli L, Elli M, Rossi M, et al. Proteomic investigation of the aggregation phenomenon in *Lactobacillus crispatus*. *Biochim Biophys Acta.* (2008) 1784:335–42. doi: 10.1016/j.bbapap.2007.11.007
70. Beck HC, Madsen SM, Glenting J, Petersen J, Israelsen H, Nørrelykke MR, et al. Proteomic analysis of cell surface-associated proteins from probiotic *Lactobacillus plantarum*. *FEMS Microbiol Lett.* (2009) 297:61–6. doi: 10.1111/j.1574-6968.2009.01662.x
71. Castaldo C, Vastano V, Siciliano RA, Candela M, Vici M, Muscariello L, et al. Surface displaced alfa-enolase of *Lactobacillus plantarum* is a fibronectin binding protein. *Microb Cell Fact.* (2009) 8:14. doi: 10.1186/1475-2859-8-14
72. González-Rodríguez I, Sánchez B, Ruiz L, Turroni F, Ventura M, Ruas-Madiedo P, et al. Role of extracellular transaldolase from *Bifidobacterium bifidum* in mucin adhesion and aggregation. *Appl Environ Microbiol.* (2012) 78:3992–8. doi: 10.1128/AEM.08024-11
73. Pérez Montoro B, Benomar N, Caballero Gómez N, Ennahar S, Horvatovich P, Knapp CW, et al. Proteomic analysis of *Lactobacillus pentosus* for the identification of potential markers of adhesion and other probiotic features. *Food Res Int.* (2018) 111:58–66. doi: 10.1016/j.foodres.2018.04.072
74. Candela M, Centanni M, Fiori J, Biagi E, Turroni S, Orrico C, et al. DnaK from Bifidobacterium animalis subsp. lactis is a surface-exposed human plasminogen receptor upregulated in response to bile salts. *Microbiology.* (2010) 156:1609–18. doi: 10.1099/mic.0.038307-0
75. Celebioglu HU, Ejby M, Majumder A, Køhler C, Goh YJ, Thorsen K, et al. Differential proteome and cellular adhesion analyses of the probiotic bacterium *Lactobacillus acidophilus* NCFM grown on raffinose - an emerging prebiotic. *Proteomics.* (2016) 16:1361–75. doi: 10.1002/pmic.201500212
76. Celebioglu HU, Olesen SV, Prehn K, Lahtinen SJ, Brix S, Abou Hachem M, et al. Mucin- and carbohydrate-stimulated adhesion and subproteome changes of the probiotic bacterium *Lactobacillus acidophilus* NCFM. *J Proteomics.* (2017) 163:102–10. doi: 10.1016/j.jprot.2017.05.015
77. Celebioglu HU, Delsoglio M, Brix S, Pessione E, Svensson B. Plant polyphenols stimulate adhesion to intestinal mucosa and induce proteome changes in the probiotic *Lactobacillus acidophilus* NCFM. *Mol Nutr Food Res.* (2018) 62:1700638. doi: 10.1002/mnfr.201700638
78. Savijoki K, Lietzén N, Kankainen M, Alatossava T, Koskenniemi K, Varmanen P, et al. Comparative proteome cataloging of *Lactobacillus rhamnosus* strains GG and Lc705. *J Proteome Res.* (2011) 10:3460–73. doi: 10.1021/pr2000896
79. Ashida N, Yanagihara S, Shinoda T, Yamamoto N. Characterization of adhesive molecule with affinity to Caco-2 cells in *Lactobacillus acidophilus* by proteome analysis. *J Biosci Bioeng.* (2011) 112:333–7. doi: 10.1016/j.jbiosc.2011.06.001
80. Konstantinov SR, Smidt H, de Vos WM, Bruijns SC, Singh SK, Valence F, et al. S layer protein A of *Lactobacillus acidophilus* NCFM regulates immature dendritic cell and T cell functions. *Proc Natl Acad Sci USA.* (2008) 105:19474–9. doi: 10.1073/pnas.0810305105
81. do Carmo FLR, Rabah H, Huang S, Gaucher F, Deplanche M, Dutertre S, et al. *Propionibacterium freudenreichii* surface protein SlpB is involved in adhesion to intestinal HT-29 cells. *Front Microbiol.* (2017) 8:1033. doi: 10.3389/fmicb.2017.01033
82. do Carmo FLR, Silva WM, Tavares GC, Ibraim IC, Cordeiro BF, Oliveira ER, et al. Mutation of the surface layer protein SlpB has pleiotropic effects in the probiotic *Propionibacterium freudenreichii* CIRM-BIA 129. *Front Microbiol.* (2018) 9:1807. doi: 10.3389/fmicb.2018.01807

Conflict of Interest Statement: The authors declare that the research was conducted in the absence of any commercial or financial relationships that could be construed as a potential conflict of interest.

frontiers in Microbiology

ORIGINAL RESEARCH
published: 05 June 2019
doi: 10.3389/fmicb.2019.01272

Growth Mode and Carbon Source Impact the Surfaceome Dynamics of *Lactobacillus rhamnosus* GG

*Kirsi Savijoki[1,2], Tuula A. Nyman[3], Veera Kainulainen[4], Ilkka Miettinen[2], Pia Siljamäki[1], Adyary Fallarero[2], Jouko Sandholm[5], Reetta Satokari[4] and Pekka Varmanen[1]**

[1] Department of Food and Nutrition, University of Helsinki, Helsinki, Finland, [2] Division of Pharmaceutical Biosciences, University of Helsinki, Helsinki, Finland, [3] Department of Immunology, Institute of Clinical Medicine, University of Oslo and Oslo University Hospital, Oslo, Norway, [4] Human Microbiome Research Program, Faculty of Medicine, University of Helsinki, Helsinki, Finland, [5] Turku Bioscience, University of Turku and Åbo Akademi University, Turku, Finland

Bacterial biofilms have clear implications in disease and in food applications involving probiotics. Here, we show that switching the carbohydrate source from glucose to fructose increased the biofilm formation and the total surface-antigenicity of a well-known probiotic, *Lactobacillus rhamnosus* GG. Surfaceomes (all cell surface-associated proteins) of GG cells grown with glucose and fructose in planktonic and biofilm cultures were identified and compared, which indicated carbohydrate source-dependent variations, especially during biofilm growth. The most distinctive differences under these conditions were detected with several surface adhesins (e.g., MBF, SpaC pilus protein and penicillin-binding proteins), enzymes (glycoside hydrolases, PrsA, PrtP, PrtR, and HtrA) and moonlighting proteins (glycolytic, transcription/translation and stress-associated proteins, r-proteins, tRNA synthetases, Clp family proteins, PepC, PepN, and PepA). The abundance of several known adhesins and candidate moonlighters, including enzymes acting on casein-derived peptides (ClpP, PepC, and PepN), increased in the biofilm cells grown on fructose, from which the surface-associated aminopeptidase activity mediated by PepC and PepN was further confirmed by an enzymatic assay. The mucus binding factor (MBF) was found most abundant in fructose grown biofilm cells whereas SpaC adhesin was identified specifically from planktonic cells growing on fructose. An additional indirect ELISA indicated both growth mode- and carbohydrate-dependent differences in abundance of SpaC, whereas the overall adherence of GG assessed with porcine mucus indicated that the carbon source and the growth mode affected mucus adhesion. The adherence of GG cells to mucus was almost completely inhibited by anti-SpaC antibodies regardless of growth mode and/or carbohydrate source, indicating the key role of the SpaCBA pilus in adherence under the tested conditions. Altogether, our results suggest that carbon source and growth mode coordinate mechanisms shaping the proteinaceous composition of GG cell surface, which potentially contributes to resistance, nutrient acquisition and cell-cell interactions under different conditions. In conclusion, the present study shows that different growth regimes and conditions can have a profound impact on the adherent and antigenic features of GG, thereby providing new information on how to gain additional benefits from this probiotic.

Keywords: ***Lactobacillus rhamnosus*, probiotic, biofilm, surface protein, fructose, mucus, adhesion**

OPEN ACCESS

Edited by:
Rosa Anna Siciliano, Italian National Research Council (CNR), Italy

Reviewed by:
Silvina Graciela FADDA, CONICET Centro de Referencia para Lactobacilos (CERELA), Argentina
Clifton Fagerquist, United States Department of Agriculture, United States

***Correspondence:**
Pekka Varmanen
pekka.varmanen@helsinki.fi

Specialty section:
This article was submitted to Food Microbiology, a section of the journal Frontiers in Microbiology

Received: *15 March 2019*
Accepted: *22 May 2019*
Published: *05 June 2019*

Citation:
Savijoki K, Nyman TA, Kainulainen V, Miettinen I, Siljamäki P, Fallarero A, Sandholm J, Satokari R and Varmanen P (2019) Growth Mode and Carbon Source Impact the Surfaceome Dynamics of Lactobacillus rhamnosus GG. Front. Microbiol. 10:1272. doi: 10.3389/fmicb.2019.01272

INTRODUCTION

Probiotic bacteria, applied in various aspects of the food and pharmaceutical industries (Sanders et al., 2013; Goldenberg et al., 2017), exploit sophisticated strategies to enable the utilization of many nutrients, maintain viability and adherence to mucosal surfaces, and modulate host immunity in a beneficial way during industrial processes and upon their consumption (Siezen and Wilson, 2010). Unlike free-living cells, the biofilm mode of growth has been shown to improve existing probiotic features (antimicrobial and anti-inflammatory functions) in some *Lactobacillus* strains (Jones and Versalovic, 2009; Rieu et al., 2014; Aoudia et al., 2016). In addition, switching from the planktonic to the biofilm mode of growth can provide bacteria, including probiotics, with means to overcome lethal conditions, including antimicrobial treatments, host immune defenses, and changes in pH, salt, temperature and nutrients (Flemming et al., 2016). Biofilms comprise cells enclosed in an extracellular matrix (consisting of nucleic acids, exopolysaccharides (EPS), lipids and/or proteins) and typically display adherent growth on either abiotic or natural surfaces (Flemming and Wingender, 2010). Probiotics must be consumed at least daily to obtain most of their benefits, and new probiotic supplements prepared as biofilms, e.g., in biocompatible microspheres or encapsulated in microcapsules, could offer longer lasting probiotic effects compared to those prepared from free-grown cells (Cheow and Hadinoto, 2013; Cheow et al., 2014; Olson et al., 2016).

One of the most documented and utilized probiotic *Lactobacillus* strains, *Lactobacillus rhamnosus* GG, is known to adhere to the human intestinal mucosa via pilus (encoded by *spaCBA*) extending from its cell surface and to persist for more than a week in the gastrointestinal tract (GIT) of healthy adults (Kankainen et al., 2009). EPS is another factor that plays an important role as a protective shield against host innate defense molecules to improve adaptation in the GIT (Lebeer et al., 2011a). However, reduced EPS synthesis has been linked to the increased adherence and biofilm formation of GG, which by uncovering specific adhesins necessary for biofilm formation, enabled the enhanced biofilm growth of this strain (Lebeer et al., 2009). The SpaCBA-pilus adhesin, which mediates the direct interaction with the host and abiotic surfaces, and MabA (the modulator of adhesion and biofilm), which strengthens the biofilm structure, are considered the central factors that mediate the biofilm formation of GG *in vitro* (Lebeer et al., 2007b; Velez et al., 2010). While the presence of biofilms in the colonic microbiome has been reported in several studies, GIT-associated probiotic biofilms have been found in specific niches of certain animal hosts (Lebeer et al., 2011b; de Vos, 2015). GG can grow as a biofilm on inert substrates (Lebeer et al., 2007a,b; Savijoki et al., 2011) and integrate well in a multispecies biofilm model with the potential to inhibit the growth of some cariogenic species (Jiang et al., 2016). However, systematic studies aiming to uncover all surface-bound proteins on GG biofilms have not been conducted.

We previously demonstrated that the biofilm formation of GG in MRS medium under microaerophilic and anaerobic (5% CO_2) conditions was protein-mediated (Savijoki et al., 2011), indicating that cell surface-associated proteins most likely affected the biofilm formation of this strain. In a multispecies biofilm model, GG was shown to reach high viable cell numbers with glucose or sucrose as the carbon source (Jiang et al., 2018). Glucose and fructose can enhance the survival of GG in simulated gastric juice at pH 2.0 (Corcoran et al., 2005), while fructose also contributes to the *in vitro* adherence and antimicrobial activity of this probiotic (Lee and Puong, 2002; Jiang et al., 2015). These simple carbohydrates were recently found to prevent the colonization of a gut commensal bacterium, *Bacteroides thetaiotaomicron*, in the gut, an effect that was not observed with prebiotic fructo-oligosaccharides (Townsend et al., 2019).

The present study aimed to uncover the effects of two simple carbohydrates, glucose and fructose, on the total surface-associated antigenicity of GG growing in planktonic and biofilm states. To explore these findings further, the surfaceome compositions from the same cells were compared, and some industrially relevant features were verified with phenotypic analyses. To the best of our knowledge, this is the first systematic study exploring surfaceomes of probiotic biofilms and demonstrating the importance of growth mode and carbon source in coordinating the adherent and industrial features of GG.

MATERIALS AND METHODS

Culture Media

Lactobacillus rhamnosus GG was routinely grown on commercial MRS agar (BD, Franklin Lakes, United States) prior to propagation in modified MRS broth for planktonic or biofilm cultivations. The composition of this modified MRS was as follows: 10 g/L tryptone pancreatic digest of casein, 10 g/L beef extract powder, 5 g/L Bacto^{TM} yeast extract, 1 g/L Tween 80, 2 g/L ammonium citrate tribasic, 5 g/L sodium acetate, 0.1 g/L magnesium sulfate heptahydrate, 0.05 g/L manganese II sulfate monohydrate and 2 g/L dipotassium hydrogen phosphate trihydrate (pH 6.5–7). When appropriate, MRS was supplemented with 2% glucose (glc) (MRS-G) or 2% fructose (frc) (MRS-F) (Sigma-Aldrich, St. Louis, MO, United States) or less (1.75, 1.5, 1.25, 1.0, 0.75, 0.5, 0.25, 0.1, or 0.05%).

Biofilm Formation and Quantification

GG colonies from MRS agar plates were suspended in MRS supplemented with glc or frc at desired concentrations to obtain an OD_{600} = 0.15–0.2, from which 200 μL was removed and added to flat-bottomed 96-well plates (FALCON; Tissue Culture Treated, polystyrene, Becton Dickinson), and the plates were incubated at 37°C under anaerobic conditions (5% CO_2) for 24 h, 48 h or 72 h. Biofilm formation efficiency was assessed with crystal violet staining essentially as previously described (Sandberg et al., 2008). Briefly, the non-adherent cells were removed from the wells, and the biofilm cells were washed twice with deionized H_2O. Adherent cells were stained with 200 μL of the crystal violet solution (0.1%, w/v) (Sigma–Aldrich, Munich, Germany) for 30 min at RT. Excess stain was removed by washing the cells twice with deionized H_2O, and the stained cells were

suspended in 200 μL of 30% acetic acid by shaking at RT (400 r.p.m. for 30 min). The density of the biofilms was recorded at 540 nm using an ELISA reader (LabSystems Multiskan EX, Thermo Scientific, Wilmington, DE, United States). Biofilm experiments were performed several times, using at least eight technical replicates.

LIVE/DEAD Staining of Biofilms and Confocal Microscopy

GG cells were suspended in MRS-G (2% glc) or MRS-F (2% frc) to obtain OD_{600} ∼ 0.15–0.2, from which 4 mL was added to uncoated 35 mm glass bottom dishes (MatTek, Ashland, MA, United States). Dishes were incubated at 37°C under anaerobic conditions (5% CO_2) for 48 h for biofilm formation. Non-adherent cells were removed, and adherent cells were subjected to LIVE/DEAD viability staining using 5 μM of Syto9 and 30 μM of propidium iodide (PI) according to the manufacturer's instructions (LIVE/DEAD® *Bac*Light™, Molecular Probes, Life Technologies, Thermo Scientific, Wilmington, DE, United States). Fluorescence images were captured with Zeiss LSM510 META confocal microscope using Zeiss LSM 3.2 software (Zeiss GmbH, Oberkochen, Germany). All biofilms were analyzed in duplicates.

1-DE Immunoblotting

Samples from planktonic and biofilm cells for 1-DE (SDS polyacrylamide gel electrophoresis) and immunoblotting were prepared as follows. GG cells were suspended in MRS-G or MRS-F to obtain an OD_{600} = 0.15–0.2. The cell suspensions were split in two; half (2.5 mL) of the suspension was cultured under planktonic conditions (Falcon tubes) and half (2.5 mL/ tube) was cultured under biofilm-formation conditions (2.5 mL per well in a flat-bottomed 24-well plate; FALCON – Tissue Culture Treated, Polystyrene, Becton Dickinson) at 37°C in the presence of 5% CO_2. The cell densities of planktonic cultures and biofilms, after suspending the adherent cells in fresh MRS, were measured at 600 nm. Surfaceome proteins from planktonic cells (1.5 mL) after overnight incubation were harvested by centrifugation (4000 × *g*, 3 min, 4°C). Cells were washed once with ice cold 100 mM sodium acetate buffer (pH 4.7). Cells from biofilm cultures after 48 h of incubation were harvested by removing non-adherent cells and washing adherent cells with ice cold acetate buffer as above. Cells normalized to equal cell densities were centrifugated (4000 × *g*, 3 min, 4°C) and then suspended gently in Laemmli buffer (pH 7.0) as described earlier (Jakava-Viljanen et al., 2002). Cells were incubated in Laemmli buffer on ice for 15 min and then an additional 5 min at RT. Supernatants were recovered by centrifugation (4000 × *g*, 3 min, 4°C) and equal volumes from each sample were subjected to 12% TGX™ Gel (Bio-Rad, Hercules, CA, United States) electrophoresis (1-DE) using 1× Tris-glycine-SDS as the running buffer. After 1-DE, proteins were transferred onto a PVDF membrane using the TransBlot Turbo™ Transfer System (Bio-Rad, Hercules, CA, United States) according to the manufacturer's instructions. The membrane was then probed first with antibodies (1:4000) detecting surface-associated factors of GG (Espino et al., 2015) and then with IRDye® 800CW goat anti-Rabbit IgG (LI-Cor® Biosciences, Lincoln, NE, United States) (1:20000). After probing, the membrane was blocked using Odyssey Blocking buffer and washed with PBS (phosphate buffered saline, pH 7.4) according to the instructions provided by LI-Cor® Biosciences. The cross-reacting antigens were detected and quantified using an Odyssey® infrared imaging system (LI-Cor® Biosciences, Lincoln, NE, United States) and the AlphaView Alpha View 3.1.1.0 software (ProteinSimple, San Jose, CA, United States), respectively. The experiment was repeated three times (each with two technical replicates).

Mucus Adhesion Assay

Adhesion to mucus was carried out as described previously (Vesterlund et al., 2006; Kainulainen et al., 2013). GG was grown in MRS-G and MRS-F with H^3-thymidine for metabolic labeling in planktonic and biofilm forms as described above in section 2.4 (1-DE immunoblotting). Briefly, the planktonic and biofilm cells were first washed with a low pH buffer (100 mM sodium acetate, pH 4.7), which prevented the release of adhesive moonlighting proteins (cytoplasmic proteins) from the cell surfaces. Then, the washed cells were allowed to bind the porcine mucin immobilized onto microtiter plate wells. After washing the cells to remove non-adherent cells, the radioactivity of the adherent cells was measured by liquid scintillation, and the percent of bacterial adhesion was determined by calculating the ratio between the radioactivity of the adherent bacteria and that of the added bacteria. The experiment was repeated twice with four to five technical replicates. An unequal variance *t*-test was used to determine significant differences between selected samples.

Indirect ELISA for Detecting Changes in SpaC Abundance

Planktonic and biofilm GG cells were grown on MRS-G and MRS-F and washed with sodium acetate buffer as above. Washed cells at the same density were treated with 10 μM 4,6′-diamidino-2-phenylindole (DAPI; Molecular Probes, Thermo Scientific, Wilmington, DE, United States) to stain all bacterial populations and with antiserum raised against His_6–SpaC to detect SpaC expression. Antiserum against purified His_6–SpaC of *L. rhamnosus* GG was raised in rabbits using routine immunization procedures as described previously (Tytgat et al., 2016). The staining was carried out by using indirect immunofluorescence as described previously (Kainulainen et al., 2012) with minor modifications. Briefly, GG cells were collected by centrifugation, washed once with 100 mM Na-acetate buffer (pH 4.7) and fixed with 4% (wt/vol) paraformaldehyde in phosphate buffered saline (PBS; pH 4.0) prior to detection with anti-His_6-SpaC primary antibody and Alexa-488 (Invitrogen)-conjugated goat anti-rabbit IgG (1 μg/ml) secondary antibody and DAPI counterstain. After staining, the optical density (OD_{600}) of the cells was adjusted to 1.0 with washing buffer, and the intensity of the fluorescence in the samples was measured using the Victor3 1420 multilabel counter (PerkinElmer, Waltham, MA, United States). The experiment was repeated twice, each with five technical replicates.

An unequal variance *t*−test was used to determine significant differences between selected samples.

Cell-Surface Shaving and LC-MS/MS Analyses

Surfaceome analyses were conducted with GG cells cultured in planktonic (24 h; stationary phase) and biofilm states (48 h) in MRS-G and MRS-F at 37°C under microaerophilic (5% CO_2) conditions. Biofilms were formed using flat-bottomed 24-well plates with 2.5 mL of the indicated media containing suspended GG cells (OD_{600} = 0.1) per well as described above. After 48 h of incubation, non-adherent cells were discarded, and the adherent cells were washed gently with ice-cold 100 mM Tris–HCL (pH 6.8). Pelleted cells suspended gently in 100 μl of TEAB were mixed with 50 ng/μL of sequencing grade modified porcine trypsin (Promega, Madison, WI, United States), and digestions were incubated at 37°C for 15 min. Released peptides and trypsin were recovered by filtration through a 0.2 μm pore size acetate membrane by centrifugation (7000 × *g*, 2 min, +4°C), and the digestions were further incubated for 16 h at 37°C. The cell samples from planktonic cultures were harvested by centrifugation (7000 × g, 2 min, +4°C) and subsequently washed and treated with trypsin as described above for biofilm cells. Digestions were stopped by adding trifluoroacetate (TFA) to a final concentration of 0.6%. The peptide concentrations were measured using a Nano-Drop (ND 1000, Thermo Scientific, Wilmington, DE, United States) at 280 nm. For each growth mode, three biological replicate cultures were used.

Trypsin-digested peptides were purified using ZipTips (C18) (Merck Millipore, Burlington, MA, United States), and equal amounts of the peptide samples were subjected to LC-MS/MS using an Ultimate 3000 nano-LC (Dionex) and QSTAR Elite hybrid quadrupole TOF mass spectrometer (Applied Biosystems/MDS Sciex) with nano-ESI ionization as previously described (Espino et al., 2015). The MS/MS data were searched against the concatenated GG protein database composed of the target (Acc. No. FM179322; 2944 entries) (Kankainen et al., 2009) and the decoy protein sequences using the Mascot (Matrix Science, version 2.4.0) search engine through the ProteinPilot software (version 4.0.8085). The Mascot search criteria were based on trypsin digestion with one allowed mis-cleavage, fixed modification of carbamidomethyl modification of cysteine, variable modification of oxidation of methionine, 50 ppm peptide mass tolerance, 0.2 Da MS/MS fragment tolerance and 1+, 2+, and 3+ peptide charges. The false discovery rate (FDR) percentages calculated using the formula 2×n*reverse*/(n*reverse* + n*forward*) (Elias and Gygi, 2007) indicated FDRs < 4% in each data set. The raw Mascot proteomic identifications and associated files are freely downloadable from the Dryad Digital Repository (doi: 10.5061/dryad.15534h9).

Protein Identifications and Surfaceome Comparisons

Mass spectra from each replica sample were searched both separately and combined against the indicated protein database. Proteins with Mascot score (ms) ≥ 30 and $p < 0.05$ and identified in at least 2/3 replicates were considered high quality identifications and used to indicate condition-specific identifications and relative protein abundance changes. The emPAI (exponentially modified Protein Abundance Index) values of the high confidence identifications were used to estimate protein abundance changes; emPAI is considered roughly proportional to the logarithm of the absolute protein concentration, which allows label-free and relative quantitation of the protein pairs (Ishihama et al., 2005). Principle component analysis (PCA) of the emPAI values was performed with IBM SPSS Statistics v.24. Missing values were substituted with half minimum emPAI value for each protein identified in at least 2/3 replicates in at least one of the conditions using MetImp 1.2[1] (Wei et al., 2018a,b) (**Supplementary Table S1**). Two proteins with zero variance (YP_003172193.1; YP_003172584.1) were excluded. PCA of the imputated emPAI data was carried out utilizing Varimax rotation with Kaiser normalization.

Proteome Bioinformatics

Theoretical molecular weights (MW) and isoelectric points (pI) for the identified proteins were acquired using the Protein Manipulation Suite Server v. 2.0 at https://www.genscript.com/sms2/proteiniep.html (Stothard, 2000). The presence of classical secretory motif (signal peptide) and lipobox was predicted using the SignalP Server v. 5.0 at http://www.cbs.dtu.dk/services/SignalP/abstract.php (Almagro Armenteros et al., 2019). The cellular location for each protein was predicted using the PSORTb Server v. 3.0 at https://www.psort.org/psortb/ (Yu et al., 2010) and the number of potential transmembrane domains (TMDs) with the TMHMM Server v. 2.0 at http://www.cbs.dtu.dk/services/TMHMM/ (Krogh et al., 2001). The identified proteins with plausible moonlighting function/entering the extracellular milieu via non-classical route were predicted using the SecP Server v. 2.0 at http://www.cbs.dtu.dk/services/SecretomeP/ (Bendtsen et al., 2005). UniProt/Proteomes[2] with the GG proteome ID UP000000955 (UniProtKB, 2,832) with Gene Ontology (GO) IDs was used to link biological process, molecular function and cellular component to each identified protein.

Analysis of Surface-Associated Aminopeptidase Activities

Cell surface-associated aminopeptidase activity (PepN and PepC) was determined from planktonic and biofilm cells cultured in the presence of 2.0 and 0.5% glc and frc for 24 h (planktonic and biofilm cells) and 48 h (biofilm cells) using a previously reported method (Varmanen et al., 1994) with the following modifications. Briefly, biofilm and planktonic cells (1.8 mL) obtained from 10 mL cultures were washed as described above and then suspended in 1 mL of cold 100 mM Tris–HCl buffer, pH 6.8. The optical density of each sample was measured at 540 nm. The incubation mixture contained 1 mM L-leucine-*para*-nitroanilide (Leu-*p*NA) substrate in

[1]https://metabolomics.cc.hawaii.edu/software/MetImp/

[2]https://www.uniprot.org/proteomes/

200 µl of the cell suspension. The inhibitory effect of the metal-ion chelator EDTA was examined by incubating the cell suspension with 5 mM EDTA for a few minutes prior to the addition of Leu-pNA. Reactions were incubated at 37°C for 5–25 min and stopped with 800 µl of 30% (v/v) acetic acid. After centrifugation (8000 × *g*, 5 min), the absorbance was measured at 410 nm. The specific aminopeptidase activity was calculated by dividing the absorbance change at 410 nm by the reaction time used for Leu-*p*NA hydrolysis and the optical density of the cells (OD_{540}). An unequal variance *t*-test was used to determine significant differences between selected samples.

RESULTS

Biofilm Formation of GG on Fructose and Glucose

Biofilm formation of GG was first tested at three time points (24, 48, and 72 h after inoculation, hpi) in MRS-G and MRS-F (2% glc and 2% frc) and MRS without carbohydrate, which indicated that frc stimulated biofilm formation by approximately 2-fold compared to glc at each time point tested (**Figure 1A**). The highest biofilm masses in MRS-F and MRS-G were detected at 48 and 72 hpi, respectively (**Figure 1A**). The cell viability analysis of biofilm cells grown on glass-bottom dishes with both carbon sources revealed that biofilms formed on frc at 48 hpi contained proportionally more living cells than those grown on glc (**Figure 1B**). In addition, the biofilm formation efficiency was higher on hydrophilic polystyrene than hydrophilic glass under the conditions used (data not shown).

Growth Mode- and Carbon Source-Induced Changes in Cell-Surface Antigenicity

The surface antigenicity of GG cells grown in biofilm and planktonic states in MRS-G and MRS-F was studied by subjecting surface-associated proteins extracted in 1× Laemmli buffer to 1-DE combined with immunoblotting using antisera raised against intact GG cells. **Figure 1C** reveals that in each sample, the most intense/abundant cross-reacting antigen signals migrated to approximately 65, 55, 40, and 35 kDa. Comparing the total antigen intensity profiles, reflecting antigen abundances (**Figure 1D**), showed that the presence of frc in the growth medium increased the surface antigenicity by ∼two-fold in planktonic and ∼ 2.5-fold in biofilm cells compared to cells grown on glc. In glc-associated cells, switching from planktonic to biofilm growth had no effect on surface-antigenicity, whereas the surface-antigenicity increased by ∼20% after switching from planktonic to biofilm growth in the presence of frc. The presence of Frc in the growth medium resulted in the appearance of unique protein bands at 15 and 20 kDa in both the planktonic and biofilm cell samples, while a higher-molecular weight protein (∼200 kDa) was specific to glc- and frc-biofilm samples. Thus, growing cells in planktonic or biofilm forms on frc increases the overall surface-antigenicity of GG along with the specific production of small-molecular-weight antigens, while a larger protein was specifically produced by biofilm cells growing on both carbon sources.

Identifying the Surfaceomes of GG Cultured Under Different Conditions

We previously demonstrated that the biofilm formation of GG is mainly protein-mediated (Savijoki et al., 2011). To explore this further, the surfaceomes of cells cultured in biofilm state were analyzed. For obtaining high amounts of biomass needed for proteome analysis without compromising cell viability, the biofilm samples were collected at 48 hpi (**Figures 1A,B**). According to previous studies the physiology of mature biofilms resembles that of stationary phase planktonic cultures (Stoodley et al., 2002; Folsom et al., 2010). Therefore, the planktonic cell samples for comparative analyses were harvested from cultures at stationary phase (24 hpi). LC-MS/MS based protein identifications ($p < 0.05$) are listed in **Supplementary Table S2**. Four surfaceome catalogs [(ms) ≥ 30, $p < 0.05$] were generated with each data set showing extensive overlap; 70–94% of the identified proteins were shared between at least two of the replica samples (**Supplementary Table S3**). The total number of high-quality identifications was 245 [(ms) ≥ 30, $p < 0.05$], consisting 94, 117, 179, and 227 proteins from the glc-planktonic, frc-planktonic, glc-biofilm and frc-biofilm cells, respectively (**Supplementary Table S4**). As no decrease in the colony forming units (CFUs) of the shaved cells was observed (data not shown), we concluded that no significant cell lysis had occurred under the trypsin-shaving conditions used. Thus, comparison of the surfaceome catalogs indicated that the number of proteins at the cell surface of GG increased with frc as the carbon source compared to glc. Similarly, growth in the biofilm state increased the number of protein identifications compared to cells grown in planktonic form, regardless of the carbon source used.

Multivariate Analysis for Screening Specific Surfaceome Patterns

A principal component analysis (PCA) was performed to identify carbon source- and growth mode-dependent patterns in the surfaceome data. **Figure 2A** shows that all biological replicate samples clustered together well, with four clearly separated and identifiable groups. PC1, correlating with the change in growth mode-, and PC2 with the carbohydrate-dependent changes, suggest that the carbon source had a greater effect on GG during biofilm growth than planktonic growth. This was further explored by Venn diagrams that compared the number of specifically identified proteins (unique to growth mode and/or carbon source) and proteins with emPAI values showing ≥ 2-fold change (**Supplementary Table S4**). Venn digrams in **Figure 2B** compares the growth-mode and carbon source-associated surfaceomes. The number of specifically identified proteins (not identified from planktonic cells) was 90 and 113 in biofilm cells grown on glc and frc, respectively. In total, 5 and 3 identifications were specific for planktonic cells grown on glc and frc, respectively. In addition, the abundance of 60 and 67 proteins increased ≥ 2-fold in biofilm cells, whereas 2

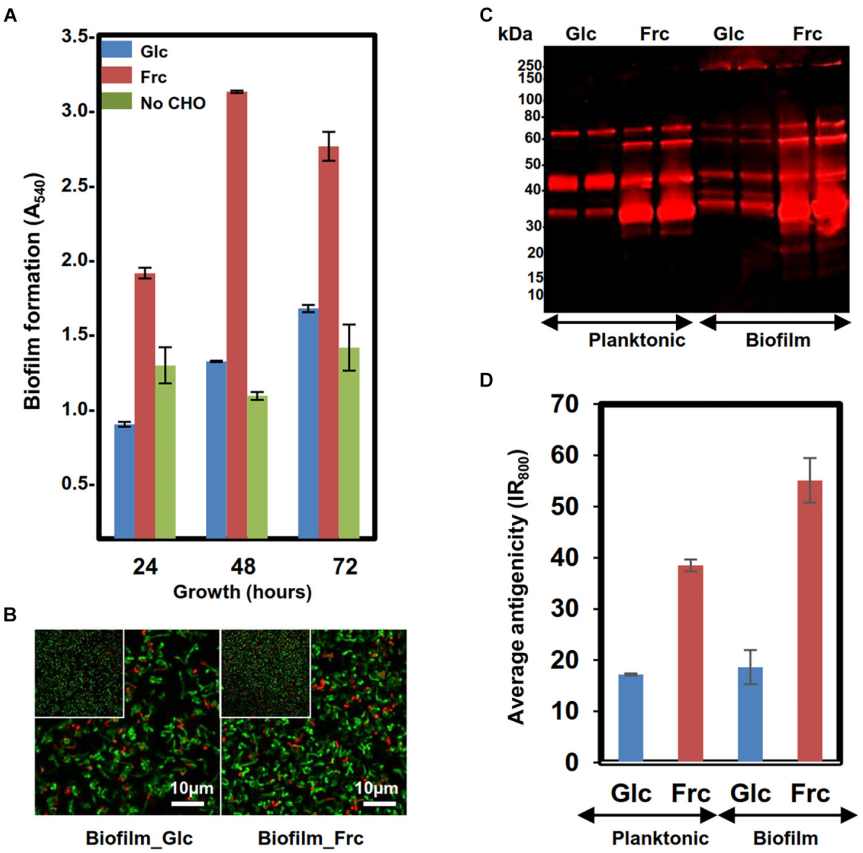

FIGURE 1 | Assessing the biofilm formation of the GG cells in MRS in the presence 2% glc, 2% frc or without carbohydrate (CHO) under anaerobic conditions (5% CO_2). **(A)** Biofilm formation efficiency of the GG cells in the presence of frc and glc on flat-bottom polystyrene wells at indicated time points of incubation. **(B)** Fluorescence images of 48 h old biofilms prepared in the presence of glc and frc. Biofilms were stained with the LIVE/DEAD *Bac*Light kit with Syto9 for staining viable cells and PI for dead cells. The scale bar is 10 μm. **(C)** 1-DE immunoblot analysis of planktonic and biofilm GG cells using anti-GG antibodies targeting the surface-associated proteins. The surface proteins were isolated from 24 h old (planktonic) and 48-h-old (biofilms) cells, and the amounts of samples separated by 1-DE were normalized to cell density. Glc and Frc indicate lanes with samples (two technical replicate) grown in presence of glucose and fructose, respectively. The antigen profiles were detected using an Odyssey® infrared imaging system. **(D)** Total fluorescence of each 1-DE antigen profile was quantified using the Alphalmager gel documentation and image analysis system.

and 3 proteins were more abundant (≥2-fold) in planktonic cells with glc and frc, respectively. With frc as the carbon source, the number of specific identifications (not identified from glc-grown cells) from the planktonic and biofilm cells was 32 and 61, respectively. For glc, 9 and 13 specific identifications were made from the planktonic and biofilm cells, respectively. Four and 19 proteins displayed ≥ 2-times higher abundances in planktonic cells grown of glc and frc, respectively. The number of more abundant proteins with ≥ 2-fold change was 11 and 33 on glc- and frc-associated biofilms. Altogether, the presence of frc in the growth medium resulted in a higher number of specifically identified proteins as well as proteins with increased abundances in comparison to cells grown on glc.

Because Venn diagrams implied that the carbon source affected the number and amount of proteins attached to the biofilm surfaces, we also explored the biofilm formation efficiency in the presence of varying carbohydrate concentrations. **Figure 2C** shows that frc enhanced the biofilm formation over a wider concentration rate compared to glc. However, 0.5% glc produced the thickest biofilms at 48 hpi, while over two-fold higher concentrations of frc were required to achieve the thickest biofilms under the same conditions. Furthermore, optical densities (at 600 nm) of the formed biofilms grown on different carbohydrate concentrations revealed only marginal changes in cell densities, indicating that increased biofilm formation was not accompanied by an increased number of cells (data not shown).

Categorizing Condition Specific Protein Identifications and Changes in Protein Abundances

Based on the proteome bioinformatics the identified proteins were next divided according to their predicted secretion motifs, subcellular location and cellular functions (**Supplementary Table S4**). Based on this categorization 48 proteins were predicted to be exported via the classical and 68 via the non-classical secretion pathway. For majority of the identifications the proteome bioinformatics tools imply

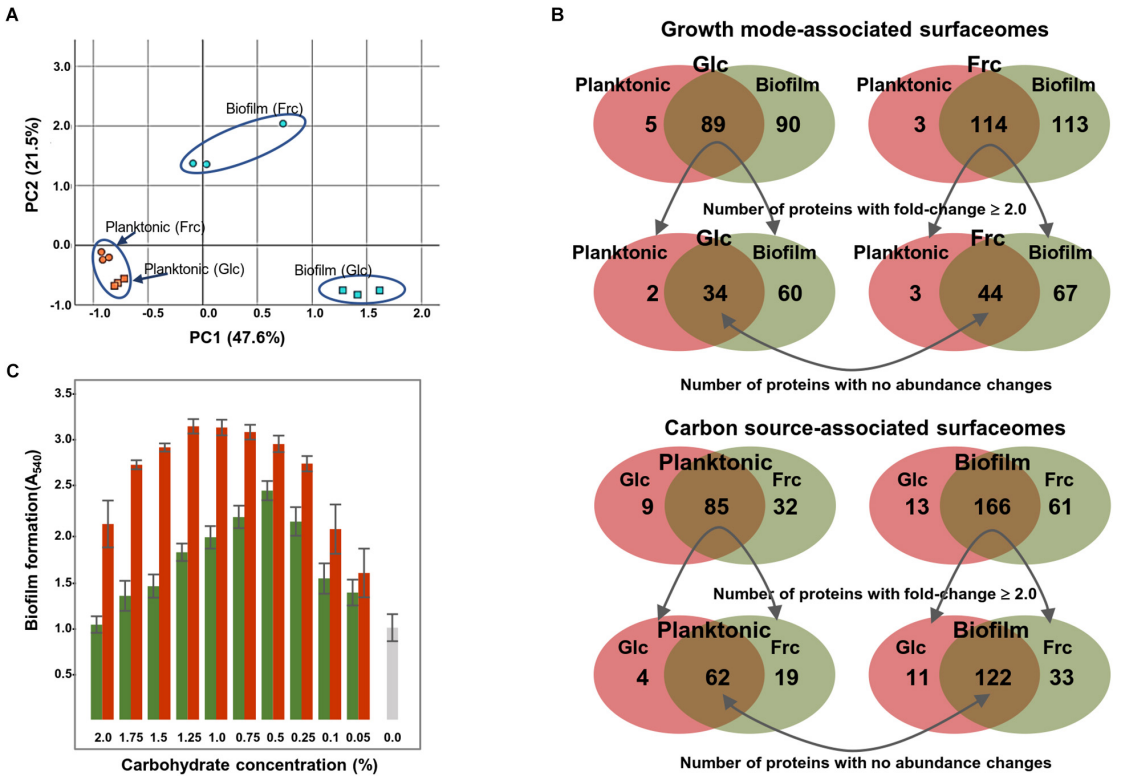

FIGURE 2 | (A) Surfaceome variability among GG cells cultured under four different conditions (two carbon sources and two growth modes) assessed by PCA. PC1 (growth mode) accounts for 47.6% and PC2 (carbon source) accounts for 21.5% of the variation. **(B)** Venn diagrams indicate the number of commonly and specifically identified surfaceome proteins. **(C)** Biofilm formation of GG in varying concentrations of fructose (red bars) and glucose (green bars) and with no carbohydrate (gray bar). The biofilm formation efficiency was monitored after 48 h of incubation at 37°C in the presence of 5% CO_2.

cytoplasmic or cytoplasmic/membrane location. Next, the most distinctive protein abundance variations, including condition-specific identifications and proteins with abundance change ≥ 2-fold between the indicated conditions were selected for visual illustration by heatmaps; **Figure 3** shows relative abundance changes estimated for classical surface proteins and known/adhesive moonlighters and **Figure 4** candidate moonlighting proteins. Altogether, these proteins could be categorized into three groups: **(i)** the classically secreted surface adhesins, transporters and enzymes, **(ii)** known surface-associated moonlighters with adherence features, and **(iii)** predicted and new candidate moonlighters lacking established extracellular function. The known and candidate moonlighters were the dominant protein group among the detected surfaceomes. Among the identified putative moonlighters, the ribosomal proteins r-proteins (42 proteins), PTS/ABC-type transporter proteins (17 proteins; several OppA paralogs) and amino acid tRNA synthetases (10 proteins) formed the largest protein groups.

Protein identifications specific to one of the four tested conditions

The greatest proportion (35 proteins) of the one-condition specific identifications was obtained from the frc-biofilm cells. The proteins identified only from frc-biofilm cells but not from any other sample type included known and candidate moonlighters (e.g., RbfA, PDHA, GreA, GPD, FrlB, IF-2, and AlaS), Clp family chaperones (ClpL, ClpA, and ClpC) and a PepN aminopeptidase, which were all proposed to be present at relatively high abundances. Seven small molecular weight (6–33 kDa) putative moonlighters (YP_003170092.1, YP_003170859.1, YP_003170536.1, YP_003171217.1, YP_003171101.1, YP_003172119.1, and YP_003170467.1) were also found to be specific to frc-biofilm surfaces. The classical surface proteins, such as a 70-kDa penicillin-binding protein (PbB3) and a 28-kDa Aes lipase, were specific to frc-biofilm surfaces and, based on the emPAI values were predicted to be produced at low levels under these conditions. Leucyl-tRNA synthetase (LeuS) and glutamine transport (GlnQ) were specifically identified from glc-biofilm surfaces. Protein identifications specific to planktonic cells growing on frc included the SpaC pilus subunit, encoded by the *spaCBA* pilin operon (Kankainen et al., 2009).

Protein identifications specific to growth mode

In total, 3 and 47 proteins were detected as specific to planktonic and biofilm cell growth, respectively, independent of the carbon source. Planktonic-specific identifications included the classically secreted 73-kDa lectin-binding protein and ClpB, a candidate moonlighting Clp family ATPase. Classical surface-proteins

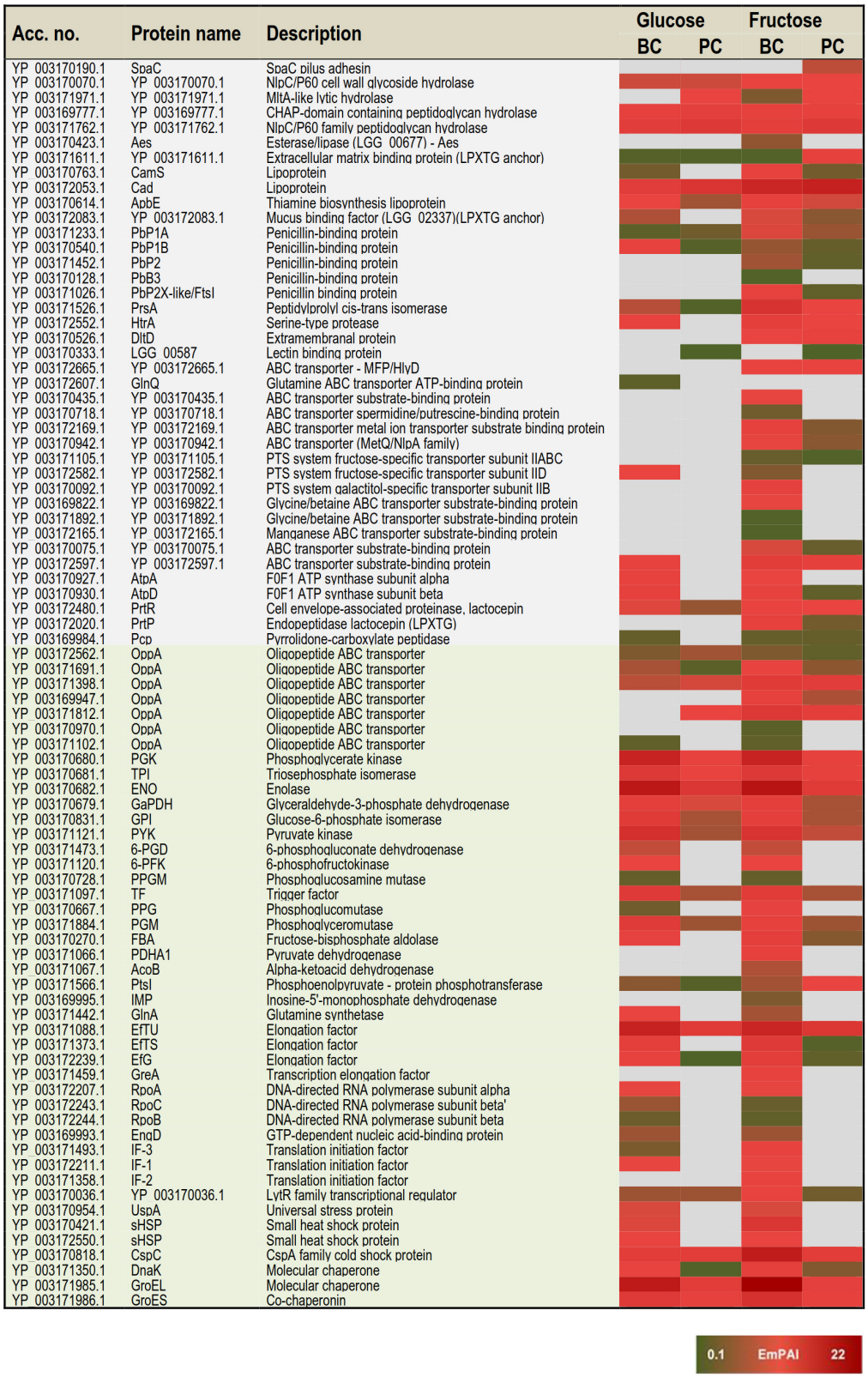

FIGURE 3 | A heat map comparing the most distinctive protein abundance changes (estimated by the emPAI values) among the classical surface proteins anchored to cell-wall/-membrane via motifs or domains (names shaded in gray) and among known and/or adhesive moonlighters (names shaded in light green). Red and green refer to higher and lower protein abundances, respectively.

FIGURE 4 | A heat map comparing the most distinctive protein abundance changes (estimated by the emPAI values) among the predicted moonlighters. Red and green refer to higher and lower protein abundances, respectively.

specific to biofilm cells included one of the OppA transporter paralogs (YP_003171102.1) and AtpA, a subunit of the F-ATPase (F_1F_o ATPase). Several known and putative moonlighters were also specifically identified from biofilm cell surfaces. These included seven amino acid tRNA synthetases (Thr, Met, Asn, Ser, Glu, Lys, and Asp); 11 known (D-LDH, PPGM, 6-PGD, UspA, IF-1, 6-PFK, RpoB/C, GlnA, PepA, and EngD); and 13 predicted moonlighters (RpsF, RplP, RpsQ, RpmE2, RplT, RpmG, RplM, RpsC, RplF, RplR, RmlA, RmlC, and RmlD). Among the predicted moonlighters, RmlA, RmlC, and RmlD are encoded by the four-gene (*rmlABCD*) operon involved in dTDP-rhamnose biosynthesis.

Protein identifications specific to available carbon source

From the two carbon sources, frc was found to induce specific surfaceome changes similar in both the planktonic and biofilm cell surfaces, whereas only one glc-specific identification (prolyl-tRNA synthetase -ProS) was shared by the planktonic and biofilm cells. The frc-specific identifications included classical surface proteins, such as the lactocepin (PrtP), an extramembranal protein (DltD), a tellurite resistance protein (TelA), five ABC/PTS-type transporters mediating type I protein secretion (MFP/HlyD), amino acid (OppA)/metal ion intake/output proteins (YP_003172665.1, YP_003169947.1, YP_003169947.1, YP_003170942.1, YP_003172169.1, YP_003170075.1, and YP_003171105) and two penicillin-binding proteins (PbP2 and PbP2X-like/FtsI). In addition, two phosphoglycerol transferase (MdoB) paralogs of different sizes (78 and 84 kDa) and an r-protein, RplX, were detected as candidate moonlighting proteins specific to frc-associated cells. From these, the greatest differences were associated with RplX, the ABC transporters for metal ion binding (YP_003172169.1) and oligopeptide uptake (OppA, YP_003169947.1), the 78-kDa MdoB paralog and the penicillin-binding proteins PbP2X-like and PbP2, which all displayed over two-fold higher abundances during biofilm growth compared to planktonic growth on frc.

Growth mode-induced protein abundance changes

Planktonic- or biofilm growth-induced surfaceome changes independent of the carbon source used were considered growth mode-induced changes. Twenty-nine proteins showed similar abundance levels in the glc- and frc-biofilm cells, and were higher (≥2-fold) in abundance compared to the glc- and frc-planktonic cells. The greatest differences in abundance were detected for candidate moonlighters, such as an elongation factor – EfG (>8.0-fold increase), an 8-kDa hypothetic protein – YP_003172198.1 (with ∼6.0-fold increase), an aminopeptidase – PepC (with ∼5.0-fold increase) and a ClpP caseinolytic peptidase (>2.0-fold increase). Known moonlighters (PGK, TPI, L-LDH, GaPDH, and RpoA) and 21 r-proteins (RplR, RplO, RpsG, RplJ, RplU, RplQ, RpsD, RpsE, RpsR, RpsD, RpsE, RpsB, RpsS, RpsA, RpsM, RpsH, RplK, RpsL, RplN, RplK, and RplB) were less abundant but still over 2-fold more abundant on biofilm than on planktonic cell surfaces. Only one of the OppA paralogs (YP_003171102.1) was found to be ∼5-times more abundant on planktonic cells on both carbon sources.

Effect of carbon source on biofilm-induced protein abundance changes

In total, 61 proteins more abundant in glc and frc biofilms than in planktonic cells were divided into four groups as follows: **(i)** Biofilm-induced proteins showing greater relative abundance difference between planktonic and biofilm growth modes when grown on glc. This group included twenty-two proteins and 14 proteins with > 5-fold higher differences in abundance and included the classically secreted penicillin-binding protein (PbP1B) as well as several known and predicted moonlighters (DnaK, L-LDH, PYK, PGM, GBI, RplA, RplD, RpsE, RpsB, RplQ, RpsG, and the 8-kDa YP_003172198.1). **(ii)** Biofilm growth induced proteins more abundant on glc-biofilm than on frc-biofilm cell surfaces included dihydrolipoamide acetyltransferase (∼4.7-fold increase), a potential Com_YlbF family protein predicted to ensure proper biofilm formation (∼2.7-fold increase) and five r-proteins (RplK, RplB, RplN, RpsF, and RpmF) with fold-changes ranging from 2.4 to 4.6. **(iii)** Biofilm-induced proteins showing greater relative abundance difference between planktonic and biofilm growth modes when grown on frc. The majority of these were identified as known and candidate moonlighters (EfTS, GroEL, AtpD, FBA, RplV, RpsR, and CspC), with fold-change 4–15 and with EfTS (∼15-fold increase) and GroEL (∼9-fold) displaying the greatest changes in abundance. The classical surface-proteins, including the PrtP protease (specific to frc-cells) and the lipoprotein CamS (∼4-fold increase), were predicted to be more abundant on frc cells than on glc cells. **(iv)** Biofilm growth induced proteins more abundantly produced on frc- than on glc-associated biofilm cell surfaces included five classical surface proteins, which included one of the OppA paralogs (YP_003171812.1), the PrsA chaperone/foldase, the serine-proteases PrtP and HtrA and the CamS lipoprotein. Of these, OppA (>15-fold increase), PrsA (∼7-fold increase) and PrtP (∼4-fold increase) displayed the greatest changes in abundance. In total, nine possible moonlighters were also more abundantly produced (≥4-fold) on frc-biofilm cell surfaces, including an 18 kDa small heat shock protein (sHSP), a cold-shock protein (CspC), two amino acid tRNA synthetases (LysS and AspS), RpsR, phosphoglucomutase (PPG), and a dTDP-glucose-4,6-dehydratase (RmlB, encoded by the *rmlABCD* operon). In addition, a dTDP-4-dehydrorhamnose reductase – RmlD, with a > 2.0-fold change in abundance, was also identified from the frc-biofilm cells.

Carbon source-induced changes in planktonic cultures

Carbon source-dependent changes in planktonic cell surfaces could be divided into two groups. **(i)** Proteins predicted to be more abundant on cells growing on frc included the extracellular matrix-binding protein (YP_003171611.1) with > 8-fold higher abundance. Another classical surface protein, PrsA, and two moonlighters (PtsI and RplC) were also predicted to be ∼5-fold more abundantly produced on frc cells. **(ii)** Proteins predicted to be more abundantly produced in the presence of glc included one of the OppA paralogs (YP_003171812.1), an

MltA lytic hydrolase, a prolyl-tRNA synthetase – ProS, and the AtpD protein.

Adherence of Biofilm and Planktonic Cells to Porcine Mucus

Because the identification data implied that the growth mode and carbon source in the growth medium could affect the adherence features of GG, we investigated the mucus-binding ability of the planktonic and biofilm cells grown on glc and frc. **Figure 5A** indicates that the biofilm cells grown on frc displayed the highest level of adherence, while planktonic cells grown on glc were the least adherent. The frc biofilms demonstrated a mucus-binding ability that was ∼2-fold more efficient than that of the glc-associated planktonic cells; $p = 0.037$). The possible role of the SpaC-adhesin, the tip pilin of the SpaCBA pilus known to mediate key interactions with the human mucus (Kankainen et al., 2009), in mediating the frc-stimulated adherence was assessed next by testing the adherence of the GG cells in the presence of anti-SpaC antiserum. **Figure 5A** indicates that the presence of SpaC antibodies markedly decreased the adherence of each type of cell to mucus. Although the final level of adherence detected for these cells was somewhat similar, the biofilm cells grown on frc displayed the greatest SpaC-mediated inhibition, whereas the level of adherence decreased the least in glc-associated planktonic cells. To readdress the possible role of the pilus structure in the observed differences, we also monitored the SpaC abundances on each GG cell type. As shown in **Figure 5B**, the highest abundance of SpaC was detected on the glc-associated biofilm cells, which was > 2-fold (p = 4.46e−09) higher than that on the planktonic cells grown on glc and ∼2-fold (p = 1.15e−07) higher than that on the frc-biofilm cells. Planktonic cells grown on frc displayed the lowest SpaC abundance.

Whole-Cell Aminopeptidase Activity

Varying abundances detected for predicted cell-surface moonlighters, such as PepN, PepC, PepA, ClpP, and several OppA paralogs, implied differences in the ability of the GG cells to utilize casein/casein-derived peptides for growth. PepN was specific to frc-biofilm cells. PepC was predicted to be equally abundant on the biofilm cells grown on frc and glc and displayed over a 4-fold higher abundance on biofilm than planktonic cells. Comparison of PepN and PepC implies that PepC is produced ∼2-fold more on the frc-biofilm cells than PepN on the same cells. To verify these results, we monitored the surface-associated aminopeptidase activity by exposing washed and intact GG cells to a chromogenic substrate, Leu-*p*NA, a specific substrate for both aminopeptidases (Varmanen et al., 1994). **Figure 5C** confirms the identification findings by showing that the surface-associated aminopeptidase activity of frc-biofilm cells was ∼4-fold higher (p = 0.001) than that of planktonic cells growing on frc. Changes from glc to frc increased the aminopeptidase activity on both the planktonic and biofilm cell surfaces but led to a proportionally greater increase in the biofilm cell surface. Lowering the carbohydrate concentration to 0.5% increased the aminopeptidase activity in planktonic cells by ∼4-fold, while only a slight decrease in the enzyme activity was observed in biofilm cells on both carbon sources. Enzyme activities were also examined in the presence of 5 mM EDTA,

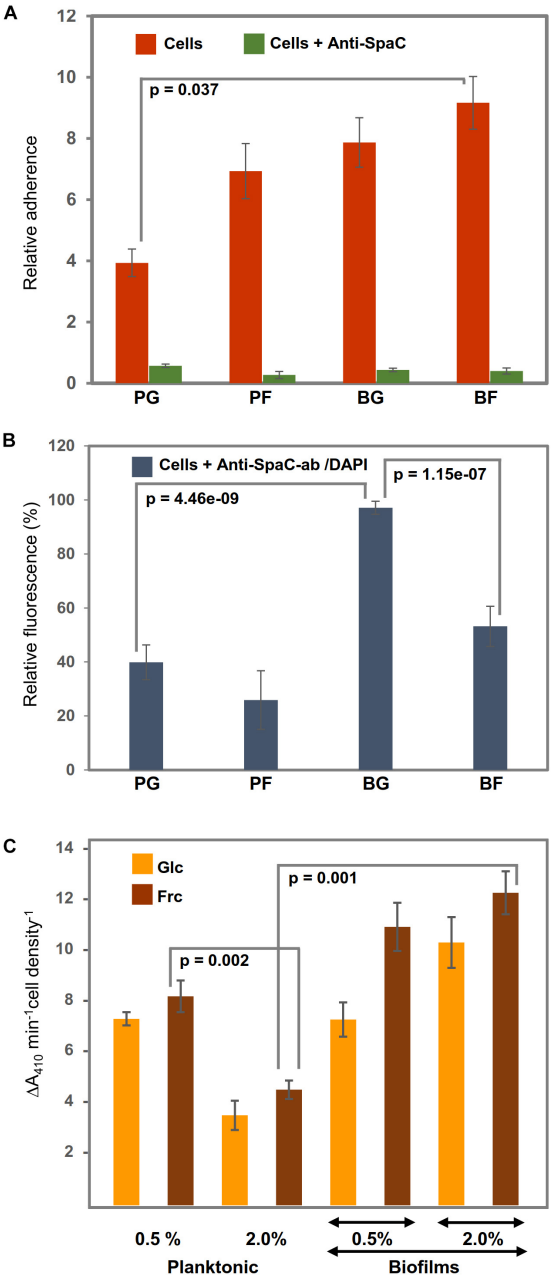

FIGURE 5 | Representative diagrams **(A)** showing the relative adherences (average adhesion percentage of the added bacteria) of planktonic (PC) and biofilm GG (BC) cells grown on frc and glc to porcine mucus and **(B)** illustrating the abundance of the SpaC pilin subunit on the cells treated first with anti-SpaC-antibody and then Alexa-488-conjugated goat anti-rabbit IgG and/or the DAPI counterstain. **(C)** The surface-associated aminopeptidase activity (PepC and PepN) of the planktonic and biofilm cells was assessed using 1 mM Leu-pNA. Significant differences are indicated with lines. The error bars indicate SD for two or more biological replicates, each with several technical repeats.

a metal-chelator that inhibits the activity of metallopeptidases such as PepN while not affecting other types of peptidases such as PepC (Varmanen et al., 1994). Since EDTA inhibited only marginally the total aminopeptidase activity only in frc-biofilm cells, PepC is the likely candidate for the hydrolysis of the substrate.

DISCUSSION

Carbon Source Controls the Protein-Dependent Biofilm Growth of GG

Environmental signals, such as O_2, CO_2, bile, mucins, non-digestible polysaccharides and carbohydrates present in the human GIT, have been shown to affect the GG biofilm formation *in vitro* (Lebeer et al., 2007b; Savijoki et al., 2011). In MRS growth medium, GG produces biofilm, which is completely disintegrated by treatment with proteolytic enzyme (Savijoki et al., 2011), indicating the presence of a large amount of proteins in the biofilm matrix and/or that biofilm formation is protein-mediated. Since both carbon metabolism (Lebeer et al., 2007b) and cell-surface exposed proteins (Savijoki et al., 2011) appear to play a role in biofilm formation, we explored this link further by investigating the effects of glc and frc as carbon sources on the surfaceome composition of GG. Our findings indicated that changing the carbon source from glc to frc resulted in enhanced biofilm formation efficiency of GG *in vitro*. GG is known to exert high *in vitro* adhesion to Intestinal Epithelial Cells (IECs) and biofilm formation capacity on polystyrene and glass (Doron et al., 2005; Lebeer et al., 2007b). Here, our findings demonstrated more efficient biofilm growth on polystyrene than on glass and more efficient biofilm growth with frc than with glc on both inert materials. Crystal violet provides a good detection of biofilm mass, but this dye stains both the bacterial cells and extracellular matrix, including proteins (Santhanalakshmi and Balaji, 2001; Welch et al., 2012). As the tested carbohydrates had only a marginal effect on the cell density, we suggest that the increase in crystal violet staining, instead of showing increased biofilm formation, related directly to changes in the protein abundance of biofilm cells. A similar observation was also made when growing the biofilm cells with varying carbohydrate concentrations; decreased carbohydrate concentrations resulted in thicker biofilms, which did not result from higher cell density (data not shown). Thus, changes in carbon sources and their concentrations regulate the changes in protein abundance on the biofilm cell surfaces.

Biofilm Growth and frc in Growth Medium Enhance the Protein Export in GG

Examining the cause-effect relationships between the identified surfaceomes revealed that the carbon source played a more important role in the biofilm mode of growth. Conditions of glc limitation have been shown to enhance the biofilm formation of GG (Velez et al., 2010). Here, decreasing the concentration of both carbon sources in growth medium resulted in similar outcomes. The presence of frc enhanced biofilm formation over wider concentrations than glc. Putative moonlighting proteins, including predicted as well as new candidate moonlighters, were the dominant protein group in the biofilm-associated surfaceomes. Comparing the frc- and glc-associated surfaceomes implied that these non-classical surface proteins are more abundantly present in both the biofilm and planktonic cells growing on frc. These results could be explained by increased cell lysis within the biofilm and the fructose containing cultures or alternatively, be a result of non-classical protein export by a yet unknown pathway. Cell lysis in biofilms is a well-reported phenomenon for model bacteria like *S. aureus* (Rice et al., 2007; Houston et al., 2011; Mashruwala et al., 2017), but remains to be studied in *L. rhamnosus* GG. In this study, three proteins potentially involved in hydrolysis of peptidoglycan and autolysis were identified, NlpC/P60, MltA and a CHAP-domain containing peptidoglycan hydrolase. Of these, NlpC/P60 was previously identified from the surface of exponentially growing *L. rhamnosus* GG cells, while the other two proteins were not detected in that study (Espino et al., 2015). Here, the results indicate constant expression of NlpC/P60 and CHAP-domain containing peptidoglycan hydrolase under the conditions used, whereas MltA appears to be more abundant on stationary phase planktonic cells than on biofilm cells. Thus, while the presence of MltA and the CHAP-domain containing peptidoglycan hydrolase could be linked to increased autolysis in stationary phase and biofilm cells compared to exponentially growing cells, these protein identification results do not support increased autolysis activity as an explanation of higher number of cytoplasmic proteins on biofilm cells compared to stationary phase planktonic cells. The presence of moonlighting proteins on the cell surface or in the culture medium has been reported for several microbial species, and for many of these, the moonlighting activity outside of the cells has been demonstrated (Kainulainen and Korhonen, 2014; Chen et al., 2018). It has been proposed that bacteria recycle conserved cytoplasmic proteins in a pH-dependent manner in the matrix to facilitate interspecies interactions without specifically recognizing the dedicated matrix components of the other species (Foulston et al., 2014). In a recent study, the strongly positively charged r-proteins were shown to be embedded in *S. aureus* biofilm matrix under acidic conditions (Graf et al., 2019). This was proposed to depend on the pH, coordinated by the formation/release of acidic fermentation end-products in the biofilm cells facing oxygen limitation (Graf et al., 2019). In the present study, the pHs of the spent culture supernatants were clearly acidic, pH < 5.0 (data not shown). Thus, while r-proteins were identified as the most abundant moonlighters in the biofilm matrices, we suggest that low pH could have promoted the interactions between the r-proteins and the biofilm cells also in the present study.

In general, the mechanisms underlying export/transport of moonlighting proteins remain unknown (Wang and Jeffery, 2016). In view of this, it is tempting to speculate that the specific appearance of HlyD/MFP in frc-associated cell surfaces indicates the role of this protein in directing moonlighting proteins out of the cell. HlyD is part of a translocon that comprises

HlyB, HlyD, and TolC, which is proposed to coordinate the transport of potential novel proteins by quite different mechanisms (Holland et al., 2016). Overexpression of PrsA, a known surface-associated chaperone or foldase acting on secreted proteins (Kontinen and Sarvas, 1993), on biofilm cells and frc-associated cells is another plausible factor contributing to protein secretion under these conditions. This chaperone/foldase is known to enhance protein secretion efficiency in bacteria (Chen et al., 2015) and act on various substrates, ranging from 20 to 80 kDa in size (Jakob et al., 2015). The serine-type surface-protease, HtrA, follows the same abundance trend as PrsA and is another classical surface-protein that could enhance protein secretion in frc-associated samples. In bacteria, HtrA is involved in degrading abnormal proteins, processing secreted proproteins and the maturation of native proteins (Poquet et al., 2000), but this protease can also affect biofilm formation and control the presence of surface-associated moonlighters, such as enolase (ENO) and glyceraldehyde-3-phosphate dehydrogenease (GaPDH) (Biswas and Biswas, 2005).

Here, ENO, EfTU, TDPA, PGK, and GroEL, each with previously reported adhesive functions (Kainulainen and Korhonen, 2014; Chen et al., 2018), were detected as the most abundant moonlighters in the biofilm cells growing on both carbon sources. In addition, stress response proteins (GroES and DnaK), glycolytic proteins (PGM, PYK, PGK, FBA, GPI, L/D-LDH, GMR, and PDCE2), the elongation factors EfTS and EfG, the RNA polymerase subunit RpoA, the translation initiation factor IF1, and the trigger factor (TF), were also detected as relatively abundant on biofilms. The r-protein moonlighters (a total of 43 proteins) were the largest protein group among the biofilm-associated surfaceomes, independent of the carbon source used. In addition to their proposed role as biofilm integrity/stability enhancing role, coordinated by the production of acidic fermentation end-products (Graf et al., 2019), some of the identified r-proteins may also have other moonlighting functions. The most abundant r-proteins were RplX, RpsE, RpsG, RplL, and RplO, from which RpIL (the 50S ribosomal protein L7/L12) was predicted to be the most abundant. The high abundance of this r-protein during biofilm growth could explain the concomitant presence of another moonlighting protein, EfG, on the biofilm cells at high abundances, as the GTPase activity of EfG is reported to require RplL for ribosomal translocation (Koch et al., 2015). For several r-proteins (e.g., L5, L11, L23, L13a, S3, S19, and S27), non-canonical functions ranging from gene expression regulation to subverting pro-inflammatory actions, apoptosis and protection against abiotic stress (Liu et al., 2014; Henderson et al., 2016; Chen et al., 2018) have been proposed. The increased abundance of the TF during the biofilm mode of growth could be explained by the concomitant presence of the ribosomal protein L23. This r-protein has been reported to have binding sites for both the TF and the signal recognition particle, which is thought to aid in protein export to the cell membrane (Hoffmann et al., 2010). The specific appearance of several moonlighting aminoacyl-tRNA synthetases (ATRSs) in biofilm cells was also interesting, as these enzymes, unrelated to their primary function, also regulated gene expression, signaling, transduction, cell migration, tumorigenesis, angiogenesis, and/or inflammation (Son et al., 2014; Chen et al., 2018), thereby forming a novel group of moonlighters in probiotic species.

Fructose and Biofilm Growth Increase the Surface-Associated Aminopeptidase Activity in GG

Several components of the proteolytic system (several OppA paralogs, PepC, PepN, and PepA) involved in the utilization of milk casein (Savijoki et al., 2011) were identified here as candidate moonlighters with higher abundances on biofilm than planktonic cell surfaces. Among these PepN and the OppA paralogs were more abundant on or specific to the frc-associated cell surfaces. The enzymatic assay performed on whole cells using a substrate specific to PepC and PepN confirmed the identification results and indicated that more PepC than PepN is associated with biofilm cells. In addition, the classical surface proteases PrtP and PrtR were predicted to be more abundantly produced on the biofilm cell surfaces. The two identified aminopeptidases are expressed in the cytoplasm, where they act on the oligopeptides that are taken up by the Opp-transport system. Thus, efficient surface-aminopeptidase activity could provide the probiotic with means to speed up growth and adaptation in conditions involving oligopeptides as the carbon source. In a recent study by Galli et al. (2019) GG was utilized as an adjunct starter culture in Camembert-type cheese production, which was found to improve the sensory characteristics of the cheese. While the mechanism behind the GG-mediated flavor formation in cheese remains to be elucidated, the efficient and diversified proteolytic system of the strain could be involved (Galli et al., 2019). It is highly likely that the robust GG cells do not undergo autolysis during cheese making, which makes the cell-surface located moonlighting aminopeptidases C and N interesting objects to be studied further in this context.

Several cytoplasmic proteins have been shown to be selectively sorted into membrane vesicles (MVs), which in some bacteria were shown to contribute to approximately 20% of the whole biofilm matrix proteome, demonstrating that MVs are also important constituents of the biofilm matrices (Couto et al., 2015). Protein targeting to MVs provides an important mechanism exploited by both gram-negative and gram-positive bacteria to export proteins in a protected and concentrated manner to aid neighboring cells or modulate the host immune system. Whether MVs play a role in *L. rhamnosus* GG biofilm formation and surface protein export, remain to be studied.

Surface-Antigenicity and Adherence of GG by Biofilm Growth in the Presence of frc

Comparison of the total antigenicity profiles of GG cells grown in planktonic and biofilm forms on glc and frc indicated that frc as the carbon source increases the abundances of many antigens (∼23, 28, 40, and 60 kDa in size) during both growth

modes. We previously demonstrated the presence of several adhesive and antigenic moonlighters at the cell surface of planktonic GG cells grown on glc (Espino et al., 2015). In that study, protein moonlighters, such as DnaK (67.2 kDa), GroEL (57.4 kDa), PYK (62.8 kDa), TF (49.8 kDa), ENO (47.1 kDa), GaPDH (36.7 kDa), L-LDH (35.5 kDa), EfTu (43.6 kDa), Adk (23.7 kDa), and UspA (16.8 kDa), were identified as highly abundant and antigenic on planktonic GG cells. The present study suggests that PYK, ENO, GaPDH, TF, L-LDH, EfTU, UspA, DnaK, and GroEL could be produced more during biofilm than planktonic growth, which is also in line with an earlier proteomic study showing that a switch from planktonic to biofilm growth in *L. plantarum* increases the abundances of several stress responses and glycolytic moonlighters (De Angelis et al., 2015). From the identified moonlighters, ENO, IMP, FBA, TDPA, GreA, GroES, and GroEL are plausible factors that aid in biofilm formation in the presence of frc, as evidenced by surfaceome predictions.

The *rmlABCD* operon products, involved in the synthesis of O-antigen lipopolysaccharide (Reeves, 1993), could have conferred increased surface antigenicity to GG cells during biofilm growth. Here, all of the operon gene products RmlA, RmlB, RmlC, and RmlD corresponding to glucose-1-phosphate thymidylyltransferase, dTDP-4-dehydrorhamnose 3,5-epimerase, dTDP-4-dehydrorhamnose reductase and dTDP-glucose-4,6-dehydratase, respectively, were detected only in biofilm cells and with ∼2-fold higher abundances in the presence of frc. In some pathogens, L-rhamnose is required for virulence, and the enzymes of the Rml pathway are considered potential targets in drug design (Trent et al., 2006). In view of this, detection of the Rml enzymes as moonlighters is interesting and points toward a novel role of these enzymes at the cell surface of non-pathogenic bacteria. The rhamnose moiety has also been shown to bind specific moonlighters (e.g., ENO and 58 other potential moonlighters) at the bacterial cell surface, proposing that rhamnose-mediated anchoring is a general mechanism for anchoring the moonlighting proteins to the cell surface in bacteria (Daubenspeck et al., 2016).

The identified DltD, encoded by part of the *dltABCD* operon involved in the formation of lipoteichoic acid (LTA), could have increased antigenicity in frc-associated GG cells. DltD is a single-pass membrane protein involved in the final transfer of D-alanine residues to LTA on the outside of the cell (Reichmann et al., 2013) that contributes to adherence and biofilm formation (Spatafora et al., 1999; Gross et al., 2001). LTA has been shown to be essential for biofilm matrix assembly and bulk accumulation over time (Castillo Pedraza et al., 2017), and the early stages of biofilm formation necessitates efficient expression of *dltD* (Klein et al., 2012). In addition, a lack of DltD has been linked to poor acid survival in planktonic cells and an inability to form biofilms *in vitro* in the presence of sucrose or glucose (Quivey et al., 2015). As DltD could not be detected in the glc-associated planktonic or biofilm cells, we hypothesize that such deficiency might also explain the lower biofilm formation efficiency on glc compared to frc.

Many of the classical surface proteins may have also contributed to the total antigenicity and/or adherence in the GG cells. The most plausible candidates include lipase and lipoproteins (Aes, AbpE, Cad, and CamS), peptidoglycan hydrolases (e.g., the NlpC/P60), MBF, a lectin-binding protein, penicillin-binding proteins and the pilus protein SpaC. The identification data implies that SpaC is specifically produced during planktonic growth on frc. From these proteins, the SpaC adhesin and MBF are best known; the first is produced through the *spaCBA* operon coding for the pilus, the key factor promoting biofilm formation *in vitro* as well as colonization and adherence *in vivo* (Lebeer et al., 2007b, 2012), while MBF has been shown to bind intestinal and porcine colonic mucus, laminin, collagen IV, and fibronectin (von Ossowski et al., 2011; Nishiyama et al., 2015). Additional mucus-adherence assays with each GG cell type in the presence of anti-SpaC antibodies complemented with indirect ELISA monitoring of the SpaC abundances indicated the importance of the pilus adhesin in coordinating the adherence in both the planktonic and biofilm cells. Surprisingly, the glc–associated biofilm cells with the highest SpaC abundance did not shown the highest mucus binding ability, which was detected for frc grown biofilm cells. Possible explanations to this discrepancy include presence of specific factors in biofilm cells grown on frc, which could enhance or strengthen the pilus mediated mucus binding. The inability to identify SpaC by LC-MS/MS from biofilm-cells implied that the complex structure of the pilus adhesin together with the overwhelming presence of moonlighting proteins on biofilm cell surfaces could be the reason why the pilus protein was identified only from the planktonic cells. The same reason applies for the lack of MabA among the identified surfaceomes. MabA (LGG_01865), the modulator of adhesion and biofilm formation, is proposed to strengthen the biofilm structure following the pilus-mediated interaction with the surface (Velez et al., 2010).

A recent study highlighted an important role of glc and frc, carbohydrates prevalent in the Western diet, in regulating the colonization of a beneficial microbe independent of supplying these carbohydrates to the intestinal microbiota (Townsend et al., 2019). In that study, both frc and glc, but not prebiotics such as fructo-oligosaccharides, were found to silence the two-component system sensor histidine kinase/response regulator Roc that activates transcription of clustered polysaccharide utilization genes in a widely distributed gut commensal bacterium *B. thetaiotaomicron*. Roc was also suggested to promote gut colonization by interacting with moonlighting proteins such as GPI or glucose 6-phosphate dehydrogenase (Sonnenburg et al., 2006). From these two moonlighters, GPI was detected here as a more abundant protein in biofilm cells with a slight increase in cells grown on glc. As the present study compared surfaceomes of cells grown only in the presence of simple carbohydrates, we cannot exclude the possibility that corresponding response regulators (e.g., WalK) could have been modulated by these carbohydrates and that the two tested carbohydrates could coordinate the colonization of GG *in vivo* in an analogous manner.

CONCLUSION

The present study provides the first in-depth comparison of the planktonic- and biofilm matrix-associated surfaceomes of GG. We show that cells growing in planktonic and biofilm forms in the presence of simple carbohydrates in growth medium could be used to modify the surfaceome composition of this probiotic. We show remarkable differences among the compositions of the classical and non-classical surface proteins (moonlighters) that have immunomodulatory, adherence, protein-folding, proteolytic or hydrolytic activities. Our study also indicated that the carbon source coordinates protein-mediated biofilm formation, as evidenced by a whole-cell enzymatic assay measuring the surface-associated aminopeptidase activity on cells cultured on different carbon sources and with varying carbohydrate concentrations. The total antigenicity and adherence were higher on biofilm and planktonic cells grown on frc, in which specific surface-adhesins and putative moonlighters were the plausible contributory factors. Our findings also demonstrated the key role of the SpaCBA pilus independent of the growth mode or carbon source used, whereas the increased protein moonlighting is suggested to strengthen the biofilm structures and/or aid in cell-cell interactions. The observed phenotypic variations in *L. rhamnosus* GG potentially includes probiotic (adherence and immunomodulatory) and industrially relevant (proteolytic activity) features. Whether the GG phenotypes could be modulated in the host or in the food conditions remains to be shown.

DATA AVAILABILITY

The datasets generated for this study can be found in the Dryad Digital Repository, https://doi.org/10.5061/dryad.15534h9.

AUTHOR CONTRIBUTIONS

KS, PV, TN, PS, VK, RS, AF, and JS conceived, designed, and performed the experiments. IM analyzed the data. KS and PV wrote the manuscript. All authors participated in the revision of the manuscript and approved the final version of the manuscript.

FUNDING

This study was supported by the Academy of Finland (Grant No. 272363 to PV and 285632 to VK) and by Sigrid Juselius Foundation's Senior Reseacher's grant to RS. Open access publication fees were covered by Helsinki University Library.

SUPPLEMENTARY MATERIAL

The Supplementary Material for this article can be found online at: https://www.frontiersin.org/articles/10.3389/fmicb.2019.01272/full#supplementary-material

REFERENCES

Almagro Armenteros, J. J., Tsirigos, K. D., Sønderby, C. K., Nordahl Petersen, T., Winther, O., Brunak, S., et al. (2019). SignalP 5.0 improves signal peptide predictions using deep neural networks. *Nat. Biotechnol.* 37, 420–423. doi: 10.1038/s41587-019-0036-z

Aoudia, N., Rieu, A., Briandet, R., Deschamps, J., Chluba, J., Jego, G., et al. (2016). Biofilms of *Lactobacillus plantarum* and *Lactobacillus fermentum*: effect on stress responses, antagonistic effects on pathogen growth and immunomodulatory properties. *Food Microbiol.* 53, 51–59. doi: 10.1016/j.fm.2015.04.009

Bendtsen, J. D., Kiemer, L., Fausbøll, A., and Brunak, S. (2005). Non-classical protein secretion in bacteria. *BMC Microbiol.* 5:58. doi: 10.1186/1471-2180-5-58

Biswas, S., and Biswas, I. (2005). Role of HtrA in surface protein expression and biofilm formation by *Streptococcus mutans*. *Infect. Immun.* 73, 6923–6934. doi: 10.1128/IAI.73.10.6923-6934.2005

Castillo Pedraza, M. C., Novais, T. F., Faustoferri, R. C., Quivey, R. G., Terekhov, A., Hamaker, B. R., et al. (2017). Extracellular DNA and lipoteichoic acids interact with exopolysaccharides in the extracellular matrix of *Streptococcus mutans* biofilms. *Biofouling* 33, 722–740. doi: 10.1080/08927014.2017.1361412

Chen, C., Zabad, S., Liu, H., Wang, W., and Jeffery, C. (2018). MoonProt 2.0: an expansion and update of the moonlighting proteins database. *Nucleic Acids Res.* 46, D640–D644. doi: 10.1093/nar/gkx104

Chen, J., Gai, Y., Fu, G., Zhou, W., Zhang, D., and Wen, J. (2015). Enhanced extracellular production of α-amylase in *Bacillus subtilis* by optimization of regulatory elements and over-expression of PrsA lipoprotein. *Biotechnol. Lett.* 37, 899–906. doi: 10.1007/s10529-014-1755-3

Cheow, W. S., and Hadinoto, K. (2013). Biofilm-like *Lactobacillus rhamnosus* probiotics encapsulated in alginate and carrageenan microcapsules exhibiting enhanced thermotolerance and freeze-drying resistance. *Biomacromolecules* 14, 3214–3222. doi: 10.1021/bm400853d

Cheow, W. S., Kiew, T. Y., and Hadinoto, K. (2014). Controlled release of *Lactobacillus rhamnosus* biofilm probiotics from alginate-locust bean gum microcapsules. *Carbohydr. Polym.* 103, 587–595. doi: 10.1016/j.carbpol.2014.01.036

Corcoran, B. M., Stanton, C., Fitzgerald, G. F., and Ross, R. P. (2005). Survival of probiotic lactobacilli in acidic environments is enhanced in the presence of metabolizable sugars. *Appl. Environ. Microbiol.* 71, 3060–3067. doi: 10.1128/AEM.71.6.3060-3067.2005

Couto, N., Schooling, S. R., Dutcher, J. R., and Barber, J. (2015). Proteome profiles of outer membrane vesicles and extracellular matrix of *Pseudomonas aeruginosa* biofilms. *J. Proteome Res.* 14, 4207–4222. doi: 10.1021/acs.jproteome.5b00312

Daubenspeck, J. M., Liu, R., and Dybvig, K. (2016). Rhamnose links moonlighting proteins to membrane phospholipid in *Mycoplasmas*. *PLoS One* 11:e0162505. doi: 10.1371/journal.pone.0162505

De Angelis, M., Siragusa, S., Campanella, D., Di Cagno, R., and Gobbetti, M. (2015). Comparative proteomic analysis of biofilm and planktonic cells of *Lactobacillus plantarum* DB200. *Proteomics* 15, 2244–2257. doi: 10.1002/pmic.201400363

de Vos, W. M. (2015). Microbial biofilms and the human intestinal microbiome. *NPJ Biofilms Microbiomes* 1:15005. doi: 10.1038/npjbiofilms.2015.5

Doron, S., Snydman, D. R., and Gorbach, S. L. (2005). *Lactobacillus* GG: bacteriology and clinical applications. *Gastroenterol. Clin. North Am.* 34, 483–498. doi: 10.1016/j.gtc.2005.05.011

Elias, J. E., and Gygi, S. P. (2007). Target-decoy search strategy for increased confidence in large-scale protein identifications by mass spectrometry. *Nat. Methods* 4, 207–214. doi: 10.1038/nmeth1019

Espino, E., Koskenniemi, K., Mato-Rodriguez, L., Nyman, T. A., Reunanen, J., Koponen, J., et al. (2015). Uncovering surface-exposed antigens of *Lactobacillus rhamnosus* by cell shaving proteomics and two-dimensional immunoblotting. *J. Proteome Res.* 14, 1010–1024. doi: 10.1021/pr501041a

Flemming, H. C., and Wingender, J. (2010). The biofilm matrix. *Nat. Rev. Microbiol.* 8, 623–633. doi: 10.1038/nrmicro2415

Flemming, H. C., Wingender, J., Szewzyk, U., Steinberg, P., Rice, S. A., and Kjelleberg, S. (2016). Biofilms: an emergent form of bacterial life. *Nat. Rev. Microbiol.* 14, 563–575. doi: 10.1038/nrmicro.2016.94

Folsom, J. P., Richards, L., Pitts, B., Roe, F., Ehrlich, G. D., Parker, A., et al. (2010). Physiology of *Pseudomonas aeruginosa* in biofilms as revealed by transcriptome analysis. *BMC Microbiol.* 10:294. doi: 10.1186/1471-2180-10-294

Foulston, L., Elsholz, A. K., DeFrancesco, A. S., and Losick, R. (2014). The extracellular matrix of *Staphylococcus aureus* biofilms comprises cytoplasmic proteins that associate with the cell surface in response to decreasing pH. *MBio* 5, e01667–e01614. doi: 10.1128/mBio.01667-14

Galli, B. D., Baptista, D. P., Cavalheiro, F. G., and Gigante, M. L. (2019). *Lactobacillus rhamnosus* GG improves the sensorial profile of Camembert-type cheese: an approach through flash-profile and CATA. *LWT* 107, 72–78. doi: 10.1016/j.lwt.2019.02.077

Goldenberg, J. Z., Yap, C., Lytvyn, L., Lo, C. K., Beardsley, J., Mertz, D., et al. (2017). Probiotics for the prevention of *Clostridium difficile*-associated diarrhea in adults and children. *Cochrane Database Syst. Rev.* 12:CD006095. doi: 10.1002/14651858.CD006095

Graf, A. L., Schäuble, M., Rieckmann, L. M., Hoyer, J., Maaß, S., Lalk, M., et al. (2019). Virulence factors produced by *Staphylococcus aureus* biofilms have a moonlighting function contributing to biofilm integrity. *Mol. Cell. Proteomics* doi: 10.1074/mcp.RA118.001120 [Epub ahead of print].

Gross, M., Cramton, S. E., Götz, F., and Peschel, A. (2001). Key role of teichoic acid net charge in *Staphylococcus aureus* colonization of artificial surfaces. *Infect. Immun.* 69, 3423–3426. doi: 10.1128/IAI.69.5.3423-3426.2001

Henderson, B., Fares, M. A., and Martin, A. C. R. (2016). "Biological Consequences of Protein Moonlighting" in *Protein Moonlighting in Biology and Medicine*, eds B. Henderson, M. A. Fares, and A. C. Martin (Hoboken, NJ: John Wiley & Sons, Inc.), 81–141. doi: 10.1002/9781118952108.ch6

Hoffmann, A., Bukau, B., and Kramer, G. (2010). Structure and function of the molecular chaperone trigger factor. *Biochim. Biophys. Acta* 1803, 650–661. doi: 10.1016/j.bbamcr.2010.01.017

Holland, I. B., Peherstorfer, S., Kanonenberg, K., Lenders, M., Reimann, S., and Schmitt, L. (2016). Type I protein secretion-deceptively simple yet with a wide range of mechanistic variability across the family. *EcoSal Plus* 7, 1–46. doi: 10.1128/ecosalplus.ESP-0019-2015

Houston, P., Rowe, S. E., Pozzi, C., Waters, E. M., and O'Gara, J. P. (2011). Essential role for the major autolysin in the fibronectin-binding protein-mediated *Staphylococcus aureus* biofilm phenotype. *Infect. Immun.* 79, 1153–1165. doi: 10.1128/IAI.00364-10

Ishihama, Y., Oda, Y., Tabata, T., Sato, T., Nagasu, T., Rappsilber, J., et al. (2005). Exponentially modified protein abundance index (emPAI) for estimation of absolute protein amount in proteomics by the number of sequenced peptides per protein. *Mol. Cell. Proteomics* 4, 1265–1272. doi: 10.1074/mcp.m500061-mcp200

Jakava-Viljanen, M., Avall-Jääskeläinen, S., Messner, P., Sleytr, U. B., and Palva, A. (2002). Isolation of three new surface layer protein genes (*slp*) from *Lactobacillus brevis* ATCC 14869 and characterization of the change in their expression under aerated and anaerobic conditions. *J. Bacteriol.* 184, 6786–6795. doi: 10.1128/JB.184.24.6786-6795.2002

Jakob, R. P., Koch, J. R., Burmann, B. M., Schmidpeter, P. A., Hunkeler, M., Hiller, S., et al. (2015). Dimeric structure of the bacterial extracellular foldase PrsA. *J. Biol. Chem.* 290, 3278–3292. doi: 10.1074/jbc.M114.622910

Jiang, Q., Kainulainen, V., Stamatova, I., Korpela, R., and Meurman, J. H. (2018). *Lactobacillus rhamnosus* GG in experimental oral biofilms exposed to different carbohydrate sources. *Caries Res.* 52, 220–229. doi: 10.1159/000479380

Jiang, Q., Stamatova, I., Kainulainen, V., Korpela, R., and Meurman, J. H. (2016). Interactions between *Lactobacillus rhamnosus* GG and oral micro-organisms in an *in vitro* biofilm model. *BMC Microbiol.* 16:149. doi: 10.1186/s12866-016-0759-7

Jiang, Q., Stamatova, I., Kari, K., and Meurman, J. H. (2015). Inhibitory activity *in vitro* of probiotic lactobacilli against oral *Candida* under different fermentation conditions. *Benef. Microbes* 6, 361–368. doi: 10.3920/BM2014.0054

Jones, S. E., and Versalovic, J. (2009). Probiotic *Lactobacillus reuteri* biofilms produce antimicrobial and anti-inflammatory factors. *BMC Microbiol.* 9:35. doi: 10.1186/1471-2180-9-35

Kainulainen, V., and Korhonen, T. K. (2014). Dancing to another tune-adhesive moonlighting proteins in bacteria. *Biology* 3, 178–204. doi: 10.3390/biology3010178

Kainulainen, V., Loimaranta, V., Pekkala, A., Edelman, S., Antikainen, J., Kylväjä, R., et al. (2012). Glutamine synthetase and glucose-6-phosphate isomerase are adhesive moonlighting proteins of *Lactobacillus crispatus* released by epithelial cathelicidin LL-37. *J. Bacteriol.* 194, 2509–2519. doi: 10.1128/JB.06704-11

Kainulainen, V., Reunanen, J., Hiippala, K., Guglielmetti, S., Vesterlund, S., Palva, A., et al. (2013). BopA does not have a major role in the adhesion of *Bifidobacterium bifidum* to intestinal epithelial cells, extracellular matrix proteins, and mucus. *Appl. Environ. Microbiol.* 79, 6989–6997. doi: 10.1128/AEM.01993-13

Kankainen, M., Paulin, L., Tynkkynen, S., von Ossowski, I., Reunanen, J., Partanen, P., et al. (2009). Comparative genomic analysis of *Lactobacillus rhamnosus* GG reveals pili containing a human-mucus binding protein. *Proc. Nat. Acad. Sci. U.S.A.* 106, 17193–17198. doi: 10.1073/pnas.0908876106

Klein, M. I., Xiao, J., Lu, B., Delahunty, C. M., Yates, J. R., and Koo, H. (2012). *Streptococcus mutans* protein synthesis during mixed-species biofilm development by high-throughput quantitative proteomics. *PLoS One* 7:e45795. doi: 10.1371/journal.pone.0045795

Koch, M., Flür, S., Kreutz, C., Ennifar, E., Micura, R., and Polacek, R. (2015). Role of a ribosomal RNA phosphate oxygen during the EF-G–triggered GTP hydrolysis. *Proc. Natl. Acad. Sci. U.S.A.* 112, E2561–E2568. doi: 10.1073/pnas.1505231112

Kontinen, V. P., and Sarvas, M. (1993). The PrsA lipoprotein is essential for protein secretion in *Bacillus subtilis* and sets a limit for high-level secretion. *Mol. Microbiol.* 8, 727–737. doi: 10.1111/j.1365-2958.1993.tb01616.x

Krogh, A., Larsson, B., von Heijne, G., and Sonnhammer, E. L. (2001). Predicting transmembrane protein topology with a hidden Markov model: application to complete genomes. *J Mol. Biol.* 305, 567–580. doi: 10.1006/jmbi.2000.4315

Lebeer, S., Claes, I., Tytgat, H. L., Verhoeven, T. L., Marien, E., von Ossowski, I., et al. (2012). Functional analysis of *Lactobacillus rhamnosus* GG pili in relation to adhesion and immunomodulatory interactions with intestinal epithelial cells. *Appl. Environ. Microbiol.* 78, 185–193. doi: 10.1128/AEM.06192-11

Lebeer, S., Claes, I. J., Verhoeven, T. L., Vanderleyden, J., and De Keersmaecker, S. C. (2011a). Exopolysaccharides of *Lactobacillus rhamnosus* GG form a protective shield against innate immune factors in the intestine. *Microb. Biotechnol.* 4, 368–374. doi: 10.1111/j.1751-7915.2010.00199.x

Lebeer, S., Verhoeven, T. L., Claes, I. J., De Hertogh, G., Vermeire, S., Buyse, J., et al. (2011b). FISH analysis of *Lactobacillus* biofilms in the gastrointestinal tract of different hosts. *Lett. Appl. Microbiol.* 52, 220–226. doi: 10.1111/j.1472-765X.2010.02994.x

Lebeer, S., De Keersmaecker, S. C., Verhoeven, T. L., Fadda, A. A., Marchal, K., and Vanderleyden, J. (2007a). Functional analysis of *luxS* in the probiotic strain *Lactobacillus rhamnosus* GG reveals a central metabolic role important for growth and biofilm formation. *J. Bacteriol.* 189, 860–871. doi: 10.1128/JB.01394-06

Lebeer, S., Verhoeven, T. L. A., Velez, M. P., Vanderleyden, J., and De Keersmaecker, S. C. J. (2007b). Impact of environmental and genetic factors on biofilm formation by the probiotic strain *Lactobacillus rhamnosus* GG. *Appl. Environ. Microbiol.* 73, 6768–6775. doi: 10.1128/aem.01393-07

Lebeer, S., Verhoeven, T. L., Francius, G., Schoofs, G., Lambrichts, I., Dufrêne, Y., et al. (2009). Identification of a gene cluster for the biosynthesis of a long, galactose-rich exopolysaccharide in *Lactobacillus rhamnosus* GG and functional analysis of the priming glycosyltransferase. *Appl. Environ. Microbiol.* 75, 3554–3563. doi: 10.1128/AEM.02919-08

Lee, Y. K., and Puong, K. Y. (2002). Competition for adhesion between probiotics and human gastrointestinal pathogens in the presence of carbohydrate. *Br. J. Nutr.* 1, 101–108. doi: 10.1079/BJN2002635

Liu, X. D., Xie, L., Wei, Y., Zhou, X., Jia, B., Liu, J., et al. (2014). Abiotic stress resistance, a novel moonlighting function of ribosomal protein RPL44 in the halophilic fungus *Aspergillus glaucus*. *Appl. Environ. Microbiol.* 80, 4294–4300. doi: 10.1128/AEM.00292-14

Mashruwala, A. A., van de Guchte, A., and Boyd, J. M. (2017). Impaired respiration elicits SrrAB-dependent programmed cell lysis and biofilm formation in *Staphylococcus aureus*. *eLife* 6, e23845. doi: 10.7554/eLife.23845

Nishiyama, K., Nakamata, K., Ueno, S., Terao, A., Aryantini, N. P., Sujaya, I. N., et al. (2015). Adhesion properties of *Lactobacillus rhamnosus* mucus-binding factor to mucin and extracellular matrix proteins. *Biosci. Biotechnol. Biochem.* 79, 271–279. doi: 10.1080/09168451.2014.972325

Olson, J. K., Rager, T. M., Navarro, J. B., Mashburn-Warren, L., Goodman, S. D., and Besner, G. E. (2016). Harvesting the benefits of biofilms: a novel probiotic delivery system for the prevention of necrotizing enterocolitis. *J. Pediatr. Surg.* 51, 936–941. doi: 10.1016/j.jpedsurg.2016.02.062

Poquet, I., Saint, V., Seznec, E., Simoes, N., Bolotin, A., and Gruss, A. (2000). HtrA is the unique surface housekeeping protease in *Lactococcus lactis* and is required for natural protein processing. *Mol. Microbiol.* 35, 1042–1051. doi: 10.1046/j.1365-2958.2000.01757.x

Quivey, R. G. Jr., Grayhack, E. J., Faustoferri, R. C., Hubbard, C. J., Baldeck, J. D., Wolf, A. S., et al. (2015). Functional profiling in *Streptococcus mutans*: construction and examination of a genomic collection of gene deletion mutants. *Mol. Oral Microbiol.* 30, 474–495. doi: 10.1111/omi.2015.30.issue-6

Reeves, P. (1993). Evolution of *Salmonella* O antigen variation by interspecific gene transfer on a large scale. *Trends Genet.* 9, 17–22. doi: 10.1016/0168-9525(93)90067-R

Reichmann, N. T., Cassona, C. P., and Gründling, A. (2013). Revised mechanism of d-alanine incorporation into cell wall polymers in Gram-positive bacteria. *Microbiology* 159(Pt 9), 1868–1877. doi: 10.1099/mic.0.069898-0

Rice, K. C., Mann, E. E., Endres, J. L., Weiss, E. C., Cassat, J. E., Smeltzer, M. S., et al. (2007). The *cidA* murein hydrolase regulator contributes to DNA release and biofilm development in *Staphylococcus aureus*. *Proc. Natl. Acad. Sci. U.S.A.* 104, 8113–8118. doi: 10.1073/pnas.0610226104

Rieu, A., Aoudia, N., Jego, G., Chluba, J., Yousfi, N., Briandet, R., et al. (2014). The biofilm mode of life boosts the anti-inflammatory properties of *Lactobacillus*. *Cell Microbiol.* 16, 1836–1853. doi: 10.1111/cmi.12331

Sandberg, M., Määttänen, A., Peltonen, J., Vuorela, P. M., and Fallarero, A. (2008). Automating a 96-well microtitre plate model for *Staphylococcus aureus* biofilms: an approach to screening of natural antimicrobial compounds. *Int. J. Antimicrob. Agents* 32, 233–240. doi: 10.1016/j.ijantimicag.2008.04.022

Sanders, M. E., Guarner, F., Guerrant, R., Holt, P. R., Quigley, E. M., Sartor, R. B., et al. (2013). An update on the use and investigation of probiotics in health and disease. *Gut* 62, 787–796. doi: 10.1136/gutjnl-2012-302504

Santhanalakshmi, J., and Balaji, S. (2001). Binding studies of crystal violet on proteins. *Colloids Surf. A Physicochem. Eng. Asp.* 186, 173–177. doi: 10.1016/s0927-7757(00)00824-4

Savijoki, K., Lietzén, N., Kankainen, M., Alatossava, T., Koskenniemi, K., Varmanen, P., et al. (2011). Comparative proteome cataloging of *Lactobacillus rhamnosus* strains GG and Lc705. *J. Proteome Res.* 10, 3460–3473. doi: 10.1021/pr2000896

Siezen, R. J., and Wilson, G. (2010). Probiotics genomics. *Microb. Biotechnol.* 3, 1–9. doi: 10.1111/j.1751-7915.2009.00159.x

Son, S. H., Park, M. C., and Kim, S. (2014). Extracellular activities of aminoacyl-tRNA synthetases: new mediators for cell-cell communication. *Top Curr. Chem.* 344, 145–166. doi: 10.1007/128_2013_476

Sonnenburg, E. D., Sonnenburg, J. L., Manchester, J. K., Hansen, E. E., Chiang, H. C., and Gordon, I. (2006). A hybrid two-component system protein of a prominent human gut symbiont couples glycan sensing *in vivo* to carbohydrate metabolism. *Proc. Natl. Acad. Sci. U.S.A.* 103, 8834–8839. doi: 10.1073/pnas.0603249103

Spatafora, G. A., Sheets, M., June, R., Luyimbazi, D., Howard, K., Hulbert, R., et al. (1999). Regulated expression of the *Streptococcus mutans* dlt genes correlates with intracellular polysaccharide accumulation. *J. Bacteriol.* 181, 2363–2372.

Stoodley, P., Sauer, K., Davies, D. G., and Costerton, J. W. (2002). Biofilms as complex differentiated communities. *Annu. Rev. Microbiol.* 56, 187–209. doi: 10.1146/annurev.micro.56.012302.160705

Stothard, P. (2000). The sequence manipulation suite: javascript programs for analyzing and formatting protein and DNA sequences. *Biotechniques* 28, 1102–1104. doi: 10.2144/00286ir01

Townsend, G. E. II, Han, W., Schwalm, N. D. III, Raghavan, V., Barry, N. A., Goodman, A. L., et al. (2019). Dietary sugar silences a colonization factor in a mammalian gut symbiont. *Proc. Nat. Acad. Sci. U.S.A.* 116, 233–238. doi: 10.1073/pnas.1813780115

Trent, M. S., Stead, C. M., Tran, A. X., and Hankins, J. V. (2006). Diversity of endotoxin and its impact on pathogenesis. *J. Endotoxin Res.* 12, 205–223. doi: 10.1179/096805106X118825

Tytgat, H. L., Schoofs, G., Vanderleyden, J., Van Damme, E. J., Wattiez, R., Lebeer, S., et al. (2016). Systematic exploration of the glycoproteome of the beneficial gut isolate *Lactobacillus rhamnosus* GG. *J. Mol. Microbiol. Biotechnol.* 26, 345–358. doi: 10.1159/000447091

Varmanen, P., Vesanto, E., Steele, J. L., and Palva, A. (1994). Characterization and expression of the pepN gene encoding a general aminopeptidase from *Lactobacillus helveticus*. *FEMS Microbiol. Lett.* 124, 315–320. doi: 10.1016/0378-1097(94)00447-1

Velez, M. P., Petrova, M. I., Lebeer, S., Verhoeven, T. L., Claes, I., and Lambrichts, I. (2010). Characterization of MabA, a modulator of *Lactobacillus rhamnosus* GG adhesion and biofilm formation. *FEMS Immunol. Med. Microbiol.* 59, 386–398. doi: 10.1111/j.1574-695X.2010.00680.x

Vesterlund, S., Karp, M., Salminen, S., and Ouwehand, A. C. (2006). *Staphylococcus aureus* adheres to human intestinal mucus but can be displaced by certain lactic acid bacteria. *Microbiology* 152, 1819–1826. doi: 10.1099/mic.0.28522-0

von Ossowski, I., Satokari, R., Reunanen, J., Lebeer, S., De Keersmaecker, S. C. J., Vanderleyden, J., et al. (2011). Functional characterization of a mucus-specific LPXTG surface adhesin from probiotic *Lactobacillus rhamnosus* GG. *Appl. Environ. Microbiol.* 77, 4465–4472. doi: 10.1128/AEM.02497-10

Wang, W., and Jeffery, C. J. (2016). An analysis of surface proteomics results reveals novel candidates for intracellular/surface moonlighting proteins in bacteria. *Mol. Biosyst.* 12, 1420–1431. doi: 10.1039/c5mb00550g

Wei, R., Wang, J., Jia, E., Chen, T., Ni, Y., and Jia, W. (2018a). GSimp: a gibbs samples based left-censored missing value imputation approach for metabolomics studies. *PLoS Comput. Biol.* 14:e1005973. doi: 10.1371/journal.pcbi.1005973

Wei, R., Wang, J., Su, M., Jia, E., Chen, S., Chen, T., et al. (2018b). Missing value imputation approach for mass spectrometry-based metabolomics data. *Sci. Rep.* 8:663. doi: 10.1038/s41598-017-19120-0

Welch, K., Yanling, C., and Strømme, M. (2012). A method for quantative determination of biofilm viability. *J. Funct. Biomater.* 3, 3418–3431.

Yu, Y., Wagner, J. R., Laird, M. R., Melli, G., Rey, S., Lo, R., et al. (2010). PSORTb 3.0: improved protein subcellular localization prediction with refined localization subcategories and predictive capabilities for all prokaryotes. *Bioinformatics* 26, 1608–1615. doi: 10.1093/bioinformatics/btq249

Conflict of Interest Statement: The authors declare that the research was conducted in the absence of any commercial or financial relationships that could be construed as a potential conflict of interest.

frontiers in Nutrition

ORIGINAL RESEARCH
published: 10 December 2018
doi: 10.3389/fnut.2018.00124

Proteolytic Surface-Shaving and Serotype-Dependent Expression of SPI-1 Invasion Proteins in *Salmonella enterica* Subspecies *enterica*

Clifton K. Fagerquist and William J. Zaragoza*

Produce Safety & Microbiology Research Unit, Western Regional Research Center, Agricultural Research Service, U.S. Department of Agriculture, Albany, CA, United States

We performed proteolytic surface-shaving with trypsin on three strains/sevovars of *Salmonella enterica enterica* (SEE): Newport, Kentucky, and Thompson. Surfaced-exposed proteins of live bacterial cells were digested for 15 min. A separate 20 h re-digestion was also performed on the supernatant of each shaving experiment to more completely digest protein fragments into detectable peptides for proteomic analysis by nano-liquid chromatography-electrospray ionization-Orbitrap mass spectrometry. Control samples (i.e., no trypsin during surface-shaving step) were also performed in parallel. We detected peptides of flagella proteins: FliC (filament), FliD (cap), and FlgL (hook-filament junction) as well as peptides of FlgM (anti-σ^{28} factor), i.e., the negative regulator of flagella synthesis. For SEE Newport and Thompson, we detected *Salmonella* pathogenicity island 1 (SPI-1) secreted effector/invasion proteins: SipA, SipB, SipC, and SipD, whereas no Sip proteins were detected in control samples. No Sip proteins were detected for SEE Kentucky (or its control) although *sip* genes were confirmed to be present. Our results may suggest a biological response (<15 min) to proteolysis of live cells for these SEE strains and, in the case of Newport and Thompson, a possible invasion response.

Keywords: *Salmonella enterica enterica*, surface-shaving, proteolysis, trypsin, pathogenicity island 1, nano-electrospray ionization, Orbitrap mass spectrometry, flagella

OPEN ACCESS

Edited by:
Sergio Uzzau, University of Sassari, Italy

Reviewed by:
Chyer Kim, Virginia State University, United States
Karl Matthews, Rutgers University, The State University of New Jersey, United States

****Correspondence:***
Clifton K. Fagerquist
clifton.fagerquist@ars.usda.gov

Specialty section:
This article was submitted to Food Microbiology, a section of the journal Frontiers in Nutrition

Received: *10 September 2018*
Accepted: *23 November 2018*
Published: *10 December 2018*

Citation:
Fagerquist CK and Zaragoza WJ (2018) Proteolytic Surface-Shaving and Serotype-Dependent Expression of SPI-1 Invasion Proteins in Salmonella enterica Subspecies enterica. Front. Nutr. 5:124. doi: 10.3389/fnut.2018.00124

INTRODUCTION

Bacterial *surface-shaving* is a technique by which surface-exposed biomolecules (usually proteins) are cleaved from the surface of live cells with proteolytic enzymes, e.g., trypsin, followed by detection by liquid chromatography tandem mass spectrometry (LC/MS/MS) (1–3). A majority of the surface-shaving experiments have been performed on Gram-positive bacteria (1–15). It was reasoned that the peptidoglycan cell wall of Gram-positive bacteria, having greater structural rigidity, would be less likely to rupture during proteolysis than the outer (and inner) membranes of Gram-negative bacteria. Cellular rupture contaminates the sample with cytoplasmic proteins complicating data analysis making it more difficult to assess which proteins are truly surface-exposed. As a certain amount of cell lysis is unavoidable during a shaving experiment, attempts to minimize its occurrence involved primarily reducing the proteolysis time as much as

possible, e.g., 15 min (2). Despite the lack of a cell wall, surface-shaving has been performed on a number of Gram-negative bacteria with mixed success (16–21).

In an early work, Grandi and co-workers demonstrated the surface-shaving technique on group A *Streptococcus* (a Gram-positive microorganism) in order to identify new vaccine targets (1). In addition to proteolytic surface-shaving, this influential paper used liquid chromatography tandem mass spectrometry (LC/MS/MS) to detect and identify peptides and their respective proteins by comparison to a proteomic database derived from a genomically sequenced *S. pyogenes* strain (SF370). In addition, proteins identified as surface or surface-associated were analyzed with *in silico* prediction software [e.g., PSORT(22, 23)] to confirm whether the peptides identified by LC/MS/MS were predicted to be surface-exposed. By this approach, new potential vaccine targets were identified.

Trypsin has been the proteolytic enzyme of choice for bottom-up proteomic experiments because it cleaves on the C-terminal side of basic residues: arginine (R) and lysine (K). It has been used to digest proteins in solution as well as in-gel. When ionized by electrospray ionization (ESI) (24) or nano-ESI, (25) tryptic-generated peptides will sequester an ionizing proton at the C-terminal basic residue which, for all practical purposes, is immobilized. Additional ionizing protons will occupy other basic residues (if present due to a missed cleavage) or at the N-terminus or along peptide backbone. During vibrational excitation, e.g., collision-induced dissociation (CID), (26) these additional protons "hop" along the peptide backbone causing fragmentation and resulting in an easily interpretable MS/MS spectrum (27).

Trypsin has been used in many (although not all) surface-shaving experiments primarily because the analysis is LC-ESI/MS/MS. However, trypsin has drawbacks for surface-shaving primarily because the target proteins are often embedded in the outer membrane or cell wall and may not have cleavage sites that are easily accessible even for the protein region that is exposed on the bacterial surface. In consequence, the number of peptides identified from trypsin surface-shaving may be quite limited. To address this issue, other proteolytic enzymes have been utilized that cleave at sites other basic residues, e.g., proteinase K (cleavage at aliphatic and aromatic residues), chymotrypsin, etc. However, the difficulty of cleaving at sites other than at basic residues is that the peptides generated may not fragment efficiently by CID and generate MS/MS spectra that are as easily interpretable compared to MS/MS of tryptic-generated peptides.

Another issue that was noted in early surface-shaving experiments is that the short digestion time (∼15–30 min) used in order to minimize cell lysis and contamination with cytoplasmic proteins may result in large protein fragments that may not fragment efficiently by MS/MS. In consequence, a re-digestion step was incorporated in which the supernatant containing peptides and protein fragments from a surface-shaving experiment were digested for a much longer period of time (e.g., 20 h). Implementation of this insight increased the number of identifiable peptides and proteins (3, 12).

Salmonella enterica subspecies *enterica* (SEE) is a Gram-negative human pathogen often associated with outbreaks of foodborne illness. There are over 2,500 different serovars of SEE, and pathogenicity and virulence across serovars (and even strains) can vary considerably. There have been very few experiments analyzing the surface-exposed biomolecules of SEE (19). In the current study, we examined three serovars/strains of SEE (Newport, Kentucky, and Thompson) by surface-shaving with trypsin. We chose these particular serovars/strains from our strain collection because each has some relevance to food safety or were associated with a foodborne outbreak. Although a number of surface-associated proteins were identified, we also observed significant proteolytic cleavage of flagella proteins as well as a secreted protein that is a negative regulator of flagella biosynthesis as well as SPI-1 invasion/effector proteins in the case of Newport and Thompson serovars. Our results may suggest an unusually rapid response (<15 min) of these pathogens to proteolytic damage of their flagella perhaps triggering a virulence response.

TABLE 1 | Strains used in this study.

Strain	Description	Source
RM1655	*Salmonella enterica* subspecies *enterica serovar* Newport	Greg Inami (CA State Health Lab, Berkeley). Strain isolated from alfalfa seeds responsible for an outbreak of S. Newport (28, 29).
RM7890	*Salmonella enterica* subspecies *enterica serovar* Kentucky	Isolated from ground chicken by Food Safety & Inspection Service, USDA (Alameda, CA)
RM1987	*Salmonella enterica* subspecies *enterica serovar* Thompson	Sharon Abbott (CADHS). Human isolate putatively part of an outbreak due to contaminated cilantro, epidemiologically linked to Cilantro.

EXPERIMENTAL SECTION

Culture Conditions

Strains utilized in this study are shown in **Table 1** (28, 29). Strains were inoculated from glycerol stocks into LB broth and incubated overnight at 37°C with 200 rpm agitation. The following morning, 5 μL of overnight culture was sub-cultured into 5 mL of fresh LB broth and incubated until mid-log phase ($OD_{600} \approx 0.4$). Cells were then harvested for the surface-shaving experiment.

Cell Preparation

Cells were removed from the incubator at mid-log phase and quenched on ice for 5 min. A 1 mL aliquot of cells was transferred to sterile 1.5 mL snap-cap tubes and centrifuged at 1,400 rpm for 15 min at 4°C. The broth media was discarded and the cells were suspended in 1 mL of sterile, ice-cold 1x phosphate buffered saline (PBS) and centrifuged at 1,400 rpm for 15 min. The PBS was discarded and the cells were suspended in 1 mL of 1x PBS to which was added 2 μg of modified, sequencing grade porcine trypsin (Product # V5111, Promega, Madison,WI). As a control, a 1 mL aliquot of cells were similarly pelleted by centrifugation, washed and re-suspended in 1 mL of 1x PBS but *without* trypsin.

Proteolytic Surface-Shaving

Cell samples with trypsin and *without* trypsin (control) were incubated for 15 min at 37°C and 75 rpm. Cells were then centrifuged at 13,000 rpm for 5 min. The resulting supernatant of both samples were collected separately, filtered through a 0.2 μm filter (Millipore) to remove cells and partitioned into two equal 0.5 mL aliquots. One trypsin surface-shaving aliquot was diluted with 0.5 mL of 1x PBS, filtered through a 10 kDa MWCO spin filter (VWA) with centrifugation at 14,000 g for 10 min to remove trypsin. The eluent was transferred to an HPLC vial and stored at −20°C for subsequent analysis. The other trypsin surface-shaving aliquot was diluted with 0.5 mL in 1x PBS to which was added 2 μg of trypsin, and the sample was incubated for 20 h at 37°C at 75 rpm. This re-digested sample was then filtered with a 10 kDa MWCO spin filter to remove trypsin and transferred to an HPLC vial and stored at −20°C for subsequent analysis.

The 0.2 μm filtered supernatants of cell samples that underwent "surface-shaving" in the *absence* of trypsin were also separated into two equal 0.5 mL aliquots. One aliquot was diluted with 0.5 mL of 1x PBS to which was added 2 μg of trypsin. The sample was incubated for 15 min at 37°C at 75 rpm and filtered through a 10 kDa MWCO spin filter with centrifugation at 14,000 g for 10 min. The eluent was transferred to an HPLC vial and stored at −20°C for subsequent analysis. The other aliquot was diluted with 0.5 mL of 1x PBS to which was added 2 μg of trypsin. This sample was incubated for 20 h at 37°C and 75 rpm and was filtered through a 10 kDa MWCO spin filter with centrifugation at 14,000 g for 10 min. The eluent was transferred to an HPLC vial and stored at −20°C for subsequent analysis.

Nano-Liquid Chromatography-Tandem Mass Spectrometry (nano-LC-MS/MS)

Samples were analyzed using a nano-LC system (Tempo™, nano MDLC, Applied Biosystems/Eksigent) with a PicoSlide nano-electrospray (nano-ESI, 3 column set-up) ion source (New Objective, Woburn, MA) coupled to a hybrid LTQ-Orbitrap Elite mass spectrometer (Thermo Fisher Scientific, San Jose, CA). An 8–10 μL aliquot of sample was loaded onto a 20 μL stainless steel loop using an Ultra-Plus II autosampler (Micro-Tech Scientific). The sample slug was then transferred to a one of the three PicoChip columns (C18-AQ, 3 μm, 120 Å, 105 mm, New Objective) at a flow rate of 400 nL/min using a NanoEasy n-LC II (Thermo Scientific) HPLC. The loading solution was 5% acetonitrile, 95% water, and 0.1% formic acid. Sample was eluted from the column at flow rate of 400 nL/min using the following gradient: 0.0 to 58.0 min, A: 98 to 70%, respectively, followed by 58.0 to 58.5 min, A: 70 to 98%, respectively, followed by 58.5 to 60.0 min, A: 98 to 98%. Buffer A was 0.1% formic acid in HPLC grade water (Optima® LC/MS grade, Fisher Chemical). Buffer B was 0.1% formic acid in HPLC grade acetonitrile (Optima® LC/MS grade, Fisher Chemical). After column elution, the next loaded column was automatically moved in-line for elution and mass spectrometry analysis. The recently eluted column was automatically moved out of alignment with the mass spectrometer and was subjected to a series of four fast ramping sawtooth washing cycles from high-to-low organic (90 to 10%).

ESI voltage was 2.5 kV. A heated metal capillary at 250°C was used for ESI desolvation. No sheath or auxiliary gas was used. A data dependent analysis was performed using a FTMS scan range of *m/z* 400–2,000 at a resolution 60,000 in profile mode using the Orbitrap mass analyzer. The top 10 putative peptide ions were selected from the MS survey scan on the basis of charge state (+2, +3, +4) and signal intensity for collision-induced dissociation (CID) tandem mass spectrometry (MS/MS) in the linear trap. MS/MS (Data type: centroid) was performed with a minimum signal threshold: 30,000; isolation width (*m/z*): 2.0; normalized collision energy: 35.0; activation Q: 0.250 and activation time (ms): 30.

Prior to and after analysis of *Salmonella* surface-shaving samples, the retention time of the LC and the mass spectrometry calibration of the instrument system were tested with a 200 fmol injection of a bovine serum albumin (BSA) digest. BSA tryptic peptides started eluting ∼12 min. The root-mean-square (rms) error of the precursor ion *m/z* was below 10 ppm as calculated by the search engine. Three technical replicates were performed on all surface-shaving samples and control samples, and two biological replicates were performed on different days.

Bioinformatics and Proteomic Analysis

Three databases were constructed for proteomic searches. The SEE Newport database consists of 347,185 protein sequences from 148 genomes downloaded from NCBI non-redundant protein database. The SEE Kentucky database was consists 452,644 protein sequences from 14 genomes. The SEE Thompson database is comprised 63,971 protein sequences from 8 genomes.

Raw MS and MS/MS data files (Xcalibur) were extracted and converted to.mgf files using the MSConvert (ProteoWizard). Database searches were performed with Mascot v2.2.04 (Matrix Science, London, UK). Searches were conducted using a fragment mass tolerance of 0.40 Da and peptide mass tolerance of 20.0 ppm. Trypsin was specified as the enzyme. Searches allowed a maximum of 3 missed cleavages and methionine oxidation was set as a variable modification.

Supplementary Materials

Raw Mascot proteomic identifications are provided in the Supplementary Materials file. This data is organized by SEE serovar, biological and technical replicates of both samples and their corresponding control samples. For each analysis, protein identifications that are highlighted in yellow are summarized in **Tables 2–4** of the manuscript (excluding cytoplasmic proteins which are the result of cell lysis during surface shaving).

Polymerase Chain Reaction (PCR)

PCR was used to verify the presence of the *sip* operon and *hilA* in *SEE* Kentucky. PCR was carried out on a Tetrad 2 (Bio-Rad, Hercules, CA) using colonies of *SEE* Kentucky with the primers listed in **Data Sheet 1** (**Supplementary Materials** Kentucky, page 65) under the following conditions: an initial denaturation step was at 94°C for 10 min followed by 29 cycles at 94°C for 30 s, 53°C for 30 s, and 72°C for 2 min with a final elongation cycle at 72°C for 7 min. PCR products were analyzed

TABLE 2 | Summary of surface-shaving of SEE Newport.

				Day 1						Day 2							
				Mascot scores			Number of peptides			Mascot scores			Number of peptides				
Accession number	**Protein description**	**MW (Da)**	**AA**	**1st**	**2nd**	**3rd**	**1st**	**2nd**	**3rd**	**1st**	**2nd**	**3rd**	**1st**	**2nd**	**3rd**		
NEWPORT 15 MIN																	
gi|50830890|gb|AAT81610.1|	Phase 1 flagellin, **FliC** [Salmonella enterica subsp. enterica serovar Newport]	52,223	502	136	78		3	2		388	267	429	3	3	3		
gi|459466347|gb|EMG61125.1|	Flagellar biosynthesis protein **FliC**, partial [Salmonella enterica subsp. enterica serovar Newport str. SH111077]	8447	79	136			3										
gi|194401173|gb|ACF61395.1|	Flagellar hook-associated protein 2 (HAP2), **FliD** [Salmonella enterica subsp. enterica serovar Newport str. SL254]	49,778	467							159	280	358	1	2	2		
gi|194404219|gb|ACF64441.1|	Flagellar hook-associated protein 3 (HAP3), **FlgL** [Salmonella enterica subsp. enterica serovar Newport str. SL254]	34,155	317	88		25	2		1	47			1				
gi|194403331|gb|ACF63553.1|	Negative regulator of flagellin synthesis, **FlgM** [Salmonella enterica subsp. enterica serovar Newport str. SL254]	10,561	97	188		127	1		2	209	244	337	3	2	3		
gi|194402702|gb|ACF62924.1|	Cell invasion protein **SipA** [Salmonella enterica subsp. enterica serovar Newport str. SL254]	72,333	670	89	67	62	2	2	2	299	242	254	5	3	4		
gi|194403640|gb|ACF63862.1|	Cell invasion protein **SipB** [Salmonella enterica subsp. enterica serovar Newport str. SL254]	62,382	593	66	103	64	2	5	2	112	59	105	3	2	2		
gi|392616945|gb|EIW99373.1|	Pathogenicity island 1 effector protein **SipC** [Salmonella enterica subsp. enterica serovar Newport str. Levine 15]	42,957	409	332	196	219	6	4	4	289	256	308	5	2	4		
gi|392616944|gb|EIW99372.1|	Cell invasion protein **SipD** [Salmonella enterica subsp. enterica serovar Newport str. Levine 15]	37,081	343	192		85	1		1	225	195	236	2	2	1		
gi|392765192|gb|EJA21981.1|	Phage immunity repressor protein [Salmonella enterica subsp. enterica serovar Newport str. CVM 19449]	21,776	196	20			1										
							21	13	12				23	16	19	104	Total
NEWPORT 20 H																	
gi|50830890|gb|AAT81610.1|	Phase 1 flagellin, **FliC** [Salmonella enterica subsp. enterica serovar Newport]	52,223	502	499	613	222	6	9	5	331	170	419	3	2	3		
gi|874404664|gb|KMU13862.1|	Flagellin **FliC** [Salmonella enterica subsp. enterica serovar Newport str. DC_10-446]	34,557	337		117			5									
gi|194401173|gb|ACF61395.1|	Flagellar hook-associated protein 2 (HAP2), **FliD** [Salmonella enterica subsp. enterica serovar Newport str. SL254]	49,778	467							89	191		1	1			
gi|194404219|gb|ACF64441.1|	Flagellar hook-associated protein 3 (HAP3), **FlgL** [Salmonella enterica subsp. enterica serovar Newport str. SL254]	34,155	317	112	48		2	1		41	32		1	1			
gi|194403331|gb|ACF63553.1|	Negative regulator of flagellin synthesis, **FlgM** [Salmonella enterica subsp. enterica serovar Newport str. SL254]	10,561	97	314	198	305	3	1	4	145	262	347	3	4	4		
gi|194402702|gb|ACF62924.1|	Cell invasion protein **SipA** [Salmonella enterica subsp. enterica serovar Newport str. SL254]	72,333	670	173	221	123	3	4	3	476	531	237	7	5	4		
gi|194403640|gb|ACF63862.1|	Cell invasion protein **SipB** [Salmonella enterica subsp. enterica serovar Newport str. SL254]	62,382	593	55	101	53	3	3	2	54			2				
gi|392616945|gb|EIW99373.1|	Pathogenicity island 1 effector protein **SipC** [Salmonella enterica subsp. enterica serovar Newport str. Levine 15]	42,957	409	662	587	354	9	6	5	262	216	380	5	2	3		

(Continued)

TABLE 2 | Continued

Accession number	Protein description	MW (Da)	AA	Day 1						Day 2					
				Mascot scores			Number of peptides			Mascot scores			Number of peptides		
				1st	2nd	3rd	1st	2nd	3rd	1st	2nd	3rd	1st	2nd	3rd
gi|392616944|gb|EIW99372.1|	Cell invasion protein **SipD** [Salmonella enterica subsp. enterica serovar Newport str. Levine 15]	37,081	343			111			1	139	214	189	1	1	1
gi|392742504|gb|EIZ99592.1|	Phage regulatory protein [Salmonella enterica subsp. enterica serovar Newport str. CVM 35199]	9236	80								21			1	
							26	29	20				23	18	15
CONTROL NEWPORT 15 MIN															131
															Total
CONTROL NEWPORT 20 H															
gi|392765192|gb|EJA21981.1|	Phage immunity repressor protein [Salmonella enterica subsp. enterica serovar Newport str. CVM 19449]	21,776	196		21			1							
								1							1
															Total

by gel electrophoresis and imaged using a GelDoc XR (Biorad, Hercules, CA).

RESULTS AND DISCUSSION

Salmonella enterica Subspecies *enterica* (SEE) Serovar Newport

Table 2 summarizes the results of 15 min surface-shaving experiment (and 20 h re-digestion) of SEE Newport strain RM1655 and their controls. Both the MASCOT identification scores and the corresponding number of peptides identified are reported for three technical replicates. In addition, two biological replicates were performed on different days. More detailed proteomic information on peptide/protein identifications (including any cytoplasmic proteins detected) is provided in **Supplementary Materials** Newport (pages 1-64). **Table 2** shows a number of tryptic peptide identifications corresponding to cleavage of flagella proteins (FliC, FliD, FlgL) in both the 15 min experiment as well as the 20 h re-digestion. We observe an overall increase in the number of peptides detected in the 20 h re-digestion (131) compared with the 15 min surface-shaving (104) as one might expect given the fact that the 15 min experiment may produce protein fragments too large to be detected by MS/MS, whereas the 20 h re-digestion allows greater time for large protein fragments to be enzymatically cleaved into smaller, more detectable peptides.

Phase 1 flagellin (FliC) is the most abundant of the flagella proteins with approximately 30,000 proteins per flagella (and 5-10 flagella per cell), and it is the primary structural constituent of the filament that extends into the extracellular space (30, 31). As such, this protein is not only abundant but also highly accessible to proteolytic degradation. Not surprising, we detect the highest number of peptides for this protein. **Figure 1** (**top panel**) shows the peptide sequence coverage for FliC. Peptide sequence coverage is highlighted in bold red. The N-terminal (5-143) and C-terminal (416-501) helical domains are underlined and the D3 (196-282) domain is in bold, black. It is interesting that the D3 domain has a total of eight basic residues (eight lysines), but no peptides were detected in this domain. **Figure 2** shows the 3-D image of FliC of *S. enterica* based on X-ray crystallographic structure from Protein Data Bank (Entry: 3A5X) (32) and viewed in PyMOL. The corresponding peptide sequence coverage is highlighted in red and specific peptides highlighted in white. Specific domains (D0, D1, D2, D3) are also indicated. Although the D3 domain is probably the most accessible of all the domains of FliC, it has a somewhat globular tertiary structure which may inhibit proteolysis even as part of a larger protein fragment. Interestingly, many (although not all) of the peptides detected appear to be located within secondary helical structures in the D2, D1, and D0 domains. This may suggest that, in the absence of denaturants, trypsin may favor cleavage of the polypeptide backbone at basic residues within alpha-helices. The toll-like receptor 5 region (TLR5) responsible for the innate immune response in eukaryotic cells (33, 34) is present in the upper half of the D1 domain which has three, nearly parallel alpha-helices (shown in **Figure 2**). The fact that we

TABLE 3 | Summary of surface-shaving of SEE Kentucky.

				Day 1						Day 2							
				Mascot scores			Number of peptides			Mascot scores			Number of peptides				
Accession number	**Protein description**	**MW (Da)**	**AA**	**1st**	**2nd**	**3rd**	**1st**	**2nd**	**3rd**	**1st**	**2nd**	**3rd**	**1st**	**2nd**	**3rd**		
KENTUCKY 15 MIN																	
gi|969071361|gb|KUB03511.1|	Flagellin **FliC** [Salmonella enterica subsp. enterica serovar Kentucky]	52,225	502	127	103		3	3		154	105	183	4	3	4		
gi|983253333|gb|KWU90600.1|	Flagellin **FliC** [Salmonella enterica subsp. enterica serovar Kentucky]	51,683	495									158			3		
gi|148644991|gb|ABR01027.1|	Phase 2 flagellin **FljB**, partial [Salmonella enterica subsp. enterica serovar Kentucky]	52,459	500		103			3									
gi|194455642|gb|EDX44481.1|	Flagellar hook-associated protein 3 (HAP3) **FlgL** [Salmonella enterica subsp. enterica serovar Kentucky str. CVM29188]	34,155	317		15			1		42	52	45	2	3	3		
gi|194456320|gb|EDX45159.1|	Negative regulator of flagellin synthesis, **FlgM** [Salmonella enterica subsp. enterica serovar Kentucky str. CVM29188]	10,561	97	183	100	116	2	2	2	69	302	123	3	5	5		
gi|194455511|gb|EDX44350.1|	Major outer membrane lipoprotein [Salmonella enterica subsp. enterica serovar Kentucky str. CVM29188]	8386	78								96			2			
gi|969072264|gb|KUB04403.1|	Major outer membrane lipoprotein 2 [Salmonella enterica subsp. enterica serovar Kentucky]	8531	80							39			3				
							5	9	2				12	13	15	56	Total
KENTUCKY 20 H																	
gi|148644993|gb|ABR01028.1|	Phase 1 flagellin **FliC**, partial [Salmonella enterica subsp. enterica serovar Kentucky]	51,551	495								456			7			
gi|969071361|gb|KUB03511.1|	Flagellin **FliC** [Salmonella enterica subsp. enterica serovar Kentucky]	52,225	502	333	353		6	6		200	430	121	5	7	3		
gi|983253333|gb|KWU90600.1|	Flagellin **FliC** [Salmonella enterica subsp. enterica serovar Kentucky]	51,683	495								326			7			
gi|115381392|gb|ABI96378.1|	Phase 2 flagellin **FljB**, partial [Salmonella enterica subsp. enterica serovar Kentucky]	48,340	462			49			1								
gi|194455957|gb|EDX44796.1|	Flagellar hook-associated protein 2 (HAP2), **FliD** [Salmonella enterica subsp. enterica serovar Kentucky str. CVM29188]	49,778	467								176			3			
gi|194455642|gb|EDX44481.1|	Flagellar hook-associated protein 3 (HAP3), **FlgL** [Salmonella enterica subsp. enterica serovar Kentucky str. CVM29188]	34,155	317	36	91		1	3		63	45	25	3	2	1		
gi|194456320|gb|EDX45159.1|	Negative regulator of flagellin synthesis **FlgM** [Salmonella enterica subsp. enterica serovar Kentucky str. CVM29188]	10,561	97	299	355	190	4	5	3	77	546	59	2	4	2		
gi|553491170|gb|ESC15085.1|	Anti-sigma28 factor **FlgM** [Salmonella enterica subsp. enterica serovar Kentucky str. 0253]	10,577	97	235	277	175	4	5	3								
gi|194459234|gb|EDX48073.1|	Outer membrane protein A [Salmonella enterica subsp. enterica serovar Kentucky str. CVM29188]	40,058	371								27			1			
gi|444820129|gb|ELX47576.1|	Tail fiber domain protein [Salmonella enterica subsp. enterica serovar Kentucky str. 29439]	35,445	332	21	18		1	1									
							16	20	7				10	31	6	90	Total

(Continued)

TABLE 3 | Continued

Accession number	Protein description	MW (Da)	AA	Day 1 Mascot scores 1st	Day 1 Mascot scores 2nd	Day 1 Mascot scores 3rd	Day 1 Number of peptides 1st	Day 1 Number of peptides 2nd	Day 1 Number of peptides 3rd	Day 2 Mascot scores 1st	Day 2 Mascot scores 2nd	Day 2 Mascot scores 3rd	Day 2 Number of peptides 1st	Day 2 Number of peptides 2nd	Day 2 Number of peptides 3rd	
CONTROL KENTUCKY 15 MIN																
gi|554231997|gb|ESG69366.1|	Outer membrane protein [Salmonella enterica subsp. enterica serovar Kentucky str. ATCC 9263]	27,757	252		15			1								
								1							1	Total
CONTROL KENTUCKY 20 H																
gi|44820129|gb|ELX47576.1|	Tail fiber domain protein [Salmonella enterica subsp. enterica serovar Kentucky str. 29439]	35,445	332	18	21	18	1	1	1							
gi|115381392|gb|ABI96378.1|	Phase 2 flagellin **FljB**, partial [Salmonella enterica subsp. enterica serovar Kentucky]	48,340	462								21	39		1	2	
gi|969071361|gb|KUB03511.1|	Flagellin **FliC** [Salmonella enterica subsp. enterica serovar Kentucky]	52,225	502									39			2	
gi|969072435|gb|KUB04565.1|	Flagellin **FliC** [Salmonella enterica subsp. enterica serovar Kentucky]	52,690	506									39			2	
							1	1	1				1	6	10	Total

detect peptides in two of the three helices is consistent with the accessibility of this region.

We also observe a few peptides of FliD (also called HAP2) which functions as the "cap" of the filament as well as FlgL (also called HAP3) which is critical at the junction between the filament and the hook. From a stoichiometric point-of-view, these proteins are significantly less abundant than FliC, so it is not surprising that the number of peptides identified are fewer. However, it is not simply the abundance of the protein but the accessibility of its trypsin cleavable sites that is critical.

The facile detection of flagellin tryptic peptides from this strain of SEE Newport suggest a robust number of flagellin filament structures. Interestingly, we also detected peptides of the negative regulator of flagellin synthesis or FlgM an anti-σ^{28} factor. FlgM is a secreted protein and its secretion is concomitant with up-regulation of flagellin biosynthesis noted by other researchers in *Salmonella typhimurium*, *Escherichia coli* and *Bacillus subtilis* (35–39). The very strong identification of FlgM (nearly 50% coverage in several analyses) suggests that this protein is highly abundant.

We also identified a number of effector proteins associated with pathogen virulence whose genes are located on pathogenicity island 1 (SPI-1): SipA, SipB, SipC, and SipD. SipA-D are also secreted proteins, and their abundance is high and reproducible as evidenced by the number of tryptic peptides identified in both the 15 min and the 20 h re-digestion analyses. This result is striking as the secretion of effector proteins is to facilitate the invasion of eukaryotic cells even though no eukaryotic cells were present in the sample. The fact that SipA-D appear to be strongly expressed as a result of trypsin proteolysis may suggest that, along with secretion of FlgM, genes related to virulence and invasion may also be activated and their protein products secreted.

Surface-shaving experiments are often accompanied with a certain amount of cell lysis caused by degradation of surface structures that weaken the cell membrane resulting in cell rupture and contamination of the sample with cytoplasmic proteins, e.g., ribosomal proteins. We detect some ribosomal and other cytoplasmic proteins, including one of the most abundant cytoplasmic proteins, i.e., elongation factor Tu (40) (shown in **Supplementary Materials** Newport, pages 1-65) which suggests a small amount of cell lysis in these experiments.

In parallel, analyses were also performed on control samples, i.e., no trypsin during the 15 min surface-shaving step (**Table 2** and **Supplementary Materials** Newport). In these samples, we did *not* observe any flagella proteins or FlgM or SPI-1 proteins. In addition, we observed very little evidence of cell lysis based upon detection of only a few peptides of cytoplasmic proteins.

The type III secretion system is responsible for flagellin biosynthesis, (36) but it is not clear the mechanism by which SEE Newport would "sense" damage to its flagella. It is possible that tryptic peptides of the flagellin filament are detected by receptors on its surface that signal to the pathogen the presence of damaging proteases in the extracellular milieu. Alternatively, proteolytic damage of the hook-filament junction (a critical structural junction) may result in impaired flagellin

TABLE 4 | Summary of surface-shaving of SEE Thompson.

				Day 1						Day 2							
				Mascot scores			Number of peptides			Mascot scores			Number of peptides				
Accession number	**Protein description**	**MW (Da)**	**AA**	**1st**	**2nd**	**3rd**	**1st**	**2nd**	**3rd**	**1st**	**2nd**	**3rd**	**1st**	**2nd**	**3rd**		
THOMPSON 15 MIN																	
gi|50830928|gb|AAT81629.1|	Phase 1 flagellin **FliC** [Salmonella enterica subsp. enterica serovar Thompson]	51,467	495	181	150		2	2									
gi|548714623|gb|AGX10263.1|	Flagellar hook-associated protein **FlgL** [Salmonella enterica subsp. enterica serovar Thompson str. RM6836]	34,155	317	68	51	33	2	1	1								
gi|548714611|gb|AGX10251.1|	Anti-sigma28 factor **FlgM** [Salmonella enterica subsp. enterica serovar Thompson str. RM6836]	10,561	97			77			1								
gi|548715882|gb|AGX11522.1|	Pathogenicity island 1 effector protein **SipA** [Salmonella enterica subsp. enterica serovar Thompson str. RM6836]	73,927	685	84	63		1	1		59			1				
gi|548715885|gb|AGX11525.1|	Pathogenicity island 1 effector protein **SipB** [Salmonella enterica subsp. enterica serovar Thompson str. RM6836]	62,412	593	117	239	151	5	6	4								
gi|548715884|gb|AGX11524.1|	Pathogenicity island 1 effector protein **SipC** [Salmonella enterica subsp. enterica serovar Thompson str. RM6836]	42,957	409	256	278	232	4	3	4	46	54	108	1	1	2		
gi|548715883|gb|AGX11523.1|	Cell invasion protein **SipD** [Salmonella enterica subsp. enterica serovar Thompson str. RM6836]	37,081	343							28			1				
gi|548714481|gb|AGX10121.1|	Enterohemolysin [Salmonella enterica subsp. enterica serovar Thompson str. RM6836]	40,698	369	134	119		2	2		39	84		2	1			
gi|548714507|gb|AGX10147.1|	Tail protein [Salmonella enterica subsp. enterica serovar Thompson str. RM6836]	112,007	1031	71	61	59	1	1	1								
gi|808222093|gb|KKD68276.1|	Tail protein [Salmonella enterica subsp. enterica serovar Thompson]	84,119	834			115			2								
gi|548714496|gb|AGX10136.1|	Head-tail joining protein [Salmonella enterica subsp. enterica serovar Thompson str. RM6836]	7380	67							99	48		1	1			
gi|548714499|gb|AGX10139.1|	Head decoration protein [Salmonella enterica subsp. enterica serovar Thompson str. RM6836]	11,916	115	19			1			76	115	91	2	2	2		
							18	16	13				8	5	4	64	Total
THOMPSON 20 H																	
gi|50830928|gb|AAT81629.1|	Phase 1 flagellin **FliC** [Salmonella enterica subsp. enterica serovar Thompson]	51,467	495			505			7	79	83	123	2	1	1		
gi|548715793|gb|AGX11433.1|	Flagellin **FliC** [Salmonella enterica subsp. enterica serovar Thompson str. RM6836]	52,487	506	1034	966		9	8									
gi|548714623|gb|AGX10263.1|	Flagellar hook-associated protein **FlgL** [Salmonella enterica subsp. enterica serovar Thompson str. RM6836]	34,155	317	62		34	1		1								
gi|548714611|gb|AGX10251.1|	Anti-sigma28 factor **FlgM** [Salmonella enterica subsp. enterica serovar Thompson str. RM6836]	10,561	97	60			1										
gi|548715882|gb|AGX11522.1|	Pathogenicity island 1 effector protein **SipA** [Salmonella enterica subsp. enterica serovar Thompson str. RM6836]	73,927	685	136	112	78	2	3	1		200			3			
gi|548715885|gb|AGX11525.1|	Pathogenicity island 1 effector protein **SipB** [Salmonella enterica subsp. enterica serovar Thompson str. RM6836]	62,412	593	72	107	107	3	3	2								

(Continued)

TABLE 4 | Continued

				Day 1						Day 2							
				Mascot scores			Number of peptides			Mascot scores			Number of peptides				
Accession number	**Protein description**	**MW (Da)**	**AA**	**1st**	**2nd**	**3rd**	**1st**	**2nd**	**3rd**	**1st**	**2nd**	**3rd**	**1st**	**2nd**	**3rd**		
gi|548715884|gb|AGX11524.1|	Pathogenicity island 1 effector protein **SipC** [Salmonella enterica subsp. enterica serovar Thompson str. RM6836]	42,957	409	567	480	350	6	5	6	48	178	281	1	3	3		
gi|548714481|gb|AGX10121.1|	Enterohemolysin [Salmonella enterica subsp. enterica serovar Thompson str. RM6836]	40,698	369	262	236	69	3	5	3	54	47		2	2			
gi|808222093|gb|KKD68276.1|	Tail protein [Salmonella enterica subsp. enterica serovar Thompson]	84,119	834	201	249	255	1	2	4	49	35		1	1			
gi|548714507|gb|AGX10147.1|	Tail protein [Salmonella enterica subsp. enterica serovar Thompson]	112,007	1031		43	40		1	1								
gi|548714105|gb|AGX09745.1|	Trigger factor [Salmonella enterica subsp. enterica serovar Thompson str. RM6836]																
gi|548714505|gb|AGX10145.1|	Minor tail protein [Salmonella enterica subsp. enterica serovar Thompson str. RM6836]	14,833	131	84	54	43	1	1	1	64	142	128	2	2	2		
gi|548716337|gb|AGX11977.1|	Integration host factor subunit alpha [Salmonella enterica subsp. enterica serovar Thompson str. RM6836]																
gi|548714525|gb|AGX10165.1	Membrane protein [Salmonella enterica subsp. enterica serovar Thompson str. RM6836]	39,940	369			18			1		54			1			
gi|548714500|gb|AGX10140.1|	Head protein [Salmonella enterica subsp. enterica serovar Thompson str. RM6836]	38,058	342	60	143	72	2	1	1								
gi|548714499|gb|AGX10139.1|	Head decoration protein [Salmonella enterica subsp. enterica serovar Thompson str. RM6836]	11,916	115	16	14	14	1	1	1		44	43		2	1		
gi|911477197|gb|KNN22204.1|	Phage tail protein [Salmonella enterica subsp. enterica serovar Thompson]	?	656								28			1			
							30	30	29				8	16	7	120	Total
CONTROL THOMPSON 15 MIN																	
gi|548714499|gb|AGX10139.1|	Head decoration protein [Salmonella enterica subsp. enterica serovar Thompson str. RM6836]	11,916	115							18	55		1	1			
													1	1		2	Total
CONTROL THOMPSON 20 H																	
gi|548714505|gb|AGX10145.1|	Minor tail protein [Salmonella enterica subsp. enterica serovar Thompson str. RM6836]	14,833	131								46	21		1	1		
														1	1	2	Total

FliC Newport

```
  1 MAQVINTNSL SLLTQNNLNK SQSALGTAIE RLSSGLRINS AKDDAAGQAI
 51 ANRFTANIKG LTQASRNAND GISIAQTTEG ALNEINNNLQ RVRELAVQSA
101 NSTNSQSDLD SIQAEITQRL NEIDRVSGQT QFNGVKVLAQ DNTLTIQVGA
151 NDGETIDIDL KQINSQTLGL DTLNVQKAYD VSATAAMDPK SFTDGTKNLT
201 APDATAIKAA LGNPAATGDS LSATLSFKDG KYYATVAGYT NAADTSKNGK
251 YEVNVDSATG AVTFNAAPTK ATVTGDTTVT KVQVNAPVAV STDVKKALED
301 GGVSNADATA AKLVKMSYTD KNGKSIDGGY ALEAGGKYYA ATYDEGTGKI
351 TANVTTYTDS TGVTKTAANQ LGGVDGKTEV VTIDGKTYNA SKAAGHDFKA
401 QPELAEAAAK TTENPLAKID AALAQVDALR SDLGAVQNRF NSAITNLGNT
451 VNNLSEARSR IEDSDYATEV SNMSRAQILQ QAGTSVLAQA NQVPQNVLSL
501 LR
```

FliC Kentucky

```
  1 MAQVINTNSL SLLTQNNLNK SQSALGTAIE RLSSGLRINS AKDDAAGQAI
 51 ANRFTANIKG LTQASRNAND GISIAQTTEG ALNEINNNLQ RVRELAVQSA
101 NSTNSQSDLD SIQAEITQRL NEIDRVSGQT QFNGVKVLAQ DNTLTIQVGA
151 NDGETIDIDL KQINSQTLGL DTLNVQKAYD VSATAAMDPK SFTDGTKNLT
201 APDATAIKAA LGNPTATGDS LSATLSFKDG KYYATVAGYT NAADTSKNGK
251 YEVNVDSATG AVTFNAAPTK ATVTGDTTVT KVQVNAPVAV STDVKKALED
301 GGVSNADATA AKLVKMSYTD KNGKSIDGGY ALEAGGKYYA ATYDEGTGKI
351 TANVTTYTDS TGATKTAANQ LGGVDGKTEV VTIDGKTYNA SKAAGHDFKA
401 QPELAEAAAK TTENPLAKID AALAQVDALR SDLGAVQNRF NSAITNLGNT
451 VNNLSEARSR IEDSDYATEV SNMSRAQILQ QAGTSVLAQA NQVPQNVLSL
501 LR
```

FliC Thompson

```
  1 MAQVINTNSL SLLTQNNLNK SQSALGTAIE RLSSGLRINS AKDDAAGQAI
 51 ANRFTANIKG LTQASRNAND GISIAQTTEG ALNEINNNLQ RVRELAVQSA
101 NSTNSQSDLD SIQAEITQRL NEIDRVSGQT QFNGVKVLAQ DNTLTIQVGA
151 NDGETIDIDL KQINSQTLGL DSLNVQKAYD VKDTAVTTKA YADNGTTLDA
201 SGLDDAAIKA AIGGTTGTAA VTGGTVKFDA DNNKYFVTIG GFTGADAAKN
251 GDYEVNVATD GKVTLAAGAT KTTMPAGAAT KTEVQELKDT PAVVSADAKN
301 ALIAGGVDAT DANGAELVKM SYTDKNGKTI EGGYALKAGD KYYAADYDEA
351 TGAIKAKTTS YTAADGTTKT AANQLGGVDG KTEVVTIDGK TYNASKAAGH
401 DFKAQPELAE AAAKTTENPL QKIDAALAQV DALRSDLGAV QNRFNSAITN
451 LGNTVNNLSE ARSRIEDSDY ATEVSNMSRA QILQQAGTSV LAQANQVPQN
501 VLSLLR
```

FIGURE 1 | Top panel. Phase 1 flagellin (FliC) sequence of *Salmonella enterica* subsp. *enterica* (SEE) serovar Newport strain SGSC2493. Bold red denotes the highest sequence coverage obtained for a single analysis of SEE Newport strain RM1655 (**Table 2**, 20 h, Day 1, 2nd analysis). Underlined residues are the N-terminal

(Continued)

FIGURE 1 | (5–143) and C-terminal (416–501) helical regions, respectively. Bold black residues denotes the D3 domain (196–282). Middle Panel. Flagellin (FliC) sequence from SEE serovar Kentucky strain CVM N38870. Bold red denotes highest sequence coverage obtained for a single analysis of SEE Kentucky strain RM7890 (**Table 3,** 20 h, Day 2, 2nd analysis). Underlined residues are the N-terminal (5–143) and C-terminal (416–501) helical regions, respectively. Bold black residues denotes the D3 domain (196–282). Bottom panel. Flagellin (FliC) sequence for SEE serovar Thompson str. RM6836. Bold red denotes highest sequence coverage obtained for a single analysis SEE Thompson strain RM1987 (**Table 4**, 20 h, Day 1, 1st analysis). Underlined residues are the N-terminal (5–143) and C-terminal (420–505) helical regions, respectively. Bold black residues denotes the D3 domain (197–284).

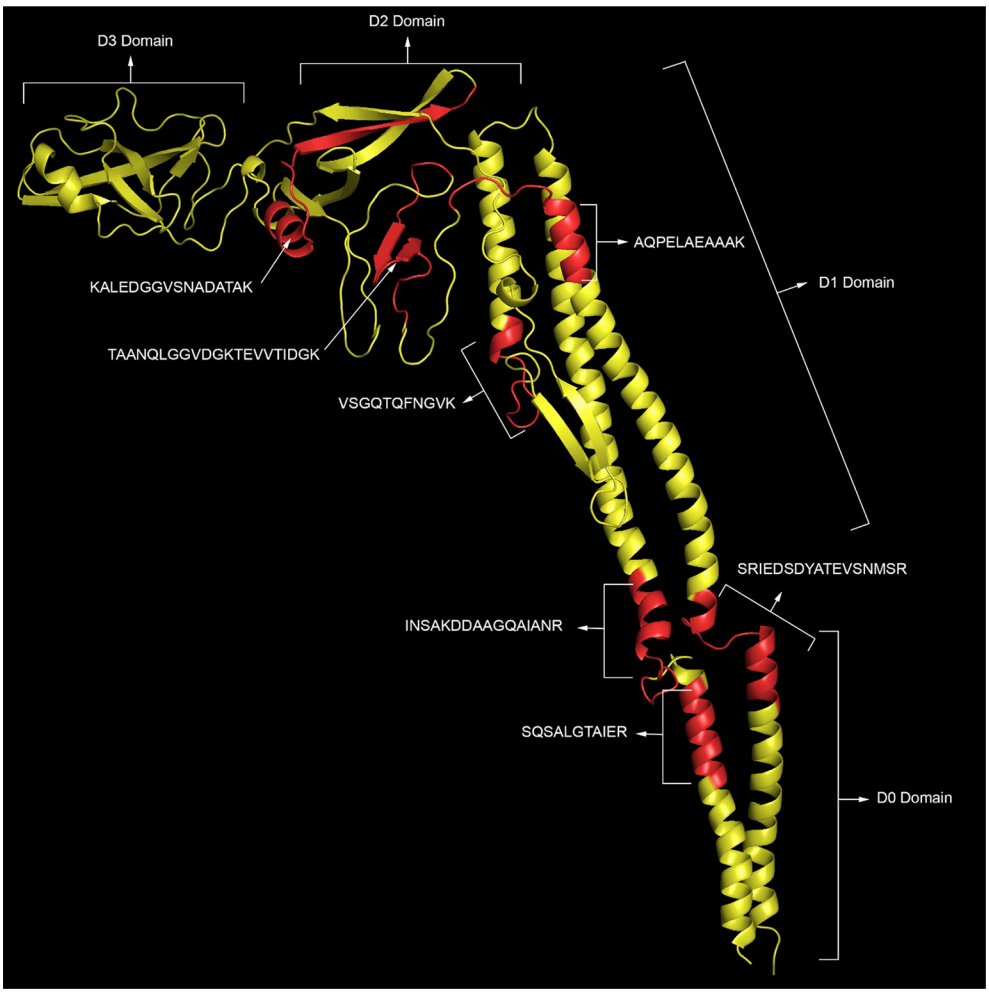

FIGURE 2 | The 3-D image of FliC of *S. enterica* based on X-ray crystallographic structure from Protein Data Bank (Entry: 3A5X) (32) and viewed in PyMOL. The corresponding peptide sequence coverage of SEE Newport is highlighted in red and specific peptides highlighted in white. Specific domains (D0, D1, D2, D3) are also indicated.

movement/operation leading to release FlgM that may re-activate flagellin biosynthesis. It is also possible that damage to the hook-filament junction may lead to detachment of the filament altogether allowing secretion of FlgM.

SEE Serovar Kentucky

Table 3 summarizes the results of the 15 min surface-shaving experiment and 20 h re-digestion of SEE Kentucky strain RM7890 and their controls. As with the SEE Newport strain, the number of peptides detected/identified is significantly increased for the 20 h re-digest compared to the 15 min shaving experiment which supports the usefulness of this secondary digestion step. Once again, peptides from proteins of the filament and hook/filament junction are detected: FliC, FljB, and FlgL. **Figure 1 (middle panel)** shows sequence coverage obtained for FliC. Peptides from the D0, D1, and D2 domains are detected but not the D3 domain which suggests that this domain appears resistant to proteolysis under the experimental conditions of our experiment. This is not entirely surprising as most bottom-up proteomic analyses incorporate denaturation of the protein prior to digestion to facilitate access to cleavable sites (basic residues). However, denaturation is contrary to the objective of

a surface-shaving experiment which is to sample only the most surface-exposed protein structures.

The negative regulator of flagellin synthesis, FlgM, was once again detected and, given the number of peptides detected, appears to be highly abundant. The appearance of FlgM under conditions of very brief exposure to trypsin (15 min) suggests a very rapid biological response to flagellin damage by the SEE Kentucky strain. Interestingly, we detected no peptides of the secreted effector/invasion proteins: SipA, SipB, SipC or SipD. The absence of detection suggested that perhaps their genes may not be present in this strain. In consequence, PCR was performed on the *sip* operon and *hilA* [a transcriptional activator of SPI1 regulation (41, 42)], and both were found to be present in this strain. The absence of *sip* expression may contribute to a lack of pathogenicity in this strain. This finding may be consistent with an assessment by the USDA in 2002 that, although the Kentucky serovar is prevalent in the food supply environment, it is not generally considered a successful human pathogen (43).

We detected only fleeting evidence of peptides of a few outer membrane proteins as shown in **Table 3**. However, reproducibility was an issue as these peptides were not detected in both biological replicates or with every analysis of a triplicate. This is probably due to their relatively low abundance as well as a portion of the protein being embedded in the membrane.

Control samples for SEE Kentucky showed detection of a few cytoplasmic proteins (**Supplementary Materials** Kentucky, pages 65–107). However, unlike the first biological replicate, the second biological replicate revealed detection of several cytoplasmic proteins (ribosomal, ef-Tu, etc.) and even flagellin (**Table 3** and **Supplementary Materials** Kentucky). This is likely the result of cell lysis releasing of cytoplasmic proteins as well as breakage of flagellin during processing.

SEE Serovar Thompson

Table 4 summarizes the results of the 15 min surface-shaving experiment and the 20 h re-digestion on SEE Thompson strain RM1987 and their controls (excluding cytoplasmic proteins detected which are shown in **Supplementary Materials** Thompson, pages 108–185). Consistent with SEE Newport and SEE Kentucky strains, we observe a significant increase in the number of peptides detected for the 20 h re-digestion (120) vs. that obtained for the 15 min surface-shaving experiment (64). Once again, peptides from FliC filament digestion were detected as well as FlgL of the hook-filament junction. The **Figure 1** (**bottom panel**) shows the sequence coverage obtained for FliC sequence of SEE Thompson. Peptides from the D0, D1, and D2 domains (but not the D3) are detected consistent with results from the other two SEE serovars. In addition to this apparent flagellin proteolysis, we observe weak detection of the anti-σ^{28} factor: FlgM.

SEE Thompson shows significant expression of SipA, SipB, SipC and SipD in both the 15 min and the 20 h re-digested samples which suggests, like the SEE Newport strain, a possible response to proteolysis including secretion of effector/invasion proteins. In addition, we detect enterohemolysin which was not detected in the SEE Newport and SEE Kentucky strains. A number of bacteriophage proteins were also detected. SEE Thompson (**Supplementary Materials**) shows a large number of cytoplasmic proteins detected in the surface-shaving samples (and even in the control samples) suggesting extensive lysis of the inner and outer membranes. It would seem that trypsin significantly weakens the integrity of the SEE Thompson envelope far more than for SEE Newport and SEE Kentucky strains. Another explanation could be that cell lysis is caused by activation of a lytic cycle of a bacteriophage in the host genome resulting in expression of bacteriophage-encoded proteins. Activation of the bacteriophage lytic cycle may be triggered by proteolytic surface-shaving.

The SEE Thompson control samples revealed a significant amount of cell lysis as evident from detection of cytoplasmic proteins in both the 15 min surface-shaving sample as well as the 20 h re-digested of the control samples. As no trypsin was used during the surface-shaving step of control samples, we can only conclude that the cellular membranes of this SEE Thompson strain were more susceptible to rupture. Cell lysis may be due to inability to respond to rapid changes in osmolarity, i.e., from broth to PBS, or membrane fragility during washing with PBS and centrifugation. In any case, the control samples showed no tryptic peptides of flagellin-associated proteins or Sip proteins (and other virulence factors) or bacteriophage proteins.

For this SEE Thompson strain, we conclude the following. The inner and outer membranes of this strain appear to be unusually susceptible to rupture and surface-shaving may exacerbate this tendency resulting in the release of a large number of cytoplasmic proteins. Surface-shaving with trypsin results in proteolytic cleavage of flagellin-associated proteins (FliC and FlgL) and the secreted FlgM and SPI-1 proteins. In addition, peptides of enterohemolysin and bacteriophage-encoded proteins were also detected. The latter may contribute to host cell lysis. Control samples were comprised of almost entirely cytoplasmic proteins.

Although sample contamination by cytoplasmic proteins is a common problem associated with proteolytic surface-shaving experiments, the amount of cell lysis observed for each strain in our study varied significantly and appeared to be strain dependent. SEE Newport was the most resistant to lysis followed by SEE Kentucky and lastly SEE Thompson which showed extensive cell lysis as evident from the number of cytoplasmic proteins detected. The use of PBS as the medium to perform all microbiological manipulations reduced the likelihood of cell lysis by maintaining mild osmotic conditions although it may have reduced the efficiency of trypsin digestion.

CONCLUSIONS

Proteolytic surface-shaving with trypsin of live SEE bacterial cells resulted in significant cleavage of flagella filament and hook-associated proteins and secretion of the negative regulator of flagellin biosynthesis: FlgM which may suggest up-regulation of flagellin biosynthesis. In addition, invasion/effector Sip proteins were also expressed in the Newport and Thompson strains. In the *absence* of trypsin during the shaving-shaving step, no significant flagella proteolysis occurred and FlgM and Sip were not detected. The Kentucky serovar/strain, although possessing *sip* genes, did

not express Sip proteins (at least not at levels detectable by our measurement).

For all three SEE strains/serovars, tryptic-generated peptides from proteolytic cleavage of the flagellin filament, FliC, were detected. Interestingly, no peptides were detected in the most accessible domain of FliC (i.e., D3) though the domain possessed seven or eight lysine residues. It is possible that the tertiary structure of the D3 domain (globular) may thwart efficient proteolysis in contrast to peptides that possess alpha-helical secondary structures.

Cell lysis can be a confounding problem of proteolytic surface-shaving experiments as it contaminates the sample with non-surface-exposed proteins (i.e., cytoplasmic proteins). In our experiments, cell lysis appeared to be serovar/strain dependent that may reflect the general robustness of the outer and inner membranes during sample processing. The greatest amount of lysis occurred with SEE Thompson which was accompanied by detection of many bacteriophage and cytoplasmic proteins that may suggest activation of a bacteriophage lytic cycle and that cell rupture may not have been entirely due to the intrinsic stability of the cell membrane. Our results suggest that brief proteolytic surface-shaving may be a useful technique to assess the potential virulence and robustness of SEE strains/serovars *in vitro*. Other techniques for assessing potential SEE virulence would be mice model, mammalian cells *in vitro* invasion assay (e.g., Caco2 cell line) or perhaps whole genome sequencing (44). Advantages of surface-shaving in assessing potential virulence would be that it does not require the use of live animals or preparation of mammalian cells *in vitro*. As surface-shaving is a mass spectrometry-based proteomic technique, we only detect expressed proteins (and by implication their genes) under specific experimental conditions.

AUTHOR CONTRIBUTIONS

CF conceptualized experiment, analyzed data and drafted and finalized manuscript. WZ performed microbiological experiments and collected mass spectrometry data and preliminary data analysis, reviewed drafts, and final manuscript.

FUNDING

This research was supported by USDA-ARS CRIS project 5325-42000-051-00D.

SUPPLEMENTARY MATERIAL

The Supplementary Material for this article can be found online at: https://www.frontiersin.org/articles/10.3389/fnut.2018.00124/full#supplementary-material

Data Sheet 1 | Mascot proteomic identifications of surface-shaving (and controls) for SEE Newport, Kentucky and Thompson.

REFERENCES

1. Rodríguez-Ortega MJ, Norais N, Bensi G, Liberatori S, Capo S, Mora M, et al. Characterization and identification of vaccine candidate proteins through analysis of the group A Streptococcus surface proteome. *Nat Biotechnol.* (2006) 24:191–7. doi: 10.1038/nbt1179
2. Tjalsma H, Lambooy L, Hermans PW, Swinkels DW. Shedding & shaving: disclosure of proteomic expressions on a bacterial face. *Proteomics* (2008) 8:1415–28. doi: 10.1002/pmic.200700550
3. Solis N, Larsen MR, Cordwell SJ. Improved accuracy of cell surface shaving proteomics in *Staphylococcus aureus* using a false-positive control. *Proteomics* (2010) 10:2037–49. doi: 10.1002/pmic.200900564
4. He Z, De Buck J. Cell wall proteome analysis of Mycobacterium smegmatis strain MC2 155. *BMC Microbiol.* (2010) 10:121. doi: 10.1186/1471-2180-10-121
5. He Z, De Buck J. Localization of proteins in the cell wall of Mycobacterium avium subsp. paratuberculosis K10 by proteomic analysis. *Proteome Sci.* (2010) 8:21. doi: 10.1186/1477-5956-8-21
6. Olaya-Abril A, Gómez-Gascón L, Jiménez-Munguía I, Obando I, Rodríguez-Ortega MJ. Another turn of the screw in shaving gram-positive bacteria: optimization of proteomics surface protein identification in *Streptococcus pneumoniae*. *J Proteomics* (2012) 75:3733–46. doi: 10.1016/j.jprot.2012.04.037
7. Wei Z, Fu Q, Liu X, Xiao P, Lu Z, Chen Y. Identification of *Streptococcus equi* ssp. zooepidemicus surface associated proteins by enzymatic shaving. *Vet Microbiol.* (2012) 159:519–25. doi: 10.1016/j.vetmic.2012.04.031
8. Bendz M, Skwark M, Nilsson D, Granholm V, Cristobal S, Käll L, et al. Membrane protein shaving with thermolysin can be used to evaluate topology predictors. *Proteomics* (2013) 13:1467–80. doi: 10.1002/pmic.201200517
9. Solis N, Parker BL, Kwong SM, Robinson G, Firth N, Cordwell SJ. *Staphylococcus aureus* surface proteins involved in adaptation to oxacillin identified using a novel cell shaving approach. *J Proteome Res.* (2014) 13:2954–72. doi: 10.1021/pr500107p
10. Flores-Ramirez G, Jankovicova B, Bilkova Z, Miernyk JA, Skultety L. Identification of *Coxiella burnetii* surface-exposed and cell envelope associated proteins using a combined bioinformatics plus proteomics strategy. *Proteomics* (2014) 14:1868–81. doi: 10.1002/pmic.201300338
11. Olaya-Abril A, Jiménez-Munguía I, Gómez-Gascón L, Rodríguez-Ortega MJ. (2014). Surfomics: shaving live organisms for a fast proteomic identification of surface proteins. *J Proteomics* 97:164–76. doi: 10.1016/j.jprot.2013.03.035
12. Tiong HK, Hartson S, Muriana PM. Comparison of five methods for direct extraction of surface proteins from *Listeria monocytogenes* for proteomic analysis by Orbitrap mass spectrometry. *J Microbiol Methods* (2015) 110:54–60. doi: 10.1016/j.mimet.2015.01.004
13. Tiong HK, Hartson SD, Muriana PM. Comparison of surface proteomes of adherence variants of listeria monocytogenes using LC-MS/MS for identification of potential surface adhesins. *Pathogens* (2016)5:40. doi: 10.3390/pathogens5020040
14. Solis N, Cain JA, Cordwell SJ. Comparative analysis of Staphylococcus epidermidis strains utilizing quantitative and cell surface shaving proteomics. *J Proteomics* (2016) 130:190–9. doi: 10.1016/j.jprot.2015.09.011
15. Rodríguez-Ortega MJ. "Shaving" live bacterial cells with proteases for proteomic analysis of surface proteins. *Methods Mol Biol.* (2018) 1722:21–9. doi: 10.1007/978-1-4939-7553-2_2
16. Cirulli C, Marino G, Amoresano A. Membrane proteome in *Escherichia coli* probed by MS3 mass spectrometry: a preliminary report. *Rapid Commun Mass Spectrom.* (2007) 21:2389–97. doi: 10.1002/rcm.3104
17. Walters MS, Mobley HL. Identification of uropathogenic *Escherichia coli* surface proteins by shotgun proteomics. *J Microbiol Methods* (2009) 78:131–5. doi: 10.1016/j.mimet.2009.04.013
18. Meoni E, Faenzi E, Frigimelica E, Zedda L, Skibinski D, Giovinazzi S, et al. CT043, a protective antigen that induces a CD4+ Th1 response during Chlamydia trachomatis infection in mice and humans. *Infect Immun.* (2009) 77:4168–76. doi: 10.1128/IAI.00344-09
19. Van Gerven N, Sleutel M, Deboeck F, De Greve H, Hernalsteens JP. Surface display of the receptor-binding domain of the F17a-G fimbrial adhesin through the autotransporter AIDA-I leads to permeability of bacterial cells. *Microbiology* (2009) 155:468–76. doi: 10.1099/mic.0.022327-0

20. Gesslbauer B, Poljak A, Handwerker C, Schüler W, Schwendenwein D, Weber C, et al. Comparative membrane proteome analysis of three Borrelia species. *Proteomics* (2012) 12:845–58. doi: 10.1002/pmic.201100211
21. Voss BJ, Gaddy JA, McDonald WH, Cover TL. Analysis of surface-exposed outer membrane proteins in *Helicobacter pylori*. *J Bacteriol.* (2014) 196:2455–71. doi: 10.1128/JB.01768-14
22. Nakai K. Protein sorting signals and prediction of subcellular localization. *Adv Protein Chem.* (2000) 54:277–344. doi: 10.1016/S0065-3233(00)54009-1
23. Doytchinova IA, Taylor P, Flower DR. Proteomics in vaccinology and immunobiology: an informatics perspective of the immunone. *J Biomed Biotechnol.* (2003) 2003:267–90. doi: 10.1155/S1110724303209232
24. Fenn JB, Mann M, Meng CK, Wong SF, Whitehouse CM. (1989). Electrospray ionization for mass spectrometry of large biomolecules. *Science* 246:64–71. doi: 10.1126/science.2675315
25. Karas M, Bahr U, Dülcks T. Nano-electrospray ionization mass spectrometry: addressing analytical problems beyond routine. *Fresenius J Anal Chem.* (2000) 366:669–76. doi: 10.1007/s002160051561
26. Jones AW, Cooper HJ. Dissociation techniques in mass spectrometry-based proteomics. *Analyst* (2011) 136:3419–29. doi: 10.1039/c0an01011a
27. Boyd R, Somogyi A. The mobile proton hypothesis in fragmentation of protonated peptides: a perspective. *J Am Soc Mass Spectrom.* (2010) 21:1275–8. doi: 10.1016/j.jasms.2010.04.017
28. Barak JD, Whitehand LC, Charkowski AO. Differences in attachment of *Salmonella enterica* serovars and *Escherichia coli* O157:H7 to alfalfa sprouts. *Appl Environ Microbiol.* (2002) 68:4758–63. doi: 10.1128/AEM.68.10.4758-4763.2002
29. Inami GB, Moler SE. Detection and isolation of Salmonella from naturally contaminated alfalfa seeds following an outbreak investigation. *J Food Prot.* (1999) 62:662–4. doi: 10.4315/0362-028X-62.6.662
30. Yonekura K, Maki S, Morgan DG, DeRosier DJ, Vonderviszt F, Imada K, et al. The bacterial flagellar cap as the rotary promoter of flagellin self-assembly. *Science* (2000) 290:2148–52. doi: 10.1126/science.290.5499.2148
31. Yamamoto S, Kutsukake K. FljA-mediated posttranscriptional control of phase 1 flagellin expression in flagellar phase variation of *Salmonella enterica* serovar *Typhimurium*. *J Bacteriol.* (2006) 188:958–67. doi: 10.1128/JB.188.3.958-967.2006
32. Maki-Yonekura S, Yonekura K, Namba K. Conformational change of flagellin for polymorphic supercoiling of the flagellar filament. *Nat Struct Mol Biol.* (2010) 17:417–22. doi: 10.1038/nsmb.1774
33. Lu Y, Swartz JR. Functional properties of flagellin as a stimulator of innate immunity. *Sci Rep.* (2016) 6:18379. doi: 10.1038/srep18379
34. Hayashi F, Smith KD, Ozinsky A, Hawn TR Yi EC, Goodlett DR, Eng JK, et al. The innate immune response to bacterial flagellin is mediated by Toll-like receptor 5. *Nature* (2001) 410:1099–103. doi: 10.1038/35074106
35. Kutsukake K. Excretion of the anti-sigma factor through a flagellar substructure couples flagellar gene expression with flagellar assembly in Salmonella typhimurium. *Mol Gen Genet.* (1994) 243:605–12.
36. Macnab, R.M. (1996). Flagella and motility. In: Escherichia coli and Salmonella typhimurium: Cellular and Molecular Biology. Neidhart, F.C., Curtiss, R. III, Ingraham, J.L., Lin, E.C.C., Low, K.B., Magasanik, B. et al. (eds). Washington, DC: American Society for Microbiology Press, pp. 123–145.
37. Karlinsey JE, Tanaka S, Bettenworth V, Yamaguchi S, Boos W, Aizawa SI, et al. Completion of the hook-basal body complex of the Salmonella typhimurium flagellum is coupled to FlgM secretion and fliC transcription. *Mol Microbiol.* (2000) 37:1220–31. doi: 10.1046/j.1365-2958.2000.02081.x
38. Calvo RA, Kearns DB. FlgM is secreted by the flagellar export apparatus in *Bacillus subtilis*. *J Bacteriol.* (2015) 197:81–91. doi: 10.1128/JB.02324-14
39. Guo S, Alshamy I, Hughes KT, Chevance FF. Analysis of factors that affect FlgM-dependent type III secretion for protein purification with *Salmonella enterica* serovar *Typhimurium*. *J Bacteriol.* (2014) 196:2333–47. doi: 10.1128/JB.01572-14
40. Brandis G, Bergman JM, Hughes D. Autoregulation of the tufB operon in Salmonella. *Mol Microbiol.* (2016) 100:1004–16. doi: 10.1111/mmi.13364
41. Ellermeier JR, Slauch JM. Adaptation to the host environment: regulation of the SPI1 type III secretion system in *Salmonella enterica* serovar *Typhimurium*. *Curr Opin Microbiol.* (2007) 10:24–9. doi: 10.1016/j.mib.2006.12.002
42. Golubeva YA, Sadik AY, Ellermeier JR, Slauch JM. Integrating global regulatory input into the Salmonella pathogenicity island 1 type III secretion system. *Genetics* (2012) 190:79–90. doi: 10.1534/genetics.111.132779
43. Dhanani AS, Block G, Dewar K, Forgetta V, Topp E, Beiko RG, et al. Genomic comparison of non-typhoidal *Salmonella enterica* Serovars Typhimurium, Enteritidis, Heidelberg, Hadar and Kentucky Isolates from Broiler Chickens. *PLoS ONE* (2015) 10:e0128773. doi: 10.1371/journal.pone.0128773
44. McWhorter AR, Chousalkar KK. Comparative phenotypic and genotypic virulence of Salmonella strains isolated from Australian layer farms. *Front Microbiol.* (2015) 23 6:12. doi: 10.3389/fmicb.2015.00012

Conflict of Interest Statement: The authors declare that the research was conducted in the absence of any commercial or financial relationships that could be construed as a potential conflict of interest.

Advantages of publishing in Frontiers

OPEN ACCESS
Articles are free to read for greatest visibility and readership

FAST PUBLICATION
Around 90 days from submission to decision

HIGH QUALITY PEER-REVIEW
Rigorous, collaborative, and constructive peer-review

TRANSPARENT PEER-REVIEW
Editors and reviewers acknowledged by name on published articles

Frontiers
Avenue du Tribunal-Fédéral 34
1005 Lausanne | Switzerland

Visit us: www.frontiersin.org
Contact us: info@frontiersin.org | +41 21 510 17 00

REPRODUCIBILITY OF RESEARCH
Support open data and methods to enhance research reproducibility

DIGITAL PUBLISHING
Articles designed for optimal readership across devices

FOLLOW US
@frontiersin

IMPACT METRICS
Advanced article metrics track visibility across digital media

EXTENSIVE PROMOTION
Marketing and promotion of impactful research

LOOP RESEARCH NETWORK
Our network increases your article's readership